Regulation of neural crest migration and patterning in zebrafish

Nikolic, Valentina

Award date:
2004

Awarding institution:
University of Bath

REGULATION OF NEURAL CREST MIGRATION AND PATTERNING IN ZEBRAFISH

Submitted by Valentina Nikolić
for the degree of PhD of the University of Bath
2004

COPYRIGHT

Signed:...Valentina Nikolić.....

ProQuest LLC
789 East Eisenhower Parkway
P.O. Box 1346
Ann Arbor, MI 48106-1346

To Tomo, '*per aspera ad astra*'

"It was the best of times, it was the worst of times, it was the age of wisdom, it was the age of foolishness, it was the epoch of belief, it was the epoch of incredulity, it was the season of Light, it was the season of Darkness, it was the spring of hope, it was the winter of despair, we had everything before us, we had nothing before us...."

Charles Dickens "A Tale of Two Cities"

Acknowledgements

I would primarily like to thank my supervisor, Dr Robert Kelsh, for his help, guidance, advice and understanding throughout my PhD, and for the many stimulating and inspiring discussions we had.

I would also like to thank all of the people who contributed to my project by sharing their results with me or providing me with the necessary materials. This includes our collaborators, Pete Currie and Georgina Hollway, who complemented our work with their studies of the *choker* muscle phenotype. I am also grateful to Jenny Reagan who provided me with the *EphA4* and *ephrinB2a* probes, Jenny Chan for the *ephrinB1* and *ephrinB2b* probes, Wataru Shoji for the *SemaZ1a* and *nrp-1* probes, Anil Challa for the *robo1* and *robo3b* probes and Samantha England for the *eng1* probe. I would also like to thank Dave Parichy for providing the lab with the *gch* probe.

In addition I would like to acknowledge the people whose technical support and expertise made the timelapse experiments possible: Richard Adams, Guy Blanchard and James Dutton. I would also like to thank Kirsten Dutton for her help during the early stages of the transplant experiments. I am particularly grateful to the computing experts in our lab who have on countless occasions helped me deal with intransigent computers, namely Bill Bennett and Tom Carney. In addition I would like to acknowledge all of the fish facility technicians, past and present, for maintaining the fish facility at a high standard: Kim Denny, Leanne Price and Richard Squire.

Finally I would like to thank all of the members of the lab, past and present, for all of the stimulating discussions, advice and input over the past three years, and for making the lab a great environment to work in. More than anything, I would like to express my gratitude to my closest friends in the lab, Sharon Kelly, Trevelyan Menheniott and Tia Smith for all the laughs and the emotional support, which I could not have done without. I am also deeply grateful to my fiancée, Tomo Svetić, and my parents for the relentless support they gave me throughout my PhD. Finally, I would like to thank Dejan Tauzer for his invaluable help with the printing of my chapters in Croatia.

This work was funded by the ORS award and the University of Bath.

Table of contents

Abbreviations

ATP	–	adenosine triphosphate
bHLHzip	–	basic helix-loop-helix/leucine zipper
BMP	–	Bone Morphogenetic Protein
BSA	–	Bovine serum albumin
C6S	–	chondoritin-6-sulfate
$CaCl_2$	–	Calcium chloride
cho	–	*choker*
cls	–	*colourless*
CNS	–	central nervous system
con	–	*chameleon*
CTP	–	cytidine triphosphate
dct	–	*dopachrome tautomerase*
DIG	–	Digoxygenin
Dll1	–	*Delta-like 1*
DMSO	–	Dimethyl Sulfoxide
DNA	–	Deoxyribonucleic acid
DRG	–	Dorsal Root Ganglia
E-cad	–	E-cadherin
ECM	–	Extracellular Matrix
EDTA	–	Ethylenediaminetetra-acetic acid
EMT	–	Epithelial-to-mesenchymal transition
engl	–	*engrailed1*
FGF	–	Fibroblast Growth Factor
fss	–	*fused somites*
gch	–	*GTPI cyclohydrolase*
GPI	–	glycosyl-phosphatidyl inositol
GTP	–	guanosine triphosphate
H_2O_2	–	Hydrogen peroxide
HCl	–	Hydrochloric acid
Hh	–	Hedgehog
HM	–	Horizontal myoseptum
HM	–	Hybridisation mix
KOH	–	Potassium hydroxide
LiCl	–	Lithium Chloride
lnfg	–	*lunatic fringe*
mitf	–	*microphthalmia related transcription factor*
MP	–	Muscle pioneers
nac	–	*nacre*
NC	–	Neural crest
NCC	–	Neural crest cell
nrp1	–	*neuropilin1*
NTP	–	nucleoside triphosphate
PAPC	–	Paraxial protocadherin
PBS	–	Phosphate Buffered Saline
Penn/Strep	–	Pennicillin/Streptomycin
PFA	–	Paraformaldehyde
pfe	–	*pfeffer*

PLLn	–	Posterior lateral line nerve
PNA	–	Peanut agglutinin lectin
PNS	–	Peripheral nervous system
PSM	–	Presomitic mesoderm
PTU	–	1-phenyl-2-thiourea
RB	–	Rohon-Beard
RNA	–	Ribonucleic acid
RPE	–	Retinal Pigmented Epithelium
Sema3A	–	*Semaphorin 3A*
Sema 3C	–	*Semaphorin 3C*
SemaZ1a	–	*Semaphorin Z1a*
Shh	–	*Sonic hedgehog*
smbp	–	*small muscle binding protein*
syu	–	*sonic you*
TAE	–	Tris-Acetate-EDTA
TE	–	Tris EDTA
TGFβ	–	Transforming Growth Factor β
TUNEL	–	Terminal deoxynucleotidyl Transferase Biotin-dUTP Nick End Labelling
ubo	–	*u-boot*
UTP	–	uridine triphosphate
xdh	–	*xanthine dehodrogenase*
yot	–	*you too*

Abstract

The neural crest is an embryonic population of cells that gives rise to numerous stereotypically patterned derivatives, including pigment cells, craniofacial cartilage and the neurons and glia of the peripheral nervous system. The mechanisms that regulate the patterning of these derivatives are still incompletely understood. Zebrafish are an excellent model for studying the processes of neural crest patterning as they have reproducible arrangements of neural crest-derived pigment cells. Our studies attempt to further the understanding of neural crest patterning in zebrafish by characterising a pigment patterning mutant and a candidate neural crest guidance molecule. The zebrafish mutant *choker* has spatially correlated defects in embryonic pigment patterning and muscle development. Our analyses show that the neural crest defects are restricted to derivatives that travel on the lateral migratory pathway: a loss of xanthophores and an accumulation of melanophores in the anterior trunk region. We show that these two defects are not causally related. We do preliminary transplant experiments to try to address the question of cell autonomy, and marker expression analyses to see whether the expression of candidate neural crest guidance molecules is affected in *choker* mutants. We use timelapse microscopy to characterise the melanophore defect, and find that it occurs due to aberrant migration of dorsal and ventral stripe melanophores into the lateral pathway during what is in wild types a post-migratory phase. Based on our findings we propose a model of how muscle-associated molecules regulate melanophore and xanthophore patterning in wild-type zebrafish embryos. Furthermore, we characterise neuropilin-1, a neural crest surface molecule thought to be involved in neural crest migration. We produce and characterise morpholino knock-downs of this protein and show that it is essential at early stages of neural crest migration. Overall, our analyses further our understanding of neural crest migration in zebrafish embryos by characterising one cellular and one molecular event required for correct neural crest patterning.

Chapter 1

Introduction

Overview of Neural Crest Development

The neural crest is an embryonic population of cells, characteristic of vertebrates, which arises at the dorsal edge of the forming neural tube and gives rise to numerous derivatives such as the neurons and glia of the peripheral nervous system, pigment cells and craniofacial cartilage. Because of the variety of cell derivatives that it generates and their stereotyped patterning, the neural crest has for many years been considered to be an excellent model for studying how cells are patterned in the developing embryo.

Neural crest induction

The neural crest is derived from the ectoderm which subdivides during neurulation to give rise to three distinct derivatives – the epidermis, the neural tube and the neural crest. Studies in the axolotl (Moury and Jacobson, 1989), and subsequently in Xenopus and chick embryos (Dickinson et al., 1995; Mancilla and Mayor, 1996; Selleck and Bronnerfraser, 1995) have revealed that the neural crest forms at the interface of neural and non-neural ectoderm. *In vitro* and *in vivo* studies found the appearance of neural crest markers, such as *slug,* whenever these two tissues were brought in contact with each other. It was thus postulated that interactions between neural and non-neural ectoderm are required for neural crest induction. Studies in Urodeles, chick and frogs suggest that both of these tissues contribute to the neural crest (Mancilla and Mayor, 1996; Moury and Jacobson, 1990; Selleck and Bronnerfraser, 1995). This was elegantly shown by grafting experiments in the axolotl where the neural tube or epidermis of a pigmented donor were grafted into an albino host and the neural crest was observed to originate from both of these tissues (Moury and Jacobson, 1990). However, although single cell labelling studies have found a common precursor for neural crest and neural tube lineages, a common epidermis/neural crest precursor hasn't been reported yet (Selleck and Bronnerfraser, 1995).

More recent studies have shown that neural crest induction is under the control of bone morphogenetic protein (BMP) levels. BMP4 and BMP7 are both expressed in the avian epidermis and treatment of neural tube explants with BMPs *in vitro* results in the induction of neural crest markers (Liem et al., 1995). Studies in Xenopus using dominant negative BMP receptors have shown that progressively higher levels of BMPs are required for the induction of neural tube, neural crest and epidermal tissues respectively (Marchant et al., 1998), thus suggesting that these tissues are induced by a BMP gradient. This gradient is achieved through the influence of molecules such as noggin, chordin and follistatin, which are secreted by the dorsal mesoderm (organiser) and inhibit the activity of BMPs produced by the ventral mesoderm. The antagonistic activities of these molecules result in a BMP gradient that is vital not just for ectoderm development but for the correct dorso-ventral patterning of the whole embryo. Elegant studies in the zebrafish confirmed this model of neural crest induction by looking at various mutations of BMP signalling (Nguyen et al., 1998; Nguyen et al., 2000). Where BMP signalling is completely abolished (*swirl/bmp2*) so is the presence of neural crest markers. By comparison, in the mutants where some BMP signalling persists (*somitabun/smad5* and *snailhouse/bmp7*), the neural crest domain is expanded. Thus the neural crest is induced only at a particular BMP concentration.

However, other studies have shown that chordin-induced BMP inhibition in both explants and whole embryos fails to give rise to the level of neural crest induction normally seen in vivo (LaBonne and Bronner-Fraser, 1998), suggesting that neural crest induction requires additional signals beside BMPs. Several lines of evidence suggest a role for Wnts and FGFs in neural crest induction. Thus, the over-expression of Wnts in the Xenopus neurectoderm leads to the dramatic expansion of neural crest markers, whereas the injection of dominant negative forms of these molecules has the opposite effect (Chang and Hemmati-Brivanlou, 1998; LaBonne and Bronner-Fraser, 1998; SaintJeannet et al., 1997). The Wnts implicated in neural crest induction (Wnt1 and Wnt3) are however only expressed following the upregulation of the earliest neural crest marker, *slug*, and thus unlikely to have a role in neural crest induction *per se*. Instead, they may have a role in the maintenance and enhancement of the initial weak neural crest induction established by BMP signalling.

The patterning of the neural plate has been proposed to involve one additional signal, whose role is to restrict the dorsalizing influence of BMP signals. Hh signals are emitted from the tail bud at early stages of neurectoderm development (Nguyen et al., 2000) and from the notochord at later stages, and they have a ventralizing activity. Thus, when dorsal neural plate explants are grown in the presence of a notochord, dorsal cell fate acquisition, including that of the neural crest lineage is suppressed (Liem et al., 1995). Hence, the ventralizing influence of Hh signals has an important role in restricting the domain where the neural crest is induced.

Epithelial-to-mesenchymal transition and delamination

Once cells become specified to the neural crest lineage they begin to express various lineage-specific markers, including *Slug,* a member of the *Snail* family of zinc finger transcription factors and the earliest known vertebrate neural crest marker (Nieto et al., 1994). Members of the *Slug/Snail* family of genes act as transcriptional repressors and may have a role in downregulating those genes which need to be excluded from the neural crest. The injection of antisense oligonucleotides designed to *Slug* mRNA into avian embryos resulted in aberrant neural crest development manifested by an inability to undergo epithelial-to-mesenchymal transition (EMT) (Nieto et al., 1994). More recent evidence has shown that the mammalian counterpart of *Slug, Snail,* directly binds the promoter of the E-cad gene (Cano et al., 2000). The downregulation of E-cad is thought to loosen homophilic neural crest contacts with neighbouring neural crest cells and thus enable the start of the epithelial-to-mesenchymal transition. This is a crucial process in neural crest development as it enables neural crest cells to lose their epithelial organisation and become mesenchymal in nature. It involves a decrease in cell-cell adhesion mediated by molecules such as E-cad and N-cad, and a greater affinity for ECM molecules (for review, see Duband et al., 1995). Following EMT, neural crest cells begin their migration and dispersion towards various sites in the embryo.

Neural crest cells segregate from the neuroepithelium in a rostrocaudal sequence which has been found to be under the control of BMP signalling in chick. Somite ablation experiments have shown that in the absence of somites, neural crest cells fail to delaminate from the neural tube and that the level of noggin expression remains high in the region of the neural tube opposite somite removal (Sela-Donenfeld and Kalcheim, 1999; Sela-Donenfeld and Kalcheim, 2000). It was thus

proposed that a signal, secreted by the somite, diffuses to the neural tube and inhibits noggin activity. This releases BMP4 from inhibition by noggin and results in locally elevated levels of BMP4, which induce neural crest segregation. This process occurs in a rostro-caudal sequence coincident with somite development and hence gives rise to the antero-posterior progression of neural crest delamination. Grafting experiments have found that the noggin inhibitor is produced by the dorso-medial quadrant of the somite. This link between somite development and initiation of neural crest migration has been proposed to be vital in ensuring that neural crest cells only begin migrating once the somite has matured enough to provide an adequate substrate for their migration.

Neural crest migration

The migration of neural crest cells is under the control of a number of factors, both environmental and intrinsic to neural crest cells themselves. There are proposed changes that occur both in the environment and in the neural crest expression profile that allow both the initiation of migration and the progression of neural crest cells along the correct pathways. The pathways of neural crest migration have been extensively studied in avian embryos where they were found to follow two distinct routes. The first wave of emigrating cells travels between the medial face of the somite and the notochord, the so called ventral pathway. Ventrally migrating cells are guided so that they travel through the rostral portion of each somite only and this gives a segmental aspect to their migration (Rickmann et al., 1985). A number of hours later, the second wave of neural crest cells begin to migrate and these follow the dorsolateral pathway, in between the lateral face of the somite and the overlying ectoderm. Dorsolaterally migrating cells are not segmentally arranged and are instead distributed randomly over the lateral face of the somite. In avian embryos melanoblasts are the only neural crest derivatives capable of migrating on the dorsolateral pathway whereas all other NCC fates utilise the ventral route (Erickson and Goins, 1995).

Zebrafish neural crest cells also migrate on two different pathways but due to anatomical differences between avian and zebrafish embryos, the two pathways are named the medial and lateral pathways, respectively (Raible et al., 1992). Zebrafish neural crest cells begin migrating on the medial pathway at around 19 hpf and although they enter the medial pathway at any location along the somite, they are

soon funnelled down the medial region and continue migrating in organised streams (Raible et al., 1992). Migration on the lateral pathway is initiated approximately 4 hours later and these cells also enter the pathway at various points along the somite, but, unlike cells migrating on the medial pathway, they are not found in organised streams, but instead migrate over the full face of the somite (RN Kelsh, personal communication). Similar to the avian model, only pigment cells have the ability to migrate on the lateral pathway in zebrafish, but all neural crest cells can migrate on the medial pathway (including melanoblasts) (Raible and Eisen, 1994; RN Kelsh, personal communication). Thus there are extensive similarities between the processes of neural crest migration in zebrafish and higher vertebrates and the factors that influence these will be discussed in more detail further on.

Neural crest specification

Finally, in order to give rise to the correct distribution of derivatives, neural crest cells must differentiate into the appropriate derivative in the appropriate location. Two models have been proposed to explain how this occurs: the progressive fate restriction (PFR) model where individual fates become specified through sequential fate restrictions both before and during migration; and the direct fate restriction (DFR) model where pluripotent cells adopt a particular fate according to the environmental signals in their postmigratory environment. There is evidence to support both of these models but recent evidence does increasingly favour the progressive fate restriction model. However, the real situation is likely to involve a combination of these two models (for a review, see Kelsh, 2002).

The exact time of neural crest specification to different lineages is not precisely understood. Although the situation is unclear from mouse and chick studies, work in the zebrafish suggests that most of the derivatives become specified prior to initiation of migration. Thus, cell labelling studies revealed that most NCCs are only capable of generating a single derivative after they have begun migrating, although some cells did undergo one restrictive cell division whilst migrating (Raible and Eisen, 1994). In addition, *in situ* analysis revealed that all pigment cell progenitors express cell-specific markers at the onset of migration. Expression of cell specific marker is seen in the premigratory and migratory crest for *mitf* (Lister et al., 1999) and for *gch* (Parichy et al., 2000). Although at these early stages there is some overlap in the expression of these markers between different pigment derivatives

(Pelletier et al., 2001) the cells are still specified to pigment lineages even if they are not unequivocally specified as a single fate. Similarly, ectomesenchymal fates also appear to be specified prior to migration as all premigratory cells that become cartilage or fin mesenchyme show fate restriction (Dutton et al., 2001; Schilling and Kimmel, 1994). In addition, the premigratory position of a non-ectomesenchymal neural crest cell appears to affect its fate choice. Medially positioned cells are close to the sources of Wnt signalling, which promotes pigment fates at the expense of neuronal ones, and become pigment cells, whereas laterally positioned cells are farther removed from these signals and choose a neuronal fate (Dorsky et al., 1998). These studies give support to the PFR model, as they reveal that single fates arise through a process of fate restriction which occurs early on in neural crest development and not during post-migratory stages.

Further evidence for the PFR model comes from the identification of pluripotent precursors in *in vitro* studies of quail neural crest cells (reviewed in Le Douarin and Dupin, 2003). When cultured, the isolated neural crest cells can give rise to colonies of distinct phenotypic assortments, such as glia and neurons, or glia and melanocytes, indicating that they are precursors with restricted developmental capacity. Recent studies have confirmed the existence of these pluripotent precursors by using endothelin 3 (ET3) to revert Schwann cells cultures into mixed cultures of melanocytes and glial cells via a reversion to the glia-melanocytic precursor state (Dupin et al., 2000; Dupin et al., 2003). These studies show that a terminal differentiation state can revert to a bipotent precursor state under particular conditions, a result entirely consistent with the progressive fate restriction model which dictates that neural crest derivatives go through a series of fate restricted precursors before becoming committed to a final fate.

Other studies do however suggest that some cell fates are specified only once a neural crest cell has reached its destination, and have identified factors which act instructively upon cell fate choice. For instance, BMP2 secreted by the dorsal aorta is thought to instruct a subset of as of yet unspecified neurons to differentiate into autonomic neurons (Shah et al., 1996).

It is thus likely that cells are specified through a series of restrictive divisions early on in neural crest development, and that, at the time of leaving the neural tube, they are only capable of giving rise to a limited number of derivatives. The environmental signals that they encounter whilst migrating and once they have

reached their final destination may be involved in the specification to a final fate and its maintenance. Thus a certain amount of fate restriction occurs prior to initiation of migration, although cell commitment to a final fate may be a post-migratory event.

The processes of neural crest development are thus complex and numerous factors are involved in their regulation. The tissues that are in close contact with migrating neural crest cells, such as somites, are of particular importance in ensuring the correct distribution of neural crest derivatives.

Somitogenesis

Paraxial mesoderm establishment

The vertebrate somites are derived from the paraxial mesoderm, a strip of tissue that flanks the developing notochord on both sides. In lower vertebrates such as amphibians and zebrafish, the paraxial mesoderm precursors are found in two symmetrical layers on either side of the Spemann organiser, or shield. In mice and chick, the progenitors of the paraxial mesoderm are located in a roughly equivalent zone. The induction of the paraxial mesoderm has been found to be under the control of various signals including those of the TGF-β and FGF families. The various mesodermal derivatives are specified by a dorso-ventral gradient of BMP signalling, established through the antagonistic activities of BMP-4 and its inhibitors, chordin noggin and follistatin, which are secreted by the Spemann organiser (for review see Kimelman and Griffin, 2000). FGF signalling also seems to have an important role in mesoderm specification as its inhibition leads to failure to develop trunk and tail structures (Amaya et al., 1991). The effects of FGF signalling on mesoderm formation in zebrafish have been shown to be primarily mediated through several T-box containing transcription factors, including Brachyury (*no tail*), *spadetail* and *tbx6* (Griffin et al., 1998). In addition to these signals, Wnt signalling also appears to have a role in paraxial mesoderm formation as the injection of XWnt-8 RNA into Xenopus embryos results in the enlargement of this tissue (Christian and Moon, 1993). XWnt-8 was postulated to have a role in specifying ventral mesoderm fate by attenuating the ability of XWnt-8 expressing cells to respond to the dorsalizing signals emanating from the Spemann organiser. The specification of mesodermal fates is thus a complex process involving numerous signalling pathways.

Following its induction, the paraxial mesoderm is established through a series of convergent extension movements which happen during gastrulation and result in the establishment of head and anterior trunk mesoderm. These movements appear to be under the control of FGF signalling as the injection of a dominant negative FGF receptor leads to defects in mesoderm involution during gastrulation (Amaya et al., 1991). FGF signalling may control the expression of genes involved in cell movement, such as paraxial protocadherin (PAPC). Thus, zebrafish mutants of the downstream effector of FGF signalling, the T-box gene *spadetail*, lose PAPC expression indicating a role for FGF signalling in the regulation this gene (Yamamoto et al., 1998). In addition, T-box genes are also known to regulate Wnt signalling. The absence of Wnt signalling in mutants such as *silberblick*, leads to convergent extension defects (Heisenberg et al., 2000).

In contrast to head and anterior trunk mesoderm, the posterior portion of the mesoderm is derived from a mass of cells found in the tail bud. Although the processes that give rise to the anterior and posterior portions of the paraxial mesoderm are therefore distinct, the transition from one process to the other is a continuous one.

PSM pre-patterning

Although the presomitic mesoderm (PSM) appears as a mass of loose mesenchymal cells, scanning electron microscopy revealed that it is pre-segmented into units that precede epithelial somite formation and are termed 'somitomeres' (Meier 1979, Jacobson 1988). These consist of units of mesenchymal cells and are found in both the head and trunk mesoderm. The head mesoderm somitomeres never form somites, although they are the functional equivalent of trunk somitomeres and as such, give rise to head muscle and bone. The trunk somitomeres do form somites and are termed as such when the borders dividing individual segments become wide enough to be seen by light microscopy. In addition to this morphological prepattern, evidence also exists for a molecular prepattern. Thus, transplantation of rostro-caudally inverted somites immediately after somite formation from donor chick embryos to a stage-matched quail host showed that the specification of antero-posterior identity occurred at the time of or prior to, somite segmentation, and was intrinsically determined (Aoyama and Asamoto, 1988). This molecular prepattern

was shown to be important for somite segmentation and the formation of morphologically distinct boundaries.

The segmentation clock

The early prepattern established in the PSM must be translated into morphologically distinct somites by a process called segmentation. Somite segmentation occurs in an antero-posterior progression and with a reproducible periodicity that is species-specific. Thus, in chick somites form every 90 minutes, and in zebrafish every 30 minutes. Various models have been put forward to explain the synchronous nature of this process, such as the 'clock-and-wavefront' and Meinhardt models. Both models postulate the existence of an oscillator in the cells of the PSM that regulates the timing of somite formation. The 'clock-and-wavefront' model states that cells in the PSM oscillate between permissive and non-permissive states while a maturation wavefront sweeps progressively posterior. When the wavefront encounters a cell in a permissive state, a somite boundary will form (Cooke and Zeeman, 1976). A more recent modification of the model states that cells in the PSM would count the number of cycles they go through and upon reaching the appropriate count they would form a somite boundary. In this model the wavefront is a direct output of the clock (Cooke, 1998). By comparison, the Meinhardt model proposes that PSM cells oscillate between signals responsible for the specification of anterior and posterior somite halves. Anterior expressing cells instruct their neighbours to express posterior signals and vice versa. This activity creates oscillations that spread through the PSM in a postero-anterior direction and stabilize at its most anterior end when they encounter signals (wave front) from the last formed somite (Meinhardt 1982, 1986).

The first molecular evidence for the existence of the oscillator was the identification of the chick homologue of the Drosophila *hairy* segmentation gene, *c-hairy1* (Palmeirim et al., 1997). The expression of this gene was found to oscillate in a cyclic pattern in the PSM and its oscillations could be subdivided into three consecutive phases. In phase I *c-hairy1* was expressed broadly in about 70% of the posterior PSM and in a narrow band in the prospective posterior half of the forming somite (somite 0). In stage II, *c-hairy1* expression was recorded in a narrower band that had moved anteriorly to the rostral part of the PSM. Finally, in stage III, *c-hairy1* expression has moved further anteriorly and had become restricted to a

narrow stripe that corresponds to the posterior half of the rostralmost prospective somite. This cycle of expression is repeated with a periodicity corresponding to the formation time of one somite.

Cell labelling and ablation studies revealed that the cyclic expression of *c-hairy1* does not depend on cell movement or a diffusible signal travelling caudo-rostrally but is instead likely to be an autonomous property of the PSM. In addition, the activity of *c-hairy1* does not depend on protein synthesis. This eliminates the possibility that *c-hairy1* regulates its own transcription by a negative feedback mechanism. Instead, the *c-hairy1* oscillations are likely to be regulated by some form of post-translational protein modification. The characterisation of *c-hairy1* suggested that this gene plays an important role in the process of somite segmentation.

Homologues of *c-hairy1* have subsequently been identified in other organisms including mice (*hes* genes) and zebrafish (*her* genes).

The role of Notch signalling in somite segmentation

The Notch signalling pathway has been shown to have roles in boundary formation and establishment of distinct territories in *Drosophila*. Notch is a transmembrane receptor that can bind two classes of transmembrane ligands, Delta and Serrate. The affinity of Notch for these ligands can be modified by differential glycosylation by the *fringe* protein, which acts as a modulator. Notch activation leads to its proteolytic cleavage at the membrane and translocation into the nucleus where it interacts with the transcription factor *RBPJκ* to activate various genes such as those of the *hairy/E(spl)* family. Notch signalling was first characterised in the formation of the *Drosophila* wing imaginal disc. The juxtaposition of *Drosophila fringe (D-fringe)* expressing (dorsal) and non-expressing (ventral) cells, leads to the activation of *fringe*-dependent cell signalling at the boundary of the two territories. This results in the activation of Notch ligands at either side of the boundary so that *Delta* expressed in ventral cells binds and activates *Notch* in dorsal cells, and *Serrate* expressed in dorsal cells binds and activates *Notch* in ventral cells. Thus, *Notch* is specifically activated along the dorso-ventral boundary and this causes the subsequent activation of downstream signalling targets, such as the signalling molecule *wingless (wg)*.

Notch has been proposed to play a similar role in vertebrate somite boundary formation. Its involvement in somitogenesis has been shown in mouse knock-out

studies. All mutants defective in components of the Notch signalling pathway show defects in somitogenesis ranging from somites with irregular size and shape, to defects in antero-posterior polarity and epithelialization (summarized in Barrantes et al., 1999).

The mammalian homologues of the *Drosophila fringe* protein have been identified and, of the three homologues (*Manic, Radical,* and *Lunatic fringe*; Johnston et al., 1997), only *lunatic fringe* (*lnfg*) was found to be expressed in the PSM in a pattern suggestive of a role in segmentation (Johnston et al., 1997). Expression analyses revealed that both in avian and mouse embryos, *lnfg* is expressed in a cyclic pattern reminiscent of *c-hairy1* expression (Aulehla and Johnson, 1999; Forsberg et al., 1998). Similar to *c-hairy1*, *lnfg* expression is not regulated by cell movement in the PSM or the caudo-rostral progression of a diffusible signal. Its expression appears to be an intrinsic property of the PSM as it is unaffected when the segmental plate is cultured in isolation from all surrounding tissues (Aulehla and Johnson, 1999). However, unlike *c-hairy1,* the dynamic expression of *lnfg* is disrupted by treatment with cycloheximide, indicating that it is protein synthesis dependent (McGrew et al., 1998). Mouse *lnfg* knock-out models display severe defects in somite segmentation and A-P polarity, thus further arguing for a role for *lnfg* in somitogenesis (Evrard et al., 1998; Zhang and Gridley, 1998).

The synchrony found between *c-hairy1* and *lnfg* oscillations in the PSM provided a link between the segmentation clock and Notch signalling. The fact that *lnfg* oscillations, unlike those of *c-hairy1,* were found to be dependent on protein synthesis led to the suggestion that Notch signalling acts downstream of *c-hairy1* and is an output of the clock (McGrew et al., 1998). It was suggested that the function of the clock is to regulate *lnfg* expression which in turn modulates the activation of Notch signalling. The disrupted A-P polarity in various mutants defective in components of the Notch signalling pathway led to the suggestion that Notch signalling regulates the establishment of A-P polarity which in turn leads to boundary formation.

However, there is evidence to suggest that Notch signalling may not only be an output of the clock, but may also be a component of the oscillator. Thus, the expression of both *lnfg* and *hes5*, the murine homologue of *c-hairy1*, was found to be perturbed in various mouse Notch pathway mutants such as *Dll1 (Delta-like 1), Notch1* and *RBPJκ* (Barrantes et al., 1999). Similarly, the oscillating expression of

her1, the zebrafish homologue of *c-hairy1*, was found to be perturbed in a Notch signalling mutant, *after eight (deltaD)* (Holley et al., 2000). Studies in Xenopus showed that the Notch targets ESR4 and ESR5 have the ability to negatively regulate themselves and Notch signalling (Jen et al., 1999), which gave rise to the idea that negative feedback loops may regulate Notch signalling during segmentation. Recent data have confirmed this by showing that loss of *lnfg* expression resulted in an inhibition of Notch signalling thus suggesting the existence of a negative feedback loop between *lnfg* and Notch. The existence of a notch-*her1*-notch regulatory loop has also been showed through epistasis experiments in the zebrafish (Holley et al., 2002).

Thus Notch signalling activates its downstream targets such as *lnfg* and the *her* and *hes* genes during segmentation and these genes in turn negatively regulate Notch signalling. This negative feedback loop is important in establishing Notch periodicity. Thus, Notch signalling acts as both the regulator and the output of the segmentation clock.

Somite boundary formation

According to Meinhardt's model of somite formation, somite boundaries form as a results of the juxtaposition of distinct anterior and posterior somite halves. The A-P polarity of somite segments is established prior to somite boundary formation and has been proposed to occur as a result of Notch signalling. Notch genes are expressed broadly in the posterior PSM and segment formation involves the periodic downregulation of Notch genes to give rise to a striped pattern. Studies in Xenopus suggest that Notch signalling is regulated in such a manner as to give rise to an ON/OFF expression pattern that corresponds to the anterior/posterior half segments respectively.

The segmental expression of Notch pathway genes enables the establishment of antero-posterior polarity through the regulation of expression of numerous other genes which become restricted to the rostral or caudal half of the prospective somite. A particularly important role appears to be played by the gene *mesp2,* which is expressed in the rostral half of the developing somite. Mouse knock-outs of this gene have severe segmentation defects caused by loss of rostral-half identity and the consequent duplication of caudal-half identity (Saga et al., 1997). This suggests that *mesp2* has a key role in specifying rostral half identity. However, aberrant expression

of Notch and FGF pathway genes in this mutant suggests that *mesp2* may have a role in also regulating Notch and FGF signalling. Studies of zebrafish mutants confirmed that the homologues of mammalian *mesp* genes, *mesp-a* and *mesp-b* have a role in establishing somite anterior half identity through the Notch/Delta and FGFR pathways (Sawada et al., 2000). The establishment of antero-posterior identity thus involves a host of molecular players and it is likely that feedback loops are in operation so that *mesp* genes lie both upstream and downstream of Notch signalling.

Studies in the zebrafish suggest that members of the Eph receptor and ephrin ligand family are pivotal in the formation of somite boundaries (Durbin et al., 1998). The ligands ephrin A-L1 and ephrin-B2 were found to be expressed in the posterior half of forming somites whereas their receptor Eph-A4 is expressed in the anterior half. The injection of dominant negative Eph receptors and soluble forms of ephrin ligands resulted in defective somite formation. Boundary formation was defective and so was differentiation, as judged by aberrant expression of the muscle marker *myoD.* Although the expression pattern of genes such as *her1* and *Delta D* was affected in injected embryos this was only apparent at later stages when boundary formation had already been disrupted. The early expression of these genes was however normal, suggesting that Eph/ephrin signalling plays no role in the establishment of the segmental prepattern in the PSM and is instead involved in translating the prepattern into morphologically distinct somite boundaries (Durbin et al., 1998). The juxtaposition of Eph-A4 and ephrin-B2 expressing cells may result in inhibition of cell movement at presumptive boundaries. This in turn may result in local de-adhesion events that lead to boundary formation. However, additional signals must also be involved as boundary formation does not occur where Eph-A4 and ephrin-B2 expressing domains meet in the middle of each somite.

Somite epithelialization

Besides segmentation, the formation of morphologically distinct somites involves somite epithelialization. This involves several changes in the adhesion properties of the somite cells. Thus, studies in culture have analysed the expression profile of somitic cells when they are dissociated and when they are in aggregates and found that the expression of N-cadherin and N-CAM varies dramatically. These molecules are both cell-adhesion molecules (CAMs) and thus mediate the attachment of a cell to its neighbours. Their expression was found to increase in the epithelial

somite. Other molecules involved in cell-ECM attachment, such as integrins, have also been found to have a role in epithelialization. The process of epithelialization has been proposed to be under the control of the gene *paraxis*, which is induced in the somite by signals in the surface ectoderm and neural tube (Sosic et al., 1997). Its expression is upregulated prior to epithelial somite formation and is maintained in the epithelial dermomyotome. However, paraxis-null embryos are still able to specify sclerotomal and dermamyotome lineages correctly suggesting that epithelialization and fate specification are under the control of different signals (Burgess et al., 1996). Similarly, in the *mesp-2* mutant segmentation fails but *paraxis* expression remains unaffected. Although the authors were unable to prove that epithelialization had occurred due to the lack of a good marker, the maintenance of the correct *paraxis* expression pattern in the absence of segmentation suggested that epithelialization and segmentation are distinct processes (Saga et al., 1997). This was also found in a separate study which showed that in the absence of surface ectoderm there is no epithelialization but some segmentation occurs as shown by the correct segmental expression of *Notch1* and *Dll1* and the presence of some weak boundaries. Combined, these data suggest that segmentation and somite epithelialization are two distinct processes. However, as complete segmentation is never seen in the absence of epithelialization and vice versa, it is likely that these two processes are linked at some level.

Muscle fibre development

After they bud off from the segmental plate, each somite is made up of a mesenchymal core, surrounded by a sheet of epithelium. The somites will then undergo a series of morphological and molecular changes which will enable them to separate into two distinct compartments – the sclerotome which gives rise to the vertebrae and the ribs; and the dermamyotome which generates skeletal muscle and the dermis of the skin, respectively. These lineages are specified by various inductive signals from surrounding tissues including Shh and Wnt signals from the notochord and neural tube.

Unlike terrestrial vertebrates, zebrafish have no need for extensive axial support structures as they are supported by the buoyancy of the water and their swim bladder. Thus the zebrafish sclerotome is a much smaller population of cells than its terrestrial counterpart. The dermatome portion of the zebrafish somite has not yet

been identified and it is unclear whether it exists at all. Thus the largest portion of the zebrafish somite consists of the myotome. This portion of the somite will develop into three different types of muscle – slow muscle, fast muscle and the muscle pioneers. Slow muscle fibres are found in a monolayer on the lateral surface of the myotome and are specialised for slow swimming. The fast muscle fibres by contrast are found deep within the myotome and are used for short and rapid bursts of swimming. The muscle pioneers are a small population of cells at the level of the horizontal myoseptum that span the width of the myotome, from the notochord to its lateral surface. They are responsible for secreting the fibrous sheet of ECM found along the midline of the zebrafish and called the horizontal myoseptum.

Slow muscle precursors can be distinguished before the onset of somitogenesis, as a population of cuboidal cells adjacent to the notochord. These cells will give rise to slow muscle fibre and muscle pioneer fates and are called the adaxials. Their commitment to a myogenic fate can be detected even before the onset of somitogenesis with the employ of molecular markers such as *myoD* and *myogenin* (Weinberg et al., 1996). Soon after somite formation a subset of the adaxial cells undergoes a change in morphology. They elongate in an antero-posterior plane and then migrate radially to form a superficial monolayer on the lateral surface of the somite (Devoto et al., 1996). Fast muscle fibre specification begins around the time of adaxial cell migration when they begin to express muscle-specific markers such as *myoD* and *myogenin* (Weinberg et al., 1996). The final myotomal fate, the muscle pioneers, becomes specified a number of hours after somite formation. The adaxial cells that had remained close to the notochord now elongate in a medio-lateral direction so that they span the entire width of the somite at the level of the future horizontal myoseptum (Devoto et al., 1996). They are distinguishable by the expression of the molecular marker Engrailed.

The acquisition of slow muscle fate has been postulated to be under the control of sonic hedgehog signalling from the notochord. The suggestion for this came from studies of mutants such as *floating head, no tail* and *bozozok,* all of which have defective notochord development and consequent defects in adaxial *myoD* expression, muscle pioneers and horizontal myosepta (Halpern et al., 1993). The muscle defects in these mutants can be rescued by the transplantation of wild-type notochord cells (Halpern et al., 1993). The analysis of hedgehog pathway mutants that have a morphologically normal notochord such as *syu* and *yot* revealed defects in

muscle development similar to those observed in notochord development mutants. It thus became clear that slow muscle fates were specified by hedgehog signals emitted by the notochord. This was further confirmed in overexpression studies where ectopic expression of *Shh* and *Ehh* led to the expansion of the muscle pioneer population (Currie and Ingham, 1996). However, the analysis of *you*-type mutants revealed that some slow muscle can form in the absence of *Shh* (Lewis et al., 1999). Thus the loss of *Shh* can be compensated for by other signals such as perhaps *echidna* or *tiggywinkle hedgehog.* However, all *Shh* mutants display a complete loss of muscle pioneers suggesting that this molecule is indispensable for muscle pioneer induction. In fact, prolonged exposure to *Shh* by virtue of remaining close to the notochord for a longer period of time is thought be the factor responsible for MP fate induction (Lewis et al., 1999). This is however in disagreement with previous studies that analysed the *no tail* mutant and found that muscle pioneer formation is impaired despite normal early *shh* signalling (Blagden et al., 1997). It is however possible that specification to a muscle pioneer fate requires a prolonged exposure to any of the Hh signals – the presence of early *shh* expression may not be enough to induce muscle pioneer fate in the absence of other signals. Thus *shh* appears to be necessary but not sufficient for MP induction.

In addition to Hh signals, muscle pioneer development is also regulated by members of the TGFβ family. Zebrafish BMP4 is expressed in the dorsal and ventral portions of the myotome and is proposed to restrict the acquisition of muscle pioneer fate to the medial portion of the myotome (Du et al., 1997). Thus, even in the presence of ectopic *Shh* signalling, supernumerary muscle pioneers form only in the medial portion of the myotome. The specification of fast muscle, by comparison, is thought to occur independently of Hh signalling. Thus, all of the Hh pathway mutants have defects in slow muscle fates only whilst fast muscle development is unimpaired. Studies suggest that fast muscle fate is a default fate that is taken by cells not instructed to become slow muscle (Blagden et al., 1997). Thus, in the presence of ectopic *Shh* signalling fast muscle cells were found to change their developmental programme and shift to a slow muscle fate.

The morphology of the somite is very important for neural crest and axon guidance. Adaxial cells and slow muscle fibres are both located in close apposition to neural crest and axon trajectories. Furthermore, fast muscle develops adjacent to the medial neural crest migratory pathway. The correct specification and differentiation

of distinct muscle cell types thus has implications for neural crest and axon patterning.

Neural Crest Patterning

The neural crest gives rise to several distinct derivatives that are distributed in a very stereotyped manner. For instance, neurogenic crest gives rise to neurons of the peripheral nervous system. Among these are the sensory neurons of the dorsal root ganglia which are found segmentally patterned at a frequency of one ganglion per somite. The sympathetic neurons are found as a chain of ganglia adjacent to the dorsal aorta. Pigment cells are equally stereotypically patterned. This is particularly clear in lower vertebrates such as the axolotl and the zebrafish. These possess several types of pigment cells and consequently have elaborate and beautiful pigment patterns. The zebrafish embryonic pigment pattern consists of three stereotypically arranged classes of pigment cells – the black melanophores, yellow xanthophores and iridescent iridophores. The melanophores are found in four longitudinal body stripes – the dorsal stripe, which is located on top of the somites and runs from the top of the head to the tip of the tail; the lateral stripe, found at the level of the horizontal myoseptum and extending from somite 5 to the tip of the tail; the ventral stripe, on the ventral surface of the somites, which runs from the ear to the tail and the yolk sac stripe which is found on the ventral surface of the yolk sac and stops at the anus. Even within the stripes the melanophores have a stereotypical morphology, arrangement and orientation. Thus, in the dorsal stripe the melanophores found on the top of the head are flat and paving-slab like. As the dorsal stripe narrows and runs along the trunk of the fish, it is composed of smaller, bilaterally arranged melanophores. The melanophores in the lateral stripe by comparison are always found elongated in an antero-posterior direction. The xanthophores have a less precise arrangement in that they are found loosely scattered throughout the head and flank of the embryo. They fill in the spaces that are devoid of melanophores but are also found mixed in with melanophores in the lateral pigment stripe. Finally the iridophores are found in three of the four melanophore stripes – the dorsal, ventral and yolk sac stripe - and scattered over the iris of the eye. Thus the arrangements of

pigment cells in the zebrafish are not only very complex but are also highly reproducible and their regulation must involve numerous factors.

The process which enables the appropriate neural crest derivatives to be distributed in the correct locations is called neural crest patterning. For neural crest cells to be patterned correctly a cell must both migrate to the correct destination and give rise to the appropriate type of derivative. Most pigment derivatives are thought be specified prior to or during migration, thus, at least for pigment cells, the guidance of already specified derivatives to the right location is the major factor in determining whether they are correctly patterned.

As previously discussed, neural crest migration occurs on two distinct pathways – in zebrafish these are referred to as the medial and the lateral migratory pathway. Each of these pathways is subject to temporal as well as spatial regulation as migration on the lateral pathway begins a number of hours after migration on the medial route has commenced. Furthermore, although neural crest cells on the lateral pathway migrate randomly over the lateral face of the somite, medially migrating cells are organised into distinct streams and are thus subject to a further level of regulation. The cues that ensure that neural crest cells migrate at the appropriate locations and times are clearly complex and they involve both environmental and cell-autonomous factors. In addition, interactions between neural crest cells themselves play a role in the correct patterning of derivatives.

The environmental cues regulating neural crest migration have most extensively been studied in avian embryos but there has also been some interesting work done on the zebrafish. There is an intimate geographical relationship between the pathways of neural crest migration and somite location, and the latter is ideally positioned to influence neural crest cells as they migrate to their destination. Thus, it was observed that changes in somite shape accompany the initiation of neural crest migration in zebrafish (Raible et al., 1992). The somites elongated in a dorso-ventral plane, thus facilitating the establishment of contacts with neural crest cells. Further studies in the zebrafish showed an even more intimate relationship between neural crest cells and somites (Jesuthasan, 1996). Prior to initiation of neural crest migration, neural crest cells were observed to extend cellular processes and to make contact with the young somite. However at these early stages the processes collapsed and the cell bodies remained associated with the space at the top of the neural tube. However, as the start of migration begun to draw near, the frequency of protrusion

collapse decreased and stable contacts begun to be established between the neural crest cells and the somite. These often thickened and led to the extension of more protrusions and establishment of more contacts. Eventually, the neural crest cell moved into the migratory pathway. However, contacts with the lateral face of the somite continued to result in protrusion collapse until a few hours later when migration on the lateral pathway begun. This collapsing activity was postulated to occur as a result of inhibitors associated with the somite (Jesuthasan, 1996).

Somite-associated inhibitors are found in the form of cell-surface or ECM molecules. Early studies found that the ECM has an important role in the regulation of neural crest migration. Thus, the transplantation of ECM from late to early axolotl embryos resulted in precocious neural crest migration, suggesting that the ECM undergoes a 'maturation' process which enables neural crest cells to start migrating (Lofberg et al., 1985). *In vitro* and *in vivo* manipulations of various ECM components have shown the pivotal role of these molecules in NC development (summarised in Perris and Perissinotto, 2000). Some molecules such as laminin and fibronectin are considered to be permissive to neural crest migration. Laminin-1 and -8 isoforms in particular appear to optimally promote neural crest motility and their spatial distribution in chick embryos is suggestive of a role in directing cells to the ventromedial pathway (Erickson and Perris, 1993). On the other hand, molecules of the aggrecan family are found in areas that neural crest cells are excluded from, such as the perinotochordal space, and are considered to be inhibitory to neural crest migration (Pettway et al., 1996). Chondroitin sulphate proteoglycans and peanut agglutinin lectin (PNA)-binding molecules have been shown to have an important role in delaying lateral pathway migration. Experiments where the dermamyotome, and consequently the associated peanut agglutinin lectin (PNA)-binding and chondoritin-6-sulfate (C6S) molecules were ablated resulted in the precocious invasion of the dorsolateral space by melanoblasts (Oakley et al., 1994). However other factors must also be involved as the precocious dorsolateral pathway migration ensued only after a short delay and no amount of somite ablation was able to abolish this delay. The absence of molecules that normally restrict dorsolateral pathway migration is important for the pigmentation of the naturally occurring chick mutant Silkie fowl. The lack of PNA-binding molecules allows melanoblasts to enter the ventral space and occupy most connective tissues thus giving them a blue-black coloration (Faraco et al., 2001).

In addition to controlling the timing of neural crest migration, somite associated molecules also have a pivotal role in guiding the ventrally migrating cells along a precise pathway in avian embryos. The segmental nature of avian neural crest migration was found to be associated with an unequal distribution of molecules in sclerotome rostral and caudal halves (summarised in Krull, 2001). Some molecules such as Tenascin-C were found to be expressed by both neural crest cells and the cells of the rostral sclerotome halves and are thus thought to be generally permissive to neural crest migration. Introduction of tenascin-C morpholinos into avian neural crest precursors resulted in impaired neural crest emigration from the neural tube into the somites. Thus tenascin-C may have anti-adhesive properties that play a vital role in neural crest detachment from the neuroepithelium (Tucker, 2001). However, mouse knock-outs of tenascin-C showed no overt phenotype suggesting that the role of this molecule can perhaps be compensated for by other members of this family (Saga et al., 1992). Thrombospondin is also expressed in the rostral somite half and has been shown to promote neural crest migration *in vitro*.

In contrast, a number of molecules are expressed in the caudal half of avian sclerotomes and are thought to be important in excluding migrating neural crest cells from this region. F-spondin, for instance is expressed by both the caudal sclerotome and perinotochordal space, both regions devoid of migrating neural crest cells. The PNA-binding molecules that have a role in regulating the timing of dorsolateral pathway migration also appear to have a prominent role in the guidance of neural crest migration through the somite as the application of PNA to avian trunk explants caused neural crest cells to begin migrating through both the rostral and caudal somite halves (Krull et al., 1995). An important role in the guidance of neural crest migration has been ascribed to members of the Eph-receptor and ephrin ligand family. Both receptors and ligands encode membrane attached proteins that are expressed in complementary expression patterns. The caudal somite half of avian embryos expresses the ligand ephrin-B1 while the rostral somite half and the migrating neural crest cells express the corresponding receptor Eph-B3 (Krull et al., 1997). The application of a soluble ephrin-B1 ligand which acts as a dominant negative to avian trunk explants resulted in neural crest migration through both rostral and caudal somite halves. This result is similar to that observed with PNA-binding molecules and suggests that both of these families have an important role in directing neural crest migration through the rostral sclerotome half. More recently,

Eph receptors and ligands of the A class have also been found to have a role in the guidance of neural crest migration (McLennan and Krull, 2002).

The attachment of ECM components to elements of the cytoskeleton in neural crest cells is mediated by integrins. For instance, binding of neural crest cells to fibronectin, a molecule whose expression shows a strong spatiotemporal correlation with neural crest migration, is mediated by the integrin $\alpha 4\beta 1$. The blockage of this integrin's function by the addition of an antibody *in vitro* impaired neural crest migration and reduced delamination from the neural tube (Testaz and Duband, 2001). Similarly, the inhibitory effects of sonic hedgehog on neural crest migration are largely mediated through a Patched-Smoothened-Gli pathway independent mechanism. Instead, *Shh* has been shown to, directly or indirectly affect integrin conformation so that they can't bind neural crest cells, resulting in an inhibition of migration. However, integrin knock-out studies show that the segmental migration of neural crest cells remains undisturbed (Kil et al., 1998). Thus, although integrins seem to have an important role in neural crest emigration from the neural tube, their role in the guidance of neural crest cells may be minor or, alternatively, compensated for by other integrins.

Although environmental factors have a pivotal role in the guidance and patterning of neural crest cells, there are a number of cell-autonomous factors that also contribute to this process. For instance, several lines of evidence indicate that chick neural crest cells can only enter the dorso-lateral pathway once they have become specified to a melanoblast fate (Erickson and Goins, 1995). Thus, grafting experiments showed that young neural crest cells grafted into host embryos where neural crest migration has just begun migrate down the ventral path only. By comparison, when older neural crest cells which have already differentiated as melanoblasts are grafted, they immediately begin migrating down the dorso-lateral pathway. Furthermore, if young neural crest cells are transplanted into older embryos, none of the grafted cells migrate dorso-laterally despite the fact that many of the host neural crest cells are doing so. Additional studies confirmed these observations and found that if early migrating neural crest cells are cultured under permissive conditions none differentiate into melanocytes. This suggests that the fate restriction is intrinsic to the cells themselves rather than being a consequence of environmental cues that cells may encounter once they begin migrating ventrally (Reedy et al., 1998). Thus it is clear that in addition to the loss of glycoconjugates

from the dorso-lateral pathway, specification to a melanoblast fate plays an important role in the initiation of dorso-lateral migration. It has been suggested that the ability of melanoblasts to invade the dorso-lateral pathway is due to the fact that they are more invasive when compared to other neural crest derivatives (Erickson and Goins, 1995). Melanoblasts may also have a different complement of cells surface molecules that enable them to interact differently with the dorso-lateral pathway environment. Studies have indicated that the gene expression profile of melanoblasts and neural crest cells in general is plastic and changes during migration. For instance, the cadherin expression profile of melanoblasts as they migrate into the skin has been studied and it has been found that the invasion of the epidermis from the dermis correlates with an increase in E-cad expression (Nishimura et al., 1999). The cytoplasmic domain of E-cad can induce stromelysin-1 expression which may in turn enable melanoblasts to degrade the basement membrane separating the epidermis from the dermis through local metalloproteinase activity (Delmas et al., 1999). Changes in neural crest cell cadherin expression have also been found to have a role in the epithelial-to-mesenchymal transition (summarised in Pla et al., 2001). It is these changes in cadherin expression that enable neural crest cells to detach from the neuroepithelium. Similarly, the integrin expression profile of neural crest cells has also been found to change according to the environment (Strachan and Condic, 2003). Examination of rates of migration and integrin expression profiles of neural crest cells migrating on different concentrations of substrates such as laminin and fibronectin revealed that the neural crest cells modulate the level of integrin expression to compensate for the differences in substrate concentration. This allows them to maintain an even speed of migration over the substratum.

Thus, the correct migration of neural crest cells is the result of a combination of environmental cues and the way that the cells themselves interact with their environment. However, to achieve correct patterning neural crest cells must not only be guided along the appropriate pathways but must also cease their migration in the appropriate locations. Here also environmental cues play an important role. Thus, the receptor Sema3A has been proposed to have a role in the patterning of the sympathetic nervous system (Kawasaki et al., 2002). This receptor is expressed in the caudal sclerotome of avian and rodent embryos whereas its ligand neuropilin-1 is expressed by the sensory neurons of the dorsal root ganglia and the autonomic neurons of the sympathetic nervous system. Nrp-1 and Sema3A mouse knock-out

mutants show defects in the development of the latter, evidenced by the presence of ectopic sympathetic neurons. It was found that the sympathetic neuron progenitors migrated through and emerged correctly from the sclerotome but then distributed widely, and not just in the region adjacent to the dorsal aorta as in wild-type embryos. These observations led to the suggestion that Sema3A probably acts as a stop signal for sympathetic neuron progenitors.

Finally, the interaction between different neural crest cells also plays an important role in achieving a correct spatial distribution. This has been best studied in the zebrafish where the transparency of the embryo and the natural label of its three different types of pigment cells make the observation of pigment cell behaviour throughout development relatively straightforward. Early studies looking at lateral stripe development saw that migrating melanophores preferentially populated the horizontal myoseptum of somites that had no melanophores already associated with them (Milos and Dingle, 1978a; Milos and Dingle, 1978b). The repulsive interaction between the melanophores thus insures that these cells are evenly spread along the lateral stripe. Even earlier studies have looked at the relationship between adult melanophores and xanthophores in the regeneration of the anal fin pigment pattern (Goodrich, 1931). After fin amputation, the regenerating tissue was transparent and unpigmented. However, as the fin grows, the melanophores increase progressively so that they are uniformly distributed throughout the growing fin. After a period of about 3 weeks, when the fin is half-grown the melanophores begin to thin out in a horizontal band near the base of the fin, which becomes invaded by xanthophores. The melanophores then become concentrated on either side of the xanthophore band, thus giving rise to the black melanophore stripes. This process mirrors stripe formation during normal development and suggests that stripe development occurs as a consequence first of localised melanophore destruction followed by their accumulation in specific regions. These studies have been extended more recently with the help of zebrafish pigmentation mutants. That xanthophores have a direct role in the patterning of adult melanophores is inferred from mutants such as *fms,* which have defects in both xanthophore and melanophore patterning (Parichy et al., 2000). *fms* is a gene required for xanthoblast dispersal and its absence results in the loss of both embryonic and adult xanthophores but also in an adult melanophore stripe defect. It was found that instead of dying in interstripe regions only, adult melanoblasts also underwent cell death in presumptive stripe regions. In addition,

fms mutants also showed a reduction in directional melanophore movement. As differentiated melanoblasts do not express *fms* it was presumed that the melanophore defect must be due to an interaction between melanophores and xanthophores. Thus, xanthophores may mediate melanophore aggregation into stripes and in their absence the melanophores are unable to coalesce into stripes, and consequently they die off. However, it is unclear whether stripe formation in the adult reflects embryonic pigment pattern development. Thus, studies of embryonic pigment pattern mutants suggest that the opposite may be the case. The absence of embryonic xanthophores in zebrafish pigmentation mutants results in no detectable melanophore phenotype (Odenthal et al., 1996). In addition, melanophore mutants such as *sparse* have xanthophores occupying the spaces normally taken by melanophores, thus suggesting that during embryonic pigment patterning melanophores populate their sites first and then the xanthophores 'fill-in' the remaining spaces (Kelsh et al., 1996). The process of pigment pattern establishment in the zebrafish thus appears to be regulated differently in the embryo and in the adult.

In summary, the patterning of neural crest derivatives is a highly complex and incompletely understood process regulated by a number of environmental and cell-autonomous factors.

Aims: Investigating the mechanisms of zebrafish neural crest migration and patterning

Some understanding of the processes of neural crest migration and the molecules involved has been reached for avian embryos, however the process is much less understood in zebrafish and there are some significant differences between these two species. Firstly, the sclerotome obviously plays an important role in the migration of neural crest cells in avian embryos. However evidence suggests that the sclerotome does not have an equivalent role in the zebrafish. The zebrafish sclerotome is a small and migratory population of cells and its ablation does not result in any neural crest phenotype with respect to peripheral nervous system segmentation (Morin-Kensicki and Eisen, 1997). The role of the sclerotome might instead have been taken over by the much larger portion of the somite – the myotome - which in zebrafish is located in an appropriate location to guide neural crest cells.

Secondly, in contrast to avian neural crest cells, zebrafish neural crest cells migrating on the medial pathway do not travel through the rostral somite half. Instead, they travel midsegmentally down the somite, and very little is known of how this is achieved. It is likely however, that this is regulated by a system of neural crest cell interaction with asymmetrically distributed environmental molecules.

In order to find out more about how neural crest migration is regulated in the zebrafish we decided to use two approaches. Firstly, we characterised a zebrafish pigment pattern mutant. Secondly, we investigated a candidate neural crest guidance molecule chosen because of its expression in the neural crest and the expression of its ligand in the somite, adjacent to neural crest migratory pathways.

Zebrafish mutants have proved a useful tool for studying the processes of neural crest development. A large-scale mutagenesis screen in Tübingen identified thousands of mutants with defects in various aspects of embryonic development. Among those, there are a large number of mutants with defective neural crest development and their characterisation contributes to our understanding of this process (Kelsh et al., 1996; Odenthal et al., 1996). Thus, the mutant locus in several mutants has been cloned and the gene's functions characterised. For instance the characterisation of the mutant *colourless*$^{-}$ found that it has an absence of pigment cells and neural crest derived neurons and glia, but normal craniofacial cartilage development (Kelsh and Eisen, 2000). Further studies showed that *colourless* is a homologue of the mouse *sox10* gene and is required cell-autonomously within the neural crest lineage for the specification of non-ectomesenchymal derivatives (Dutton et al., 2001). The zebrafish pigment pattern mutant *fms*$^{-}$ has an embryonic xanthophore defect and studies using xanthoblast markers found that labelled cells were confined to the vicinity of the neural tube (Parichy et al., 2000). Thus, it was postulated that *fms* has a role in xanthoblasts dispersal. As *fms*$^{-}$ mutants also have an adult melanophore defect, their study was important in elucidating the importance of xanthophores in adult melanophore patterning. Finally, the gene mutated in *nacre*$^{-}$, a mutant that has a complete absence of melanophores, was found to be vital for the specification of neural crest cells to a melanoblast fate (Lister et al., 1999).

The *choker*^{tm26} allele was identified during the 1996 Tübingen mutagenesis screen, according to its pigmentation and muscle development defects (Kelsh et al., 1996). The pigmentation defect consisted of a band of ectopic melanophores in the anterior trunk (Kelsh et al., 1996). This band bridges the dorsal and ventral

melanophore stripes in the region of the anteriormost 4-5 somites (Figure 1.1B). Spatially correlated with this melanophore band there is a 'hindbrain indentation' which was later found to be due to aberrant muscle development (van Eeden et al., 1996). This region of ectopic melanophore accumulation and aberrant muscle development will hereafter be referred to as the 'collar'.

In addition to the anterior trunk abnormalities, *choker* was found to have a number of other defects indicative of aberrant muscle patterning (van Eeden et al., 1996), and according to these was classified as a *you*-type mutant. This class of mutants was characterised by their U-shaped somites, reduced or absent horizontal myoseptum and a morphologically normal notochord. It included *you (you), you-too (yot), sonic-you (syu), chameleon (con), u-boot (ubo)* and *choker (cho)*. Antibody staining with the muscle pioneer marker 4D9 revealed that all of the *you*-type mutants, with the exception of *choker*, had reduced muscle pioneer staining. *choker* mutants were not analysed with molecular markers but muscle pioneer cell presence was judged by their characteristic early striation. In addition to the muscle pioneer defects, most of the *you*-type mutants also had varying degrees of defects in adaxial cell development. *In situ* hybridisation with the adaxial cell marker *myoD* revealed that *myoD* expression is most reduced in *yot*, the mutant with the strongest phenotype. The reduction in *myoD* expression was also detected, although to a lesser degree, in *syu, con* and *you* mutants, whereas *ubo* had normal *myoD* staining. As *choker* appeared to have normal muscle pioneers it was also assumed that adaxial cell development would be unaffected and thus *myoD* expression was not investigated in this mutant.

The *you*-type mutants were found to have a host of other developmental defects including aberrant primary motor neuron patterning and defective motility in response to touch. Furthermore, most *you*-type mutants, with the exception of *ubo* and *cho* had defective circulation resulting from the delayed or aberrant formation of the dorsal aorta. However, the *choker* mutant had none of these defects and this, along with the fact that it was the only *you*-type mutant to have a pigment phenotype, set it apart from the other mutants in its class.

According to these observations it was assumed that most of the *you*-type genes, including *yot, syu, you* and *con,* have roles in adaxial cell development. *ubo* was suggested to have a role in muscle pioneer development and, as *choker* appeared to have normal muscle pioneers, it was placed downstream of the other *you*-type genes and assumed to act on horizontal myoseptum development (van Eeden et al., 1996).

Figure 1.1. *choker* mutants have a melanophore defect, and a muscle extension defect at 5 dpf

(A, B) Live microscopy of 5 dpf *choker* mutants and wild-type siblings (Kelsh *et al,* 1996). Lateral views revealed that wild-type melanophores are arranged in 4 longitudinal stripes (A). By comparison, the mutants have a band of ectopic melanophores located over somites 1-5 (B). Spatially correlated with the pigment defect the mutants also have a hindbrain indentation. (C-F) Transverse sections of 5 dpf *choker* mutants and wild-type siblings (RN Kelsh, unpublished data). The wild-type muscle extends beyond the neural tube at all axial levels (C, E). Although the extension of posterior muscle blocks is normal in the mutant (F), the anteriormost myotomes fail to extend fully dorsally, thus accounting for the apparent hindbrain indentation (D).

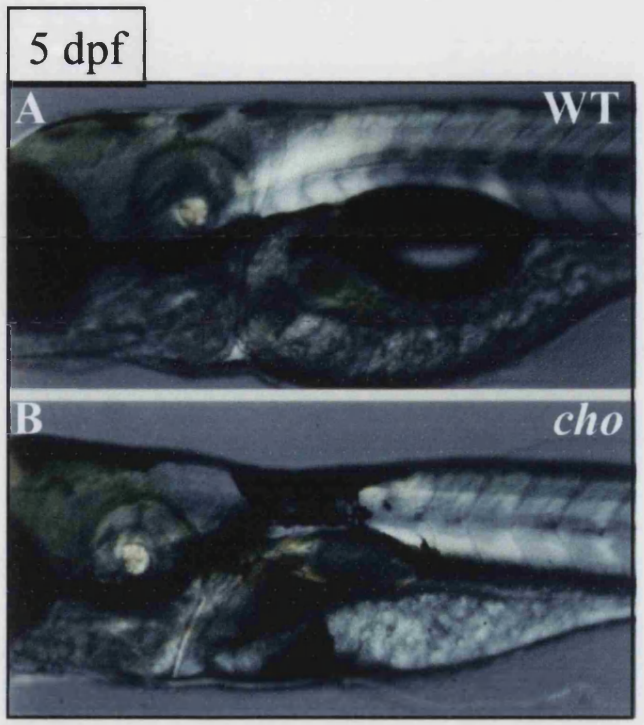
5 dpf
A
WT
B
cho

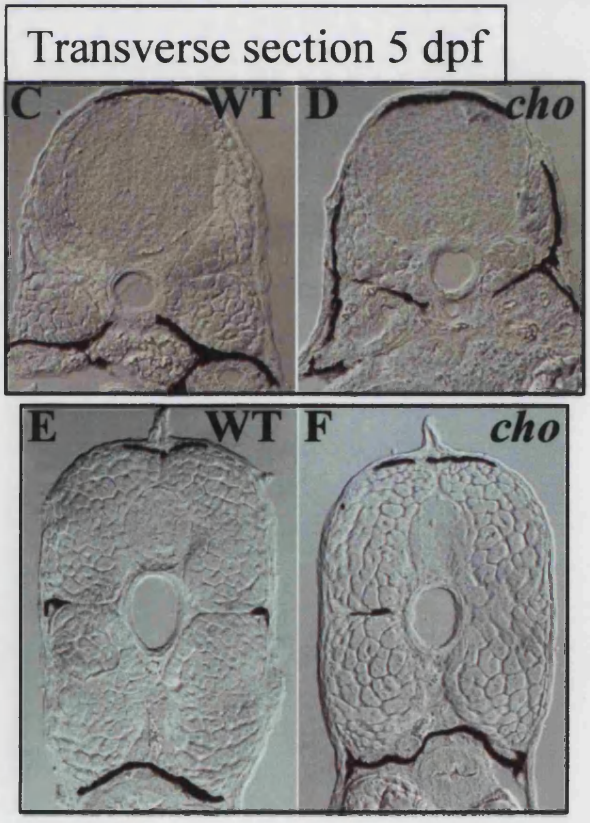
Transverse section 5 dpf
C
WT
D
cho
E
WT
F
cho

However, as it had not been analysed with molecular markers its position remained unclear.

The *choker* muscle development defect was further analysed in studies done by Kelsh R, and Hollway and Currie (personal communication) and was found to be extensive. Transverse sections of 5 dpf *choker* mutants and their wild-type siblings revealed that the hindbrain indentation was a result of defective dorsal extension of the anteriormost 4-5 somites (RN Kelsh, unpublished data; Figure 1.1C, D). This defect was restricted to the foremost five somites as more posterior somites appeared normal in transverse view (Figure 1.1E, F). Furthermore, antibody staining at 24 hpf with the slow muscle marker F59 revealed a severe disorganisation of slow muscle fibres in the anteriormost 5 somites (RN Kelsh, unpublished data; Figure 1.2A, B). By comparison, the more posterior somites had only a low level of muscle fibre disorganisation (Figure 1.2C, D). Adaxial cell labelling at 24 hpf with the molecular marker Engrailed revealed that the foremost 5 somites in *choker* mutants had aberrant adaxial cell migration. Instead of migrating laterally and forming a monolayer on the surface of the somite as they do in the wild types, *choker* adaxial cells remained close to the notochord (RN Kelsh, unpublished data; Figure 1.2E, F). Subsequent studies done by Hollway and Currie confirmed the slow muscle and adaxial cell defects and found that the muscle defect in *choker* also extended to fast muscle fibres. There was a strong reduction of fast muscle fibres when compared to wild-type embryos at 24 hpf (G Hollway, unpublished data; red, Figure 1.3A, B). Furthermore, staining with the pectoral fin precursor marker *mox* revealed that this population of cells was also severely reduced in the mutant (G Hollway, unpublished data; Figure 1.3C, D). This phenotype was reported to be rather variable between different individuals, however could be quite striking and sometimes resulted in a loss of 90% of the pectoral fin muscle fibres (Figure 1.3G, H).

Thus it is clear that *choker* mutants have defects in all anterior trunk muscle derivatives, including pectoral fin muscle. These observations distinguish *choker* from other *you*-type mutants, which have unimpaired fast muscle development and defects restricted to slow muscle and muscle pioneer patterning only. All of the *you*-type genes cloned to date have been found to be members of the hedgehog-signalling pathway (Karlstrom et al., 1999; Roy et al., 2001; Schauerte et al., 1998), which is known to have a role in both slow muscle and muscle pioneer development. *choker* defects however appear to reflect a more generalised disruption of all myotomal fates, including

Figure 1.2. *choker* mutants have slow muscle development defects restricted to the anteriormost somites

(A-D) Antibody staining of wild types and *choker* mutants with the slow muscle marker F59 (RN Kelsh, unpublished data). Lateral views revealed that wild-type embryos have a high number of slow muscle fibres in each somite (A, C). The *choker* slow muscle fibres were however highly disorganised, particularly in the anteriormost five somites (B, D). (E, F) Antibody staining of wild types and *choker* mutants with the adaxial cell marker *engrailed* (RN Kelsh, unpublished data). Transverse sections revealed that the wild-type adaxial cells migrated to form a monolayer of cells on the outer surface of the myotome (arrows, E). The mutant adaxial cells however failed to migrate and remained associated with the notochord (arrows, F).

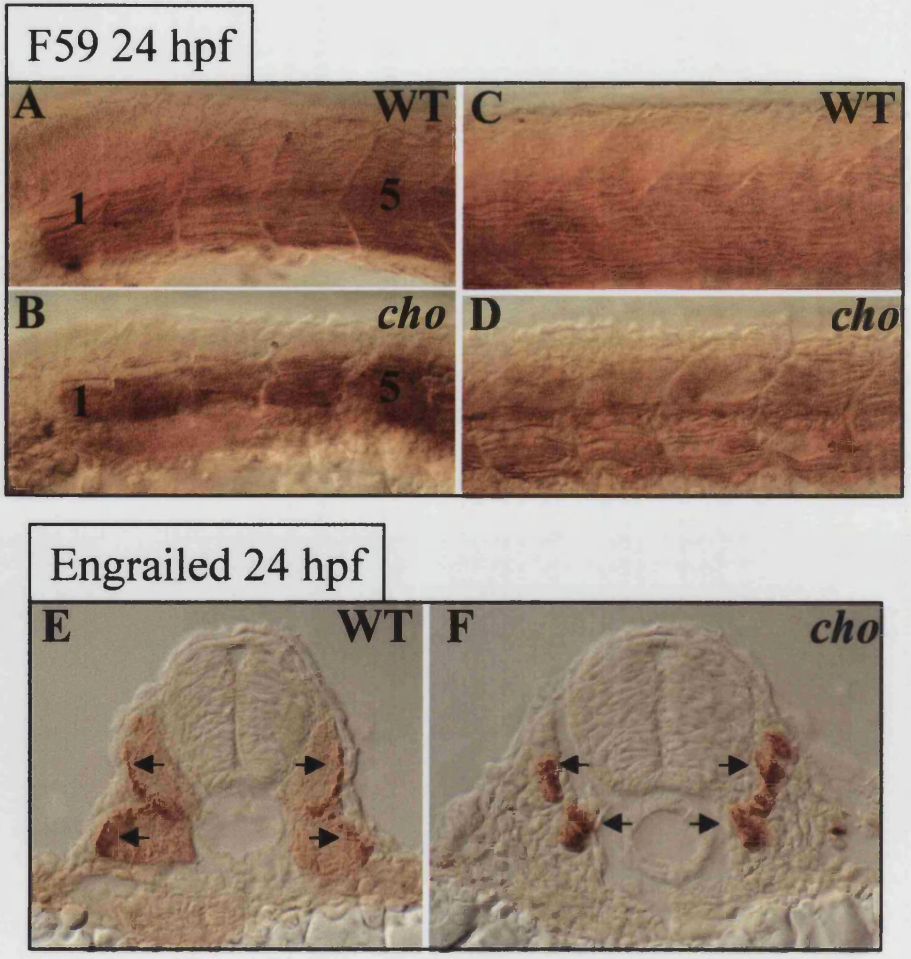
F59 24 hpf
A
WT
1
5
C
WT
B
cho
1
5
D
cho
Engrailed 24 hpf
E
WT
F
cho

Figure 1.3. *choker* mutants have defects in fast muscle and pectoral fin muscle development

(A, B) Transverse views of *choker* mutants and wild-type siblings labelled with a fast-muscle marker (red) (G Hollway and P Currie, unpublished data). The majority of the wild-type myotome is made up of fast muscle fibres (red, A). There was however a strong reduction of fast muscle fibres in *choker* mutants (red, B). (C-F) Labelling with various pectoral fin muscle markers revealed that this population is defective in *choker* mutants (G Hollway and P Currie, unpublished data). Dorsal views of wild types stained with the pectoral fin muscle precursor marker *mox* revealed a number of migrating cells (arrows, C). These were reduced in the mutant (arrows, D). This resulted in a reduction of pectoral fin muscle fibres, which was sometimes as extensive as 90% (F).

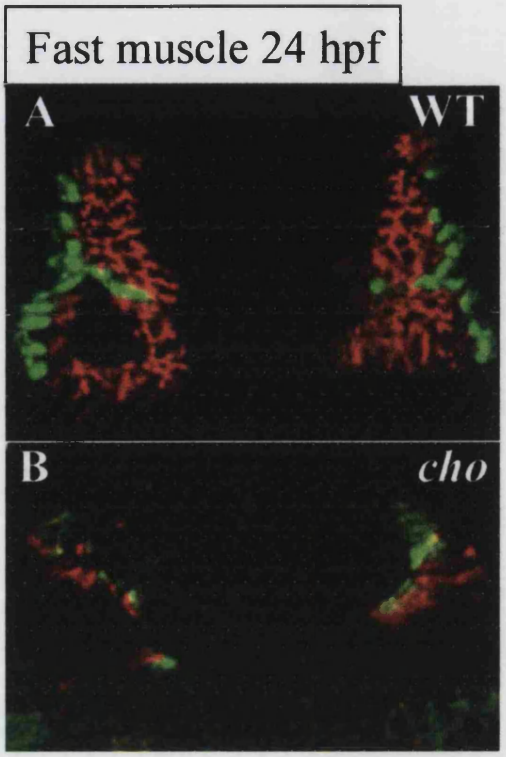
Fast muscle 24 hpf
A
WT
B
cho

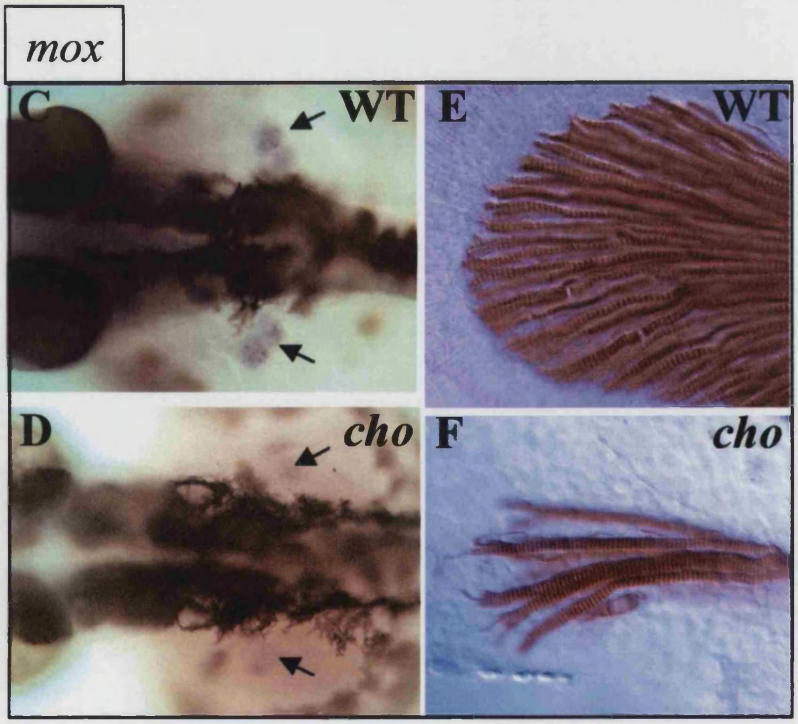
mox
C
WT
E
WT
D
cho
F
cho

those of the pectoral fin and consequently it was suggested that *choker* may not be a true *you*-type mutant. In addition to the muscle development and pigmentation defects *choker* was also found to have abnormal posterior lateral line nerve (PLLn) patterning (Figure 1.4). Antibody staining with the axon marker acetylated tubulin revealed that the nerve follows an abnormal trajectory in *choker* mutants. This patterning defect was presumed to occur as a consequence of the absence of horizontal myoseptum-derived cues.

The muscle aspect of the *choker* phenotype was studied prior to, and in parallel with our investigation. Our studies have focused on the relatively uncharacterised pigment phenotype. The *choker* mutant promised to be a good tool for finding out more about the process of neural crest patterning in zebrafish embryos. There were thus a number of questions we wanted to ask:

1. How extensive is the neural crest defect in *choker* - does it affect other neural crest derivatives?
2. How does the melanophore phenotype develop over time?
3. What are the cellular and molecular bases of the melanophore phenotype?
4. Are the muscle and melanophore phenotype causally related?

The intriguing correlation between the pigment and muscle defects in the anterior trunk raised the possibility that aberrant muscle development may result in the anomalous melanophore patterning. The characterisation of the pigment defect and the study of the relationship between the muscle and the pigment defects may provide us with a better understanding of how neural crest cells are patterned in wild type embryos. We employed a variety of molecular markers to determine whether any other neural crest derivative was affected in *choker* mutants and found that xanthophore patterning was also defective. We used epistasis experiments to try and understand the relationship between the two pigment defects and transplantation studies in a preliminary attempt to determine whether the melanophore defect in *choker* is cell autonomous. We also used timelapse microscopy to monitor melanophore behaviour in the mutant collar. Finally, on the basis of these studies we present a model to explain why *choker* melanophore patterning is aberrant.

In addition, as very few of the molecules that play a role in the pathfinding of zebrafish neural crest cells have been identified, we decided to characterise the function of a potential candidate neural crest guidance molecule, *neuropilin-1* (*nrp-1*). We were trying to answer the following questions:

Figure 1.4 *choker* mutants have defective patterning of the posterior lateral line nerve

(A, B) Lateral views of 48 hpf *choker* mutants and wild-type siblings stained with the acetylated tubulin marker (RN Kelsh, unpublished data). The posterior lateral line nerve in wild-type embryos extends along the horizontal myoseptum (arrowheads, A). This nerve was found to project aberrantly in *choker* mutants (arrowheads, B).

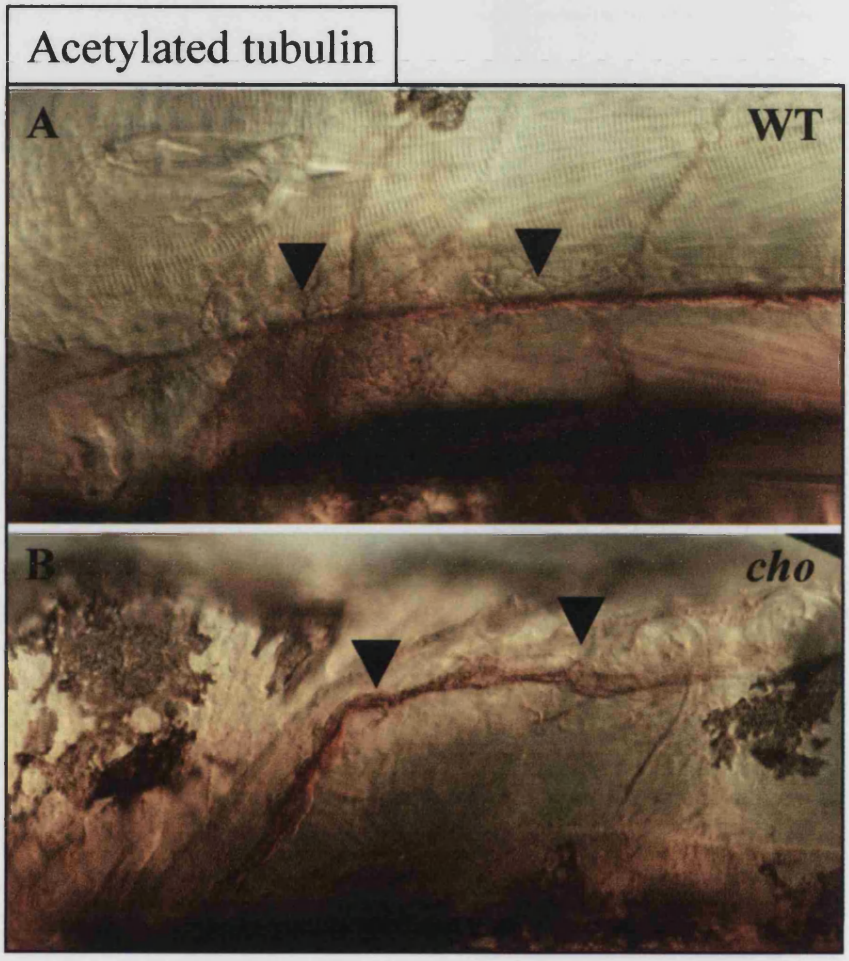
Acetylated tubulin
A
WT
B
cho

1. What is the expression pattern of *nrp-1*?
2. Does *nrp-1* have a role in neural crest patterning in zebrafish?
3. If so, then at what stages and how does *nrp-1* influence neural crest patterning?

We used morpholino injections to analyse the defects resulting from the absence of *nrp-1* protein. On the basis of this, we present a hypothesis as to the role of *nrp-1* in neural crest migration.

We hoped that these two studies combined might help enhance our understanding of how zebrafish neural crest migration and patterning is regulated.

Chapter 2

Materials and methods

Fish Husbandry

Fish were kept at the zebrafish facility at the University of Bath. Embryos were obtained by setting up natural crosses, staged according to Kimmel (Kimmel et al., 1995) and placed in Embryo Medium (5mM NaCl, 0.17mM KCl, 0.33mM $CaCl_2$, 0.33mM $MgSO_4$, 10^{-5} methylene blue). Fish were typically reared at 28.5°C but when necessary their development was slowed down by placing them at 21°C, or sped up by leaving them at 32°C. For PTU treatment embryos were placed into embryo medium containing 0.003% 1-phenyl-2-thiourea (PTU) immediately after egg collection. They were then reared as normal and fixed at the required timepoint. Fish to be sorted or mounted live were first anaesthetised in 0.2% solution of Tricaine (Sigma).

The tm26 allele of *choker* (Kelsh et al., 1996; van Eeden et al., 1996), the tq211 allele of *pfeffer* (Kelsh et al., 1996; Odenthal et al., 1996) and the w2 allele of *nacre* (Lister et al., 1999) were used. Double mutants were created by crossing *choker* and *pfeffer* identified carriers for the *choker;pfeffer* double mutant, and a *choker* identified carrier with a *nacre* homozygote for the *choker;nacre* double mutant. Offspring were reared to adulthood and carriers of both alleles were identified in the expected Mendelian ratios.

Whole mount *in situ* hybridisation

Probe synthesis

10μg of plasmid was linearised with a suitable restriction enzyme that cut at the 3' end of the probe sequence. The DNA was purified through a phenol:chloroform extraction followed by ethanol precipitation and then resuspended in 20μl of MiliQ water.

All probes used were DIG-labelled and thus synthesised using the Boehringer-Mannheim DIG RNA Labelling Kit protocol. 1μg of linearised DNA was typically used and combined with 2μl of 10X NTP labelling mixture containing DIG-labelled UTP (10mM ATP, CTP, GTP, 6.5mM UTP, 3.5mM DIG-11-UTP), 2μl 10X transcription buffer, 1μl RNase inhibitor (20 units/μl), 2μl of an appropriate polymerase (20 units//μl) that will produce an antisense strand (either T3, T7 or SP6) and finally, MiliQ water to a final volume of 20μl. The reaction was left for two hours at 37°C and then the DNA template was removed through a 15 minute incubation at 37°C with 2μl of RNase-free DNaseI (10 units/μl). The reaction was stopped by adding 2μl of 0.2M EDTA, followed by an RNA extraction with 4M LiCl and 100% cold ethanol. The purified RNA was resuspended in 100μl RNase-free water and stored at -70°C.

In situ *hybridisation*

All embryos were dechorionated prior to fixation with a pair of Watchmaker's forceps, fixed overnight at 4°C, in 4% paraformaldehyde in PBS (PFA/PBS), and then dehydrated by washing three times for 5 minutes and once for 10 minutes in 100% methanol. They were left at –20°C for at least an hour and then rehydrated in a series of Methanol/PBS, followed by PBT washes (0.1% Tween20 in PBS). Embryos older than 10 hpf were digested in a 10μg/ml solution of proteinase K in PBT. 10-15 hpf embryos were digested for 5minutes, 15-20 hpf for 10 minutes, 20-25 hpf for 15 minutes, 25-30 hpf for 20 minutes, 30-35 hpf for 30 minutes, 35-40 hpf for 35 minutes, 40-45 hpf for 40 minutes, 45-50 hpf for 40 minutes, 50-55 hpf for 45 minutes, 55-60 hpf for 50 minutes, 60-65 hpf for 55 minutes, and 65-70 hpf or older for one hour. The embryos were then refixed for 20 minutes in 4% PFA/PBS. After a series of 5 minute PBT washes, the embryos were prehybridized at 65°C in hybridization mix (50 ml of hybridization mix contains 25 ml formamide, 12.5 ml 20xSSC, 0.5 ml 5mg/ml heparine, 0.5 ml 50mg/ml yeast RNA, 0.25 ml 20% Tween20, 0.46 ml 1M citric acid and 10.7 ml sterile water) for 3-5 hours. Following prehybridization, embryos were hybridized overnight at 65°C in a 1:200 probe:hybridization mix dilution.

On the following day, the embryos were washed once in hybridization mix (HM), and then in 10 minute 75% HM/25% 2xSSC, 50% HM/50% 2xSSC, 25% HM/75% 2xSSC and 2xSSC washes, all at 65°C. Two 30 minute 0.2xSSC washes were then carried out at 65°C, followed by 5 minute room temperature washes with 75%

0.2xSSC/25% PBT, 50% 0.2xSSC/50% PBT, 25% 0.2xSSC/75% PBT and PBT. The embryos were blocked in a solution of PBT/2% sheep serum/2 mg/ml BSA. After blocking for several hours, the embryos were incubated overnight at 4°C in a 1:5000 dilution of anti-DIG alkaline phosphatase conjugated antiserum in blocking solution. The embryos were rotated on a shaker throughout the pre-blocking and antibody incubation steps.

On the following day, one fast and six 15-minute PBT washes were performed, followed by three 5 minute washes with NBT/BCIP buffer (100mM TrisHcl, pH 9.5, 50 mM $MgCl_2$, 100mM NaCl, 0.1% Tween20). Finally, the embryos were incubated in blue staining solution (one NBT/BCIP tablet from Boehringer/Roche in 10ml MiliQ water), in the dark for a period of up to 24 hours. The reaction was stopped by washing once in PBT, followed by PBS. The embryos were cleared by rotating in 50% glycerol in PBS for 30 minutes and then stored in PBS at 4°C. Zebrafish probes for the following genes were used: *GTP-cyclohydrolase I* (*gch* (Parichy et al., 2000)), *nacre/microphtalmia related transcription factor* (*nac/mitfa,* (Lister et al., 1999)), *dopachrome tautomerase* (*dct,* (Kelsh et al., 2000b)), *engrailed1* (*eng1* (Ekker et al., 1992); kind gift of England S), *EphA4, ephrinB2a* ((Durbin et al., 1998); kind gift of Reagan J), *ephrinB1, ephrinB2b* ((Chan et al., 2001); kind gift of Chan J), *neuropilin-1* (*nrp1,* (Lee et al., 2002); kind gift of Shoji W), *robo1* and *robo 3b* ((Challa et al., 2001); kind gift of Challa A) and *sema Z1a* ((Yee et al., 1999); kind gift of Shoji W).

Antibody staining

All embryos were dechorionated prior to fixation with a pair of Watchmaker's forceps and fixed in 4% paraformaldehyde in PBS (PFA/PBS) for either 2 hours at room temperature, or for a maximum of 2 days at 4°C. The embryos were then washed 3 times for 5 minutes in PBT (0.5% Triton X-100 in PBS) with gentle agitation on a rotating shaker. Three one hour long MiliQ washes were then carried out using a rotating shaker, followed by a 2-3 hour long pre-incubation step in PBT/1% DMSO/5% horse serum. The embryos were then rotated overnight at room temperature in a 1:700 dilution of primary antibody (anti-Hu mAb, University of Oregon) in blocking solution.

The following morning, one fast, and three 1 hour long washes in PBT were carried out, and the embryos were then gently agitated on a rotating shaker overnight, at

room temperature, in a 1:800 dilution of secondary antibody (Alexa Fluor 546 goat anti-mouse, Molecular Probes) in blocking solution. One fast and three 30-minute long PBT washes were performed on the following day, and followed by a clearing step in 50% glycerol in PBS. Embryos were stored in PBS or 50% glycerol/PBS at 4°C.

Alcian Blue Staining

The embryos were dechorionated with a pair of Watchmaker's forceps and fixed overnight, at room temperature in 4% paraformaldehyde in PBS (PFA/PBS). The following morning, they were washed once in a solution of acid-alcohol (1.85% HCl/70% ethanol) and then incubated overnight at room temperature in a 0.1% solution of Alcian green in acid-alcohol.

The following day, the embryos were destained in a series of 5 to 10 acid-alcohol washes then rehydrated by washing for 10 minutes in 25% PBS/75% acid alcohol, 50% PBS/50% acid-alcohol, 75% PBS/25% acid-alcohol and PBS. Embryos were bleached for 5 to 10 minutes in a solution of 1% KOH and 3% H_2O_2, cleared in 0.25% KOH/50% glycerol in PBS, and then stored in the same solution at 4°C.

TUNEL

Embryos were fixed for 1-2 hours in 4% paraformaldehyde in PBS (PFA/PBS), and then dehydrated by 5 minute washes in 50% methanol/50% TBST (a solution of 10x TBST contains 10x TBS, 2% Triton X-100 and 5% Tween20; a 10x TBS stock contains 1M Tris, 1.5M NaCl and is pH'd to 7.5 with HCl), 75% methanol/25% TBST, 85% methanol/15% TBST, 95% methanol/5% TBST and 100% methanol. The embryos were bleached for one hour at room temperature in a 5:1 solution of methanol: H_2O_2 and then washed twice for 10 minutes in 100% methanol. Rehydration was then performed by doing 5 minute washes in 95% methanol/5% TBST, 85% methanol/15% TBST, 75% methanol/25% TBST, 50% methanol/50% TBST followed by two 5 minute washes in 100% TBST. All embryos older than 24 hpf were then incubated for 30 minutes in a 1μg/ml solution of proteinase K in TBST. Embryos younger than 24 hpf were also digested, however, for 15 minutes only. Two 5 minute washes in 2mg/ml glycine in

TBST were then performed, followed by an optional refixation step in TBST for 5 minutes, then 4% PFA/PBS for 20 minutes. The embryos were then washed 3 times for 10 minutes in TBST, and then two times in Terminal Transferase buffer (a 5x TTase buffer stock contains 12.5ml of 1M tris, 6g of Na Cacodylate, 125g of BSA and 1ml Tween20. To make a 1x stock, the 5x solution was diluted in sterile water and 1x of a 100x stock of $CoCl_2$ was added). Pre-incubation with 0.5µl TTase enzyme and 0.25µl DIG-labelled dUTP in 100µl TTase buffer was carried out for one hour on ice, protected from light. 100µl of the above solution sufficed for one tube of 25-50 embryos. The embryos were then incubated for one hour at 37°C, protected from light and then washed 3 times for 10 minutes in TBST. Blocking in blocking solution (10% goat or horse serum, 2% BSA, 0.1% sodium azide in TBST) was performed for at least 3 hours or overnight. Following blocking, the embryos were incubated for 2-3 hours in a 1:4000 dilution of anti-Flu alkaline phosphatase conjugated antibody in blocking solution, and then washed in TBST for 2-3 hours or TBS overnight. Three 15 minute washes in Fast Red buffer (0.1M Tris, pH 8.0, filtered) were then carried out and then the embryos were incubated in staining solution (one tablet of Fast Red from Roche in 2ml of filtered Fast Red buffer) in the dark for a period of up to a few hours. The reaction was stopped by performing three 15 minute washes in TBST and the embryos were cleared in a graded series of methanol to 100% followed by a 1:1 solution of Glycerol/TBS.

Microscopy and Photography

All embryos were cleared in a solution of 50% Glycerol in PBS for at least 30 minutes before viewing. They were then mounted either on cold (4°C) methylcellulose or in 100% glycerol and examined using the Nikon Eclipse E800. Photographs were taken both with a Nikon FDX-35 camera, and a digital spot camera. When necessary, the yolk was dissected away with a pair of dissecting scissors and a scalpel.

Timelapse Microscopy

Embryos were dechorionated using a pair of watchmakers forceps and anaesthetised in a solution of 0.2% Tricaine in Embryo Medium. They were then immobilised in 0.5% agarose/0.2% Tricaine in Embryo Medium on a circular glass coverslip, which was placed into a ring-shaped metal chamber. The chamber was filled with Embryo Medium to prevent embryo desiccation, and a small amount of Fluorocarbon (Sigma). Oxygen was bubbled through the fluorocarbon solution for several minutes prior to addition to the chamber, in order to ensure sufficient oxygen supply to the immobilised embryo. The system was sealed with another circular glass coverslip and observed under an Eclipse E1000 (Nikon) microscope, using a 20X dry objective lens. The microscope stage was surrounded by a heated chamber, which was maintained at approximately 30°C throughout the experiment. Images were collected with a Hamamatsu C4880 CCD camera, and processed using the Metamorph software program. Images were taken of ten different focal planes between the skin and notochord of the embryo and were collected every ten minutes.

Embryos were successfully immobilised and kept under anaesthetic for a period of more than two days, although restriction of embryo growth by surrounding agarose resulted in distortion after a certain timepoint, thus timelapses were rarely useful beyond approximately 30 hours. Embryo development appeared normal, although somewhat slowed throughout this period, despite incubation under a higher temperature than normally used for rearing embryos. Timelapses were started at either 24 or 48 hours post fertilisation with wild-type and *choker* sibling embryos mounted together and timelapsed in parallel to ensure comparability.

General molecular biology techniques

Agarose Gel Electrophoresis

1% gels were typically made by heating 1 g of agarose (Sigma) and 100ml of 1x TAE in the microwave for approximately 90 seconds until all the agarose has melted. Ethidium Bromide was added to a final concentration of 0.5μg/ml and then the gel was poured and left to cool. Gels were usually run at 100V for approximately 60-90 minutes, analysed under an ultraviolet light source (UVP), and photographed using a black and white video camera (UVP) and a video graphic thermal printer (Sony).

Restriction Digestion

0.5-1μg of plasmid DNA was typically digested with 1μl of the enzyme of choice enzyme (NEB), 2μl of a 10x buffer compatible with the enzyme used (NEB) and water up to the final volume of 20μl. The reaction was incubated for 90 minutes typically at 37°C although some enzymes, such as SmaI, had to be incubated at the lower temperature of 25°C. The products of the reaction were analysed by running on a 1% agarose gel.

Transformation of plasmid DNA into competent cells

Most transformations were carried out with chemically competent DH5α cells made competent by the $CaCl_2$ method and provided by Dr. Kim Jones and Jo Allsop. 1μl of DNA was mixed with 50μl of competent cells and left on ice for 30 minutes. The cells were heatshocked at 42°C for 90 seconds and then placed back on ice for 2 minutes. 1ml of LB medium prewarmed to 37°C was then added, followed by an hour-long shaking incubation at 37°C. Finally, 100μl of cells were plated on LB agar plates containing 50μg/ml ampicillin and left at 37°C overnight.

Commercially available XL 10-Gold Ultracompetent cells (Stratagene) were occasionally used. Prior to the transformation, 2μl of XL 10-Gold β-mercaptoethanol was added to 45μl of cells, followed by a 10-minute incubation on ice during which the cells were periodically swirled gently. The cells were transformed in the same manner as described above but they were heatshocked for 30 seconds only and the LB medium added to them after the heatshock was prewarmed to 42°C.

DNA purification

DNA extraction was carried out by adding an equal volume of phenol:chloroform (Sigma) to the DNA solution, vortexing briefly and then spinning in a microcentrifuge for 2 minutes at 14,000rpm. The upper layer was then removed to a fresh tube and the DNA precipitated by adding 2 volumes of ethanol and 1/10 the volume of 3M Sodium Acetate and leaving at room temperature for 10 minutes. The DNA was then spun for 10 minutes at 14,000rpm, washed with 70% ethanol, re-spun and air-dried. Finally the DNA was resuspended in an adequate amount of MiliQ water.

Plasmid preparation

Large scale plasmid purification was carried out using the Concert High Purity Plasmid Purification Systems kit (GibcoBRL). For a maxi-prep protocol the cells were grown in a 100ml overnight culture and harvested the next morning by spinning them down for 10 minutes at 6,000rpm in an Avanti J-25 centrifuge (Beckman Coulter). They were re-suspended in 10ml of E1 buffer containing RNase A and lysed for 5 minutes with 10ml of E2 buffer, followed by neutralisation in 10ml of E3. The cell debris was pelleted out by spinning the cells at 15,000g for 10 minutes. The supernatant was poured into the column provided, after equilibration with 30ml of E4 buffer, and left to drain by gravity flow. The column was washed with 2 X 30ml E5 washes and the flow-through discarded. Following the washes, the DNA was eluted with 15ml of E6 and precipitated by spinning at 15,000g at 4°C for 30 minutes. The pellet was washed with 70% ethanol and spun again for 5 minutes, following which the DNA was air-dried. The resulting pellet was usually resuspended in 300µl of TE buffer but, depending on the size of the pellet, the re-suspension volume used could be less. The DNA was stored at –20°C.

Cell transplantation

Cells were transplanted from wild type embryos of the AB strain into *choker* mutants.

The day before the transplantation at least five pairs of identified carriers for the *choker* allele were set up in mating boxes. Similarly, at least five wild-type pairs of the AB strain were set up concomitantly and the following morning all the eggs were harvested. The host embryos were cleaned, staged, and left to develop in Embryo Medium at 28.5°C until the afternoon.

At least 40 donor eggs were injected with 5% Rhodamine/5% Biotin dye at the one to two cell stage, using a SMZ1500 dissecting microscope (Nikon) and the PV 820 pneumatic pico pump injector (World Precision Instruments). Injection needles were made from borosilicate glass capillaries of the following dimensions: 1.2mm outer diameter x 0.94mm inner diameter (Harvard Apparatus Ltd). The needles were pulled on a model P-97 Flaming/Brown micropipette puller (Sutter Instruments Co.) using the

following parameters: Heat - 270, Pull - 35, Velocity - 150, Time - 50. After pulling, a razor blade was used to break the needle tip. The needles were of the following shape:

The injected eggs were placed in a Petri dish containing Embryo Medium and left to develop at 21°C. The donor embryo development was thus sufficiently slowed so that when the hosts were at the 6h shield stage the donors were approximately at the 3-4 hour stage.

During cell transplantation, cells were taken out of 3-4 hour old donors and placed into the neural crest fate map region of 6h old hosts. The transplant needles were made by pulling some 1.0mm outer diameter x 0.78mm inner diameter borosilicate glass capillaries on the micropipette puller. The tip was broken using a razor blade and then polished and pulled them into a fine point on the Beaudoin Microforge No. 620. The needle opening typically varied between 30 and 50 microns. The needles were of the following shape:

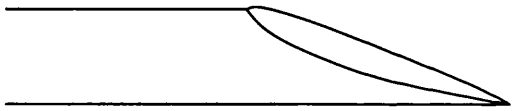

Immediately prior to the transplantation both the host and donor eggs were dechorionated and the embryos hereafter kept in an agarose coated Petri dish (1.2% agarose in Embryo Medium). One donor and four hosts were typically immobilised on a microscope slide using a coating of 4% methylcellulose which was then covered by a drop of Embryo Medium. The cell transplantation was carried out on the Eclipse inverted microscope (Nikon) using a motorised joystick (Narishige).

Following cell transplantation, microscope slides containing the immobilised embryos were immersed in Penn/Strep Embryo Medium in a Petri dish coated with agarose + Penn/Strep (25,000U/litre). The embryos were then left to develop at 28.5°C, as normal. At 1 dpf the embryos were placed into Penn/Strep Embryo Medium + 0.0015% PTU to partially inhibit melanization and prevent melanin obstruction of faintly labelled cells.

The embryos were examined at the 2 dpf stage under a green filter on the Nikon Eclipse E800 microscope and a 40X wet objective lens. The whole axis of the embryos was analysed from both lateral and dorsal views and all labelled derivatives were recorded.

Morpholino injections

The *neuropilin1* morpholino and the control 4-base mismatch morpholino were designed with the help of the Genetool website (http://www.gene-tools.com). The sequences used were:

Neuropilin1: 5'-GAATCCTGGAGTTCGGAGTGCGGAA-3'
Neuropilin1 mismatch: 5'-GAATCgTGGAcTTCGGAGTcCGcAA-3'

The morpholinos were diluted in 1x Danieau's (58mM NaCl, 0.7mM KCL, 0.4mM $MgSO_4$, 0.6mM $Ca(NO_3)_2$, 5.0mM HEPES, pH 7.6) to a stock concentration of 1mM. On the day of injection, they were diluted further in 1 x Danieau's to a concentration of 0.1mM. Some Phenol Red (typically one quarter of the volume) was also added to the solution to aid viewing of injected liquid. The morpholino injection was carried out on the SMZ1500 dissecting microscope (Nikon) using the PV 820 pneumatic pico pump injector (World Precision Instruments). The injecting needles were made from borosilicate glass capillaries of the following dimensions: 1.2mm outer diameter x 0.94mm inner diameter (Harvard Apparatus Ltd). The needles were pulled on a model P-97 Flaming/Brown micropipette puller (Sutter Instruments Co.) using the following parameters: Heat - 270, Pull - 35, Velocity - 150, Time - 50. The needles were of the following shape:

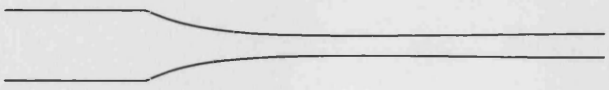

A range of morpholino volumes (2.5nl – 10nl) was injected to find the optimal concentration where the morpholino-specific defects were significant while keeping the rate of non-specific deformities low. Following injection, the embryos were grown as normal at 28.5°C.

Microangiography

The protocol was carried out according to (Lee et al., 2002).

The injection was carried out using the same microscope, injector and needles as specified for the morpholino injections.

Embryos were typically injected at 48-52 hpf and were anaesthetised with 0.2% Tricaine prior to injection. The embryos were immobilised with the aid of a holding glass pasteur pipette which was flamed to narrow the opening to approximately yolk sac size. Approximately 10μl of 2mg/ml FITC-dextran (Mw=2,000,000, Sigma) in 1x Danieau's was injected into the sinus venosus of each embryo. Following injection, embryos were immediately screened for vascular defects under the blue filter of a Leica MZFLIII fluorescent dissecting microscope.

Chapter 3

Preliminary characterisation of the *choker* mutant

Introduction

The *choker*^{tm26} mutant allele was identified in the 1996 Tübingen mutagenesis screen by the pigmentation and somitogenesis defects of homozygotes (Kelsh et al., 1996; van Eeden et al., 1996; RN Kelsh, unpublished). Subsequent studies done by Hollway and Currie (personal communication) have investigated the *choker* muscle phenotype but the pigment defect remained largely uncharacterised. A number of questions were left open as to when the ectopic pigment collar is first detectable, how the collar is built up over time and whether the patterning of other neural crest derivatives that originate from this trunk region is affected? In addition, the spatial correlation between the pigment collar and the muscle defect raised the possibility that the two were causally related. It was necessary to find out more about the spatio-temporal aspects of the pigment phenotype in order to begin to address some of these questions.

As discussed previously (see chapter 1), neural crest patterning is a multi-step process influenced by both environmental and cell-autonomous factors. Neural crest cells first segregate away from the neural tube in a rostro-caudal progression. They then interpret various guidance cues and migrate, either on the medial or the lateral migratory pathways. Some derivatives, like melanoblasts, are able to migrate on both. Finally, after the cells have reached the appropriate destinations, their migration must be arrested, and the migratory pathways must be shut down in order to prevent further cell movement. One or more of these processes may be affected in *choker*. For instance, *choker* melanophores may begin to migrate normally, but be unable to leave the lateral pathway environment and over time give rise to the ectopic collar. Alternatively, collar formation may be initiated at later stages, once lateral pathway migration had been completed, due to the lack of an inhibitory factor preventing further melanophore emigration. In addition, there may be an excess of melanophores emigrating from the neural tube or an excess of proliferation during migration, thus accounting for the supernumerary collar pigment cells. The defect may not necessarily be lateral pathway-

specific. It is conceivable that the medially migrating melanophores may aberrantly invade and accumulate in the lateral pathway environment due to lack of adequate guidance cues. It was necessary to further characterise the timing of onset of the pigment phenotype to investigate some of these possibilities.

In order to find out more about the nature of the *choker* defect it was also necessary to determine whether there were any additional, undiscovered, aspects of the phenotype. It is known that, beside melanophores, neural crest cells from the anterior trunk axial level give rise to a wide range of derivatives. Extensive fate mapping studies in chick have shown that anterior trunk neural crest contributes to craniofacial cartilage, melanocytes, and neurons and glia of the sensory, sympathetic and enteric nervous systems (Le Douarin and Kalcheim, 1999). Fate mapping in zebrafish has not been as extensive. However Schilling et al demonstrated an origin for craniofacial cartilage from neural crest, including that adjacent to somite one (Schilling and Kimmel, 1994). Other studies have shown that trunk neural crest gives rise to pigment cells and neurons and glia of the peripheral nervous system, although none have specifically analysed anterior trunk neural crest (Dutton et al., 2001; Raible and Eisen, 1994). It is thus possible to infer that, analogous to the situation in chick, zebrafish anterior trunk neural crest gives rise to a wide range of derivatives and that these may be affected in *choker.* The defect in *choker* may be broader than suspected, affecting several neural crest derivatives. Conversely, it is conceivable that only a small subset of derivatives is affected. The analysis of the patterning of other NC derivatives will provide useful clues as to the precise extent of the neural crest defect in *choker.*

Finally, although the *choker* muscle phenotype has been characterised by Hollway and Currie, there were some issues we wished to resolve. Firstly, we wanted to see whether we could identify live mutants by their muscle phenotype at early developmental stages and without the aid of muscle-specific markers. *choker* mutants could be separated from their siblings at 24 hpf according to the slow muscle and adaxial cell defects however this could only be done in batches of embryos labelled with the appropriate marker. Secondly, we wanted to look at the muscle pioneer (MP) population and establish whether it was unaffected in *choker* mutants. The muscle pioneers are thought to give rise to the fibrous sheet of ECM that is known as the horizontal myoseptum (HM) (Halpern et al., 1993). Reportedly, *choker* has normal muscle pioneers (van Eeden et al., 1996; Hollway, unpublished observation), however this contradicts the observation that the horizontal myoseptum is reduced or absent in

this mutant (van Eeden et al., 1996). We thus used a MP-specific marker at two different developmental stages to see whether the *choker* muscle pioneer population is present in normal numbers.

We hoped that these analyses might allow us to build a more complete picture of the *choker* muscle defect.

Results

Comparison of melanophore number in the anterior trunk of choker *mutants and wild-type siblings*

We compared the number of melanophores in the anterior trunk lateral pathway of *choker* mutants and wild-type siblings to characterise the timing of *choker* collar development and to get a better understanding of melanophore lateral pathway migration in wild-type embryos.

Melanophores are naturally strongly labelled so it is relatively straightforward to count the cells and characterise their distribution using live microscopy. Melanophores were first counted at 30 hpf, when individual melanised cells are clearly visible. After this timepoint, they were counted at intervals to monitor collar development, until a robust ectopic melanophore band was established at 60 hpf. The ectopic collar forms in the lateral pathway of the anteriormost five somites, thus our counts were restricted to this region. Melanophores were counted on both sides of the embryo, and cells that had more than half their cell body emerging from either the ventral or dorsal stripes were counted as 'collar melanophores'. Subsequently, these counts will be referred to as 'anterior trunk lateral pathway counts'.

Our counts revealed that, despite being initially comparable, after several hours the number of melanophores in the wild-type anterior trunk begun to decrease, whereas the number of *choker* melanophores continued to accumulate. Thus, at the earliest timepoint investigated (30 hpf), the number of melanophores in *choker* and wild-type anterior trunk lateral pathway was equivalent (3.9 ± 0.5 and 4.2 ± 0.4 respectively) (Figure 3.1). By 36 hpf the number of melanophores in the mutant collar begun to increase and there was a comparable decrease in wild-type sibling anterior trunk melanophores. However at this stage the difference was found not to be significant (4.4 ± 0.8 and 3.3 ± 0.4 respectively). By 48 hpf however there was a striking and

Figure 3.1. Melanophore number in the anterior trunk lateral pathway of *choker* mutants continued to increase even after wild-type migration had ceased

Mean number ± SEM of pigmented melanophores migrating on the anterior trunk lateral pathway is given at each of 5 timepoints. At the earliest timepoint tested, wild types had several melanophores in the anterior trunk lateral pathway but these begun to decrease at 36 hpf, and by 48 hpf there were essentially none there. By comparison, the number of melanophores in the collar region of *choker* embryos initially mirrored that of wild types but continued to increase throughout the timepoints tested, so that by 48 hpf there was a statistically significant difference between the number of melanophores in mutant and wild type anterior trunks.

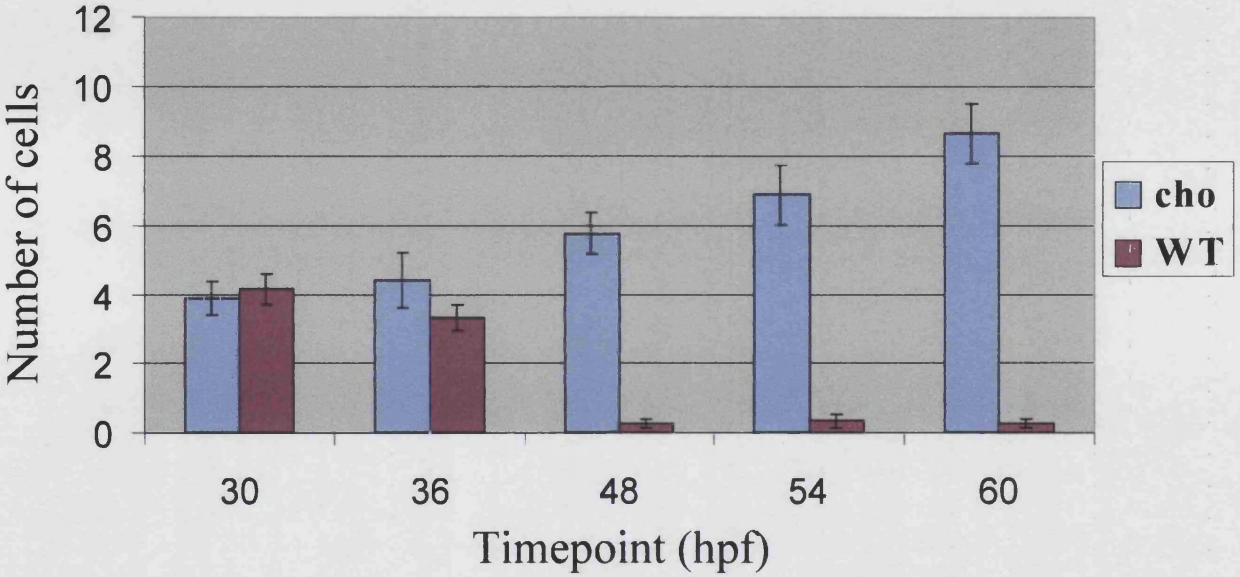
12
10
8
6
4
2
0
Number of cells
30
36
48
54
60
Timepoint (hpf)
cho
WT

statistically significant difference in the mean number of melanophores found in mutant and wild type anterior trunks (5.8 ± 0.6 and 0.3 ± 0.1 respectively). Over the next 12 hours, the number of melanophores in the wild-type anterior trunk remained essentially at 0 whereas the melanophore number in *choker* collars continued to climb until it reached an average of 8.7 ± 0.9 cells at 60 hpf. The cells in the ectopic location were observed to spread out and adopt a stellate shape.

Analysis of neural crest derivatives in choker *mutants*

We used a range of *in situ* and antibody markers to analyse the patterning of several neural crest derivatives thought to originate from the anterior trunk.

Craniofacial cartilage

We used Alcian Blue staining to look at craniofacial cartilage of 5 dpf embryos. At this stage the wild-type jaw structures were well developed and consisted of seven clearly visible pharyngeal arches – the first, mandibular arch, which forms the jaw; the second, hyoid arch, which forms the jaw support structures; and the remaining five arches, which form branchial (gill) structures (Schilling and Kimmel, 1994). Fate mapping studies in zebrafish have shown that neural crest forming adjacent to somite one contributes to the posteriormost four of the seven arches (Schilling and Kimmel, 1994).

Mutants were separated from their wild-type siblings according to the collar pigment phenotype. At 5 dpf we were unable to detect any differences between wild-type and mutant jaws; all of the cartilages were in the correct location and were of appropriate size and shape (Figure 3.2A, B). To exclude the possibility that there was an earlier defect that may have recovered with time we also used Alcian Blue staining to look at 3 dpf embryos. We were unable to detect any differences at this stage either (data not shown) and therefore concluded that craniofacial cartilage was unaffected in *choker* mutants.

Neurons and glia of the peripheral nervous system

The peripheral nervous system of zebrafish embryos consists of the cranial ganglia, sensory neurons in the dorsal root ganglia, the sympathetic neurons, neurons of the enteric nervous system, and associated glial cells. We used the anti-Hu antibody

Figure 3.2. Most neural crest derivatives were unaffected in *choker* mutants

(A, B) Ventral view of Alcian blue stained 5 dpf embryos revealed that craniofacial cartilage is indistinguishable in wild types and *choker* mutants. (C-F) Immunofluorescent detection of Hu-antigen at 3 dpf reveals peripheral neurons. Lateral views of wild types and *choker* mutants showed no differences in the patterning of the cranial ganglia (C, D), dorsal root ganglia posterior to somite 7 (arrows C, D) and enteric neurons (E, F). Dorsal root ganglia in the anteriormost 6 somites however appeared slightly disorganised (discussed below). (G, H) Immunofluorescent detection of Hu-antigen at 5 dpf highlights a chain of sympathetic ganglia dorsal to the swim bladder. Lateral views of wild types and mutants revealed that, perhaps due to the absence of an inflated swim bladder in *choker* embryos, the sympathetics were found in close proximity to the enteric neurons and it was thus impossible to distinguish the two (arrows, H). We were thus unable to determine whether there is a sympathetic neuron phenotype in *choker* mutants.

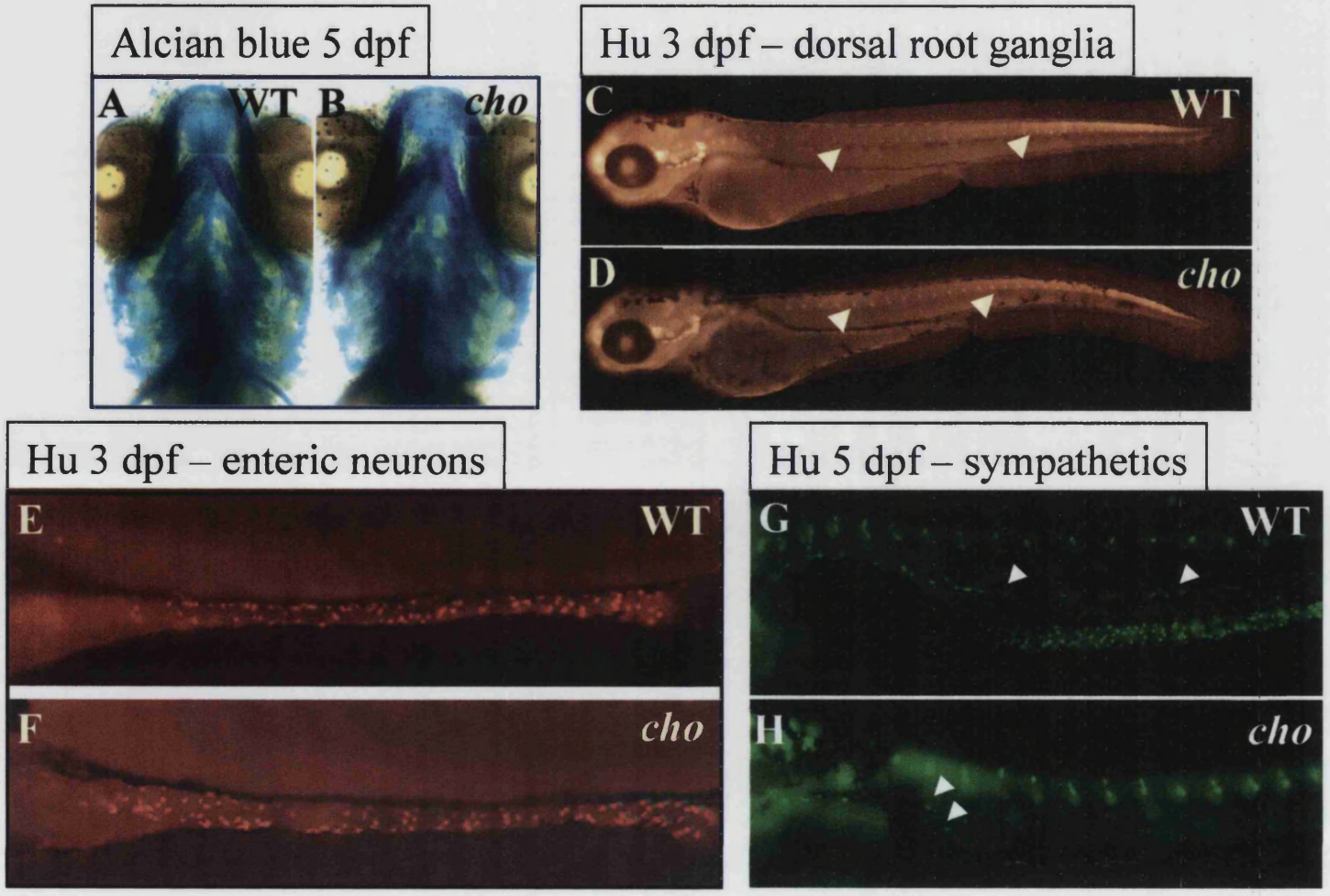
Alcian blue 5 dpf
A
WT
B
cho
Hu 3 dpf – dorsal root ganglia
C
WT
D
cho
Hu 3 dpf – enteric neurons
E
WT
F
cho
Hu 5 dpf – sympathetics
G
WT
H
cho

which detects the pan-neuronal marker Hu (Marusich et al., 1994) to investigate neural crest-derived neurons.

Studies in chick have shown that cranial ganglia are derived from both neural crest and ectodermal placodes (Ayer-Le Lievre and Le Douarin, 1982). Although studies in zebrafish have been limited, fate mapping has demonstrated a neural crest contribution to at least the trigeminal ganglion (Schilling and Kimmel, 1994). We examined the cranial ganglia at 3 dpf and at this stage wild-type embryos had four well-developed cranial ganglia – the trigeminal (located posterior to the eye), the anterior lateral line ganglion (found posterior to the trigeminal), the acoustic (located ventro-medially to the developing otic vesicle), and the posterior lateral line ganglion (posterior to the otic vesicle) (Andermann et al., 2002). *choker* mutants showed cranial ganglia indistinguishable in location, shape and size from those of wild-type siblings (Figure 3.2C, D).

Immunofluorescent detection of the Hu-antigen at 3 dpf enabled us to score enteric neurons. These are found scattered around the gut and extend to the anus. Their number and distribution was comparable in *choker* mutants and wild-type siblings (Figure 3.2E, F).

The sympathetic neurons form a readily identifiable chain of metameric ganglia located adjacent to the dorsal aorta, which can be identified in wild types at 5 dpf using anti-Hu. At this stage the chain of sympathetic neurons was found to extend up to somite 15 in some wild types (arrows, Figure 3.2G). However, the majority of wild types examined only had one or two sympathetic neurons posterior to the swim bladder. Similarly, sympathetic neurons in *choker* mutants were also predominantly found over the swim bladder region. However, due to the absence of the swim bladder in *choker* embryos the enteric and the sympathetic neurons were found too close in proximity to be able to precisely distinguish them (arrows, Figure 3.2H). We were thus unable to establish whether there was a sympathetic phenotype in *choker* embryos.

We also looked at the dorsal root ganglia that extend along the trunk of the embryo in a segmental pattern of one ganglion per somite, and are formed of clusters of typically 2-6 individual neurons. We found that the size, morphology and distribution of *choker* dorsal root ganglia posterior to somite 6 generally paralleled that seen in wild types (arrows, Figure 3.2C, D). However there seemed to be some disorganisation in the more anterior *choker* somites, which we decided to investigate further. To quantify this defect, we examined DRG number in *choker* mutants and wild-type siblings at 48 hpf

when the dorsal root ganglia are just forming, and at 5 dpf when each larval DRG contains 4-7 individual neurons (An et al., 2002). To analyse the DRG phenotype in 5 dpf embryos, we treated batches of wild type and mutant embryos with the melanin synthesis inhibitor PTU, so as to prevent pigmentation of the *choker* collar melanophores. Separation of the mutants from their wild-type siblings was readily performed using the *choker* hindbrain indentation. The embryos were then fixed and the Hu-antigen detected by immunofluorescence.

At 48 hpf each wild-type DRG is composed only of 1-2 neurons and they are not detectable beyond the trunk with anti-Hu. At this stage the total number of neurons in the anterior trunk of choker mutants and wild-type siblings was comparable (Table 3.1). However, we found that *choker* mutants were more likely to show ectopic neurons (64%) in the anteriormost 6 somites when compared to wild types (20%) (Table 3.1; arrowhead, Figure 3.3A, B). If a somite contained more than one DRG neuron and one of these was found outside the usual position in the dorso-caudal portion of the somite, then it was called an ectopic neuron. This difference was found to be statistically significant using a t-test, and is suggestive of a patterning defect. In addition to the higher occurrence of ectopic neurons, the segmental arrangement of the *choker* DRGs was slightly irregular in these embryos. At 5 dpf, the overall number of neurons per embryo was comparable in *choker* mutants and wild-type siblings (Table 3.1). At this stage ectopic neurons were detected in both mutants and wild-types (arrowheads, Figure 3.3C, D). Interestingly, there was now no statistically significant difference in the number of ectopic neurons in the anteriormost 6 somites of mutants and wild-type siblings, nor elsewhere in the trunk and tail (Table 3.1). However, some mutant embryos still had the irregular segmentation first observed at 48 hpf.

Besides neurons, the neural crest also gives rise to the glia of the peripheral nervous system and we therefore decided to investigate the glial cells found along the posterior lateral line nerve (PLLn). The posterior lateral line nerve itself was found to be disrupted in *choker* mutants (RN Kelsh, unpublished) and to project aberrantly, however this was presumed to be a secondary consequence of the absence of the horizontal myoseptum. We decided to use the glial marker *foxD3* (Kelsh et al., 2000a) to examine the posterior lateral line glia. *foxD3*-positive cells have been shown to align at the horizontal myoseptum in the first five somites at 24 hpf and to subsequently follow the posterior lateral line primordium as it migrates posteriorly along the horizontal

Table 3.1 *choker* mutants showed an early defect in anterior trunk dorsal root ganglia patterning, which recovered by 5 dpf

Mean number ± SEM of total dorsal root ganglia neurons and ectopic neurons is given for each trunk region at two developmental stages. Counts of dorsal root ganglia neurons in *choker* mutants and wild-type siblings at 48 hpf revealed a statistically significant difference in the number of anterior trunk ectopic neurons. This defect however recovered by 5 dpf as counts revealed an equivalent number of ectopic neurons in both wild-type and mutant anterior trunks.

Table 3.1 Counts of peripheral sensory neurons in wild types and mutants for anterior (somite 1-6) and posterior (somite 7-14) trunk and tail revealed that *choker* mutants show disorganised DRGs at 48 hpf.

Trunk section	**Somite 1-6**		**Somite 7-14**		**Tail**	
Genotype	WT	*Choker*	WT	*choker*	WT	*choker*
Total neuron number at 48hpf	11± 1.0 n=10	11 ± 0.72 n=14	13 ± 1.3 n=4	15 ± 2.2 n=4	N/A	N/A
Ectopic neuron number at 48hpf	0.20 ± 0.20 n=10	0.71 ± 0.19 n=14	N/A	N/A	N/A	N/A
Total neuron number at 5dpf	39 ± 1.4 n=10	46 ± 2.1 n=10	35 ± 2.0 n=10	39 ± 1.7 n=10	80 ± 2.9 n=10	75 ± 1.6 n=10
Ectopic neuron number at 5dpf	2.3 ± 0.47 n=10	3.3 ± 1.1 n=10	0.50 ± 0.22 n=10	0.70 ± 0.70 n=10	4.9 ± 0.98 n=10	5.6 ± 1.4 n=10

Figure 3.3. Anterior trunk dorsal root ganglia in *choker* mutants showed an early patterning defect which recovered by 5 dpf

(A-D) Immunofluorescent detection of the Hu-antigen at 48 hpf and 5 dpf reveals a chain of dorsal root ganglia. Lateral views of 48 hpf embryos revealed that the anterior trunk DRGs are present and correctly segmented in both wild types (A) and mutants (B). There was however a higher incidence of ectopic neurons in mutant anterior trunks at 48 hpf (arrowhead, B) (Table 3.1). If a somite contained more than one DRG neuron and one of these was found outside the usual position in the dorso-caudal portion of the somite, then it was called an ectopic neuron. Lateral views of 5 dpf embryos revealed that by this stage both wild types and mutants have equivalent numbers of anterior trunk ectopic neurons (arrowheads, C, D) (Table 3.1).

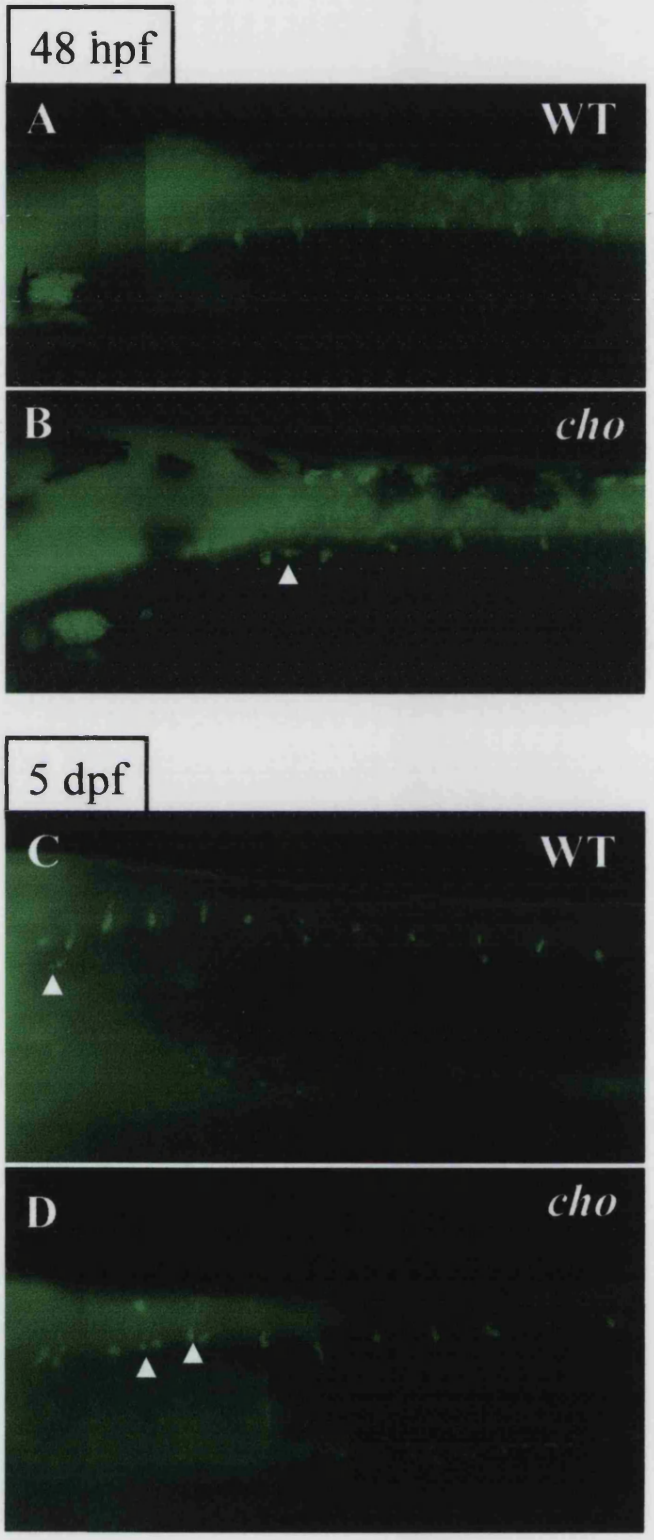
48 hpf
A
WT
B
cho
5 dpf
C
WT
D
cho

myoseptum, thus giving rise to a chain of glial cells along the PLLn. We looked at timepoints between 24 hpf and 36 hpf to analyse the glial phenotype throughout their migration along the horizontal myoseptum. At these early stages we were unable to separate mutants from wild types according to the pigment defect or the hindbrain indentation so we analysed mixed batches of embryos. At 24 hpf all embryos showed labelled cells in the expected peripheral locations (data not shown): in the posterior lateral line ganglion, and in a chain of cells extending along the horizontal myoseptum. There was much variation in the rostrocaudal spread of PLLn glia and thus it was difficult to identify potential mutants. By 30 hpf all embryos had glia in the posterior lateral line ganglion and the majority of embryos had a chain of labelled cells extending posteriorly from the ganglion (arrows, Figure 3.4A). Although there was still a great deal of variation in the degree of progression of the labelled cells along the horizontal myoseptum, some embryos clearly had aberrant glial patterning (arrow, Figure 3.4B). In these embryos, the glial migration was either prematurely truncated or projected dorsally, in a direction perpendicular to the horizontal myoseptum (2/12). Occasionally, the glia initially followed the horizontal myoseptum for a few somites but failed to extend posteriorly. At 36 hpf the migration of the wild type posterior lateral line primordium and hence the glial migration in its wake is nearly complete and therefore at this stage we were able to unambiguously separate mutants from their siblings according to aberrant or prematurely truncated projections (arrows, Figure 3.4C, D). We found that the ratio of mutants to wild types (4/15) conformed to the expected 1:3 Mendelian ratio.

Thus, although glia appear to form and initiate their migration correctly in *choker* mutants, their subsequent migration and projection is severely disrupted and they are unable to correctly pattern along the horizontal myoseptum.

Pigment cells

Since melanophores show a striking phenotype, we were interested to examine the anterior trunk of *choker* mutants for the distribution of two other types of pigment cells – the iridescent iridophores and yellow xanthophores.

Due to their natural coloration it is possible to view iridophores under incident light and we were therefore able to observe these cells directly in live embryos. By 3

Figure 3.4 PLLn glia became prematurely truncated and projected aberrantly in *choker* mutants.

(A-D) *In situ* hybridisation with the glial marker *fkd6* revealed a chain of glial cells extending along the horizontal myoseptum. Lateral views of 30 and 36 hpf wild-type and mutant embryos showed that the mutant glia failed to migrate posteriorly and instead either projected aberrantly (arrow, B) or their migration became prematurely truncated (arrow, D).

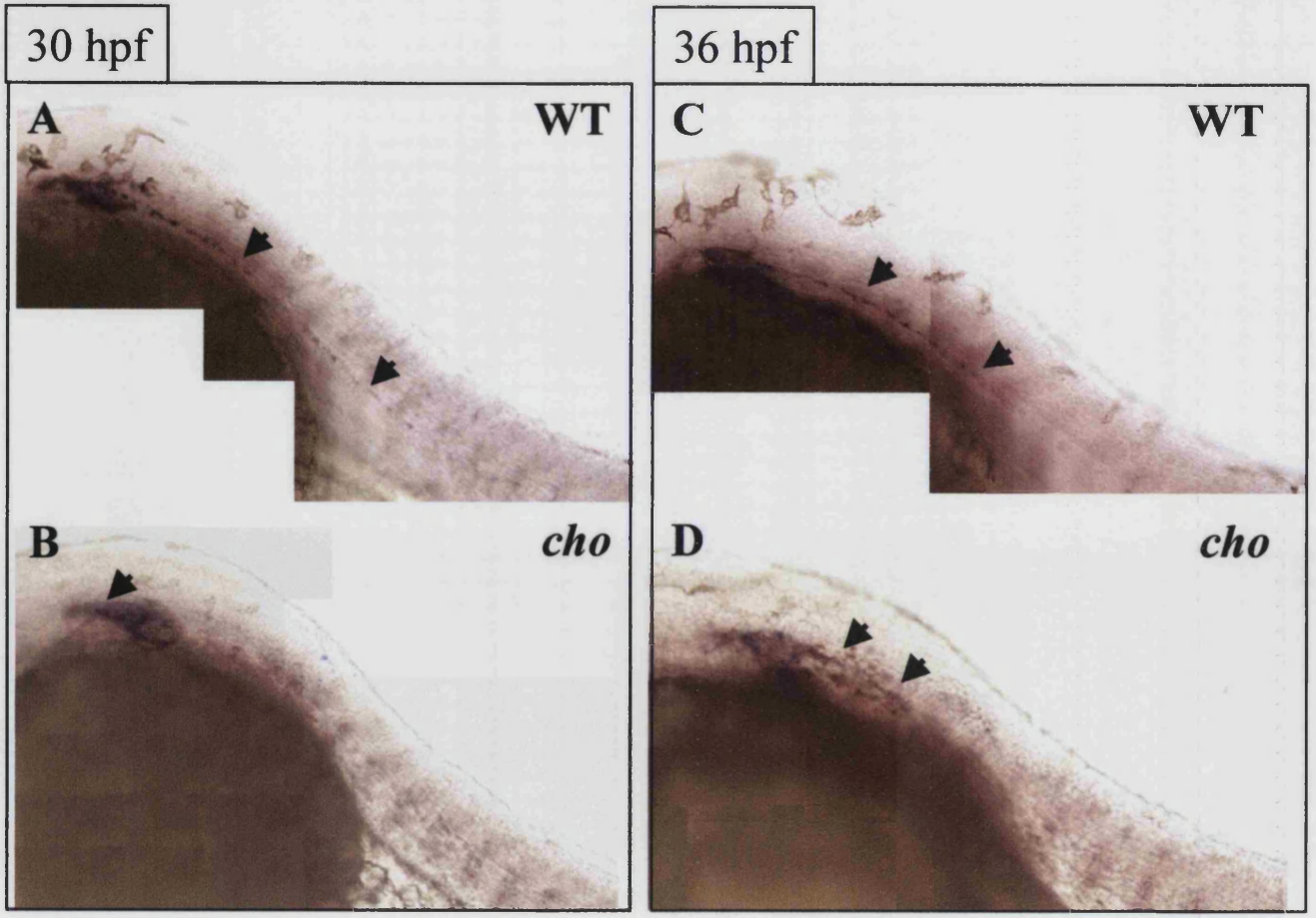
30 hpf
36 hpf
A
WT
C
WT
B
cho
D
cho

dpf wild-type iridophores are found in three (dorsal, ventral and yolk sac stripe) of the four melanophore stripes, as well as scattered over the eye. Although wild type and mutant embryos can be readily distinguished at this stage by the *choker* pigment defect, we saw no differences in iridophore number or distribution (data not shown). We concluded that iridophores are unaffected in *choker* mutants.

Xanthophores are found throughout the head and flank of the embryo and due to their very pale, yellow coloration individual cells are not readily discernible by light microscopy in live embryos. We thus used the xanthophore lineage marker *GTP cyclohydrolase I (gch;* Parichy et al., 2000) to label xanthoblasts. It has been reported that there is some overlap in *gch* expression in early melanoblasts and xanthoblasts as *gch* catalyses the conversion of GTP to dihydroneopterin triphosphate (Pelletier et al., 2001), a compound required for both *de novo* pteridine synthesis and for the production of the cofactor H_4biopterin, which is required for melanogenesis. Hence, melanoblasts express *gch* in the early stages of embryonic development, prior to melanisation (Pelletier et al., 2001). In the xanthophore lineage this marker become progressively downregulated after 60 hpf and completely disappears around 72 hpf. We thus examined embryos at 48 hpf when this marker is specific to xanthoblasts. We separated *choker* mutants from their wild-type siblings at 48 hpf by their incipient melanophore collar. The *gch* marker revealed a network of labelled cells in the head and along the whole flank of the wild-type embryos (Figure 3.5G). In addition, we detected some lateral stripe xanthoblasts that were distinguished by being elongated in an antero-posterior direction along the horizontal myoseptum. *choker* mutants had the expected xanthoblast cells in the head and in the posterior trunk, but showed a striking absence of xanthophores in the anteriormost trunk (Figure 3.5H). This defect was restricted to the anteriormost 4-5 myotomes and was therefore tightly spatially correlated with the melanophore collar defect. *choker* mutants also displayed an absence of lateral stripe xanthophores, consistent with previous reports of horizontal myoseptum reduction. To pinpoint the time of onset of the xanthoblast defect we tested earlier timepoints with the same marker. Although at the earliest timepoints tested *gch* expression is observed in both melanoblasts and xanthoblasts we hoped to be able to detect any differences in the patterning of a subpopulation of *gch*-expressing cells. At 18 hpf labelled cells are found on top of the neural tube throughout the trunk, and slightly more laterally in the head, but at this stage we could detect no differences in the *gch* expression of a mixed batch of mutants and wild-type siblings (data not shown). At 24 hpf, neural crest migration is

Figure 3.5 *choker* mutants had a strong reduction in anterior trunk xanthophores
(A-H) *In situ* hybridisation with the xanthophore marker *gch* revealed labelled cells in the head and trunk of tested embryos. Lateral views of 24 hpf embryos revealed that wild types and mutants appeared to have comparable numbers of xanthophores in the anterior trunk lateral pathway at this stage (A, B). Lateral views of 30, 36 and 48 hpf wild types (C, E, G) and mutants (D, F, H) revealed that the number of xanthoblasts in the *choker* anterior trunk decreases over time so that by 48 hpf the mutant anterior trunk is entirely devoid of xanthophores (H).

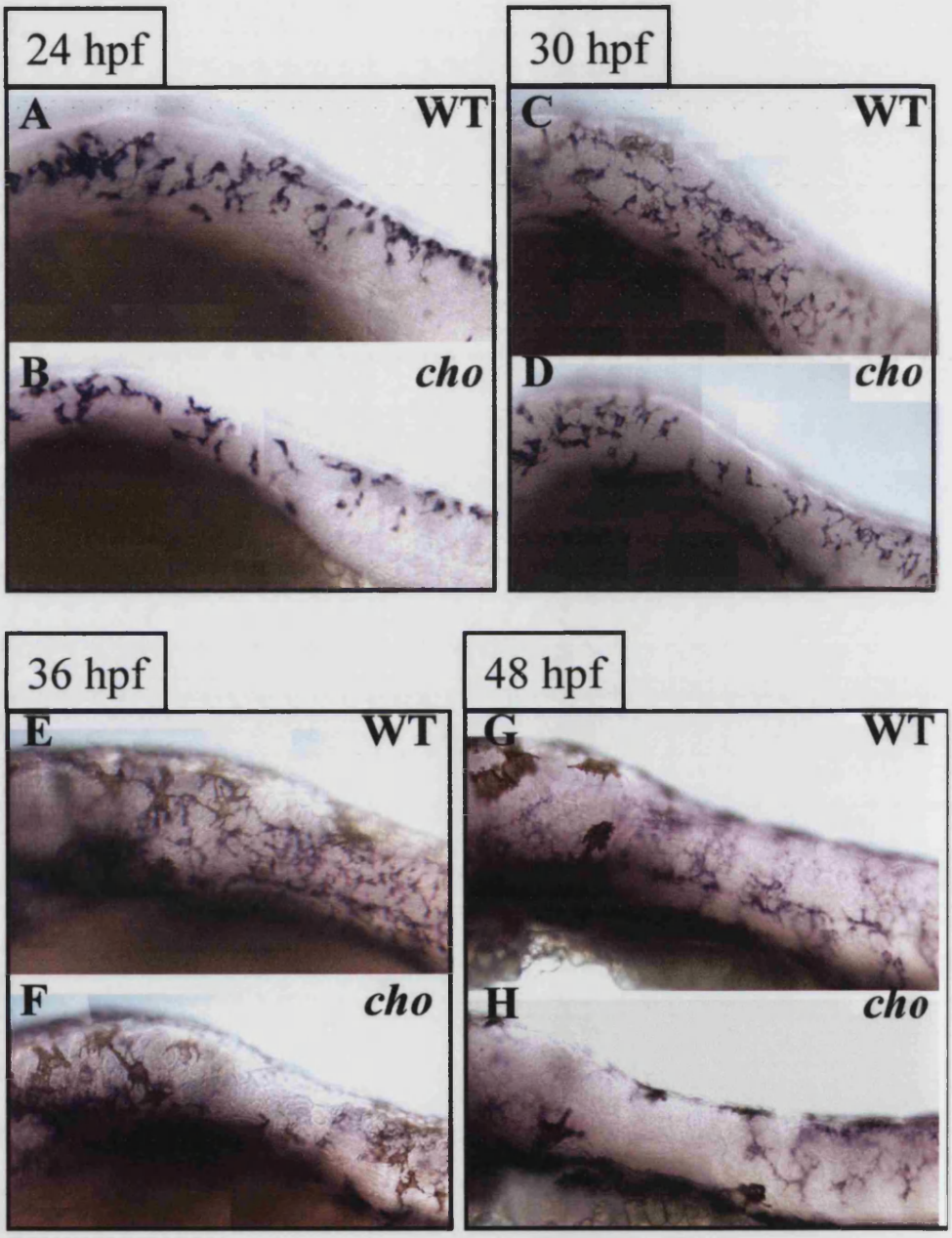
24 hpf
30 hpf
A
WT
C
WT
B
cho
D
cho
36 hpf
48 hpf
E
WT
G
WT
F
cho
H
cho

underway and xanthoblasts are detected on the lateral pathway at the anterior trunk level in all embryos (Figure 3.5A, B). At 30 hpf we observed a decrease in the number of migrating *gch*-positive cells in the anterior trunk of a subset of embryos (Figure 3.5C, D). By 36 hpf there was a dramatic decrease in the number of *choker* anterior trunk xanthoblasts (Figure 3.5E, F). At this stage we could tentatively sort mutants from wild types according to the one or two ectopic collar melanophores. We saw a tight correlation between the melanophore and *gch* expression pattern defects.

In summary, *choker* mutants have normal patterning of most neural crest derivatives, with the exception of dorsal root ganglia, posterior lateral line glia and xanthophores. Although xanthoblasts begin to migrate normally and are initially found in the anterior trunk of *choker* embryos, by 30 hpf the number of xanthoblasts in this region begins to decrease. This defect becomes exacerbated over the next 18 hours with the collar region becoming completely devoid of xanthoblasts by 48 hpf.

Characterisation of the choker muscle phenotype

For convenience when examining *choker* mutants, we wanted to see whether it was possible to sort live mutants from wild types at early stages prior to pigmentation using DIC optics. Examination of a mixed batch of *choker* mutants and wild-type siblings at 24 hpf revealed that a subset of embryos had U-shaped somites and a large number of blebby cells, reminiscent of an apoptotic phenotype, in the most newly formed somites in the posterior trunk. Surprisingly, by 36 hpf the posterior somites of mutants and wild types were indistinguishable. Thus there was a narrow time window when this defect was detectable. This finding provided us with a useful tool in that we were now able to separate live *choker* mutants from their wild type siblings as early as 24 hpf.

To confirm that the cells observed were in fact apoptotic we carried out a TUNEL (Terminal deoxynucleotidyl Transferase Biotin-dUTP Nick End Labelling) assay on mixed batches of 24 hpf embryos. At this stage, approximately 75% of embryos had a very low number of apoptotic cells in the somites (red, Figure 3.6A). By comparison, the remaining 25% of embryos had a large number of dying cells, a process which was most pronounced in the posterior, most recently formed somites (red, Figure 3.6B). These embryos were presumed to be *choker* mutants.

In addition, we were intrigued by two previous observations on *choker* mutants.

Figure 3.6 *choker* mutants had previously undetected muscle defects

(A, B) TUNEL staining revealed apoptotic cells in the posterior trunk of embryos tested. Lateral views of wild types and mutants showed that at 24 hpf *choker* embryos had a higher number of apoptotic cells in the posteriormost regions of the trunk (red, B). (C-F) *In situ* hybridisation with the muscle pioneer-specific probe *eng* revealed a chain of labelled cells extending along the horizontal myoseptum. Lateral views of 24 hpf embryos showed that at this stage *choker* mutants had slightly weaker *engrailed* expression than their wild-type siblings (C, D). At 30 hpf, the reduction in *engrailed* expression in mutants was more pronounced (E, F).

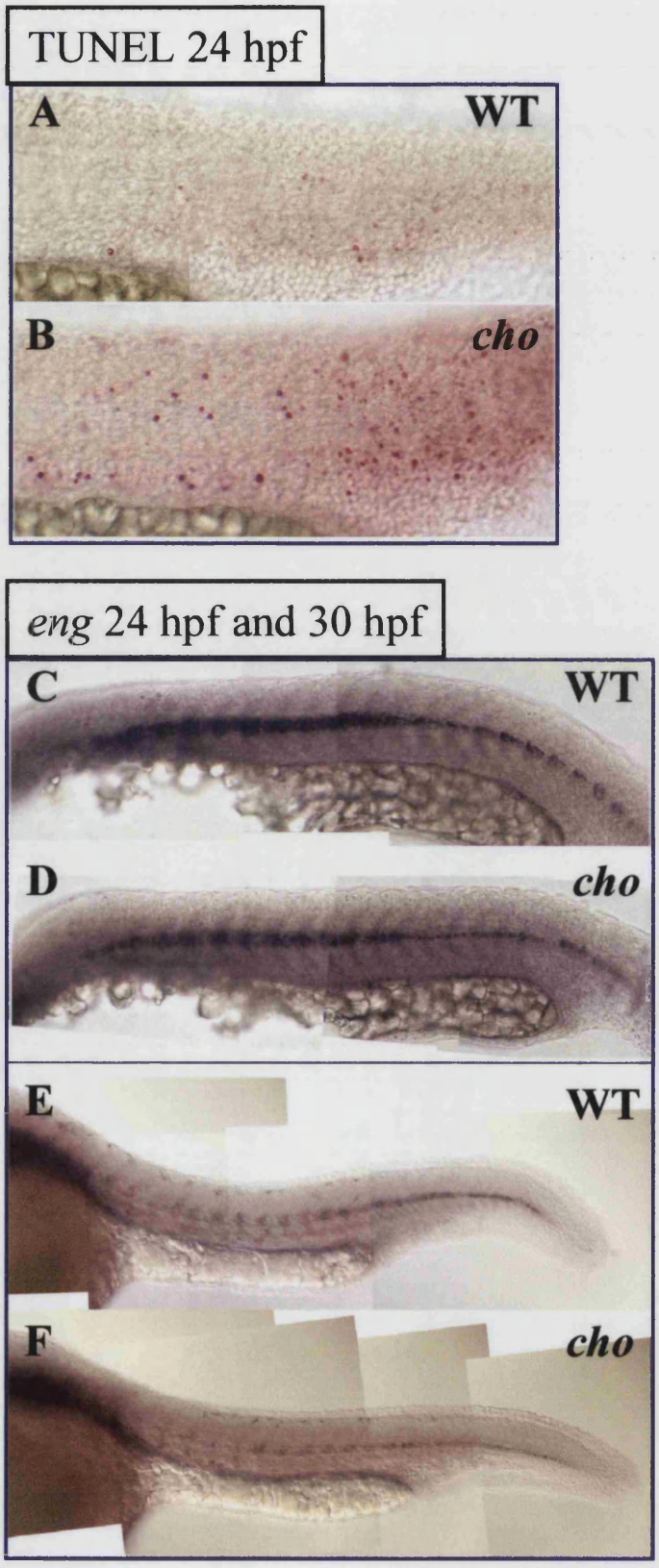
TUNEL 24 hpf
A
WT
B
cho
eng 24 hpf and 30 hpf
C
WT
D
cho
E
WT
F
cho

Thus, previous studies have reported that *choker* mutants have defects in both slow muscle and fast muscle development but not in muscle pioneers (van Eeden et al., 1996; Georgina Hollway, personal communication). The latter phenotype was judged by the presence of the characteristic muscle pioneer early striation, and was tested with the muscle pioneer-specific marker *engrailed 1* at 18 hpf (*engl*; Ekker et al., 1992), which showed an identical pattern in wild-types and mutants.

The latter finding was surprising in light of the fact that the sheet of ECM produced by the muscle pioneers, the horizontal myoseptum, is reduced in *choker* embryos. We therefore used the muscle pioneer marker *engrailed 1* (*engl*; Ekker et al., 1992) to characterise the muscle pioneers in more detail. Mutants and wild types from crosses of heterozygous parents were separated according to the apoptotic muscle phenotype discernible at 24 hpf and fixed at 24, 30 and 36 hpf. *In situ* hybridisation with the *engl* marker revealed that at 24 hpf the muscle pioneers were visible as a line of cells extending along the horizontal myoseptum in both wild-type and *choker* embryos (Figure 3.6C, D). In *choker* mutants however, the staining appeared weaker (Figure 3.6D). The *engl* expression at the midbrain-hindbrain boundary was equivalent in both mutants and wild types suggesting that the differences observed in muscle pioneers were not due to variability of staining between embryos. By 30 hpf *engl* is being downregulated and by now muscle pioneer staining in wild types can only be observed in the posterior somites (Figure 3.6E). *engl* downregulation occurs in a similar fashion in *choker* mutants, however, the difference in strength of staining is now more pronounced (Figure 3.6F). By 36 hpf *engl* expression in muscle pioneers has been completely downregulated in all embryos (data not shown).

Our analysis has revealed that, although *choker* mutants do develop muscle pioneers, these are abnormal, probably being either reduced in number or poorly differentiated.

Discussion

Melanophore accumulation in the choker *anterior trunk occurs during the post-migratory stage that follows lateral pathway shutdown*

Previous studies have shown that melanophores begin to migrate on the lateral pathway from approximately 20hpf, as they make their way towards their final

destination (Jesuthasan, 1996; Raible et al., 1992). This study complements those findings as at the earliest timepoint tested (30 hpf) melanophores were regularly observed in the wild type anterior trunk lateral pathway. However, the rapid decrease in melanophore number observed between 36 and 48 hpf in wild types probably reflects a shut down of this migratory pathway. The first decrease in anterior trunk melanophore number in wild types occurred around 36 hpf indicating that the process of pathway shutdown gets initiated at this stage and is complete by 48 hpf when this region becomes essentially devoid of all melanophores. We did not analyse timepoints between 36 hpf and 48 hpf, however, future studies will be able to elucidate the exact timing of lateral pathway shutdown in wild-type embryos and characterise in more detail the behaviour of migrating melanophores at this time.

This analysis also revealed that the time of onset of the *choker* collar pigment phenotype was much earlier than had previously been suggested. By 48 hpf, mutants and wild-type siblings could be sorted with 100% accuracy based on the pigment phenotype alone. At 30 hpf, the number of melanophores in mutant and wild-type anterior trunks was comparable suggesting that the process of lateral pathway melanophore migration in *choker* embryos is probably normal at this stage. This suggests that, at least at this early stage, there is no excess of melanophores emigrating from the neural tube or proliferating in the lateral pathway environment. The first indication of abnormality was around 36 hpf when there was a slight increase in melanophore number in the collar region. Thus, the *choker* melanophores begin to accumulate in the collar environment around the time of lateral pathway shut down in wild types.

On the basis of these observations, we would like to suggest that the processes of melanophore dispersion from the neural tube and the initial migration on the lateral pathway occur normally in *choker* mutants. The defect occurs subsequent to this and it could be due to a number of reasons including defective lateral pathway shutdown, initiation of aberrant melanophore proliferation or anomalous medial pathway melanophore invasion of lateral pathway territory.

The defect in choker *is restricted to neural crest derivatives that migrate on the lateral migratory pathway*

Our examination of the patterning of most major anterior trunk-derived neural crest derivatives revealed that, with the exception of dorsal root ganglia sensory

neurons, glia and xanthophores, all neural crest derivatives derived from the anterior trunk had normal patterning. However it is worth noting that, although the cranial ganglia appeared correctly patterned, if the situation is analogous to that found in chick, the crest contribution to the zebrafish ganglia can be expected to be partial and can perhaps be compensated for by placodal elements. Therefore the absence of a detectable phenotype does not necessarily negate the possibility that there may be a neural crest patterning defect in the cranial ganglia. A quantitative analysis of neuron number in each ganglion is required to address this question.

We found that glia were present in *choker* mutants and, judging by their correct peripheral alignment in the posterior lateral line ganglion, were correctly patterned. Their position and abundance in the ganglion mirrored that seen in wild types and their initial alignment along the horizontal myoseptum was correct, indicating that the glia both form correctly and are able to respond to guidance cues. Their failure to extend along the horizontal myoseptum is likely to be a secondary consequence of a defect in the posterior lateral line nerve. Previous studies have shown that the patterning of glia along the zebrafish horizontal myoseptum is dependent on the posterior lateral line nerve (Gilmour et al., 2002). In mutants where patterning of the nerve is affected, such as *sonic you* and *fused somites,* the glia always follow the abnormally patterned axon trajectory, suggesting that the axon produces instructive guidance cues that direct glial migration. Furthermore, timelapse studies have shown that glia migrate along the growing axons. It has been shown (RN Kelsh, unpublished) that the PLLn fails to migrate correctly in *choker* mutants, presumably due to the poorly formed horizontal myoseptum. The nerve initially projects correctly but then the axon either stops migrating, or projects aberrantly. This is reminiscent of the glial behaviour observed in our study. It is thus likely that the aberrant patterning of the *choker* glia is a secondary consequence of the axonal defect.

Analysis of the dorsal root ganglia revealed that in the early stages of DRG formation, 64% of mutant embryos had ectopic neurons in the anteriormost 6 somites, whereas only 20% of wild types showed a similar defect. Nevertheless, a large proportion of neurons were correctly patterned, even in *choker* mutants. Thus there was an early but incomplete sensory neuron patterning defect. By 5 dpf this phenotype appeared to have recovered as the number of ectopic neurons in wild types and *chokers* was statistically indistinguishable. The DRG phenotype is thus not fully penetrant as it does not affect all mutant embryos at all stages analysed. The early phenotype in *choker*

might be a consequence of a defect in the patterning cues that coalesce DRG neurons into a ganglion. The explanation for the later recovery is unclear but previous studies have shown that wild-type embryos also have ectopic neurons at 5 dpf, which recover by 14 dpf (An et al., 2002). Thus, since a similar recovery is shown in wild types, it may reflect a normal mechanism for ensuring correctly patterned DRGs. Perhaps the absence of community effects may cause the isolated, ectopic neurons to die off at later stages, thus accounting for the recovery of the phenotype in both mutants and wild-types.

The analysis of xanthophore patterning provided us with another intriguing aspect of the *choker* phenotype. Intriguingly, the xanthoblasts begin to pattern normally but are lost from the collar at later stages. Thus, the xanthophore defect is similar to the melanophore phenotype, in that migration is initially normal and is followed by a failure to maintain the wild-type pattern. Like the melanophores, xanthoblasts evidently initiate their migration and follow the appropriate migratory guidance cues correctly. At 24 hpf they are found laterally in the anterior trunk of the embryo and they thus appear to begin to populate the correct regions, however from 30 hpf onwards they start being lost from the anterior trunk. It is unclear whether this loss occurs through cell death, emigration or some other mechanism. The *choker* mutants may be lacking some form of maintenance molecule, which normally maintains xanthophore position in this region. Alternatively, the defect may lie in a trophic factor important for xanthophore survival. Finally, there is the intriguing possibility that the defect is in a cell fate maintenance factor. The timing of onset and the tight spatial correlation of the two pigment defects immediately suggests the possibility that the xanthoblasts begin to downregulate xanthoblast-specific markers at 30 hpf and start to transfate into melanophores which are first detectable in the collar after 36 hpf. Alternatively there is a possibility that the xanthoblasts are being repulsed from the anterior trunk by the invading melanophores. It is equally possible that the two defects may be independent of each other and that they may both occur as a secondary consequence of the underlying muscle defect. Some of these possibilities are further tested in the next chapter.

Whatever the nature of the *choker* molecular defect, it is clear that it does not affect all neural crest cell fates. Neuronal and glial fates, craniofacial cratilage and iridophores largely pattern normally. The only fates affected are melanophores and xanthophores. Studies in chick have shown that melanoblasts are the only neural crest derivative capable of migrating on the lateral pathway; all other derivatives usually migrate medially (Erickson and Goins, 1995). Evidence suggests that the situation is

similar in zebrafish (Raible and Eisen, 1994). Although melanophores are capable of travelling on both the medial and lateral pathways, neuronal and glial fates always migrate medially (Raible and Eisen, 1994). In addition, iridophores also appear to be restricted to the medial pathway whereas xanthophores are only ever observed on the lateral pathway (S.S. Lopes and R.N. Kelsh, unpublished observations). Thus, melanophores and xanthophores, the only neural crest derivatives that migrate on the lateral pathway are also the only crest fates that are affected in *choker*. This suggests that the defect in *choker* lies in the lateral pathway environment or in the ability of the neural crest cells themselves to interact with components of this environment. In either case, the cues that normally ensure correct patterning of cells migrating on this pathway seem to be defective in some way.

The choker *mutant shows apoptosis of muscle cells and defective muscle pioneer development*

Our analysis of the muscle defects in *choker* mutants revealed two aspects of the phenotype not studied by Currie and Hollway.

We observed large numbers of apoptotic cells in the posteriormost mutant somites, a defect which presented us with the means of reliably and easily distinguishing mutants from wild-type siblings 24 hours before the collar pigment phenotype is first detectable. The mutant somites may undergo excessive cell death as they are forming, which may explain why at 24 hpf this phenotype was restricted to the posteriormost, most recently formed somites. Although the *choker* muscle defect is most pronounced in the anteriormost 4-5 somites, the posterior somites also show some fibre disorganisation. This defect may occur as a result of the muscle cell death documented here. It might be expected to be much more pronounced in the anterior trunk, at earlier stages, when the anteriormost somites are just forming, as there is a strong reduction in both slow and fast muscle fibres in this region, but further studies are required to elucidate this.

Our muscle pioneer findings complemented the studies done by Hollway and confirmed that all aspects of muscle development are aberrant in *choker* mutants (Nikolic *et al*, unpublished). The fact that muscle pioneer cells are present initially might explain van Eeden's observation that the horizontal myoseptum in *choker* is reduced and not altogether absent. Unfortunately, due to the lack of known markers that

label muscle pioneer cells at stages after 30 hpf we were not able to find out what happens to the muscle pioneer population after this timepoint.

Our preliminary characterisation of the *choker* phenotype established the timing of the melanophore defect and the extent of the neural crest abnormalities. The identification of the xanthophore defect has presented us with further evidence for a strong spatial correlation between the muscle and neural crest defects. This relationship suggests that some or all of these defects may be causally related, a possibility which we test further in the next chapter.

Chapter 4

Further characterisation of the origin of *choker* neural crest defects

Introduction

The *choker* mutant has several muscle development defects which are restricted to the anteriormost five somites. Spatially correlated with this region there are also two neural crest defects – an accumulation of ectopic melanophores and a loss of xanthophores. The tight spatial correlation between the melanophore and xanthophore phenotypes raises the possibility that these two defects might be causally related.

The ectopic melanophores may arise through xanthophore transdifferentiation

To investigate the possibility that the melanophore and xanthophore defects are causally related we must first examine the temporal correlation between the two pigment phenotypes. The first timepoint at which we clearly begin to see a decrease in anterior trunk xanthoblasts is at 30 hpf. Several hours later, at 36 hpf, we begin to detect ectopic melanophores in the same region. The timing of onset of the two defects suggests that the ectopic melanophores may be arising through xanthophore transdifferentiation. The xanthoblasts may start downregulating xanthophore-specific markers and begin to upregulate the expression of melanophore-specific genes, such as enzymes required for melanin production, at 30 hpf, so that by 36 hpf we may expect to see the first melanised cells in this region.

There are a number of reported cases of pigment cell transdifferentiation and the best-studied ones involve the transdifferentiation of the retinal pigmented epithelium (RPE) into neural tissue and, to a lesser extent, vice versa. This process has so far been found to occur in urodeles, larval anurans, embryonic chicks and rodents (reviewed in Zhao et al., 1997) and has been extensively studied, resulting in the identification of some of the molecules involved, and a better understanding of the process of transdifferentiation. Thus, studies of the Japanese silver quail mutant, whose RPE spontaneously transdifferentiates into an ectopic neural retina, have shown that the bHLHzip transcription factor mitf and members of the fibroblast growth factor (FGF) family have a key role in this process. The silver mutant has a substitution in the *mitf*

gene which attenuates the activity of the protein and is thought to be responsible for the RPE transdifferentiation (Mochii et al., 1998). Concomitant with the decrease in *mitf* activity, an increase in the activity of FGF proteins at the site of transdifferentiation was also detected (Araki et al., 2002). Parallel studies have found that the implantation of FGF beads close to the RPE of cultured mouse optic vesicles resulted in *mitf* downregulation and retinal transdifferentiation, thus confirming the important role of these genes in the process of retinal to neural transdifferentiation (Nguyen and Arnheiter, 2000).

The studies of neural crest-derived pigment cell transdifferentiation are, however, fewer. Neural crest cells have been postulated to derive from a multipotent precursor which gives rise to all of the derivatives through a process of sequential fate restrictions (reviewed in Le Douarin and Dupin, 2003). Multipotent neural crest cells with stem cell properties have been isolated from mammalian embryos (Stemple and Anderson, 1992) however it is still unclear whether the multipotent precursors can generate all types of neural crest derivatives. *In vitro* clonal analysis of quail neural crest cells revealed the existence of several totipotent precursors that can, under the right conditions, give rise to neuronal, glial, pigment and mesenchymal derivatives (reviewed in Le Douarin and Dupin, 2003). Furthermore, several pluripotent, intermediate precursors have been identified that gave rise to colonies of distinct phenotypic assortments, such as glia and neurons or glia and melanocytes. It is thus likely that a chromatophore precursor which gives rise exclusively to pigment derivatives also exists. The idea that all pigment cells originate from the same precursor was proposed as early as 1979, upon the observation that several organisms have 'mosaic' pigment cells (Bagnara et al., 1979). For instance, cells containing both reflecting platelets and melanosomes have been identified in the dove iris and in the teleost *Dasyatis sabina,* (Arnott, 1970). A similar phenomenon has also been observed in the mutant zebrafish *parade,* which has ectopic pigment cells of mixed melanophore and iridophore character (Kelsh et al., 1996). The mutant might be missing a gene function that has an important role in fate maintenance. Studies of pigment cell marker expression give further support to the theory that all pigment cells are generated from a chromatophore precursor, as overlap of distinct pigment cell markers is seen at early stages of development. For instance, the xanthoblasts marker *gch* and the melanoblast marker *mitfa* are co-expressed until 30 hpf (Pelletier et al., 2001). If all pigment cells are derived from a common precursor then their fate restriction and commitment to a single

fate is probably dependent upon both cell intrinsic and environmental factors. Consequently, it is hypothetically possible for a cell to transdifferentiate into another if those factors were manipulated.

Transdifferentiation of one neural crest derivative into another has been shown in culture. Thus, cells derived from avian embryos and expressing Schwann cell markers were able to reverse their developmental program and give rise to melanocytes upon treatment with the tumor-promoting phorbol ester drug 12-*O*-tetradecanoyl phorbol-13-acetate (TPA) (Sherman et al., 1993). More recent studies have found that, upon exposure to endothelin-3, cultured Schwann cells change their developmental program and give rise to a mixture of melanocytes, glia and cells bearing both markers (Dupin et al., 2003). Endothelin-3 has been previously identified as a factor that promotes the generation of bi-potent glial and melanocytic precursors (Dupin et al., 2000), thus its addition to cultured Schwann cells probably promotes their reversal to the precursor state and the production of both glial and melanocytic progeny.

Of particular interest however, is the relationship between melanophores and xanthophores. Studies have shown that a decrease in melanophore number and a concomitant increase in the number of iridophores and xanthophores occur if axolotls are placed on a guanosine supplemented diet (Frost et al., 1987). These findings have been confirmed by more recent studies with cultured axolotl neural crest cells, which found that xanthophores differentiate at the expense of melanophores in guanosine-supplemented conditions (Thibaudeau and Holder, 1998).

It is conceivable that the *choker* xanthophores could be transdifferentiating into melanophores due to the lack of some factor required to maintain xanthophore fate. We wanted to test this model, and determine whether the ectopic melanophore collar forms in *choker* embryos that have no xanthophores. We thus crossed the *choker* mutant against another pigmentation mutant which lacks xanthophores, in order to give rise to a *choker* double mutant that is devoid of xanthophores. If xanthophores were required for the accumulation of the ectopic melanophores, we would expect a double mutant that has no xanthophores to also have no ectopic melanophore collar. Conversely, if the melanophore accumulation were xanthophore-independent, the double mutant would have the ectopic collar despite the absence of xanthophores. As there are no known pigmentation mutants that have a complete absence of xanthophores we instead used a mutant which has been described to lack xanthophores laterally, *pfeffer* (Odenthal et al., 1996). *pfeffer* is an orthologue of the zebrafish gene *fms* (DM Parichy, personal

communication). The analysis of xanthophore markers such as *GTP-cyclohydrolase I* (*gch*) and *xanthine dehydrogenase* (*xdh*) has shown labelled cells to be confined to the vicinity of the neural tube in *fms* mutants, suggesting that this gene has a role in xanthoblast dispersal (Parichy et al., 2000). Thus, in the *fms/pfeffer* mutant the xanthoblasts are unable to migrate and remain in premigratory positions at the dorsal edge of the neural tube in the trunk, and slightly more lateral regions in the head.

A further prediction of the transdifferentiation model is that we will be able to detect the presence of early melanoblast markers in the anterior trunk. If xanthophores were transdifferentiating, we would expect a downregulation of xanthophore-specific markers to be succeeded by an upregulation of melanophore-specific markers such as the gene involved in melanin production, *dopachrome tautomerase* (*dct*; (Kelsh et al., 2000b)). The expression of this marker precedes the appearance of melanin by 5 hours and when detectable in unmelanised cells would indicate melanophore differentiation was underway.

Anterior trunk xanthophores may be lost as a consequence of melanophore invasion

We also wanted to test the converse hypothesis that xanthophore loss occurs as a consequence of melanophore invasion. Although the onset of the melanophore phenotype is a number of hours after xanthophores begin to be lost from the anterior trunk, it is conceivable that unpigmented melanoblasts invade this region several hours before we begin to see the presence of melanised cells, force out the xanthophores through emigration or apoptosis, and then pigment *in situ*. Studies of adult zebrafish pigment pattern development have suggested that melanophore patterning is dependent on xanthophores. Early studies looking at fin regeneration after amputation revealed that, as the fin grows, it becomes uniformly dotted with melanophores (Goodrich, 1931). Shortly afterwards, a melanophore-free zone is established through localised destruction, and becomes populated by xanthophores. A similar process is observed during metamorphosis. Melanophores distribute evenly throughout the body of the fish and consequently are selectively lost from interstripe regions through apoptosis or emigration, a process that has been proposed to be xanthophore-dependent (Parichy et al., 2000). The study of adult zebrafish pigmentation mutants, such as *fms,* concurs with this hypothesis, as the absence of xanthophores results in severely disrupted adult melanophore stripes. Thus, although the embryonic melanophore pattern is normal, the

adult melanophores show an increased apoptosis rate which is not localised to interstripe regions and thus results in aberrant patterning. Together, these data suggest that xanthophores have an important role in organising melanophores into stripes in adult zebrafish. However, if this were also applicable to the way pigment cells are patterned in embryos we would expect embryonic mutants that lack xanthophores, such as *salz* and *pfeffer,* to have ectopic melanophores in the regions where xanthophores are absent. Instead, the xanthophore absence does not appear to have any effect upon embryonic melanophore patterning – the latter are still found in their stereotypic locations. Furthermore, it appears that melanophores and iridophores are directed to their positions first, and then xanthophores fill in the remaining positions in the skin. Thus, in the melanophore mutant *sparse,* xanthophores invade the spaces normally occupied by melanophores (Kelsh et al., 1996). Hence, during embryonic stages the patterning of xanthophores may be dependent on melanophores. We wanted to test this prediction by crossing *choker* against the pigmentation mutant *nacre,* which has a complete absence of melanophores. The lack of melanised cells in these mutants is not simply due to a fault in melanin synthesis, as the gene encoding *nacre* is a microphthalmia-related basic helix-loop-helix/leucine zipper transcription factor required for melanoblast specification, and in its absence cells are unable to specify to a melanoblast fate (Lister et al., 1999). If the melanophores were responsible for the xanthophore loss we would expect the double mutant to have undisturbed anterior trunk lateral xanthophores in the absence of melanophores. Conversely, if the xanthophore defect were independent of melanophores we would expect the double mutant to lose xanthophores from the anterior trunk despite the lack of melanophores.

Timelapse analysis of melanophore behaviour in choker *mutants*

In addition to trying to understand the link between the xanthophore and melanophore phenotypes we used timelapse microscopy to compare the behaviour of mutant and wild-type anterior trunk melanophores. As it is carried out on live embryos, timelapse microscopy can provide dynamic information of a cell's behaviour. Timelapse studies have been previously used to study the timing and pathways of neural crest migration (see Chapter 1) (Raible et al., 1992). In addition, more recent studies have used timelapse analysis to record a cell's behaviour prior to and during migration (Jesuthasan, 1996). These studies have shown that before they begin to migrate, between the 12- and 14-somite stage, neural crest cells extend their processes and

explore their environment by making contact with the young somite. The rate of retraction of these processes is initially very high and begins to decrease around the 14-somite stage, as neural crest migration on the medial pathway begins. However, neural crest protrusions continue to collapse as they make contact with the lateral face of the somite, until the lateral pathway opens a few hours later, at the 19-somite stage. The process of extension retraction is reminiscent of growth cone collapse and suggestive of an inhibitor being produced in this region that prevents precocious neural crest emigration and delays lateral pathway migration (Jesuthasan, 1996).

We used timelapse microscopy on 24 hpf and 48 hpf embryos to compare the behaviour of anterior trunk melanophores in *choker* mutants and wild-type siblings. We hoped this would allow us to determine which of the processes underlying neural crest patterning are aberrant in this mutant - differentiation, proliferation or migration. If any of the above processes were taking place, we expected to be able to see them using timelapse analysis - for instance, melanophores pigmenting in the ectopic location, melanophores dividing, or melanophores migrating into this region from surrounding areas. We also hoped that the timelapse experiments may help us gain further insight into the processes of wild-type melanophore migration.

Results

Analysis of choker;pfeffer *double mutants*

To test whether xanthophore transdifferentiation was responsible for the accumulation of ectopic melanophores in *choker* mutants, we crossed carriers for the *choker* and *pfeffer* alleles. The offspring resulting from this cross was reared and when the fish reached adulthood they were screened for carriers of both alleles. The identified double heterozygotes were crossed against each other and the resulting embryos screened for double mutants at 5 dpf, as we expected to be able to readily detect both the *choker* and the *pfeffer* phenotypes at this stage. By 5 dpf, the wild-type xanthophores were visible as a yellow-green hue dispersed over the head and flank of the embryo, and *pfeffer* mutants were readily identifiable by the lack of this coloration (Figure 4.1A, C). Similarly, at 5 dpf *choker* mutants had a prominent melanophore collar and hindbrain indentation (Figure 4.1B). The latter defect would enable us to

Figure 4.1. The *choker* ectopic melanophore collar formed even in the absence of xanthophores

(A-D) Live microscopy of 5 dpf single and double mutants, and wild-type siblings. Lateral views of a wild type revealed melanophores in the dorsal, lateral, ventral and yolk-sac stripes, and xanthophores scattered throughout the head and flank of the embryo (A). *choker* embryos had an accumulation of ectopic melanophores in the anterior trunk and normally distributed xanthophores (B). *pfeffer* mutants showed stereotypical melanophore patterning and an absence of lateral xanthophores (C). Lateral views of a *choker;pfeffer* double mutant revealed that the ectopic melanophore collar forms despite the absence of lateral xanthophores (D). (E-F) Whole mount *in situ* hybridisation of 48 hpf *pfeffer* single and *choker;pfeffer* double mutants. Lateral views of *pfeffer* mutants revealed the presence of some xanthoblasts in the anteriormost regions of the trunk (E). These xanthoblasts largely overlapped with the most anterior portion of the incipient *choker* collar (F).

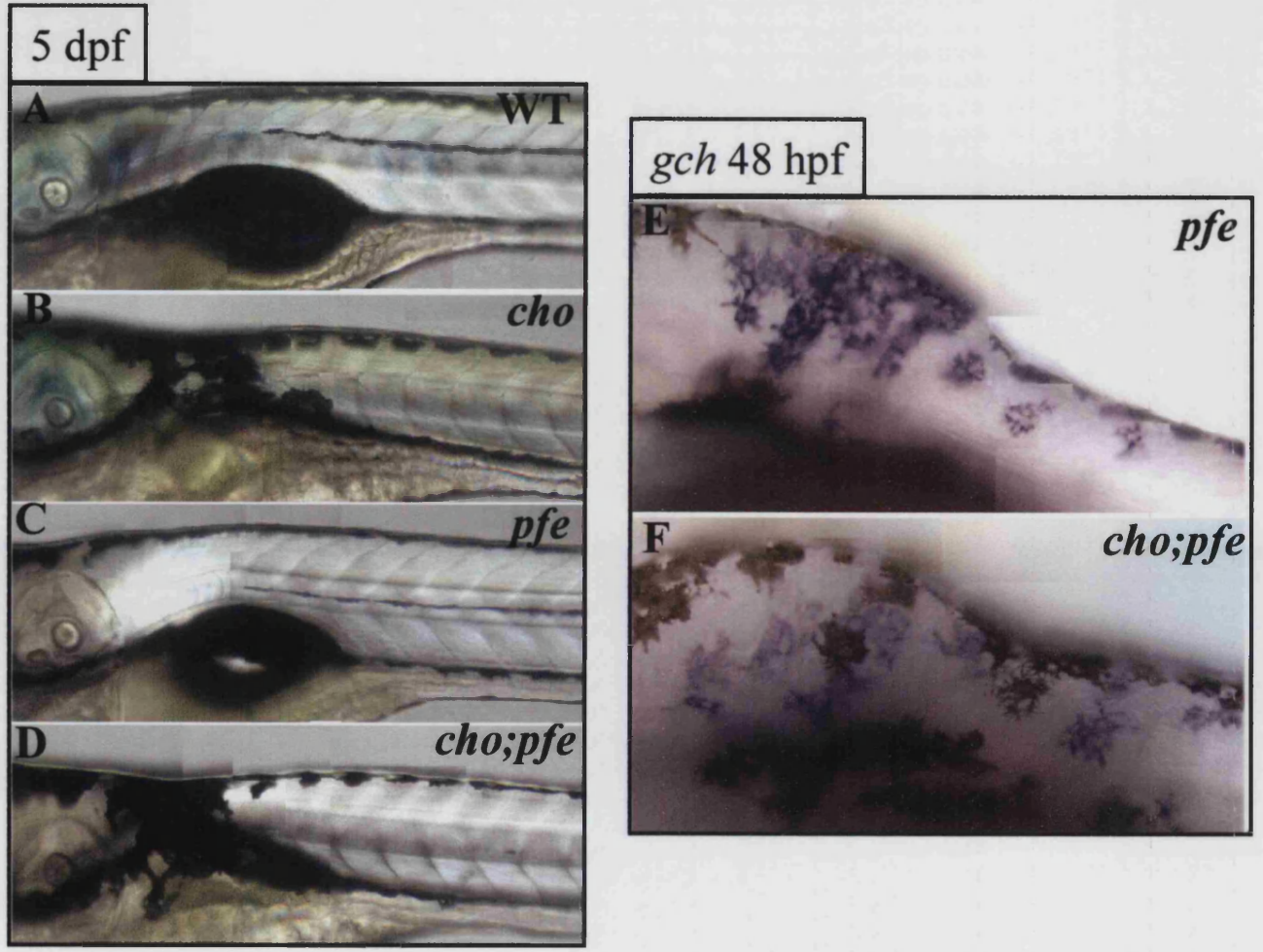
5 dpf
A
WT
B
cho
C
pfe
D
cho;pfe
gch 48 hpf
E
pfe
F
cho;pfe

identify *choker* embryos if the double mutants turned out to have no melanophore phenotype. Live embryos were screened under a dissecting scope and double mutants were identified in the expected 1:15 ratio. They all had both a lack of lateral xanthophores, judged by the absence of the yellow-green hue, and a melanophore collar (Figure 4.1D). Thus, the build up of melanophores in the collar region does not appear to be a result of xanthophore transdifferentiation.

To exclude the possibility that *pfeffer* mutants had some remaining lateral xanthophores we had to be able to see individual cells. We therefore used whole mount *in situ* hybridisation with the xanthophore marker *gch* (Parichy et al., 2000) to label batches of embryos obtained from crosses of carriers for both *choker* and *pfeffer* alleles. We opted to perform an *in situ* at 48 hpf as at that stage *gch* is strongly expressed in xanthophores, and we expected to be able to identify double mutants by their incipient melanophore collar and an absence, or a reduction of, lateral xanthophores. According to these criteria we were able to identify double mutants in the expected ratio. Both *pfeffer* single and *choker;pfeffer* double mutants lacked lateral labelled cells at all axial levels except in the head and anteriormost trunk (Figure 4.1E, F). We observed a cluster of labelled cells laterally in the head and the foremost region of the anterior trunk, specifically, lateral and dorsal to somite one. In addition, we detected two to three individual *gch*-positive cells found more posteriorly, over somites 2-5. The identity of these cells was further confirmed by their characteristic xanthophore spider-like morphology. Thus, although xanthophore number in the anterior trunk was clearly decreased as compared to wild types, this region was not altogether free of xanthophores. Nevertheless, we confirmed the previously described severe xanthophore reduction in *pfeffer* mutants.

Analysis of melanoblast differentiation in the choker *anterior trunk*

To further test the possibility that the melanophore collar arises through xanthophore transdifferentiation we looked for an early melanoblast marker in the *choker* anterior trunk. We chose to use the melanoblast marker *dct* as it is specific to melanoblasts, is expressed a number of hours before they start to melanise and is maintained strongly thereafter. It is thus a good marker for melanoblast differentiation (Kelsh et al., 2000b). Our previous observations have suggested that the highest increase in the number of ectopic melanophores appears to occur between 50 and 60 hpf (see Chapter 3). We would expect to see an increase in differentiating melanoblasts a

few hours before the appearance of melanised cells, and hence decided to look for melanoblast markers at 49 hpf and 52 hpf. To exclude the possibility that the absence of labelled cells in mutants may be due to the *in situ* not working we included PTU-treated, stage-matched mutant controls in our experiment. As *dct* continues to be expressed in differentiated melanophores even after they have melanised we would expect to be able to see signal in mature melanophores as well as differentiating, unmelanised melanoblasts. However, as the melanin may mask the signal, we PTU-treated the control embryos to aid detection of the *in situ* label. The controls were developed under the same conditions as the experimental embryos.

Our controls showed a number of *dct*-expressing cells in the anterior trunk both at 49 hpf and 52 hpf, and they were all in the areas where we expected to find *choker* melanophores – in the dorsal and ventral stripes, and in the anterior trunk lateral pathway (Figure 4.2B, D). Similarly, untreated *choker* mutants had a number of melanophores in the anterior trunk, both in the stripes and in between. However, all of these were fully melanised and we detected no unmelanised *dct*-expressing cells in the *choker* collar region (Figure 4.2A, C). Thus, all of the melanophores in the mutant collar were already differentiated and we were unable to detect any sign of new melanoblast differentiation in this region.

Preliminary analysis of xanthophore loss from choker *anterior trunk*

Our analysis of *choker;pfeffer* double mutants and melanoblast marker expression argues that *choker* anterior trunk xanthophores do not appear to be lost through transdifferentiation into melanophores. We thus wanted to investigate what other mechanism might account for xanthophore loss from the *choker* collar. To test whether the loss of xanthophores from the mutant collar was due to apoptosis we used the TUNEL (Terminal deoxynucleotidyl Transferase Biotin-dUTP Nick End Labelling) reaction on mixed batches of 30 hpf *choker* mutants and wild-type siblings. Our analyses revealed that three quarters of the embryos tested (12/16) had a low level of apoptosis throughout the head and trunk (Figure 4.3A, C). In contrast, one quarter of embryos (4/16) had an excess of apoptotic cells in the anterior trunk (arrows, Figure 4.3B, D). These cells appeared to be located on the lateral surface of the somite and in the region of somites 1-5, where the xanthophores are normally found. That these embryos were *choker* mutants was confirmed by the elevated levels of apoptosis in their posterior trunks (arrowheads, Figure 4.3B) (see Chapter 3).

Figure 4.2. *choker* ectopic melanophores did not differentiate *in situ*

(A-D) Whole mount *in situ* hybridisation of 49 and 52 hpf *choker* mutants and stage-matched PTU-treated mutant controls, with the *dct* probe. Lateral views of *choker* embryos revealed no unmelanised melanoblasts in the anterior trunk region at either stage (A, C). PTU-treated controls revealed a number of labelled cells in the dorsal stripe and the anterior trunk lateral pathway, suggesting that the *in situ* protocol had worked (B, D).

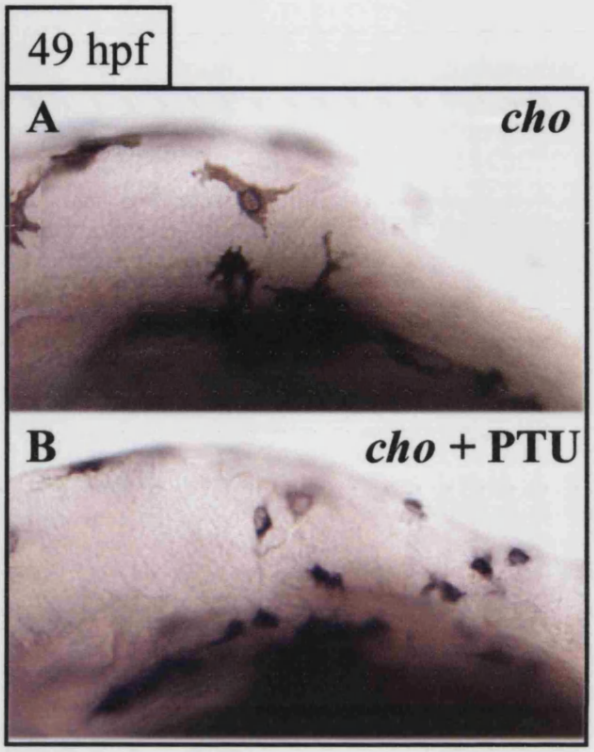
49 hpf
A
cho
B
cho + PTU

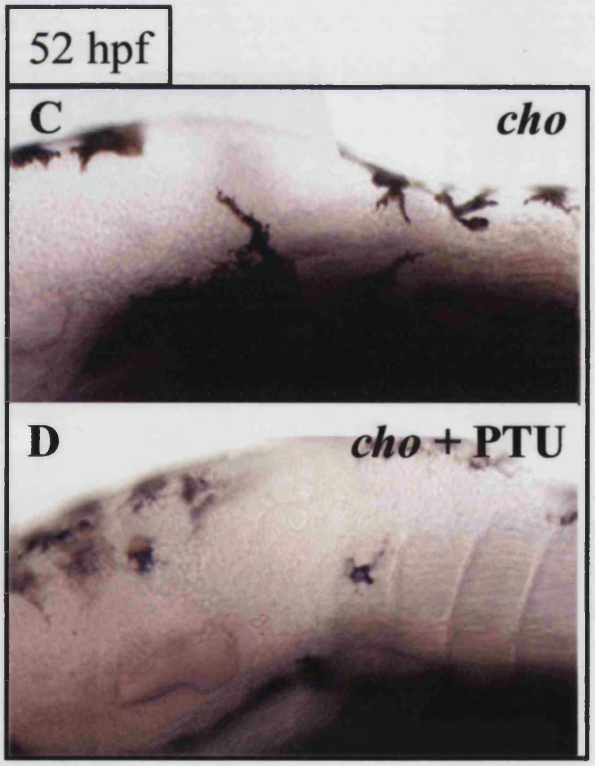
52 hpf
C
cho
D
cho + PTU

Figure 4.3. Preliminary analyses revealed that xanthophore loss from the *choker* collar region may occur through apoptosis

(A-D) TUNEL labelling of 30 hpf *choker* mutants and wild-type siblings. Lateral views of wild-type embryos revealed a low level of apoptosis in the head and trunk (A, C). Lateral views of *choker* embryos displayed elevated levels of apoptotic, labelled cells in the anterior trunk region, where xanthophores are lost from (arrows, B, D). These embryos also had apoptotic cells in the posteriormost trunk, indicating that they were *choker* mutants (arrowhead, B).

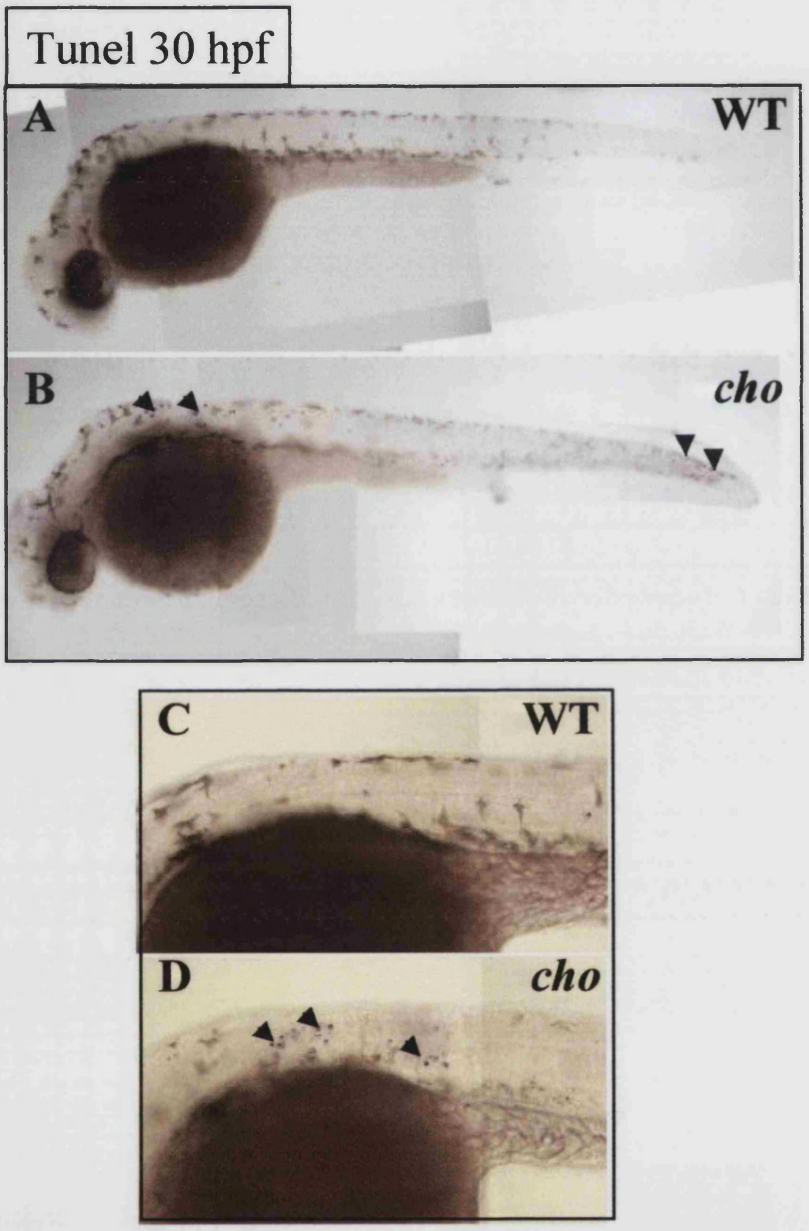
Tunel 30 hpf
A
WT
B
cho
C
WT
D
cho

These results suggest that xanthophore loss in the mutant anterior trunk might occur through cell death. However, double labelling with the TUNEL reaction and a xanthophore marker is required to conclusively prove these observations.

Analysis of choker;nacre *double mutants*

To test whether the loss of xanthophores from the anterior trunk occurs as a consequence of melanophore invasion we created *choker;nacre* double mutants. These mutants were created by crossing *choker* carriers against *nacre* homozygotes, which are homozygous viable. This eliminated the need to screen offspring for the *nacre* allele as all the embryos resulting from this cross were carriers. The offspring of the cross were reared to adulthood and screened for the *choker* allele. Carriers for both the *nacre* and *choker* alleles were crossed and the offspring screened for the presence of double mutants. By 48 hpf the xanthophore loss from the collar is complete and we therefore expected to be able to readily detect the xanthophore phenotype at this stage, if there was one. As the xanthophore phenotype is best detectable by *in situ* analysis, we collected batches of 48 hpf embryos from a cross of identified *choker;nacre* carriers and labelled them with the xanthophore marker *gch.* Following *in situ* hybridisation we screened embryos for the *nacre* phenotype by looking for the absence of melanophores. These had a network of labelled cells throughout the trunk and head regions (Figure 4.4A). As the absence of melanophores made it impossible to screen for *choker* mutants by the melanophore collar, we screened the identified *nacre* mutants for the presence of the hindbrain indentation instead, and identified double mutants in the expected 1:15 ratio. The double mutants all displayed an absence of *gch*-positive cells over somites 1-5 (Figure 4.4B). Thus, the xanthophore phenotype does not appear to be dependent on melanophore invasion.

Timelapse analysis of choker *and wild-type anterior trunk melanophores*

24 and 48 hpf *choker* mutants and wild-type siblings were analysed by timelapse microscopy for a period of up to 33 hours to monitor the behaviour of anterior trunk melanophores. As *choker* melanophores accumulate in the lateral migratory pathway, we tried to focus our analysis on the focal planes between the skin and the lateral surface of the myotome. At 48 hpf the mutants are readily distinguished from the wild types by their pigment phenotype and it is straightforward to identify embryos for timelapse analysis. In addition, previous observation has suggested that the most

Figure 4.4. *choker* xanthophores were lost from the collar even in the absence of melanophores

(A-B) Whole mount *in situ* hybridisation of 48 hpf *nacre* single and *choker;nacre* double mutants with the xanthoblast marker *gch.* Lateral views revealed a network of labelled cells and an absence of melanophores throughout the flank of the *nacre* embryos (A). *choker;nacre* double mutants showed an absence of *gch*-positive cells in the anterior trunk, although xanthoblast patterning in more posterior regions of the embryo appeared normal (B).

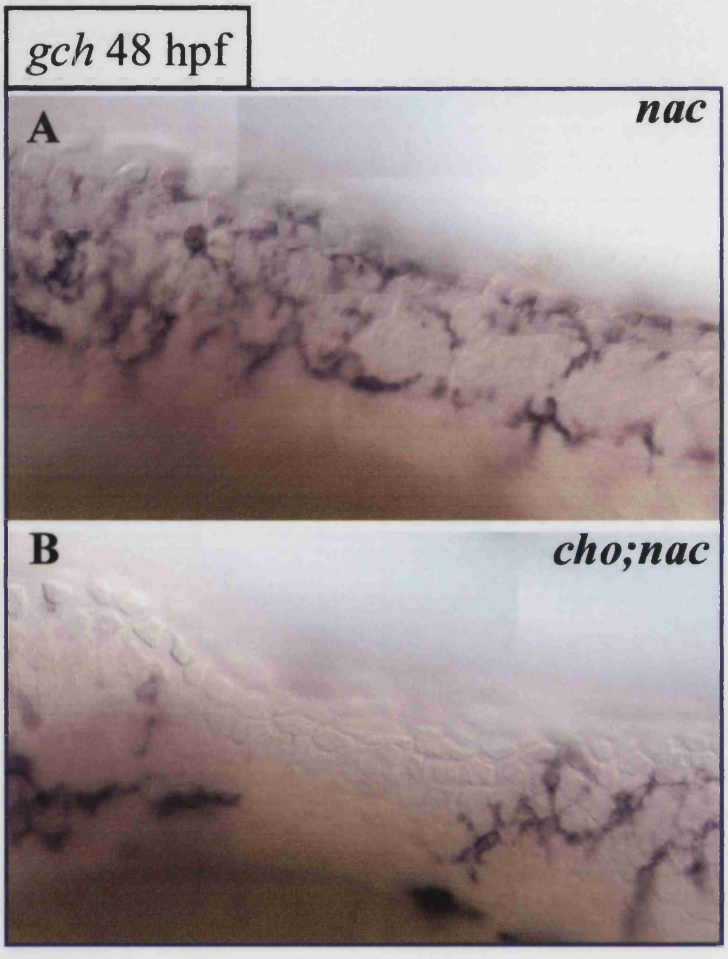
gch 48 hpf
A
nac
B
cho;nac

striking collar build up occurs between 50 and 60 hpf (see Chapter 3) and we thus expected this stage to be the most informative regarding the nature of the melanophore accumulation. To try and characterise melanophore behaviour at earlier stages, we also conducted a small number of timelapses with 24 hpf embryos (WT=3; *cho*=3). For this experiment, we first separated *choker* embryos from wild types according to the muscle apoptotic phenotype, which is detectable at 24 hpf. A wild type and a mutant were usually timelapsed alongside each other, under the same conditions, and were thus considered to be comparable.

Our timelapses of 24 hpf embryos revealed that melanophore behaviour in mutants and wild type siblings was indistinguishable over the first 15 hours of the experiment, and all melanophores displayed highly motile behaviour (Table 4.1). Wild-type melanophores were observed to emerge from the dorsal stripe and to migrate across the anterior trunk, to join the ventral stripe. Conversely, we observed melanophores emerging from the ventral stripe and migrating across the trunk to the dorsal stripe. Thus, we observed cell movement in both dorso-ventral and ventro-dorsal directions. In addition, there was also some antero-posterior and postero-anterior movement observed. Thus, following their entry into the lateral pathway, melanophores were sometimes observed to 'shuffle' anteriorly or posteriorly from their original location. Sometimes, cells were observed to stop migrating or change direction of migration upon contact with the ventral or dorsal stripes (Figure 4.5A). Thus, contact between melanophores often resulted in cell retraction and change of direction of movement (Table 4.1). After approximately 15 hours, wild-type melanophores ceased to migrate through the collar, and cells in the anterior trunk lateral pathway emigrated out of this region and seemed to settle in one of the stripes (not shown).

The behaviour of the mutant melanophores in all aspects resembled that of their wild-type counterparts for the first 15 hours of the experiment (Table 4.1). However, after this timepoint the mutant melanophores did not cease to migrate through the anterior trunk but continued to display motile behaviour throughout the remainder of the timelapse experiment, although the frequency of migration into the anterior trunk lateral pathway seemed to decrease. In all cases (n=3) one or two cells seemed unable to emigrate out of the collar and stayed in an ectopic location. These cells adopted a stellate shape and remained in this location until the end of the timelapse.

We have analysed and recorded melanophore behaviour in a number of 48 hpf *choker* mutant (n=8) and wild type embryos (n=5). At the start of the experiment, in the

Table 4.1. Melanophore migratory behaviour in *choker* mutants and wild-type siblings was comparable from 24 hpf to 39 hpf

Timelapse microscopy was used to view melanophore migration in 24 hpf *choker* mutants and wild-type siblings. At these early stages both *choker* and wild-type melanophores migrated actively in all planes. They often made contact with other melanophores, either in the lateral pathway or in one of the stripes. This contact resulted in cessation of cell movement and sometimes caused the migrating melanophore to begin moving in a different direction.

Table 4.1. Table shows the number of times that melanophore migration was observed in a particular direction, and the number of times that melanophores ceased to migrate upon contact with other melanophores over a period of approximately 15 hours, from 24 hpf to 39 hpf.

	Number of melanophores migrating in different planes (total per 15 hours)				Number of melanophores temporarily ceasing migration upon contact with other melanophores (total per 15 hours)		
Genotype	Dorso-ventral	Ventro-dorsal	Antero-posterior	Postero-anterior	Contact with dorsal stripe	Contact with ventral stripe	Contact with free melano-phore
cho		3	3	1	1		
cho	1	5		1	1	1	1
cho	2	6		2	1		
WT	2	1	2				2
WT	3	6	1	1	1	2	
WT		4	1	1		2	

Figure 4.5. Melanophores displayed distinct behaviour at early and late developmental stages

(A-B) Timelapse microscopy of a 24 hpf and a 48 hpf embryo. Four timepoints from two separate timelapse experiments are shown. (A) Lateral view of a 24 hpf wild-type embryo revealed that contact between different melanophores resulted in process retraction and the movement of the two melanophores away from each other. (B) Timelapse analysis of a 48 hpf *choker* embryo revealed that at this stage contact between different melanophores resulted in the extension of more processes and the formation of more contacts between neighbouring melanophores (arrow).

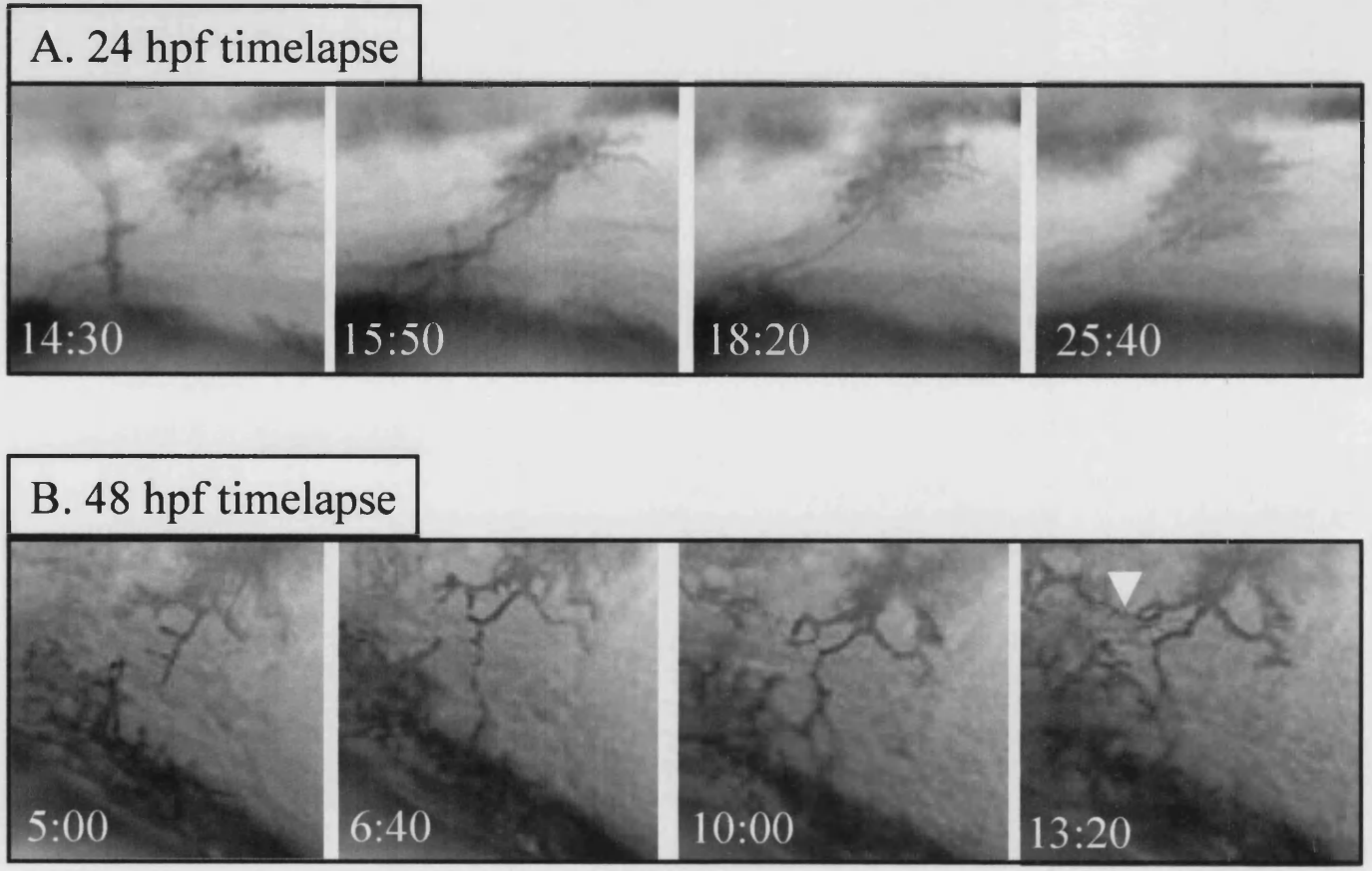
A. 24 hpf timelapse
14:30
15:50
18:20
25:40
B. 48 hpf timelapse
5:00
6:40
10:00
13:20

majority of cases (in 4 embryos out of 5), the wild-type anterior trunk lateral pathway was entirely devoid of melanophores and remained so for the remainder of the timelapse (Figure 4.6C). In one case only, there was a melanophore in the anterior trunk region (arrow, Figure 4.6A; http://www.bath.ac.uk/bio-sci/Nikolic/movies.html). The melanophore had the characteristic migratory morphology, was elongated in a dorso-ventral plane and continued to slowly migrate towards the ventral stripe. A number of hours later this melanophore was completely incorporated within the ventral stripe. In all wild-type embryos, the melanophores remained within the dorsal and ventral stripes throughout the time of observation. However, the melanophores were not static, instead displaying active behaviour by continually extending processes into the anterior trunk lateral pathway to explore their environment. These processes, however, always retracted, and the cell body remained in the stripe environment.

By comparison, all *choker* mutants (n=8) already had at least one melanophore in the collar region at the start of timelapsing (Figure 4.6B, D, E). These often had a stellate, spread out morphology and proved to be static in their location. Others continued to explore their environment with processes and to migrate over short distances, but nonetheless remained in an ectopic location. In 4 out of 8 embryos we observed melanophores that were initially in the anterior trunk lateral pathway, migrate out of this region and join the dorsal stripe (5 melanophores in total). In 2 out of 8 embryos we observed some cells emerge from the ventral stripe and then proceed to migrate through the entire anterior trunk until they joined the dorsal stripe (3 melanophores in total). It is thus not unusual for cells to migrate all the way through the collar, although we only detected this movement in a ventro-dorsal direction. In 7 out of 8 cases, we witnessed an accumulation of ectopic melanophores in the mutant anterior trunk. The melanophores clearly arrived at their ectopic location solely through migration, as we never observed any pigmentation *in situ* or proliferation. In 6 out of 8 embryos the melanophores invaded the collar region as single cells from the ventral stripe (17 melanophores in total) (arrows, Figure 4.6D, E). In a smaller number of cases (3 embryos out of 8), cells of the dorsal stripe contributed to the collar too, although they often moved as a sheet rather than individual cells (arrows, Figure 4.6B; http://www.bath.ac.uk/bio-sci/Nikolic/movies.html). Prior to invasion of the collar region, melanophores in the dorsal and ventral stripes extended processes into the anterior trunk lateral pathway. This exploratory behaviour was often followed by the cell body moving into the anterior trunk. We also observed a large number of contacts

Figure 4.6. *choker* melanophores were observed to arise in the ectopic locations through aberrant melanophore migration

(A-B, C-E). Timelapse microscopy of 48 hpf *choker* mutants and wild-type siblings revealed differences in melanophore migratory behaviour. Four timepoints from two separate timelapse experiments are shown. Lateral views of wild-type embryos showed that the wild-type anterior trunk lateral pathway was often completely devoid of melanophores (C). Occasionally, we observed a single melanophore in the wild-type anterior trunk lateral pathway (arrow, A). However, this cell emigrated out of the ectopic location by the end of the timelapse. *choker* mutants already had some melanophores in the ectopic location at the beginning of the experiment. The number of ectopic melanophores increased throughout the timelapse through sheet-like dorsal stripe migration (arrows, B), or invasion of individual cells from the ventral stripe (arrows, D, E).

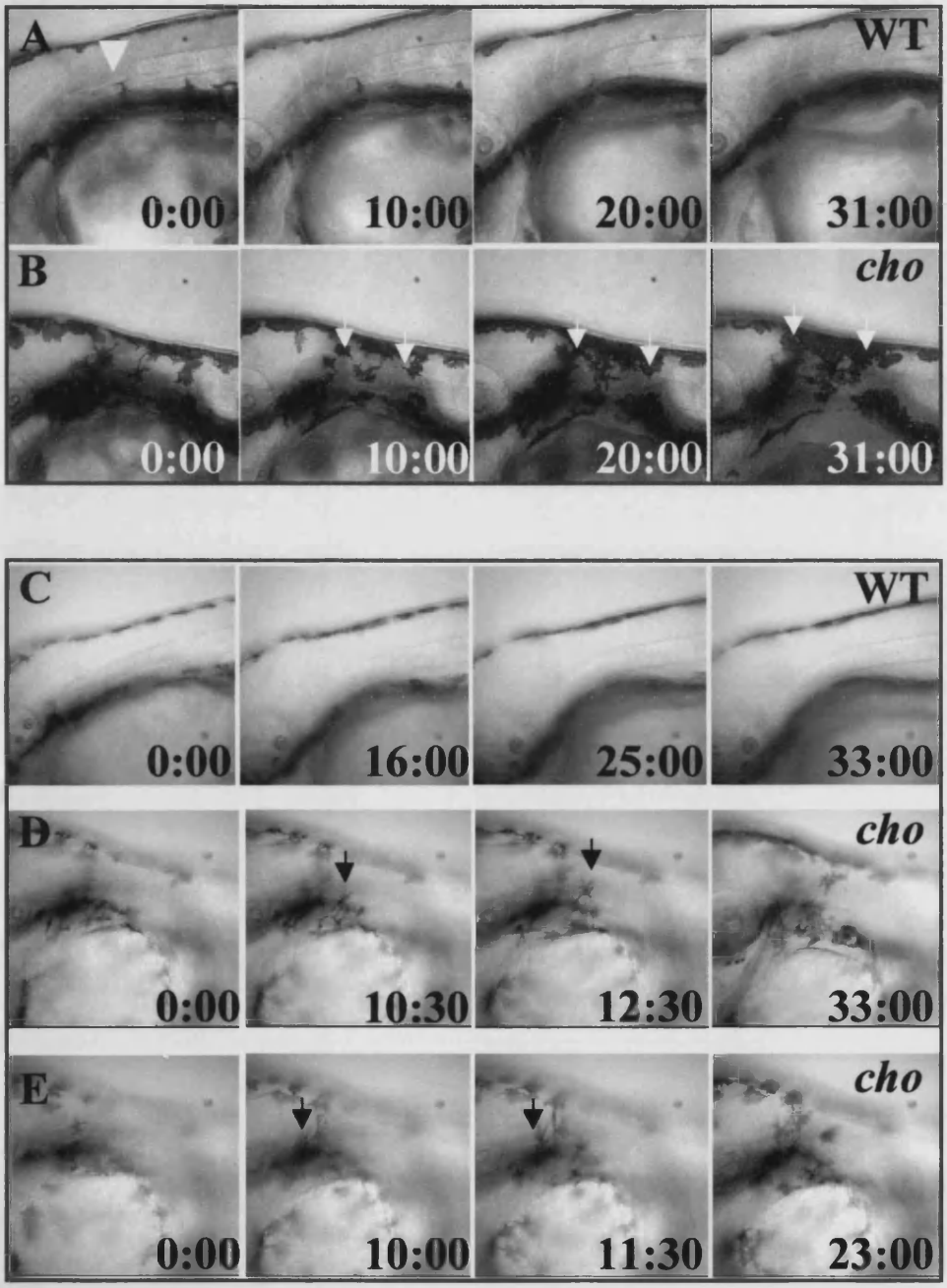
A
WT
0:00
10:00
20:00
31:00
B
cho
0:00
10:00
20:00
31:00
C
WT
0:00
16:00
25:00
33:00
D
cho
0:00
10:30
12:30
33:00
E
cho
0:00
10:00
11:30
23:00

being established between the processes of different melanophores throughout their migration, and most often, this resulted in the thickening of individual protrusions and establishment of more contacts between neighbouring melanophores (arrow, Figure 4.5B). This aberrant migratory behaviour was in all cases restricted to the anteriormost 5-6 somites of *choker* mutants. Only in one case did we observe no melanophore accumulation in the mutant collar region. However, even in this case numerous protrusions were extended into the lateral pathway environment and the cell bodies of three melanophores began to edge into this region. The melanophores in more posterior somites also displayed protrusive activity however they remained associated with the dorsal and ventral stripes at all times.

Our observations show that the *choker* melanophores accumulate in the anterior trunk through a process of aberrant migration.

Discussion

The melanophore collar does not arise through xanthophore transdifferentiation

Analysis of the *choker;pfeffer* double mutant suggests that the melanophore collar does not arise through xanthophore transdifferentiation. Despite the reduction of lateral xanthophores in *pfeffer*, *choker;pfeffer* double mutants were still able to form a melanophore collar. *pfeffer* was characterised in the 1996 Tubingen screen but its phenotype was not analysed with xanthophore-specific markers. Our analysis using the xanthophore-specific marker *gch* revealed that *pfeffer* does indeed have an absence of lateral xanthophores throughout the more posterior trunk regions. However, there were a low number of xanthophores still present in the region coinciding with the head and anterior trunk. As *pfeffer* is a gene involved in xanthophore migration these cells are unable to disperse from the neural tube (Parichy et al., 2000). However, in the head region neural crest cells tend to form more laterally and it is therefore not surprising that we find differentiating xanthophores laterally in the head and the foremost region of the trunk. However, it is unlikely that the low number of xanthophores, which are located over a small proportion of the anterior trunk area, can give rise to the full extent of the melanophore collar. This is conceivable only if the melanophores undergo extensive proliferation upon transdifferentiation to populate the whole 5 somites of the anterior trunk. Our timelapse data however suggests that this is not the case as we never saw any

dividing melanophores. This is also unlikely as melanoblast have been reported to have a small clone size (Raible and Eisen, 1994).

To strengthen the argument that xanthophores do not transdifferentiate into melanophores we looked for early melanoblast markers in the anterior trunk at 49 hpf and 52 hpf. Although our PTU-treated control embryos had labelled cells in the expected places, suggesting that the *in situ* protocol had worked, we never saw any unmelanised melanoblasts in the *choker* collar region. However, the collar melanophore accumulation occurs slowly, over a period of time and we would only expect to detect one or two transdifferentiating cells at any one time. Despite the fact that we did our analysis at the timepoints when we expected there to be the highest number of transdifferentiating cells, we cannot exclude the possibility that there was transdifferentiation underway before and after, but not at the time of, analysis. However, given the combined analysis of the *choker;pfeffer* double mutants and the melanoblast marker expression, we conclude that the melanophore collar is unlikely to arise through xanthophore transdifferentiation.

Our preliminary studies of apoptosis levels in the anterior trunk of mutants and wild-type siblings have reinforced the argument that melanophore accumulation is independent of xanthophore loss. We have shown an elevated level of apoptosis in the mutant anterior trunk, where the xanthophores are normally found. This suggests that the xanthophores do not undergo transdifferentiation but might instead undergo cell death through the absence of a survival factor. However, further analyses with xanthophore markers are required to confirm that the apoptotic cells we detected were indeed xanthophores.

Xanthophore loss from the collar is not dependent on melanophore accumulation

Previous studies have suggested a role for melanophores in patterning of embryonic xanthophores. We thus expected there to be a causal relationship between the two defects. However, the analysis of the *choker;nacre* double mutants revealed that xanthophore loss occurs independently of melanophore accumulation. Thus, *choker;nacre* double mutants which were completely devoid of melanophores, as judged by the absence of melanised cells, still had the xanthophore loss from the anterior trunk.

Our combined analyses of the *choker;pfeffer* and *choker;nacre* double mutants suggest that the two pigment defects are not causally related and might occur as separate consequences of some other primary defect, such as abnormalities in muscle patterning.

The ectopic melanophore collar forms as a direct result of aberrant melanophore migration into the anterior trunk lateral pathway

Our timelapse analyses have extended our understanding of both the *choker* defect and the process of melanophore migration in wild-type embryos. We have characterised wild-type and mutant melanophore behaviour at early stages (24 hpf onwards) as they migrate on the lateral pathway, and later (48 hpf onwards), as that pathway shuts down.

Initially, wild-type melanophores display highly motile behaviour and migrate in both dorsal-ventral and anterior-posterior planes. They frequently extend their processes and make contact with one another suggesting that they could be influencing each other's migration. In concordance with previous studies reporting on melanophore migratory behaviour we have observed melanophores often change direction of migration (Milos and Dingle, 1978a; Milos and Dingle, 1978b). On several occasions this occurred upon contact with other melanophores. Thus, melanophores that migrated towards the ventral stripe made contact with the cells already there and if the region was already densely populated, they begun to migrate in a different direction. This is consistent with studies that suggested the existence of a population-based mechanism for regulating melanophore dispersal in the lateral stripe (Milos and Dingle, 1978a; Milos and Dingle, 1978b). Thus, two consecutive waves of melanophore migration are involved in establishing the lateral stripe. Second wave melanophores, which appear in the lateral stripe around 4-5 dpf, populate the horizontal myoseptum preferentially by occupying somites that have no melanophores associated with them. Thus, melanophores only invaded an already occupied somite in 5.1% of cases, compared with the 93.5% frequency of invasion of empty somites. Our studies suggest that such may be the case for ventral stripe population too. However, more extensive studies of wild type melanophore behaviour and tracking of single cells are necessary to confirm these preliminary observations.

Approximately 15 hours after the start of the timelapse (around 39 hpf), wild-type melanophores ceased to migrate into the anterior trunk lateral pathway, and the cells already in this region emigrated out to join one of the stripes. This decrease in

melanophore number has already been shown in our cell counts (see Chapter 3). It is likely to reflect a shutdown of the lateral migratory pathway, which occurs in a rostro-caudal direction, and our melanophore counts suggest that this process occurs around 36 hpf. We have observed that timelapsed embryos appear to be somewhat slowed in their development. Thus, our timelapse data suggests that lateral pathway shutdown in the anterior trunk occurs slightly later, at approximately 39 hpf.

Timelapse analyses of older wild-type embryos revealed that, following lateral pathway shutdown, melanophores remain tightly associated with their stripes but still display exploratory behaviour. We saw melanophores extending processes into the lateral pathway environment, making contact with the lateral face of the somite and then collapsing. Similar observations in other timelapse studies have led to the suggestion that the delay in initiation of lateral pathway migration is due to an inhibitory activity associated with the lateral face of the somite (Jesuthasan, 1996). Studies have shown that inhibitors such as chondroitin sulphates, glycoconjugates and members of the Eph receptor and ephrin ligand family have a role in delaying melanophore migration on the lateral pathway in chick (Oakley et al., 1994; Santiago and Erickson, 2002). We propose that the case is similar at the time of lateral pathway shutdown in zebrafish. We propose that one or more inhibitors of neural crest migration become upregulated in the lateral pathway environment or on the neural crest cell surface, and act as effectors of lateral pathway shutdown by preventing further neural crest migration on this pathway.

The migratory behaviour of *choker* melanophores at early stages largely resembled that of wild type ones. Melanophores were observed to actively migrate through the collar for a number of hours and there was no sign of static cells until the time of lateral pathway shutdown. At this stage, as in wild types, many melanophores emigrated out of the anterior trunk lateral pathway and joined the dorsal or ventral stripes. However, 1-2 cells in each embryo did not leave this environment and instead adopted a non-migratory shape and remained in the ectopic location. Melanophores continued to migrate into the mutant collar region but they now did so with a lower frequency than at earlier stages.

The analysis of later stages, when there are already a number of ectopic melanophores in the *choker* collar, revealed that stripe melanophores continued to invade the anterior trunk environment long after their wild type counterparts had stopped migrating. Just like wild type melanophores, they extended protrusions into the lateral pathway but no process retraction was observed, instead, the whole cell body

followed into the lateral pathway environment. Protrusions of distinct melanophores often came into contact with one another and resulted in the production of more contact points between neighbouring melanophores. In this way melanophores made contact with each other and established the 'network' of ectopic cells in the anterior trunk. This behaviour is reminiscent of the way neural crest cells have been reported to behave before the onset of neural crest migration (Jesuthasan, 1996). However, in our analyses of early wild type and *choker* embryos we have shown that migrating melanophores retract upon making contact with each other. This suggests that the way melanophores influence one another can vary; at stages prior to initiation of migration, and following completion of migration, when melanophores have to maintain their position, they may contact and 'stabilise' each other. In contrast, during the time of lateral pathway migration melanophores are encouraged to migrate and populate empty spaces and thus contact with each other may result in retraction and reversal of movement.

Our timelapse studies show that the ectopic melanophore collar in *choker* mutants arises through aberrant migration of stripe melanophores into the lateral pathway environment. We propose that *choker* mutants have a defect in a molecule that act as an inhibitor of migration, and effector of lateral pathway shutdown in wild -type embryos. In the absence of this molecule, *choker* melanophores interpret the lateral pathway environment as being permissive and continue to migrate into it. In addition to effecting lateral pathway shutdown, this putative inhibitor also has an important role in the maintenance of discrete melanophore stripes as in its absence melanophores do not remain associated with the stripe environment.

There may be one or more molecules responsible for lateral pathway shutdown. Studies in other organisms suggest that there are a plethora of molecules involved in the control of cell and axon migration and often, knocking out one of these molecules results in no gross phenotype due to this great redundancy. We propose that as a result of the aberrantly patterned muscle, a number of somite-associated molecules might be incorrectly distributed. The xanthophore loss and melanophore invasion may occur as a direct consequence of the aberrant patterning of these molecules in *choker* mutants. Alternatively, the defect in the *choker* gene might be the primary cause of both the defective neural crest patterning and the aberrant muscle development. The defect underlying many aspects of the *choker* phenotype appears to be one of migration. The ectopic melanophores accumulate in the anterior trunk due to aberrant migration. One aspect of the muscle defect is the inability of the adaxial cells to migrate to the surface

of the somite. It is thus conceivable that the mutation lies in a gene whose role is in regulating the migration of several distinct cell types. Whether the melanophore defect is cell autonomous or caused by aberrant environmental cues are possibilities that will be tested in the following chapter.

Chapter 5

Preliminary attempts to address cell autonomy

Introduction

Our studies revealed that *choker* mutants have defects in the patterning of two neural crest derivatives: melanophores and xanthophores. We have shown that there is no causal relationship between these two defects (see Chapter 4). However, they are spatially restricted to a region of aberrant muscle development (RN Kelsh, personal communication; G Hollway, personal communication) and it is conceivable that both neural crest defects might occur as a secondary consequence of the defective muscle patterning.

Somites have been shown to have an important role in several aspects of neural crest migration, from initiation to guidance (see chapter 1). Following their dispersal from the neural tube, neural crest cells migrate along one of two migratory pathways, both of which are adjacent to the somite. Hence, the somite is ideally positioned to produce cues that will neural initiate crest migration and guide neural crest cells as they migrate.

The role of somites in neural crest delamination has been shown in somite ablation experiments. The dorso-medial quadrant of the somite was shown to secrete a factor which releases BMP4 from its inhibition by *noggin* and consequently triggers neural crest delamination (Sela-Donenfeld and Kalcheim, 1999; Sela-Donenfeld and Kalcheim, 2000). The importance of somite-associated cues has also been shown in the initiation of neural crest migration on both the medial and lateral migratory pathways. Thus, timelapse studies in the zebrafish have shown that protrusions extended by neural crest cells during pre-migratory stages collapse upon contact with the immature somite (Jesuthasan, 1996). Similarly, protrusion collapse is seen when neural crest cells explore the lateral face of the somite prior to the opening of the lateral migratory pathway. In addition to their importance in the initiation of neural crest migration, somites have a well-documented role in the guidance of neural crest cells during migration (see Chapter 1). This has been especially well-studied in the chick, where neural crest migration on

the medial pathway is restricted to the rostral portion of the sclerotome, and a number of somite-associated molecules that play a role in controlling the segmental nature of medial pathway migration in avian embryos have been identified (reviewed in Bronner-Fraser, 2000; Krull, 2001). By comparison, the zebrafish sclerotome is a very small population of cells, and ablation experiments have shown that it has no role in peripheral nervous system development. Hence it is thought to be unlikely to have a role in the patterning of other neural crest derivatives (Morin-Kensicki and Eisen, 1997). The role of the zebrafish sclerotome may therefore not be analogous to its role in chick. Instead, zebrafish neural crest migration might be influenced by cues from the myotome, which is the larger portion of the somite in zebrafish, and is spatially correctly positioned to influence NC migration.

Testing cell autonomy by gastrula transplantation

Given the pivotal role of somites in neural crest migration it is conceivable that a severe disruption of somite patterning would result in an aberrant distribution of key neural crest guidance molecules and consequently, in anomalous neural crest patterning. Our studies have shown that the ectopic melanophore accumulation in *choker* mutants is caused by aberrant melanophore migration into the lateral pathway environment (see Chapter 4). We wanted to test the hypothesis that this defect is not autonomous to melanophores but that it occurs as a consequence of aberrant environmental cues. We therefore transplanted labelled undifferentiated wild-type cells from a 1000-cell donor embryo into a shield-stage host *choker* embryo to try to establish whether the environmental signals present in the mutant host embryo can induce the transplanted, wild-type cells to behave in a mutant fashion. We attempted to transplant cells into a region of the host embryo that is predicted to give rise to the neural crest. In this way, many of the undifferentiated, transplanted cells will develop into neural crest cells and a subset of these will give rise to melanophores. A small proportion of wild-type labelled melanophores will be found in the anterior trunk region where we can monitor their behaviour and see whether they contribute to the ectopic melanophore collar. If our prediction is correct and the *choker* melanophore defect is not cell-autonomous we would expect wild-type melanophores transplanted into a *choker* environment to behave as mutant cells, and accumulate in the anterior trunk lateral pathway location despite their wild-type origin. Conversely, if the melanophore defect is cell autonomous we

would expect never to detect the transplanted wild type cells in the ectopic location. Instead, they should always to be found in one of the melanophore stripes.

This method has been previously successfully used in zebrafish to test for cell autonomy in various mutants, including *colourless*, *nacre* and *shady* (Kelsh and Eisen, 2000; Lister et al., 1999; SS Lopes, personal communication). The *colourless* mutant has defects in non-ectomesenchymal neural crest derivatives, including pigment cells and the neurons and glia of the peripheral nervous system. To establish whether the mutation affects non-ectomesenchymal cells autonomously, labelled wild-type cells were transplanted into *colourless* embryos. These gave rise to numerous neural crest derivatives which were able to migrate on both lateral and medial pathways and developed into wild-type pigment cells. Conversely, *colourless* cells transplanted into *albino* hosts were never observed to generate wild-type melanophores. It was thus concluded that the *colourless* gene acts cell-autonomously. In a similar experiment, cell autonomy was established for the *shady* mutant, which has a reduction in iridophore number. When labelled wild-type cells were transplanted into a *shady* host they were observed to give rise to normal, wild type iridophores. Thus, it was concluded that the iridophore defect in *shady* mutants is cell-autonomous. The same approach was used to determine cell autonomy in *nacre*, a zebrafish mutant that has a melanophore specification defect. Labelled wild-type cells were placed into a *nacre* donor and on the following day the injected donors were screened for the presence of melanophores. Melanised, labelled cells of wild-type origin were detected in a *nacre* mutant background and this gene was thus deduced to be acting cell-autonomously.

In addition to targeting neural crest cells, we also conducted a preliminary experiment to test whether transplanting wild-type somite cells into the anterior trunk of a *choker* embryo can rescue the mutant melanophore phenotype and prevent melanophore accumulation in the ectopic location. We attempted to inject undifferentiated wild-type donor cells into a region of a host gastrula that has been shown to give rise to somitic muscle. If the *choker* melanophore defect is not cell-autonomous we would expect the transplantation of a sufficiently high number of wild-type somite cells into the *choker* anterior trunk to, at least partially, rescue the ectopic melanophore defect. Alternatively, if the melanophore defect is cell-autonomous then the transplantation of wild-type somite cells into the *choker* anterior trunk will not affect melanophore accumulation in the collar region.

Zebrafish shield stage fate map

The fate map of a zebrafish shield-stage embryo has been studied in various single cell injection and caged fluorescein studies (Kimmel et al., 1990; Kozlowski et al., 1997; Woo and Fraser, 1995). The first of these studies has roughly mapped the neural crest region to the ventral half of the gastrula, relatively near to the margin (n, Figure 5.1A) (Kimmel et al., 1990). A later study confirmed these initial observations and complemented them by revealing that, instead of being restricted to a belt near the margin, cells that give rise to the neural crest appear to be located in a wide domain between 20° latitude and the animal pole (yellow, Figure 5.1B) (Woo and Fraser, 1995). This region was also found to give rise to other ectodermal derivatives including the ear placodes and epidermis. Cranial neural crest and head epidermis were placed in the more dorsal region of this domain, 70°-110° from the midline, and trunk neural crest and trunk and tail epidermis more laterally, beyond 110°. Thus, there is a dorso-ventral order to neural crest distribution, with cranial neural crest being located closer to the shield.

Muscle progenitors have been mapped to a ring of cells near the margin – the more dorsal cells in this ring give rise to muscle in the head, whereas their ventral counterparts generate trunk and tail somite muscle (Figure 5.1C) (Kimmel et al., 1990). Thus, there is a correlation between the position of cells at this stage and the ultimate anteroposterior location of the somite. These findings were confirmed in later studies and the correlation between cell position and anteroposterior location of somite was found to be diagonal (Kozlowski et al., 1997). Thus, cells in a more dorsal/animal position were found to give rise to more anterior somites.

Results

Neural crest transplantation

In order to test our hypothesis, we had to inject a high number of undifferentiated donor cells into a region of the shield-stage host embryo that will go on to generate the neural crest. The donor cells were labelled at the one-cell stage with 5% Rhodamine/5% Biotin dye (see Chapter 2) which is red and easily seen, thus it was possible to determine which region of the embryo we were injecting cells into.

Figure 5.1 Published fate maps of the zebrafish 6 hour gastrula show the areas that neural crest and somitic muscle are derived from

The region of the shield-stage embryo that the neural crest is derived from has been found to correspond to a domain on the ventral half of the gastrula, between 20° latitude and the animal pole (n, A; yellow, B). This region also gives rise to other ectodermal derivatives such as the ear placodes and the epidermis. Somitic muscle is found below this domain, in a belt of cells located close to the margin on the ventral side of the gastrula (C). The corresponding belt of cells on the dorsal side of the gastrula gives rise to head muscle. A (animal pole); V (ventral); D (dorsal).

A. Kimmel *et al,* 1990

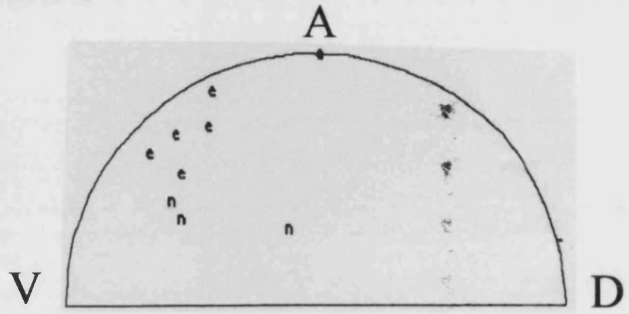

B. Woo and Fraser, 1997

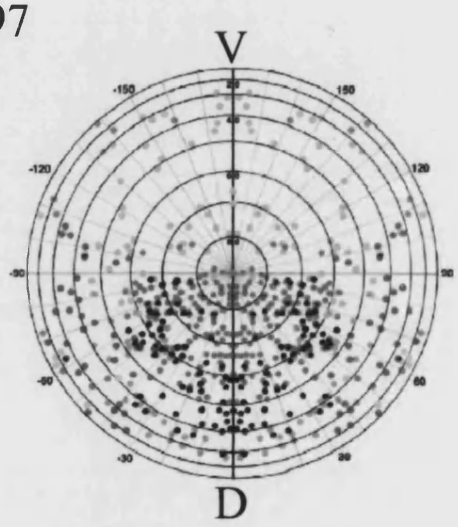

C. Kimmel *et al,* 1990

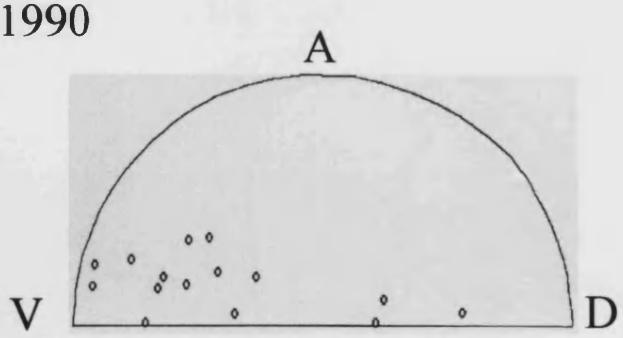

We attempted to inject approximately 50 wild type cells into each mutant host. However, as we were unable to distinguish *choker* embryos from wild-type siblings at such an early stage we had to inject whole batches of embryos obtained from crosses of heterozygous parents. Typically, we injected approximately 40 embryos per transplant experiment and expected a quarter of those to be mutant.

Following labelling, the embryos were reared to 2 days of age and then screened for the presence of labelled neural crest derivatives. The donor embryos were readily identified by the red coloration lent them by rhodamine injection, and the *choker* mutants were distinguished from their wild-type siblings by their ectopic melanophore collar. If labelled neural crest derivatives were found in the anterior trunk of *choker* mutants at 2 dpf, their position was monitored by repeating the screening process at 3 dpf.

During cell transplantation we initially immobilised host embryos so that the shield was facing right (Figure 5.2A). We transplanted cells into the ventral half of the exposed side of the gastrula, beyond 20° latitude (Figure 5.2A), which was expected to target the neural crest. Although we tried to place our transplanted cells accurately into the desired area, precise targeting was not always possible and cells were often injected more broadly into the neural crest area and surrounding regions. As a result, we labelled numerous cell types including neurons in the hindbrain and neural tube, somitic muscle, and skin. In a lower number of cases we also labelled endothelial cells. In 67% of cases (n = 12) we successfully labelled neural crest cells, both undifferentiated and differentiated (Table 5.1, Appendix A). The undifferentiated crest cells were either seen on top of the neural tube, in migrating positions on the lateral and medial pathways or in one of the pigment stripes. They were identified as crest cells by their position and characteristic spindly morphology. The only differentiated neural crest cells we observed at this stage were fin mesenchyme, lateral stripe glia and cells that had a spider-like morphology but were as yet unpigmented. These could be either xanthoblasts or melanoblasts and were recorded as such. Only in a low number of cases were we able to label anterior trunk neural crest cells (8.3%) (Table 5.1).

To improve the frequency of neural crest labelling, particularly in the anterior trunk, we tried to immobilise the host embryos in a different orientation, with the ventral half of the gastrula facing upwards and the shield facing downwards (Figure 5.2B). In this position the whole exposed side of the gastrula beyond 20° latitude is expected to give rise to the neural crest. We found that, by positioning the embryos in

Figure 5.2 Host embryos were immobilized in various orientations to improve the efficiency of cell injection into the neural crest region

The host embryo was initially positioned with the shield facing right and cells were injected into the region highlighted on panel A. This was expected to give rise to all types of trunk neural crest derivatives. Subsequently, the embryos were rotated so that the shield faced downwards. This way, the ventral side of the gastrula was face up and most of its exposed side was expected to give rise to neural crest (B). Finally we attempted to target anterior trunk neural crest by injecting cells into a region close to the animal pole (C). This area was expected to give rise to predominantly anterior trunk neural crest.

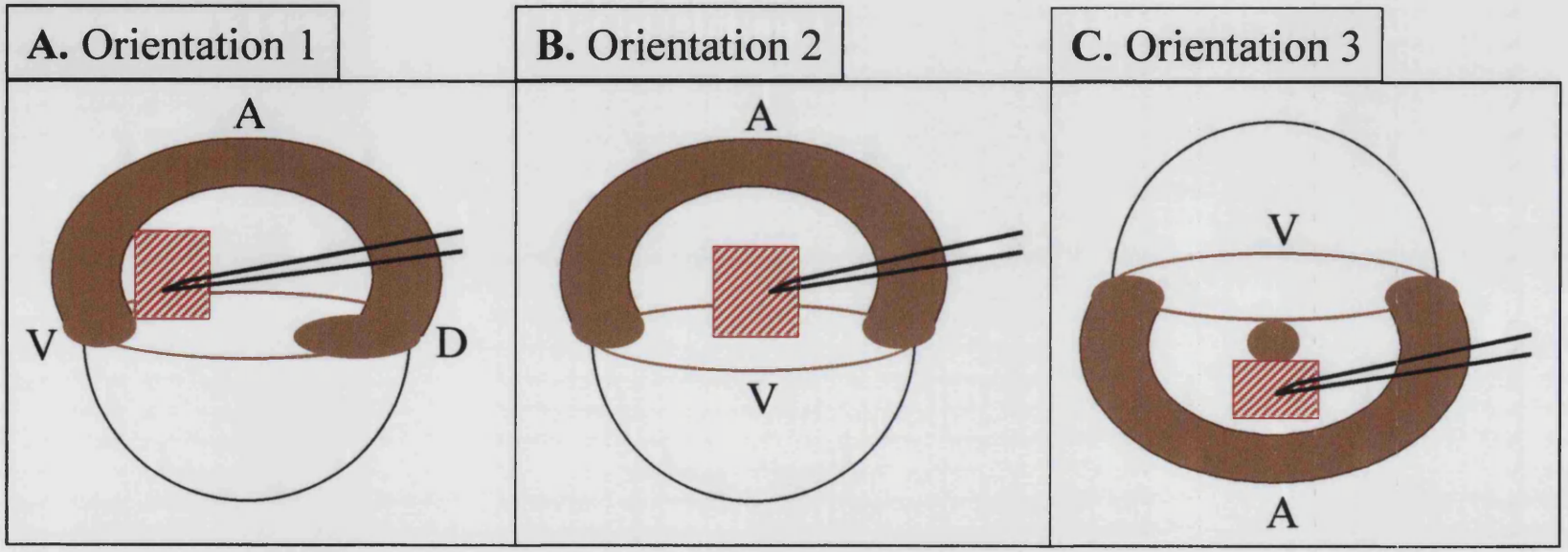

Shield

A – animal pole

V – ventral

D – dorsal

Table 5.1 The overall efficiency of neural crest targeting, and the proportion of anterior trunk neural crest labelled varied with different embryo orientations

Neural crest cells were successfully targeted when host embryos were immobilized in orientation A. However, the efficiency of neural crest labelling was significantly improved when embryos were immobilized in orientation B. In both orientations the vast majority of neural crest labelled was in the tail, while the efficiency of neural crest labelling in the anterior trunk remained low. Immobilising the embryos in orientation C resulted in a large decrease in neural crest targeting efficiency. Consequently, the efficiency of anterior trunk neural crest labelling remained low. However, the proportion of labelled anterior trunk neural crest with respect to total neural crest targeted was now higher.

Table 5.1. The overall efficiency of neural crest targeting, and the proportion of anterior trunk neural crest labelled varied with different embryo orientations.

	Orientation 1	Orientation 2	Orientation 3
Total number of embryos	12	21	53
Number of embryos with labelled NC	8	19	31
Proportion of embryos with labelled NC	66.7%	90.5%	58.5%
Number of embryos with labelled head NC	3	1	9
Proportion of embryos with labelled head NC	25%	4.76%	17.0%
Number of embryos with labelled anterior trunk NC	1	4	9
Proportion of embryos with labelled anterior trunk NC	8.33%	19.0%	17.0%
Number of embryos with labelled posterior trunk NC	3	5	13
Proportion of embryos with labelled posterior trunk NC	25.0%	23.8%	24.5%
Number of embryos with labelled tail NC	4	17	17
Proportion of embryos with labelled tail NC	33.0%	81.0%	32.1%
Ratio anterior trunk NC:total NC targeted	approx.1:8	approx. 1:5	approx. 1:3

this fashion, we still labelled a variety of cells including hindbrain and neural tube neurons, somitic muscle, skin cells and, in a lower number of cases, neuromasts, endothelial cells and blood cells. However, we found that the efficiency of neural crest targeting was now much improved and we labelled neural crest cells in 90.5% of cases (Table 5.1). We again labelled a mixture of undifferentiated and differentiated neural crest cells (Appendix B). The latter included fin mesenchyme and unpigmented cells with a morphology of xanthoblasts or melanoblasts. In a low number of cases we also labelled pigmented melanophores and xanthophores. However, we still largely targeted neural crest cells in the tail and posterior trunk regions. Anterior trunk neural crest was only labelled in 19% of cases, compared with tail neural crest which was targeted in 81% of cases (Table 5.1, Appendix B).

To improve the accuracy of anterior trunk neural crest targeting we attempted to inject cells into a region of the host embryo that is expected to give rise to anterior trunk neural crest. As previous studies have shown a correlation between cell position in the gastrula and final anteroposterior location for somitic cells (Kimmel et al., 1990; Kozlowski et al., 1997), we assumed that a similar relationship might exist for neural crest cells. If cranial neural crest is derived from more dorsal regions of the neural crest domain then we assumed that cells at progressively more ventral positions might ultimately develop into neural crest cells at more posterior axial levels. Thus, we might expect anterior trunk neural crest to be derived from the region adjacent to the border of cranial and trunk neural crest – beyond 20° latitude and between 110°-140° longitude. Hence, we tried injecting cells into a band close to the animal pole where we expected to label a mixture of cranial and anterior trunk neural crest (Figure 5.2C). By immobilising the embryos in this position we again labelled all of the cell types previously described, including neurons, somitic muscle and skin. By using this orientation the frequency of neural crest labelling was decreased to 58.5% (Table 5.1). Again we most frequently labelled undifferentiated neural crest cells, fin mesenchyme, melanophores and xanthophores (Appendix C). The overall efficiency of anterior trunk neural crest targeting remained low, presumably due to the decrease in overall neural crest labelling (17%). However, the ratio of anterior trunk neural crest labelled to total neural crest labelled was now higher indicating that, although we didn't target neural crest as often as in previous attempts, when we did, it often developed into anterior trunk neural crest (Table 5.1).

On the whole, we found that labelled neural crest cells were observed at high frequencies in the tail and posterior trunk and at a lower frequency in the anterior trunk and head (Table 5.2). This was due to the fact that, although the distribution of labelled pigment cells appeared relatively even across the whole trunk, labelled fin mesenchyme and unidentified neural crest cells were found at a much higher frequency at the more posterior axial levels (Table 5.3 and Figure 5.3). We only detected labelled anterior trunk melanophores on two occasions, but in both cases the melanophores were located posterior to our region of interest, over somites 6-8. However, anterior trunk xanthophores were detected a little more frequently (7/86). In *choker* mutants, these were always observed in the region immediately anterior to and bordering on the first somite, or posterior to somite 4. When neural crest cells were detected in the anterior trunk region of *choker* mutants at day 2, the screening was repeated on day 3. This only occurred in a limited number of cases (4/86). On two of these occasions there appeared to have been a slight change in cell number with respect to that recorded on day two. Thus, on two separate occasions we observed one xanthophore in a particular position on day two and found that on the following day there were two xanthophores there. Furthermore, on two occasions we also recorded a melanophore and some xanthophores in a particular position at day 2 and found they were no longer there at day 3. These apparent redistributions could be due to proliferation or migration of pigment cells. However, despite the changes in cell number and position we still observed no labelled wild-type xanthophores between somites 1 and 4 of *choker* mutants. We occasionally observed anterior trunk xanthophores in wild types, and in one case these were found over somites 1-2.

The results of our neural crest transplantations are summarised in Table 5.1, Table 5.2, Table 5.3 and Figure 5.3.

Transplantation into cho/nac *double mutants*

Due to their large number, dark coloration and small clone size, labelled melanophores may be difficult to detect. We thus attempted to transplant cells from a wild-type donor into a *cho/nac* double mutant. A *cho/nac* double mutant is characterised by its complete lack of melanophores, thus any melanophores observed in this mutant would have originated from the donor embryo and would be easily detectable. In addition, we hoped that, in the absence of their neighbours, the donor melanophores might be induced to proliferate at a higher rate than normal and migrate away from their

Table 5.2 The overall efficiency of neural crest targeting in posterior trunk and tail regions was progressively higher than the labelling of anterior trunk neural crest

The number of embryos in which we detected labelled neural crest derivatives and the axial level at which these were found has been recorded. A similar number of embryos had labelled crest in the head and the anterior trunk, whereas the efficiency of targeting posterior trunk and tail regions was progressively higher.

Table 5.3 Pigment cells were labelled with similar efficiency at all axial levels whereas the targeting of fin mesenchyme and unidentified derivatives was highest in the tail

The main types of labelled neural crest derivatives observed in host embryos were xanthophores and fin mesenchyme. The frequency of labelled melanophores was, by comparison, relatively low. Although labelled melanophores and xanthophores were evenly distributed across all trunk regions, the total number of labelled crest derivatives was the highest in the tail, where we observed numerous fin mesenchyme cells and several unidentified neural crest cells.

Table 5.2 The overall targeting efficiency of posterior trunk and tail neural crest was progressively higher than that of neural crest in the anterior trunk

	Number of embryos with labelled neural crest				
Injected	**Overall NC**	**Head NC**	**Anterior trunk NC**	**Posterior trunk NC**	**Tail NC**
86	58	13	14	21	38

Table 5.3 Pigment cells were labelled with similar efficiency at all axial levels whereas the targeting of fin mesenchyme and unidentified derivatives was highest in the tail

Region	NC derivative labelled	Number of embryos
Head	Melanophore	3
	Xanthophore	3
	Xanthoblast/Melanoblast	8
	Unidentified	3
	No labelled NC	73
Anterior Trunk	Glia	1
	Melanophore	2
	Xanthophore	7
	Xanthoblast/Melanoblast	5
	Unidentified	3
	No labelled NC	72
Posterior Trunk	Melanophore	1
	Xanthophore	8
	Xanthoblast/Melanoblast	5
	Fin Mesenchyme	3
	Unidentified	8
	No labelled NC	65
Tail	Melanophore	2
	Xanthophore	9
	Xanthoblast/Melanoblast	4
	Fin Mesenchyme	25
	Unidentified	18
	No labelled NC	48

Figure 5.3 Pigment cells were labelled with similar efficiency at all axial levels whereas the targeting of fin mesenchyme and unidentified derivatives was highest in the tail

The main types of labelled neural crest derivatives observed in host embryos were xanthophores and fin mesenchyme. The frequency of labelled melanophores was, by comparison, relatively low. Although labelled melanophores and xanthophores were evenly distributed across all trunk regions, the total number of labelled crest derivatives was the highest in the tail, where we observed numerous fin mesenchyme cells and several unidentified neural crest cells.

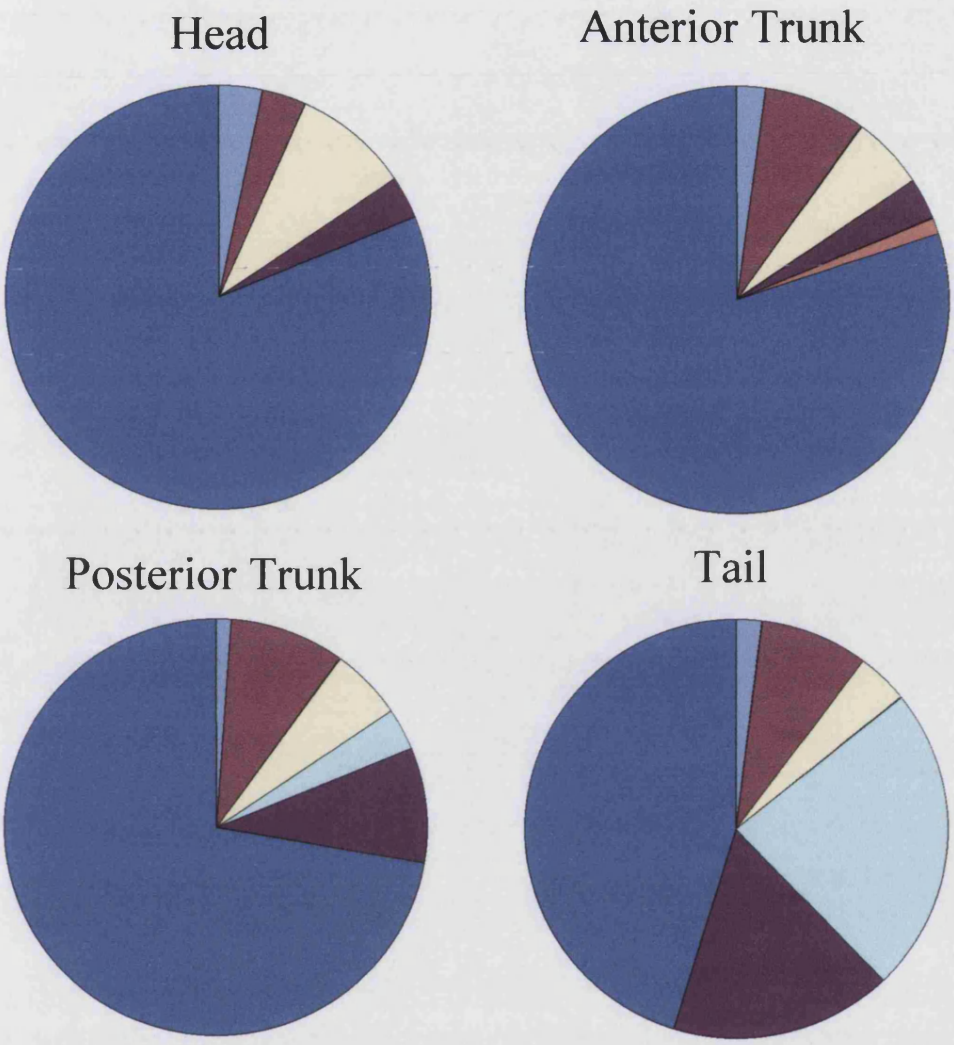
Head
Anterior Trunk
Posterior Trunk
Tail
LEGEND:
Melanophore
Xanthophore
Xanthoblast/Melanoblast
Glia
Fin Mesenchyme
Unidentified
No labeled NC

origin in order to populate other areas of the trunk. The double mutants were obtained from a cross of parents that were identified carriers for both alleles. The transplantation was carried out as detailed before and the embryos were reared as normal until 24 hpf. At this stage we separated the embryos carrying the *choker* mutation from their wild-type siblings by screening for the *choker* apoptotic muscle phenotype (see Chapter 3). The embryos carrying the *nacre* mutation were easily identified by their lack of melanophores. Both single and double mutants were kept for screening, and the wild types discarded.

Out of the 56 host embryos injected in this transplant experiment, 6 were *choker,* 3 were *nacre* and only one was a *choker;nacre* double mutant. We were unable to detect any melanophores in the latter. However, we also analysed three *nacre* mutants for the presence of any labelled or unlabelled melanophores. In 2 of 3 of the *nacre* mutants we readily detected some labelled melanophores in the head and in the tail. These were however all clustered together in a group of 2-3 cells and showed no indication of over-proliferation or migration to other axial levels. These preliminary results suggest that there appears to be no overt advantage in transplanting cells into *choker;nacre* double mutants.

Transplantation of somite cells

As we encountered problems with targeting anterior trunk neural crest we decided to attempt targeting muscle cells. In our previous transplants we noted that we often labelled contiguous sets of muscle fibres and sometimes even a whole somite. We thus hypothesised that if we specifically targeted muscle we might be able to rescue whole somites in the anterior trunk and, if the melanophore defect is non cell-autonomous, to observe a partial rescue. Previous studies have determined the location of somitic muscle on the zebrafish shield stage fate map and have also found that the ultimate antero-posterior location of a somite correlates with its dorso-ventral position on the fate map. Thus, more anterior somites are derived from more dorsal regions of the muscle band on the fate map. Consequently, we attempted to target a band of cells lying between 100° and 120° longitude and 10°-20° latitude. As in previous transplants, we found that we labelled numerous cell types including neural tube neurons, skin cells and even some neural crest cells which were largely fin mesenchyme and xanthophores. However, as in previous attempts, although we frequently observed labelled muscle in the tail and, to a lesser degree, in the posterior trunk, we saw no labelled muscle fibres

in the anterior trunk (Table 5.4 and 5.5. and Figure 5.4). Thus, although we labelled tail muscle fibres in 90% of cases, we never targeted any somitic muscle in the anterior trunk.

Discussion

Targeting anterior trunk neural crest

Our transplantation experiments didn't give us a conclusive result. The fate map for the zebrafish shield stage gastrula has been comprehensively studied and the region that gives rise to the neural crest identified. However, there is still no information on the location that various subsets of trunk neural crest originate from and whether there is any correlation between position at shield stage and ultimate antero-posterior location. In our experiments we tried to vary both the orientation of the host embryo during injection, and the region that we injected cells into, in order to maximise labelling of anterior trunk neural crest. The varying of embryo orientation was reflected in the efficiency of neural crest targeting. Thus, changing the embryo orientation so that the whole exposed side of the gastrula gave rise to the neural crest (orientation 2) dramatically improved neural crest labelling efficiency from 66.7% to 90.5%. Although this also resulted in an improvement of anterior trunk neural crest labelling, the latter still remained relatively low. Immobilising the host embryos in position 3, so that we injected cells into a region where we assumed anterior trunk neural crest to be generated from, decreased the overall efficiency of neural crest targeting. Consequently the overall efficiency of anterior trunk neural crest labelling was also decreased. This might be due to the fact that we were injecting cells quite close to the border of the neural crest area on the fate map and consequently didn't label neural crest as efficiently as before due to 'spill-over' of injected cells into surrounding areas. However, on the occasions when we successfully labelled neural crest cells they often developed into anterior trunk derivatives. Thus, when we immobilised host embryos in orientation 1 and orientation 2, anterior trunk neural crest only made up one eight and one fifth of total neural crest labelled (Table 1). In orientation 3 however, anterior trunk neural crest made up one third of total neural crest labelled. This suggests that we were injecting cells close to the area where anterior trunk neural crest is derived from. However, despite several

Table 5.4 Posterior trunk and tail muscle were targeted with a high efficiency, whereas we never labelled any head or anterior trunk muscle cells

The number of embryos in which we detected labelled somitic muscle cells and the axial level at which these were found has been recorded. The efficiency of targeting somitic muscle in the posterior trunk and tail regions was very high. However, we never labelled any muscle cells in the anterior trunk or head region.

Table 5.5 Muscle cells were successfully targeted in the posterior trunk and tail, while the labelling of skin cells and neurons was high throughout the trunk

During the transplantation of somitic muscle precursors we successfully targeted posterior trunk or tail muscle in almost every embryo. However, in 10 attempts, we never observed any labelled muscle cells in the anterior trunk of host embryos. By comparison, the labelling of neurons and skin cells was high throughout the trunk, but absent in the head.

Table 5.4 Posterior trunk and tail muscle were targeted with a high efficiency, whereas we never labelled any head or anterior trunk muscle cells

	Number of embryos with labelled muscle cells				
Injected	**Overall muscle**	**Head muscle**	**Anterior trunk muscle**	**Posterior trunk muscle**	**Tail muscle**
10	10	0	0	10	9

Table 5.5 Muscle cells were successfully targeted in the posterior trunk and tail, while the labelling of skin cells and neurons was high throughout the trunk

Region	Cell type labelled	Number of embryos
Head	Muscle	0
	Neural Crest	1
	Neurons	0
	Skin	0
	No label	9
Anterior Trunk	Muscle	0
	Neural Crest	1
	Neurons	6
	Skin	3
	No label	2
Posterior Trunk	Muscle	10
	Neural Crest	1
	Neurons	7
	Skin	5
	No label	0
Tail	Muscle	9
	Neural Crest	3
	Neurons	8
	Skin	4
	No label	1

Figure 5.4 Muscle cells were successfully targeted in the posterior trunk and tail, while the labelling of skin cells and neurons was high throughout the trunk

During the transplantation of somitic muscle precursors we successfully targeted posterior trunk or tail muscle in almost every embryo. However, in 10 attempts, we never observed any labelled muscle cells in the anterior trunk of host embryos. By comparison, the labelling of neurons and skin cells was high throughout the trunk, but absent in the head.

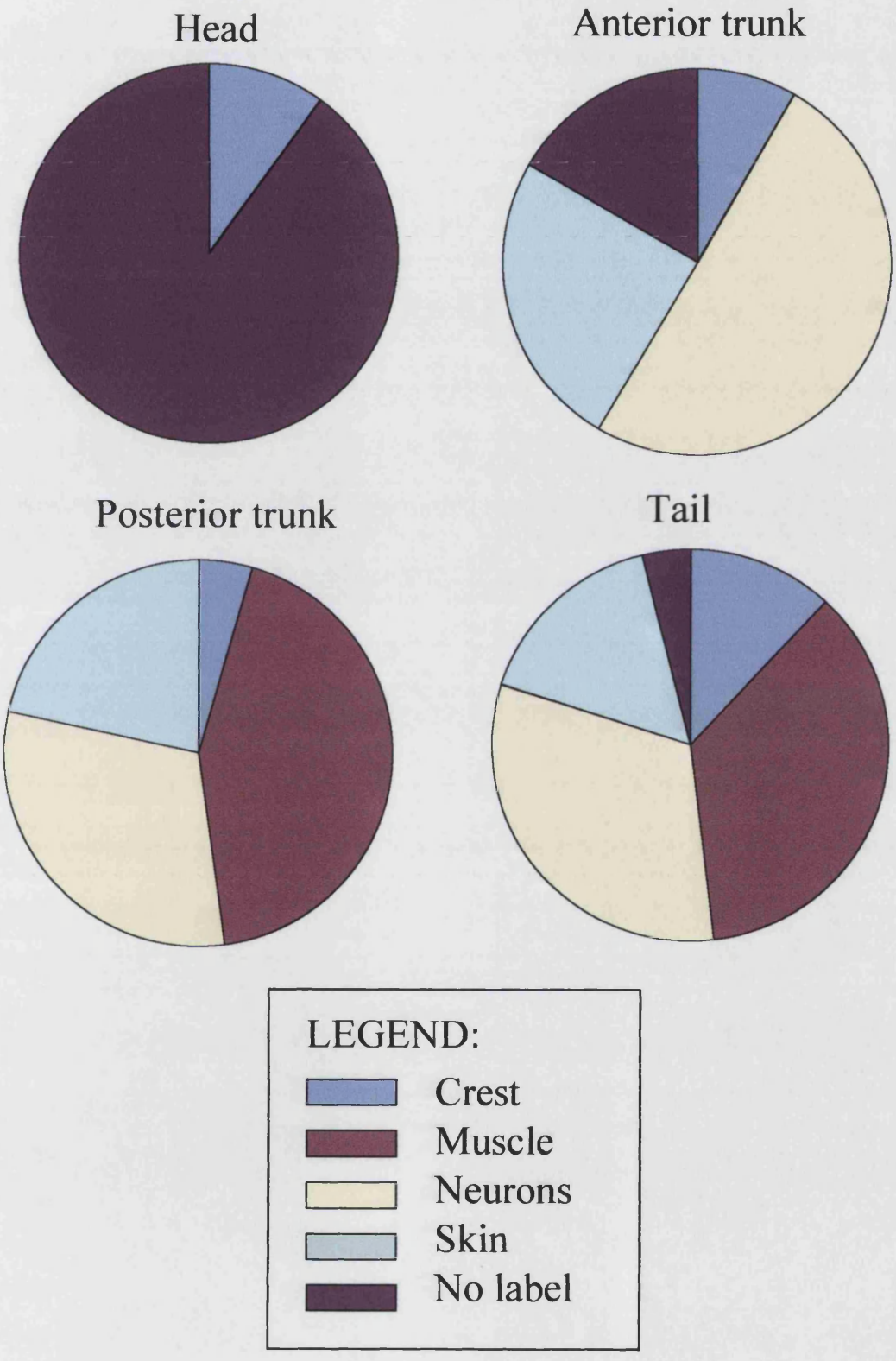
Head
Anterior trunk
Posterior trunk
Tail
LEGEND:
Crest
Muscle
Neurons
Skin
No label

attempts, we did not label anterior trunk neural crest a sufficient amount of times to address the cell autonomy question.

Out of 86 attempts, we successfully labelled crest 58% of times suggesting that we were targeting the correct region on the fate map. However, our overall hit rate for anterior trunk neural crest was poor (15%). The labelling of posterior trunk and tail regions was, by comparison, increasingly more efficient (24% and 44% respectively). Previous studies have also encountered problems with targeting anterior trunk neural crest (D Raible, personal communication). Thus, a study that attempted to label enteric neurons, which are thought to originate from the anterior trunk neural crest and then migrate posteriorly to populate all regions of the gut, had difficulties in doing so (D Raible, personal communication). It is conceivable that anterior trunk neural crest originates from a small domain on the fate map that has so far remained unidentified and might thus be particularly difficult to target. If this were the case, further single cell labelling and fate-mapping studies are required to determine the position of this domain. Only then will it be possible to start labelling anterior trunk neural crest with a sufficiently high efficiency to address the cell-autonomy question.

Previous studies have successfully used the cell transplantation technique to establish cell-autonomy (Kelsh and Eisen, 2000; Lister et al., 1999; SS Lopes, personal communication). However none of these studies aimed to label crest in a particular region of the embryo. In contrast, our study is looking for labelled cells in a small region of the trunk which comprises approximately a sixth of the body of the embryo. Due to its small size this region also contains a proportionately smaller amount of crest, and this decreases our chances of seeing labelled neural crest cells in our area of interest. Thus the chance of us observing labelled neural crest cells in the anterior trunk is 6-fold less than if we were looking for labelled neural crest cells in the whole embryo. This might explain why our neural crest targeting efficiency is more than 2-fold higher in the tail – this region is twice as large as the anterior trunk (14 somites as opposed to 7) and the chance of observing labelled neural crest cells in this location is thus proportionately higher. Only if we knew the precise area on the fate map that anterior trunk neural crest originates from might these difficulties be overcome. However as there is no information on that nor were we able to precisely pinpoint this region, our neural crest transplants were unsuccessful.

Targeting melanophores

Despite our low rate of success, we have occasionally been able to target anterior trunk neural crest. These cells were most commonly xanthophores and we only ever observed melanophores in this region twice. This presented us with the additional problem of very poor melanophore labelling. Compared to xanthophores, which we labelled in 18% of cases, and often observed multiple cells in one embryo, we only ever labelled melanophores in 7.5% of cases and even then, these were usually found alone, or in groups of two-three cells. This may be accounted for by the fact that melanophores have a smaller clone size than xanthophores and that they are harder to detect, due to their dark pigment. Previous studies often transplanted labelled wild-type cells into a mutant background devoid of melanophores (Kelsh and Eisen, 2000; Lister et al., 1999). This made detection of labelled donor melanophores comparatively easier. However, when cells had to be transplanted into a background of pigmented wild-type melanophores, problems with detection of labelled cells were reported (Kelsh and Eisen, 2000). Thus, despite the usage of PTU to partially inhibit melanisation of our host embryos, the remaining pigment may have interfered with melanophore detection. Consequently, in one of our experiments we utilised *choker;nacre* embryos to aid detection of labelled melanophores. The melanophores were very easily detectable in these embryos however this approach was found to be impractical for two reasons. Firstly, the ratio of double mutants in a batch of embryos obtained from a cross of carriers for both alleles is 1:15. In addition, the preliminary data we collected suggests that there appeared to be no extra benefits to placing melanophores in an environment devoid of any. The melanophores did divide in the host embryos however they did not appear to proliferate at a higher rate than normal nor did they migrate across long distances. Instead, they remained clustered together. This is surprising in view of reports suggesting that melanophores have an ability to regulate their own numbers to a certain extent. Studies of lateral stripe population have shown that melanophores populate stripes in two waves – the first wave which populates the lateral stripe prior to day 3 and a second wave which contributes to stripe growth between days 4 and 5 (Milos and Dingle, 1978a; Milos and Dingle, 1978b). When some first wave melanophores were extirpated from the lateral stripe, second wave melanophores compensated for this and filled-in the gaps in the lateral stripe created by the extirpations (Milos and Dingle, 1978a; Milos and Dingle, 1978b). This was also observed when all of the first wave

melanophores were ablated, suggesting that more melanophores are produced to compensate for the deficit, and that melanophores have the ability to compensate for large defects in numbers. However it is likely that the regulative ability of melanophores is dependant upon a threshold number of cells being present. Thus it is unlikely that the small number of transplanted cells could compensate to a significant extent for the complete lack of melanophores in our *choker;nacre* double mutants. However, further studies with a larger sample size have to be carried out before any firm conclusions about melanophore proliferative capacity can be drawn from this preliminary experiment.

In a low number of cases we detected labelled xanthophores in the anterior trunk. These were usually found bordering the collar region of *choker* mutants. We saw xanthophores anterior to and on top of somite 1, and posterior to somite 4 but, despite the quite high number of xanthophores labelled in these exceptional cases, we never saw them forming a network across the affected region. On only one occasion did we see xanthophores crossing this region and spreading over somites 1 and 2, and this was in a wild type embryo. Our analyses at day 3 confirmed these observations – there seemed to be a redistribution of xanthophores in *choker* mutants compared to day 2, but despite this, they were still excluded from the region between somites 1 and 5. Thus, although xanthophore number increased between days 2 and 3 on two occasions, presumably due to proliferation, the new cells did not invade the collar region but instead remained at its border.

Our experiment was designed to look for labelled wild-type melanophores in the collar region of *choker* mutants. Due to low targeting efficiency of anterior trunk melanophores we were unable to address the cell autonomy question in this manner. However our preliminary observations of xanthophore behaviour may argue that our hypothesis is correct and that the pigment defects in *choker* are in fact not cell-autonomous. Thus, wild type xanthophores placed in a *choker* environment are unable to populate the collar region in the mutant embryo. However, although the efficiency of anterior trunk xanthophore targeting was higher than that of melanophores, we still didn't target xanthophores a sufficient number of times to obtain a conclusive result. Similarly, the absence of wild-type xanthophores in the mutant anterior trunk cannot be taken as conclusive evidence of non cell-autonomy as the xanthophores may be absent from the collar through sheer chance. This could be resolved by designing the experiment differently and placing labelled *choker* xanthophores into a wild-type host.

The *choker* xanthophore phenotype consists of an absence of xanthophores in the mutant anterior trunk region. Thus, the presence of a labelled mutant xanthophore in the wild-type anterior trunk could be taken as conclusive evidence of non cell-autonomy. However, due to time restrictions we were unable to carry out a transplant experiment designed to look at xanthophore behaviour.

Targeting muscle cells

In all of our transplants we have observed a high number of labelled skin cells, CNS neurons and muscle cells. This is not surprising as the neural crest region on the fate map is adjacent to the regions where somitic muscle, epidermis and the spinal cord are derived from. However, the high muscle targeting efficiency suggested that we might be able to rescue enough muscle fibres in the anterior trunk somites to potentially rescue the pigment defect in *choker* embryos. However, despite very efficient labelling in the posterior trunk and tail, we did not label any muscle cells in the anterior trunk. Our neural crest transplant data showed that most of the muscle cells we observed previously were also found in more posterior trunk and tail regions (31% and 47% respectively). In contrast, we only managed to label anterior trunk muscle cells in 10% of cases. Thus, the transplantation of muscle cells as an approach to addressing cell autonomy might be invalid due to the same caveats we encountered when attempting to label anterior trunk neural crest. However, our sample sizes were too small to firmly establish whether the muscle transplant could have been a successful approach to addressing the question of cell autonomy in *choker* mutants.

We have been unable to ascertain whether the pigment defect in *choker* mutants is non cell-autonomous. However, our preliminary observations of xanthophore behaviour suggest that the *choker* neural crest defects may occur as a consequence of aberrant environmental cues. This, taken with the strong spatial correlation between the muscle and neural crest defects and the known role for somites in neural crest patterning, prompts us to tentatively propose that the *choker* neural crest defect occurs as a result of aberrantly distributed somite-associated neural crest guidance molecules.

Chapter 6

Expression patterns of candidate guidance molecules in choker mutants

Introduction

choker mutants have neural crest patterning defects that are spatially correlated with a region of aberrant muscle development. Although the results of our transplant experiments were not conclusive, they nonetheless suggest that the neural crest defects in *choker* may be not cell-autonomous. We would thus like to propose that *choker* might be a gene involved in muscle development and not directly in neural crest patterning. In its absence, muscle patterning is severely disrupted and consequently, a host of muscle-associated neural crest guidance molecules may have altered expression patterns. To attempt to find out more about the molecular basis of the *choker* melanophore defect we decided to compare the expression pattern of a number of candidate neural crest guidance molecules in the anterior somites of *choker* mutants and their wild type siblings. In this way, we hoped to identify molecules that show aberrant expression in *choker* mutants and that may therefore be involved in the development of the ectopic melanophore collar.

The importance of somite-associated cues in neural crest pathfinding is well established. There are a multitude of molecules thought to play a role in this process and several have been well characterized. In this study we focused on three families of genes which have been implicated in neural crest migration in zebrafish or other higher vertebrates.

The family of Eph receptor tyrosine kinases and ephrin ligands have roles in various developmental process including hindbrain and somite segmentation, angiogenesis, axon guidance and cell migration (for review see Holder and Klein, 1999). Both receptors and ligands are membrane-bound and they have been divided into two subfamilies, based on receptor-ligand binding specificities. Class A ephrin ligands are tethered to the membrane via a glycosyl-phosphatidyl inositol (GPI) linkage and the receptors that they interact with are termed the EphA receptors, whereas the ephrin B ligands have a transmembrane domain and exhibit binding specificities to EphB receptors (Eph Nomenclature Committee, 1997). The only exception to this rule is

EphA4 which can bind ligands of both classes. As ligands of the B class are transmembrane molecules they can engage in bidirectional signalling. Members of the EphB receptor family and their ligands have been shown to have a role in establishing segmental neural crest migration in avian and rodent embryos (Krull et al., 1997; Wang and Anderson, 1997). Neural crest cells express an Eph receptor, and somite cells in the caudal somite half express the corresponding ligand. The binding of the two results in a repulsive interaction between the molecules which prevents crest cells from invading the caudal half of the sclerotome. The particular type of receptor/ligand involved varies in different organisms. More recently, receptors and ligands of the A class have also been found to have a role in neural crest migration. Surprisingly however, stripe assays showed that some combinations of EphA receptors appeared to be able promote migration of neural crest cells (McLennan and Krull, 2002). A similar result has been found for ligands of the B class. Thus, ephrinB1 has been shown to have distinct effects on neural crest cells at different stages of development; at early stages, it prevents neural crest cells from invading the dorsolateral pathway, but at later stages, the presence of ephrinB ligands in the dorsolateral pathway environment promotes melanoblast migration into it (Santiago and Erickson, 2002). Thus, the role of Eph receptors and their ligands in neural crest guidance is complicated and can alter depending on the different combination of receptors and ligands involved, and on the state of the expressing cell. The expression of Eph receptors and their ligands has been studied in the zebrafish and a number of molecules have been found to be expressed in somites (Chan et al., 2001; Durbin et al., 1998). Based on these studies, we decided to analyse the expression of some somite-associated ephrin ligands and an Eph receptor that may have a role in neural crest migration in zebrafish, and whose patterning may be affected in *choker*.

We also looked at a family of molecules whose role has been best characterized in the development of the nervous system. Members of the roundabout (robo) family of transmembrane receptors have first been identified as axon guidance molecules in the Drosophila midline (Kidd et al., 1998). Since then, robo homologues have been identified in several organisms including rat, mouse, human and zebrafish. The ligands for this family of receptors were found to be a family of secreted molecules, termed slits (Kidd et al., 1999). Binding assays showed that multiple slit molecules can interacts with single robo receptors (Yuan et al., 1999). Analysis of the expression patterns of both robo and slit molecules revealed that they are expressed in complementary

patterns, and in places that suggest a role in numerous developmental processes such as midline axon guidance, axon pathfinding, neural crest migration, and limb bud development. Studies in Drosophila and rat have shown that the interaction of robo and slit molecules can mediate attractive as well as repulsive responses, depending on the receptor type employed (Englund et al., 2002; Kramer et al., 2001; Wang et al., 1999). The zebrafish robo family is composed of three members and their expression patterns reflect those already documented in the mouse (Challa et al., 2001; Lee et al., 2001). Although the complementary expression pattern of robo receptors and their ligands in both the mouse and the zebrafish somite suggests a role in axon pathfinding and neural crest migration, the evidence for a role of these molecules in neural crest migration has remained circumstantial. A recent study has shown that morpholino knock downs of the robo3b protein in zebrafish display a convergent extension defect, and intriguingly, an ectopic melanophore collar bridging the anteriormost somites (Challa, personal communication). This phenotype is strongly reminiscent of the *choker* pigment defect. Although this could be a non-specific effect of the morpholino injection we decided to further investigate the role of robo family members in zebrafish neural crest migration by looking at the expression pattern of the two robo family members (*robo1* and *robo3b*) expressed in the zebrafish somite.

Finally, we looked at members of the semaphorin family, which were initially examined for a role in neural crest migration because of their demonstrated involvement in axon guidance (Eickholt et al., 1999). The semaphorin family is large and diverse, contains both membrane-associated and secreted ligands, and its members are grouped into several classes (number 1 to 7) on the basis of structural similarity. Studies in chick have found that a Semaphorin III class ligand is expressed in the caudal half of the sclerotome and its receptor, neuropilin-1 is found on neural crest cells. *In vitro* studies have shown that neuropilin-1 expressing neural crest cells avoid Semaphorin III "stripes" (Eickholt et al., 1999). In addition, a role for semaphorins has also been demonstrated in the development of mouse cardiac neural crest (Brown et al., 2001) and mouse sympathetic nervous system (Kawasaki et al., 2002). Thus, Sema3C mutant mice have cardiac abnormalities reminiscent of cardiac neural crest defects and Sema3A mouse mutants develop ectopic sympathetic neurons. A role of the zebrafish homologues of Semaphorin III has been demonstrated in the pathfinding of motor neurons and the posterior lateral line axon (Roos et al., 1999; Shoji et al., 1998), and more recently in angiogenesis (Shoji et al., 2003) however there is no evidence yet for a

semaphorin role in zebrafish neural crest guidance. A number of semaphorin family members have been identified in zebrafish and their expression characterized. The best candidate for a role in neural crest guidance in zebrafish, based on its expression pattern within the somite, and on the fact that it is the receptor for the crest-associated molecule, neuropilin-1 (Shoji, personal communication), is the zebrafish homologue of Sema III; SemaZ1a.

Our studies of the *choker* mutant have revealed that the cellular basis of the melanophore defect lies in defective lateral pathway shutdown. Around 36 hpf the lateral pathway shuts down in wild type embryos and neural crest cells are thought to be prevented from further migration on this pathway through the upregulation of a putative inhibitor. This molecule is possibly either absent or expressed in an anomalous pattern in *choker* mutants, thus accounting for the continued melanophore migration into the mutant lateral pathway environment. For a molecule to have a role in lateral pathway shutdown, we would expect it to be expressed throughout the lateral face of the somite at 36 hpf, the time of lateral pathway shutdown. If this molecule was responsible for the melanophore defect in *choker* embryos we would expect it to be aberrantly expressed or absent from the mutant somite.

Results

We used *in situ* hybridisation to analyse the expression pattern of various candidate neural crest guidance molecules in *choker* mutants and their wild-type siblings. The probes used were *EphA4, ephrinB2a* (Durbin et al., 1998), *ephrinB1, ephrinB2b* (Chan et al., 2001), *sema Z1a* (Yee et al., 1999), *robo1* and *robo 3b* (Challa et al., 2001).

In order to confirm the specificity of our probes we analysed batches of choker mutants and wild type siblings at early stages when we expected all of these molecules to be expressed. Most of these stages have been previously documented but for some stages we were able to generate new expression data. Once we established that our probes were working, we looked at our stage of interest, 36 hpf, to see whether any of these molecules are expressed at this time and whether there are any differences in the expression pattern in *choker* mutants and wild-type siblings. However, the latest

timepoint at which we documented the expression of most of these molecules is at 24 hpf, as that is when their downregulation usually occured.

We tested batches of *choker* mutants and wild-type siblings derived from a cross of *choker* heterozygotes. As it is not possible to separate wild types from *choker* mutants as early as 18 hpf we tested mixed batches of embryos and looked for any differences in the somitic expression pattern, particularly in the anteriormost 5 somites. Although an expression defect at such an early stage is probably unlikely to account for the much later onset of the *choker* melanophore defect, it is possible that a molecule which displays aberrant expression at early stages would also have an anomalous late expression pattern. For all the later stages tested we separated mutants from wild type siblings according to the *choker* early muscle apoptotic phenotype. We anticipated that the separation of wild types and mutants would enable us to detect any differences with greater accuracy.

Eph receptors and their ligands

Mixed batches of 18 hpf *choker* mutants and wild-type siblings were probed with the *ephrinB1* probe. As expected (Chan et al., 2001), we saw staining throughout the formed somites, which was strongest in the posterior half, and in the presomitic mesoderm (PSM), just posterior to the last formed somite (Figure 6.1A). We were unable to detect any differences in any of the embryos. When we looked at 24 hpf mutants and wild type siblings we could not detect any somitic staining except for a very faint signal in the tip of the notochord, which is likely to be non-specific (Figure 6.1B, C). The *ephrinB1* expression thus appears not to be maintained in formed somites and is downregulated between 18 and 24 hpf. To ensure that this gene is not expressed at later stages, we also looked at 36 hpf and there was no somitic staining in mutants or wild types (data not shown).

EphrinB2a has been reported to have a dynamic expression pattern during somitogenesis (Durbin et al., 1998). Initially, it is expressed in the posterior half of formed somites and in the PSM, but as somitogenesis progresses this expression expands to include the whole lateral domain of the somite. From 16 hpf onwards *ephrinB2a* expression becomes restricted to dorsal and ventral lateral domains of mature somites. Our expression analyses at 18 hpf confirmed that at this stage *ephrinB2a* expression is found in the caudal half of the most newly formed somites, and is restricted to the dorsal and ventral-most domains of anterior somites (Figure 6.2A).

Figure 6.1. No differences in *ephrinB1* expression were detected in 18 hpf and 24 hpf *choker* embryos and wild-type siblings

(A-C) *EphrinB1* expression was analysed by *in situ* hybridisation in mixed batches of wild types and *choker* mutants derived from crosses of heterozygote carriers. Lateral views of labelled embryos reveal that at 18 hpf *ephrinB1* was expressed in the formed somites of all embryos analysed and this expression appeared stronger in the posterior somite half (arrows, A). There was also some expression in the presomitic mesoderm, posterior to the last formed somite, and in the eye. By 24 hpf ephrinB1 expression was completely downregulated in both wild types and *choker* mutants (B, C).

Ephrin B1 18 hpf

Ephrin B1 24 hpf

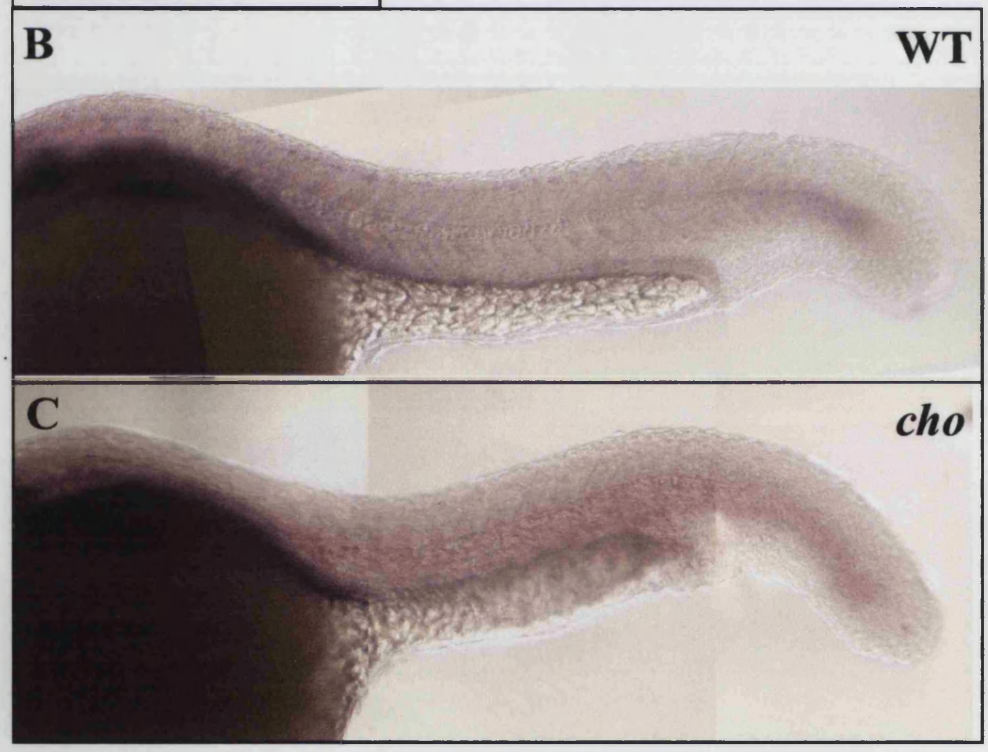

Figure 6.2. *EphrinB2a* had a dynamic expression pattern in 18 hpf and 24 hpf *choker* mutants and wild-type siblings

(A-D) Mixed batches of 18 hpf and 24 hpf wild-type embryos and *choker* mutants were tested for *ephrinB2a* expression. The majority of 18 hpf embryos had expression in the posterior half of most recently formed somites (asterisk, A, B) and in dorsal and ventral most domains of older somites (arrows, A). However, a small number of embryos had expression throughout the dorso-ventral domain of formed somites (arrows, B). These were presumed to be mutants. We also observed some expression in the eye and brain of both wild types and mutants. The restriction of *ephrinB2a* expression to dorsal and ventral somite domains is apparent at 24 hpf only in the posteriormost somites of wild-type embryos (arrows, C). Furthermore, *ephrinB2a* is now also faintly expressed at somite boundaries. This expression appears strongest in the anterior somites and at the ventral half of boundaries (asterisk, C). *choker* embryos still display the lack of dorso-ventral restriction of expression in the posteriormost somites (arrows, D), and also have no *ephrinB2a* expression at the boundaries of anteriormost somites (D).

Ephrin B2a 18 hpf

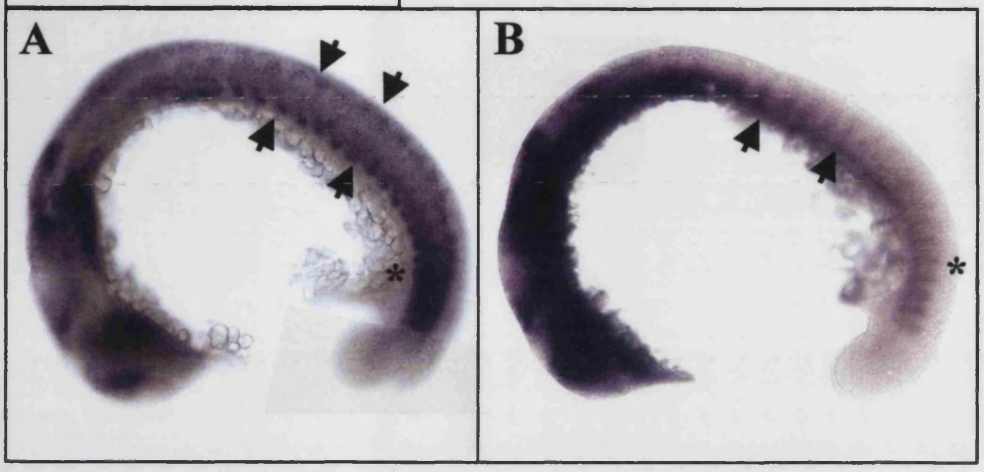

Ephrin B2a 24 hpf

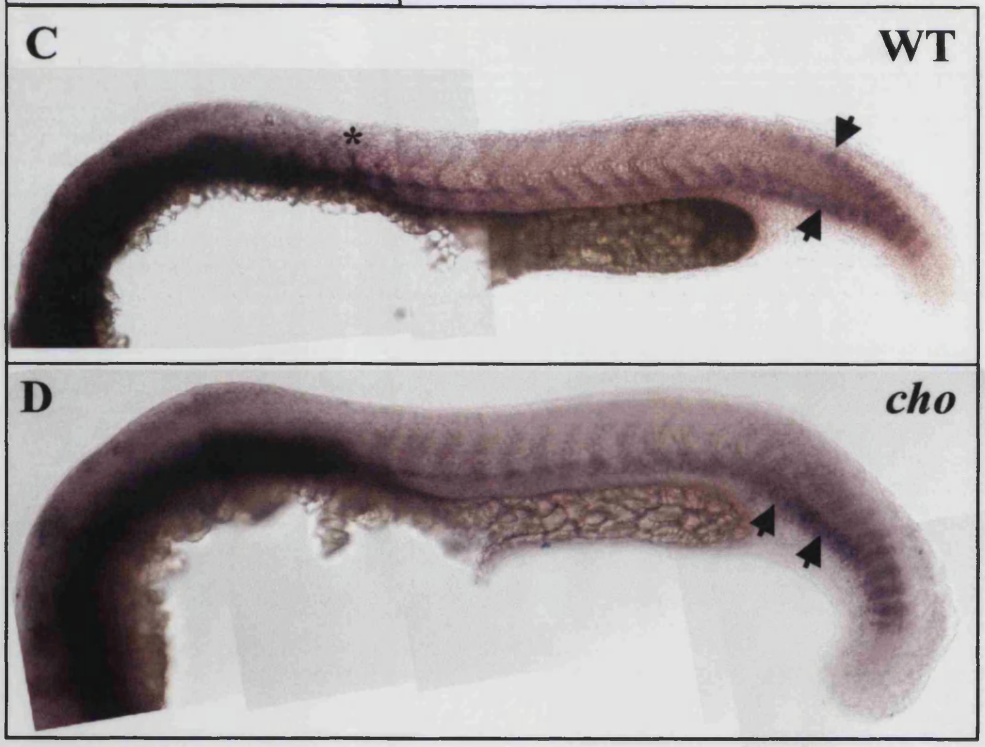

However, we found that some embryos had a different expression pattern. Thus, the mature somites in these embryos continued to express *ephrinB2a* throughout the somite, with no dorso-ventral restriction (2/13) (arrows, Figure 6.2B). By 24 hpf, the somitic expression of *ephrinB2a* has been largely downregulated in both wild types and *choker* mutants, which agrees with the published antero-posterior loss of *ephrinB2a* expression. Staining in the wild types is still visible in only the most posterior somites and is restricted to the dorsal and ventral somite halves (arrows, Figure 6.2C). However, at this stage, we also detected some low level *ephrinB2a* staining at somite boundaries. This seemed strongest in the ventral somite half and at the boundaries of the anteriormost 5 somites (asterisk, Figure 6.2C). Although present in the mid and posterior trunk, this staining was absent in the anteriormost somites of *choker* mutants (Figure 6.2D). Furthermore, where the wild-type posteriormost somites displayed the dorso-ventral restriction that characterised mature somites at earlier stages, the mutant tail somites continued to express *ephrinB2a* throughout their dorso-ventral plane (arrows, Figure 6.2D). Despite these interesting differences at 24 hpf, at 36 hpf *ephrinB2a* was not expressed in the somites of *choker* mutants or wild-type siblings (data not shown).

Previous studies of the *ephrinB2b* expression pattern have not documented any timepoints between the 10-somite and 24 hpf stage. Our *in situ* hybridisation studies at 18 hpf revealed that this ephrin was expressed in a similar fashion to the other ephrin ligands – staining was found in the PSM, just rostral to the caudalmost somite and in the most newly formed somites (arrows, Figure 6.3A). *EphrinB2b* appeared to be expressed throughout the newly formed somite, but was stronger in the anterior somite half. By 24 hpf however, the somitic expression was no longer detectable in wild types or mutants (Figure 6.3B, C). Studies at 36 hpf revealed no staining in *choker* mutants or wild-type siblings (data not shown).

Of the Eph receptors, *EphA4* was the only one tested in this study, as it was the only one reported to have somitic expression. Previously, expression has been assessed at early stages. It was reported to be expressed in the PSM and in the anterior halves of already formed somites. At 18 hpf we saw *EphA4* expression only in the most posterior somites; by 24 hpf, the somitic expression has been completely downregulated in both wild types and mutants (Figure 6.4A-C). At both timepoints we also observed the previously reported notochord staining which made the somitic expression more difficult to discern. We saw no evidence for the weak crest expression of *EphA4*, seen in chick embryos, despite leaving *in situs* to develop for a number of days. *In situ*

Figure 6.3. No differences in *ephrin B2b* expression were detected in 18 hpf and 24 hpf *choker* mutants and wild-type siblings

(A-C) *EphrinB2b* expression was analysed in mixed batches of *choker* mutants and wild-type siblings. At 18 hpf *ephrinB2b* is expressed in the anterior somite halves of recently formed somites and in the presomitic mesoderm, caudal to the most newly formed somite (arrows, A). In addition, there was also some eye expression in all embryos examined. By 24 hpf the somitic expression has been completely downregulated in both wild types and mutants (B, C).

Ephrin B2b 18 hpf

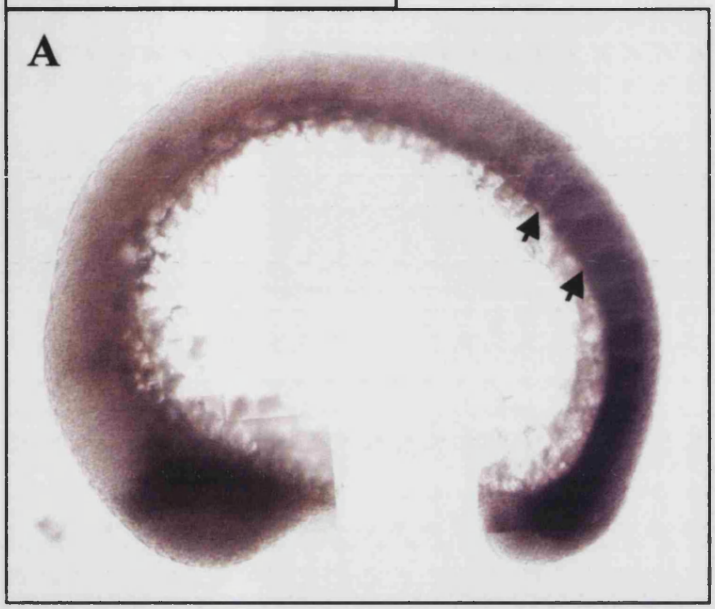

Ephrin B2b 24 hpf

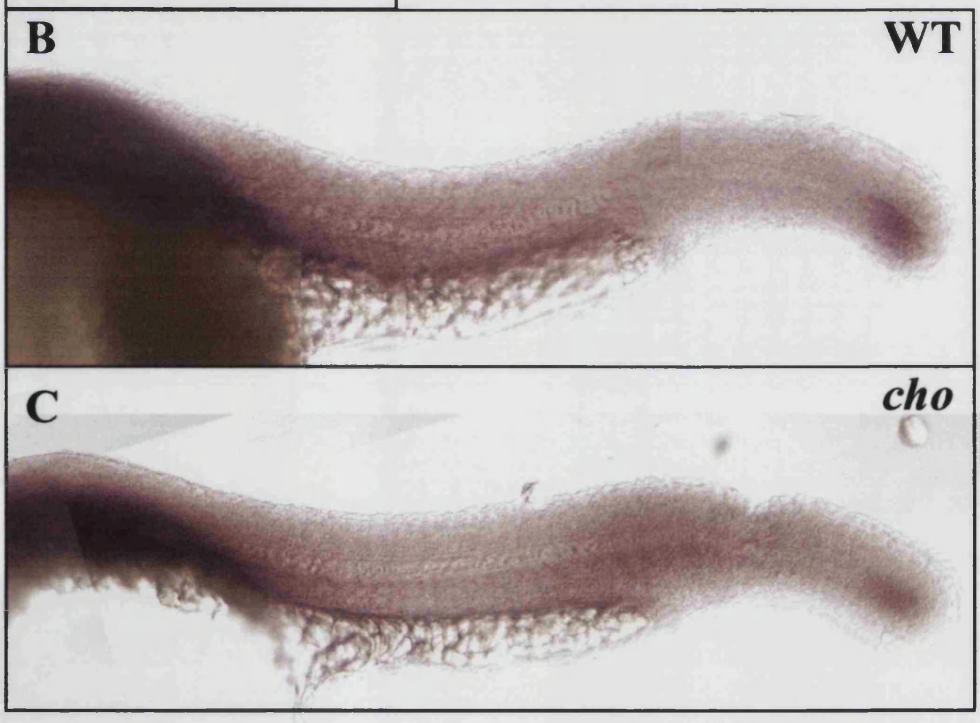

Figure 6.4. No differences in *EphA4* expression were detected in 18 hpf and 24 hpf *choker* mutants and wild-type siblings

(A-C) Mixed batches of wild types and *choker* embryos were probed with an *EphA4 in situ* probe. At 18 hpf all embryos analysed expressed *EphA4* in the brain, neural tube and in the anterior half of posteriormost somites (arrows, A). By 24 hpf the brain and neural tube expression are still prominent but the somitic expression has been completely downregulated in both wild types and mutants (B, C).

Eph A4 18 hpf

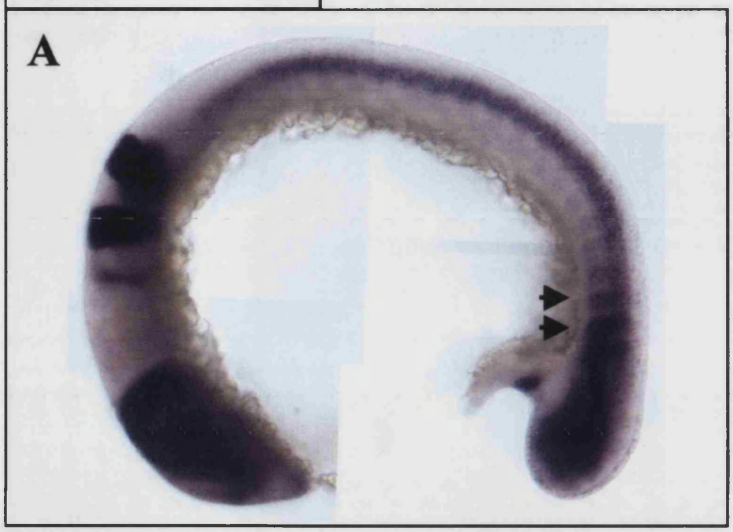

Eph A4 24 hpf

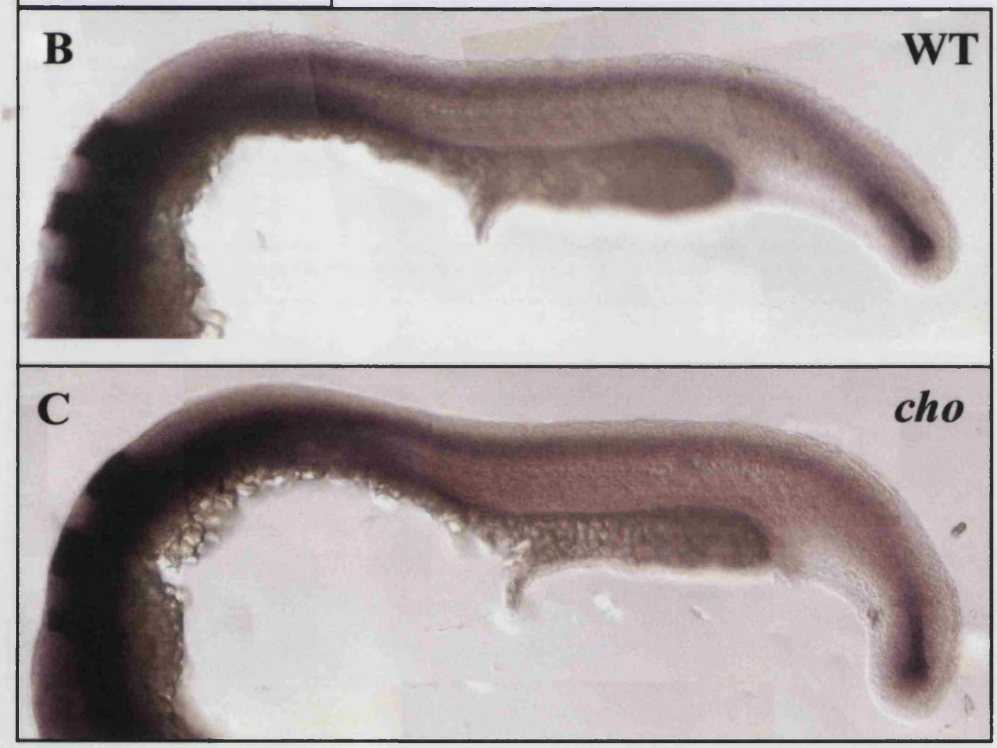

hybridisation at 36 hpf revealed that there is no somitic *EphA4* expression at this stage, in wild types or mutants (data not shown). Our analyses revealed that in most cases there appeared to be no differences in the expression of the Eph receptors and ephrin ligands tested in *choker* mutants and their wild-type siblings. The only exception was *ephrinB2a*, which displayed a different expression pattern in the trunk of the mutants at both stages tested. However, as none of these molecules are expressed at the time of lateral pathway shutdown in wild types we conclude that they are not involved in the *choker* melanophore defect.

robo1 and robo3b

The zebrafish *robo1* and *robo3b* genes have been cloned, and had their expressions patterns characterised, by two different groups (Challa et al., 2001; Lee et al., 2001). Both appear to have quite complex somitic expression patterns. *Robo1* has been reported to have broad somitic expression at 19 hpf. This is downregulated, and at 24 hpf *robo1* expression is only detectable in the posterior two thirds of the trunk. In contrast, a separate study reported that somitic *robo1* expression was not discernible before 24 hpf and after this was detectable only in the ventral somite half. Our *in situ* hybridisation showed that at 24 hpf, *robo1* expression was detectable in the mid and posterior trunk somites of both wild types and mutants (Figure 6.5A, B). We found that the expression of *robo 1* varied at different axial levels. There was no discernible expression in the anterior trunk somites in wild types or mutants, consistent with the documented rostro-caudal downregulation of *robo1* expression at this stage. In mid and posterior trunk somites, *robo 1* was expressed in a stripe down the middle of each somite (arrows, Figure 6.5A, B). Although staining was observed throughout the dorso-ventral plane of the somite, it seemed stronger in the ventral domain. By comparison, the posteriormost somites showed expression only in the posterior somite halves (asterisk, Figure 6.5A, B). At this stage we observed no differences in the expression of *robo1* in wild-type and mutant embryos. The only difference detected involved smaller domains of expression throughout the mutant trunk, probably reflecting smaller somite size. The somitic expression was completely downregulated by 36 hpf in both wild-types and mutants (data not shown).

By comparison, *robo3b* expression at 24 hpf was reported in the more caudalmost somites and was stronger in the dorsal and ventral portions of the somite, with an expression-free zone at the level of the horizontal myoseptum (Lee et al., 2001).

Figure 6.5. No differences in *Robo1* and *Robo 3b* expression were detected in 24 hpf *choker* mutants and wild-type siblings

(A-D) Batches of separated *choker* mutants and wild type siblings were probed with the *robo1* and *robo3b in situ* probes. At 24 hpf *robo1* expression has already been downregulated in the anteriormost somites of both wild types and *choker* mutants (A, B). However, expression is still evident in a stripe down the middle of mid-trunk somites (arrows, A, B) and in the posterior somite half of caudalmost somites (asterisk, A, B). There were no differences in the wild type and *choker* expression pattern, except for a smaller somitic expression domain in mutant embryos. *Robo3b* expression is also downregulated in the anteriormost somites of both *choker* mutants and wild-type siblings by 24 hpf. The mid and posterior trunk somites were however expressing *robo3b* in dorsal and ventral somitic domains, with an expression-free stripe at the horizontal myoseptum (C, D). No differences were observed in *robo3b* expression in wild types and mutants.

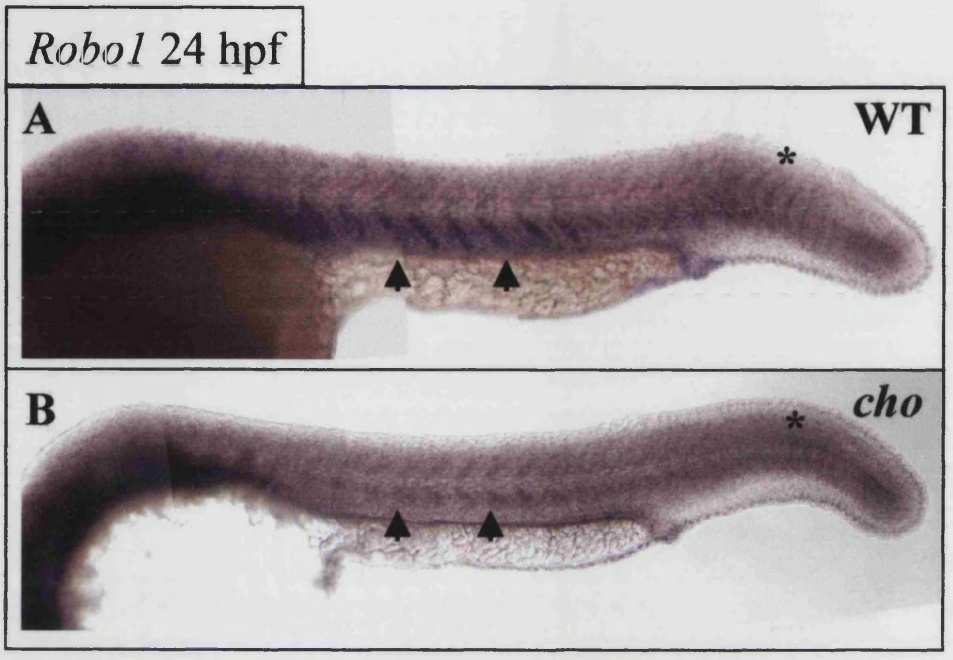
Robo1 24 hpf
A
WT
B
cho


Robo3b 24 hpf
C
WT
D
cho

A parallel study reported that expression in the midtrunk and caudal somites was restricted to the posterior somite half (Challa et al., 2001). We found *robo3b* expression throughout the dorsal and ventral somite halves of the mid and posterior trunk (Figure 6.5C, D). There was however a very strong CNS signal that masked the somitic expression in the dorsal somite halves. We were unable to detect an antero-posterior restriction but did observe the previously documented expression-free zone at the horizontal myoseptum. As previously documented, *robo3b* expression is being downregulated at this stage and we therefore saw no expression in the anterior somites of either wild types or mutants. Except for the smaller expression domains in the mutant, which probably reflect smaller somite size, we observed no differences in the somitic expression of *robo3b* in wild types and mutants. By 36 hpf the somitic expression has been completely downregulated in both wild types and mutants (data not shown).

Neither *robo1* nor *robo3b* are expressed at 36 hpf and they are therefore unlikely to have a role in lateral pathway shutdown or the *choker* melanophore phenotype.

Sema Z1a

SemaZ1a expression has been reported in the dorsal and ventral lateral domains of mature somites at 24 hpf, with an expression-free band at the horizontal myoseptum. Our *in situ* hybridisation studies at 24 hpf mirrored the published data. We detected no differences in the staining of *choker* mutants and wild-type siblings, although the expression domains again appeared smaller in the mutant somites (Figure 6.6A, B). When we looked at 36 hpf embryos we saw staining in the dorsal and ventral domains of both mutant and wild-type somites (Figure 6.6C). The staining appeared strongest in the anteriormost somites and there was an expression-free band at the horizontal myoseptum. Although the somites once again appeared smaller in *choker* mutants, the staining was in all other respects the same. To make sure that the expression of Sema *Z1a* was equivalent in mutants and wild types we looked at transverse sections of 36 hpf embryos. These revealed that at the level of both anterior (somite 1-5) and more posterior somites, the wild-type somite is expressing *Sema Z1a* throughout its medio-lateral domain (Figure 6.6D, F). The only exception was the expression-free zone at the horizontal myoseptum which also extended throughout the width of the somite. This expression was mirrored by the *choker* somites (Figure 6.6E, G) and, except for the

Figure 6.6. No differences in *SemaZ1a* expression were detected in 24 hpf and 36 hpf *choker* mutants and wild-type siblings

(A-C) *SemaZ1a* expression was analysed in 24 hpf and 36 hpf *choker* mutants and wild type siblings. At this stage the expression is seen in the dorsal and ventral somite halves of both wild types and mutants (A, B). This expression pattern is also observed at 36 hpf (C). There were no differences in *SemaZ1a* expression in *choker* mutants and wild-type siblings, besides a smaller somitic expression domain in mutant embryos. (D-G) Transverse sections of 36 hpf embryos confirm that *SemaZ1a* expression is found in the dorsal and ventral somite halves of both anterior and posterior trunk somites of wild-type embryos (D, F). There were no differences between the wild-type and *choker* somite expression pattern in transverse view (E, G).

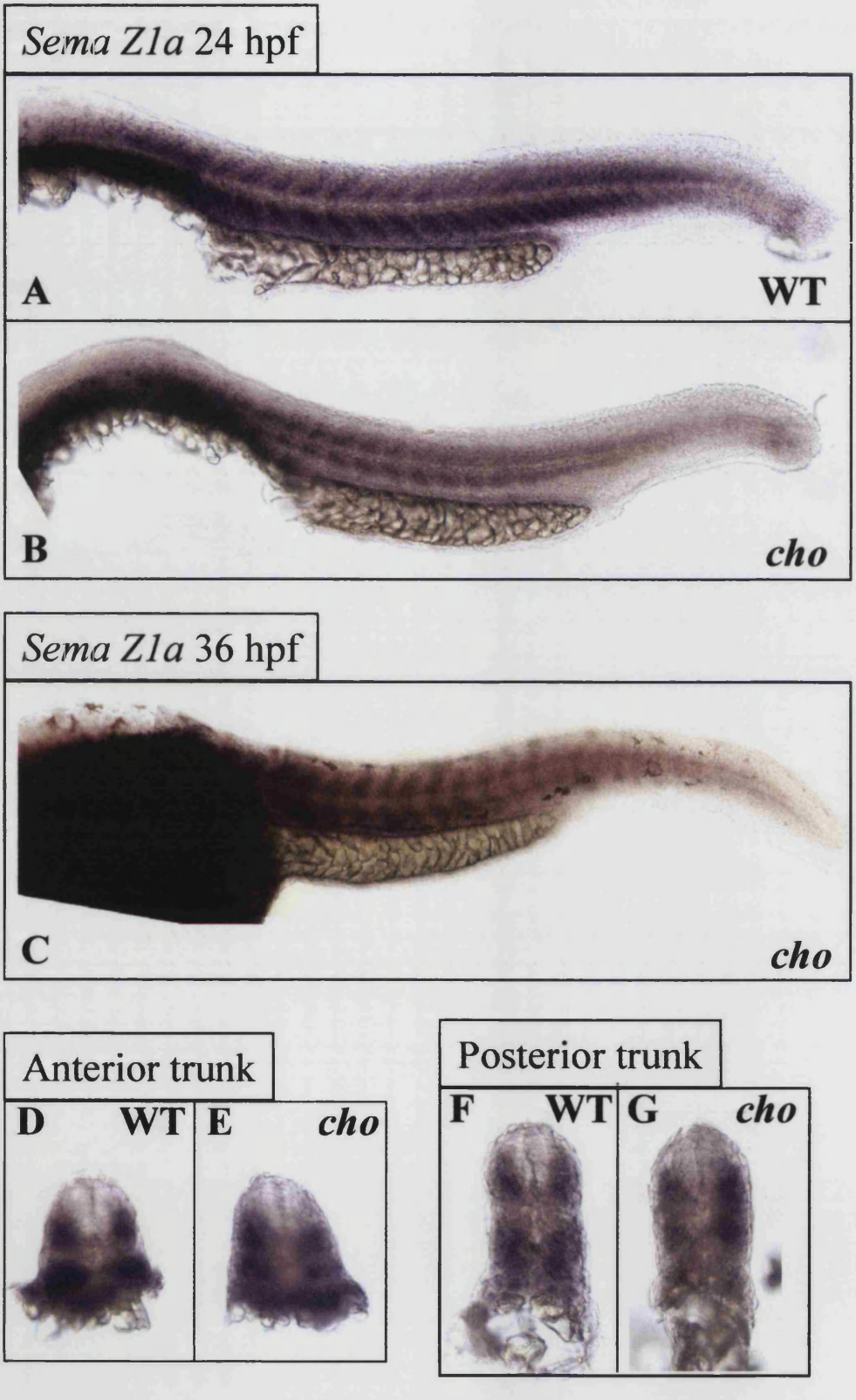
Sema Z1a 24 hpf
A
WT
B
cho
Sema Z1a 36 hpf
C
cho
Anterior trunk
D
WT
E
cho
Posterior trunk
F
WT
G
cho

smaller size of the somitic expression domains, there was no detectable difference in the expression pattern of wild-type and mutant somite sections. We observed no differences in the expression pattern of *SemaZ1a* in *choker* mutants and wild-type siblings. Thus, despite being expressed in the somite at the time of lateral pathway shutdown, this molecule is unlikely to be responsible for the *choker* melanophore phenotype.

Discussion

Eph receptors and their ligands

We have looked at the expression pattern of an Eph receptor and a number of ephrin ligands in 36 hpf zebrafish embryos. Our analyses have shown that none of these molecules are expressed at this late stage and are therefore unlikely to play a role in lateral pathway shutdown. We can therefore exclude the possibility that these members of the Eph/ephrin family have a role in the *choker* melanophore defect. We also saw no differences in the expression of most of the molecules we tested in *choker* mutants and their wild-type siblings at earlier stages. Thus, it seems that the disorganised somites are still able to express most molecules in the right locations. An alternative explanation for this might be that we only looked at expression at early stages, when the somite is still immature and the muscle defects are as yet not very pronounced.

The only difference we detected was in *ephrinB2a* expression which lacked the dorso-ventral restriction throughout the trunk, possibly as a direct consequence of the mild somite disorganisation present at all axial levels. In addition, we detected an anterior somite-specific defect in the lack of the somite boundary expression seen in wild-types and more posterior mutant somites at 24 hpf. This latter defect is probably due to the more severely disrupted somite architecture in the anterior trunk.

Although the role of Eph receptors and ephrin ligands has been extensively studied in the chick, and to a lesser degree in rodents, it is not known which, or if any, of the members of this family is involved in zebrafish neural crest development. This is particularly difficult to determine as different combinations of Eph receptors and ephrin ligands have analogous roles in different organisms. Thus, chick neural crest migration is influenced by the interaction between the Eph B3 receptor expressed on the surface of neural crest cells and the ligand ephrinB1 found in the caudal half of the somite (Krull et al., 1997). By comparison, rat neural crest cells express Eph B2 and the posterior

somite halves express the ligand ephrin-B2 (Wang and Anderson, 1997). Although the expression patterns of all of the molecules used by us have been analysed in previous studies, there were some stages that remained undocumented. Thus, we were curious to see whether any novel expression patterns we may uncover in our study might suggest a role for these molecules in zebrafish neural crest migration. Our analyses of the Eph/ephrin family however revealed that most of the molecules tested have expression patterns suggestive of a role in somitogenesis only. They are expressed in newly formed somites, and usually display some form of antero-posterior restriction consistent with a role in somitogenesis. The restriction of Eph receptors to the rostral half, and ephrin ligands to the caudal half has been shown to be required for the formation of somite boundaries (Durbin et al., 1998; Durbin et al., 2000). Following somitogenesis, the expression in the somites is downregulated in a rostro-caudal manner. For any of these molecules to be involved in neural crest migration we would expect their expression to be maintained during neural crest migration. As most of these molecules had begun to be downregulated before neural crest migration had started we assume that they play no role in neural crest guidance. The only exception to these observations was *ephrinB2a*, which, according to its published expression pattern, seemed like the most likely candidate for a role in neural crest migration. Published studies state that *ephrinB2a* is initially expressed in the whole lateral domain of the somite and that this expression is subsequently restricted to the dorsal-most and ventral-most somite regions (Durbin et al., 1998). Out of the ephrin ligands analysed, this molecule is the only one that has such a dynamic expression pattern and whose expression is maintained in mature somites. This suggests that it may have additional roles beside somitogenesis. In addition to the dynamic expression pattern of *ephrinB2a* reported at early stages, we also observed an interesting pattern at 24 hpf. The *ephrinB2a* staining at somite boundaries may have a role in guiding medially migrating neural crest cells and ensuring that they only migrate down the middle of each somite. However, analysis of the *ephrin-B2a* expression pattern in transverse sections is required to confirm that it is expressed adjacent to the medial pathway and not just on the lateral face of the somite. This molecule was the only one of all the molecules tested to show such an intricate and intriguing expression pattern.

Although the expression of Eph receptors and ephrin ligands in the zebrafish somite has been well documented, there is no data regarding the Eph/ephrin expression profile of zebrafish neural crest cells. Chick expression analyses revealed that *EphA4* is

weakly expressed in chick neural crest cells and *in vitro* studies suggested that it may have a role in their migration. We hoped that we might see expression in zebrafish neural crest however we saw no evidence for this. Therefore the role of *EphA4* in chick may not to be analogous to its role in zebrafish. This role may instead be played by one of the many zebrafish Eph-receptor tyrosine kinases whose expression has not been analysed.

The family of Eph receptors and their ligands is extremely complex and studies in chick have suggested that there is an interplay of several receptors and ligands that can act as inhibitors or attractants, depending on the developmental stage and their interactions with other molecules. In zebrafish too, the story is likely to be complex and more than a single receptor or ligand is likely to be involved. However, despite the putative role for Eph receptors and their ligands in the early stages of neural crest development, it appears that, at least the molecules we tested do not have an involvement in lateral pathway shutdown.

robo1 and robo3b

Our analyses of the expression pattern of *robo1* and *robo3b* at 36 hpf revealed that neither of these molecules showed any somitic expression at this late stage. Thus, they are unlikely to have a role in lateral pathway shutdown or to be involved in the *choker* phenotype. This result is somewhat surprising in view of the fact that *robo3b* morpholino knock-downs have an ectopic melanophore collar. However the *robo3b* morphant also has severe convergent extension defects and the melanophore phenotype might be a secondary consequence of the latter, and not a direct result of *robo3b* knock down.

Similar to our studies of the Eph/ephrin family, we were unable to detect any difference in the *robo1* and *robo3b* expression pattern in *choker* mutants and wild-type siblings. This is not surprising given that we looked at stages when the expression in the anterior somites was being downregulated.

The expression patterns of these molecules at 24 hpf are intricate and reflect their complex roles in axon guidance and the development of the nervous system. Their somitic expression pattern is as intricate, showing dorso-ventral and antero-posterior restriction. Their role has already been demonstrated in axon guidance and their somitic expression puts them in the ideal location to influence motor axon pathfinding. Furthermore, the expression of *robo1* in the middle of each somite suggests that they

might be involved in the migration of medial pathway neural crest cells. Although the role of *robo1* is traditionally repulsive, studies in Drosophila found some plasticity in the way that robo receptors and slit ligands interact (Englund et al., 2002). The response varied from repulsive to attractive depending on which combinations of receptors and ligands were employed. The Eph receptors and their ligands have been shown to have dual roles in neural crest migration; they can be both inhibitory and permissive to migrating neural crest cells (Santiago and Erickson, 2002). Thus, like the Eph receptors and ephrin ligands, the robo family may also have dual roles and *robo1* expression along neural crest migratory pathways might, under certain conditions, be permissive to migration. However, further analysis of the *robo1* expression pattern in transverse sections is required to establish whether it is expressed on the medial face of the somite.

The absence of *robo3b* expression at the horizontal myoseptum may have a role in delineating the pathway for the posterior lateral line axon. A role in neural crest guidance is also conceivable. *Robo3b* is expressed broadly in dorsal and ventral somite domains and is in the process of being downregulated at 24 hpf. There is a temporal correlation between *robo3b* downregulation and the initiation of neural crest lateral pathway migration and it is possible that *robo3b* plays a role in the delay of emigration. However, although the expression pattern of the ligands for robo, slits, has been characterised, there seems to be no evidence for slit expression in the neural crest. Thus, the roles of robo receptors in the somites may be limited to axon guidance. Alternatively, there may be other as yet undiscovered robo ligands that are expressed in the neural crest.

Sema Z1a

The analysis of the *SemaZ1a* expression pattern has provided us with a very good candidate for a molecule that has a role in lateral pathway shutdown. Its distinct expression pattern at 24 hpf has previously been shown to have a role in posterior lateral line axon guidance. *SemaZ1a* is expressed throughout the somite except for an expression-free zone at the horizontal myoseptum. The lateral line axon migrates along the horizontal myospetum, through the *Sema Z1a*-free region and is prevented from branching into adjacent territories by the repulsive action of *Sema Z1a*. More recent studies found that this specific *Sema Z1a* expression also has a role in the guidance of migrating angioblasts. The 24 hpf expression pattern of *SemaZ1a* suggests additional roles. It is ideally positioned to influence the migration of neural crest cells on the

lateral pathway. Furthermore, its expression at 36 hpf suggests that it is a prime candidate for a molecule involved in lateral pathway shutdown. It is expressed throughout the lateral face of the somite, except for a band at the horizontal myoseptum. Disappointingly however, there were no differences in 36 hpf *SemaZ1a* expression between *choker* mutants and wild-type siblings. The only difference we detected was that the expression domain was smaller in the dorso-ventral plane in *choker* embryos. However, this was evident throughout the trunk and was not restricted to the anterior trunk somites. We concluded that the smaller expression domains reflected a smaller somite size in *choker* embryos. Thus, although an interesting candidate, *SemaZ1a* is probably not the molecule responsible for the *choker* defect.

We have analysed the expression pattern in *choker* mutants of a total of seven different molecules. We found that the expression of most of these molecules was correct in the mutant somites, despite the disorganisation. This makes it more plausible that the melanophore migration defect in *choker* mutants is caused by a single molecule, rather than a host of molecular defects. The various processes of neural crest migration are regulated by a number of different molecules and it is thus likely that the process of lateral pathway shutdown will also be under the control of more than one gene. Thus, although *SemaZ1a* may have a role in lateral pathway shutdown, there might be other molecules that also contribute to this process and the expression of these might be aberrant in *choker* mutants.

Although we have chosen gene expression analysis as a tool to look for defects in *choker* mutants there are some caveats to this approach. The *in situ* method may not be sensitive enough to pick up small differences in expression. In addition, there is a possibility that a protein may have a long enough half-life to be active some hours after transcription of the gene has ceased. Thus, the absence of expression at 36 hpf does not unequivocally negate a role in lateral pathway shutdown. In addition, it is conceivable that lateral pathway shutdown is mediated by the upregulation of an attractant in the stripe region, as opposed to the switching on of an inhibitor in the pathway environment. This is relatively unlikely given that melanophores undergo protrusion collapse upon contact with the lateral pathway environment, which is suggestive of an inhibitor being present in this region. However, even allowing for this possibility, we never saw the expression of any of the molecules we analysed in stripe regions. Finally, we have analysed only a small number of molecules that may have roles in neural crest

migration. This was not intended to be an exhaustive study as we have only analysed the most obvious candidates and there are a number of other molecules which have intriguing expression patterns and which may be affected in the anterior somites of *choker* mutants. The second zebrafish homologue of Sema III, *SemaZ1b,* for instance is initially expressed in the posterior half of the somite, but coincident with the initiation of neural crest migration its expression expands to envelop the whole width of the somite (Roos et al., 1999). There is a strong possibility that this molecule has a role in neural crest migration and, as such, may also have a role in lateral pathway shutdown. Future studies of other candidate neural crest guidance molecules may uncover the molecular players involved in the generation of the *choker* melanophore defect.

Chapter 7

Characterisation of the role of neuropilin-1 in zebrafish neural crest migration and patterning

Introduction

The expression analysis of putative neural crest guidance molecules in *choker* mutants and wild-type siblings revealed several intriguing expression profiles. Although the involvement of some of these molecules in neural crest migration has been shown for higher vertebrates, there is no direct evidence to suggest that this is also the case in zebrafish. The expression patterns uncovered by us and in previous studies however, were consistent with a possible role in neural crest guidance, and we were thus keen to explore the involvement of at least one of these molecules in the patterning of zebrafish neural crest cells.

There is strong evidence from chick and mouse models to suggest that Eph receptors and ephrin ligands play an important role in guiding neural crest cells along their migratory pathways (see chapters 1 and 6). However, although the zebrafish somite is known to express several ephrin ligands, it is not known which, if any, of the Eph receptors are expressed by zebrafish neural crest. Similarly, no neural crest expression has yet been shown for slits, the ligands for the roundabout family of receptors, despite quite extensive expression studies in the mouse. In contrast, the semaphorin Z1a receptor, neuropilin-1, has been reported to be expressed by premigratory neural crest cells and downregulated at the time of their migration (Shoji, personal communication). The only published study of zebrafish neuropilin-1 documented no neural crest expression; however, no timepoints were investigated between the 5- and 22- somite stage. Our own studies have shown that the ligand is expressed in an intriguing pattern that is suggestive of roles, not only in the early processes of neural crest migration, but also in the later event of lateral pathway shutdown. Based on these expression data we decided that neuropilin-1 was plausibly involved in neural crest guidance and decided to investigate it further.

Although the role of semaphorins and neuropilins has been studied with respect to axon guidance, the understanding of the exact role they play in neural crest migration is limited. The first member of the semaphorin family that was identified was collapsin, so named due to the collapsing activity it induced in neuronal growth cones *in vitro* (Luo et al., 1993). Semaphorin family members have since then been identified in a number of invertebrate and vertebrate organisms including Drosophila, mouse, human and zebrafish. They are found as both transmembrane and secreted molecules while their receptors, the members of the neuropilin family, are type I transmembrane receptors (Kolodkin et al., 1997). An additional role for this family of receptors and ligands, beside their already well characterised involvement in axon guidance and pathfinding, has been proposed after studying the expression of collapsin-I and its effect on migrating neural crest cells *in vitro* (Eickholt et al., 1999). Chick collapsin-I was found to be expressed in hindbrain and somite regions that neural crest cells are excluded from, namely hindbrain rhombomeres r3 and r5, and the caudal portion of the sclerotome. The receptor for collapsin-I, neuropilin-1, was found to be expressed in a complementary expression pattern in the hindbrain and somite, and in addition was also expressed by cultured neural crest cells. *In vitro* stripe assays confirmed that, upon contact with collapsin-I stripes migrating crest cells round up, lose their lamellipodia and stop migrating. Despite early studies that examined mouse knockouts of semaphorin and neuropilin molecules and found no gross neural crest defects (Behar et al., 1996; Kitsukawa et al., 1997; Taniguchi et al., 1997), more recent evidence suggests that the members of these two families may indeed have a role in neural crest development. For instance, semaphorin 3C deficient mouse embryos have cardiac defects reminiscent of a cardiac neural crest phenotype (Brown et al., 2001) whereas Sema 3A and neuropilin-1 mouse mutants have defects in the patterning of the sympathetic nervous system (Kawasaki et al., 2002).

A number of zebrafish homologues of the semaphorin family members have been identified and their roles best characterised with respect to axon guidance and angiogenesis (Roos et al., 1999; Shoji et al., 2003; Shoji et al., 1998). The expression of some of these molecules mirrors that observed in higher vertebrates and is consistent with a possible role for semaphorin in neural crest guidance. The only zebrafish neuropilin homologue to have been identified is neuropilin-1 and although it has been shown to have a role in vasculogenesis, its role in neural crest patterning has not been examined (Lee et al., 2002).

Neuropilin-1 expression has been reported in the neural crest at stages prior to the onset of migration (Shoji, personal communication). The expression of its ligand, SemaZ1a, is found in the dorsal and ventral portions of the myotome prior to, and during the early stages of neural crest migration. Coincident with the start of neural crest migration, neuropilin-1 expression in neural crest cells begins to be downregulated and we would thus like to propose that the role of neuropilin-1 is to regulate the timing of neural crest emigration. At stages prior to the initiation of neural crest migration the repulsive interaction between the neuropilin-1 receptor and its semaphorin ligand would prevent neural crest cells from leaving the neural tube. At the time of initiation of migration, the downregulation of neuropilin-1 in neural crest cells would enable them to start migrating as they would no longer find the SemaZ1a expressing somite substrate repulsive. We predict that, in the absence of neuropilin-1, neural crest cells would all start migrating simultaneously, as soon as the migratory pathway opens.

In order to test our hypothesis, we used *in situ* hybridisation to confirm, and further analyse, neuropilin-1 expression in the neural crest. We then produced morpholino knock-downs of neuropilin-1 and examined the morphant phenotype to see whether it had the expected disruptions in neural crest migration and patterning.

Results

Expression of neuropilin-1 *in zebrafish neural crest*

We used a *neuropilin-1* (*nrp1;* kind gift of W Shoji) antisense *in situ* probe to examine batches of wild-type embryos for neural crest expression. We looked at several timepoints between 12 hpf and 24 hpf and the first stage when we could see *nrp-1* expression in distinct cell types was at 14 hpf. At this stage, *nrp-1* staining was observed in a stripe located on top of the neural tube, where the neural crest is found (arrows, Figure 7.1A). The expression domain started at the axial level of somite 1 and extended posteriorly, and thus did not appear to include cranial crest. At 16 hpf neural crest *nrp-1* expression was stronger, in addition to which we had begun to see strong staining in the floor plate (arrows, Figure 7.1B). By 18 hpf crest *nrp-1* expression was stronger still and the domain of expression had expended medio-laterally (Figure 7.1C). At 21 hpf *nrp-1* expression had extended to the hypochord and several cells scattered along the ventral boundaries of somites, previously shown to be angioblasts (asterisk,

Figure 7.1. *Nrp1* expression was detected in neural crest cells from 14 hpf to 21 hpf
(A-D) *In situ* hybridisation with the *nrp1* probe revealed labelling in several distinct cell types. Lateral views of 14 hpf embryos revealed faint expression at the top of the neural tube (arrows, A), which we believe to be neural crest. At 16 hpf the neural crest labelling became more pronounced (B). In addition, *nrp1* labelling was detected in the floor plate (arrows, B). At 18 hpf the neural crest signal was more pronounced still (C). By 21 hpf the neural crest signal was being downregulated and could only be detected in more posterior regions of the trunk (arrows, D). At this stage we also observed labelling in the hypochord, and in a number of cells at ventral somite boundaries (asterisk, D). These are likely to be migrating angioblasts.

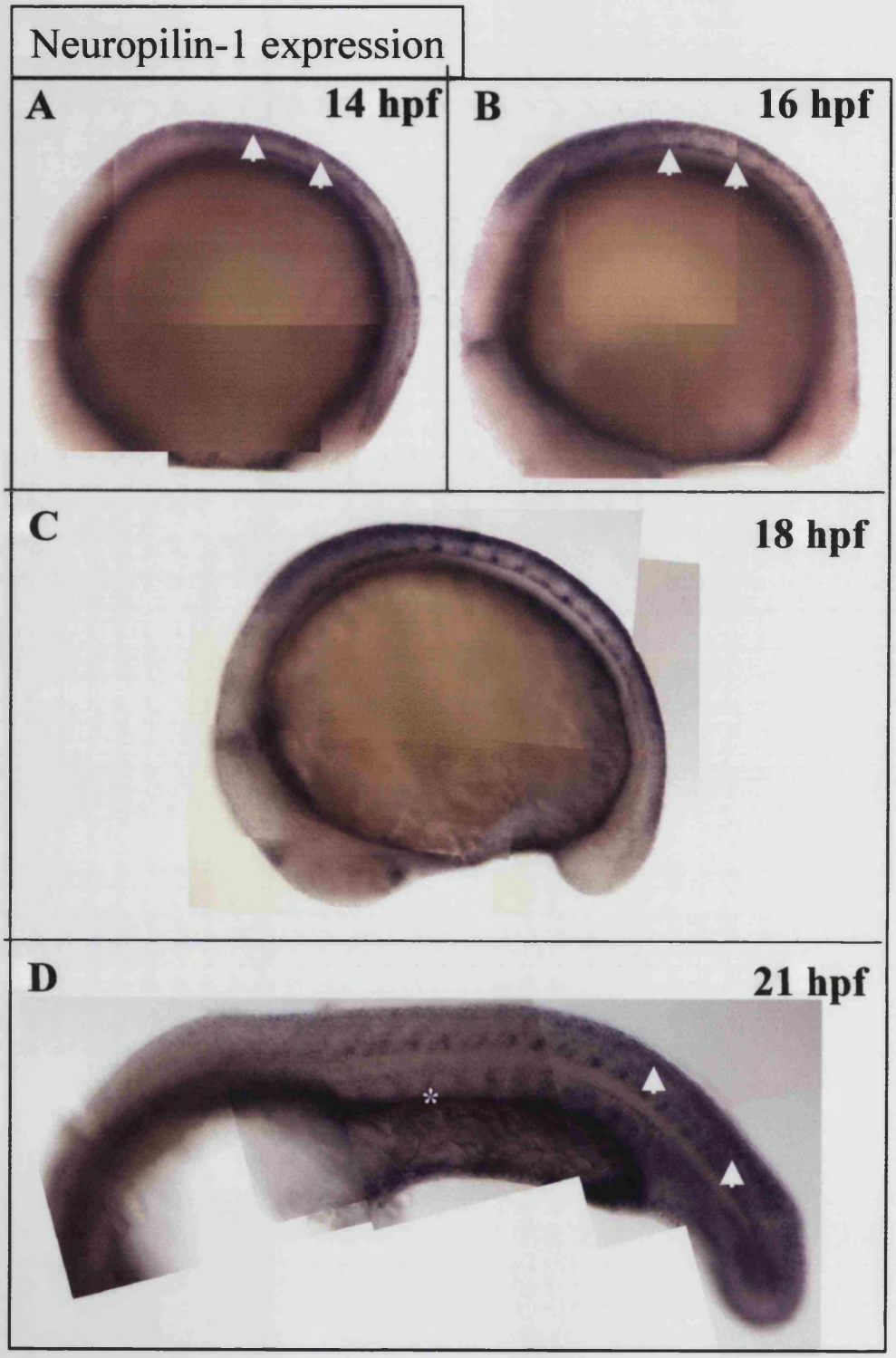
Neuropilin-1 expression
A
14 hpf
B
16 hpf
C
18 hpf
D
21 hpf

Figure 7.1D) (Shoji et al., 2003). By this stage, neural crest expression persisted only in the posterior trunk (arrows, Figure 7.1D). Neural crest migration on the medial pathway was now underway however we never saw any labelled migrating neural crest cells. By 24 hpf the crest expression of *nrp-1* had disappeared completely (data not shown).

In summary, *nrp-1* appears to be switched on early after neural crest induction and is downregulated in neural crest cells as they begin to migrate.

Late effects of neuropilin-1 morpholino knock-down

We predicted that in the absence of the neuropilin-1 protein, neural crest migration would be aberrant and this might result in defective patterning of derivatives. To see whether knocking-down the neuropilin-1 protein will have an effect on neural crest migration and patterning we used a morpholino. The effects of neuropilin-1 knock-down in zebrafish have been previously analysed with the use of a morpholino, in a study that characterised the role of this gene in vasculogenesis (Lee et al., 2002). As a consequence of morpholino injection, the morphants displayed vascular defects, specifically a loss of intersegmental vessels. The axial vessels, however, remained unaffected. As this morpholino had been successfully used before, we decided to use the same morpholino sequence in our study. In addition, to ensure that the morpholino is working properly under our conditions, we used the predicted absence of intersegmental vessels in nrp-1 morpholino injected embryos as a positive control. To ensure that any effects we might observe are specific to neuropilin-1 knock-down and not just a side effect of the injection process we also injected a 4-base mismatch morpholino into stage-matched wild-type embryos. The mismatch morpholino was usually injected at twice the dose used for nrp-1 morpholino injections.

Wild-type embryos were injected with the nrp-1 and control morpholinos at the one cell stage. Initially, a range of concentrations was used to establish the dose required to give rise to the vascular defect whilst keeping the number of deformities low. For the lowest dose we injected approximately 2.5nl of a 100μM solution. To increase the dose we simply doubled, tripled and quadrupled the volume injected so that the respective injection volumes were approximately 5, 7.5 and 10nl of a 100μM solution. The dose of mismatch morpholino injected was approximately double that of the highest nrp-1 morpholino dose – 10nl of a 200μM solution.

We reared the injected embryos to around 48-52 hpf and then looked for vascular defects. To enable observation of blood vessels, we injected FITC-dextran in 1

x Danieau's into the sinus venosus of all morpholino injected embryos and then analysed the live morphants for vascular defects. The embryos injected with the mismatch morpholino had normal vasculature, consisting of numerous intersegmental vessels extending dorsally from the dorsal aorta, at a frequency of one per somite (arrows, Figure 7.2A). Depending on the dose of morpholino used, the neuropilin-1 morphants displayed intermediate or severe vascular defects. At the lower dose (7.5nl) the most severe defect displayed was approximately 75% loss of intersegmental vessels, but many were less severe (arrows, Figure 7.2B). At higher doses however (10nl) the loss of intersegmental vessels was complete in all embryos (Figure 7.2C). In concordance with the previous study, the large axial vessels remained unaffected.

Having confirmed that the morpholino gave specific knock-down, we asked whether injecting different doses of it into wild-type embryos and then rearing them to 3 dpf would result in pigment patterning defects. By this stage neural crest migration is nearing completion and most of the pigment cells are found in their final destinations, thus we expected to be able to see any overt patterning defects. Observation of mismatch morpholino injected embryos revealed that, except for a slight edema that is probably a non-specific injection defect they had an overall normal morphology and looked like uninjected controls. Furthermore, they appeared to have normal pigment patterning - the xanthophores were evenly distributed in the head and flank of the embryos, and were slightly more concentrated dorsally. The melanophores were found in one of the three incompletely formed melanophore stripes running along the length of the embryo – the dorsal, lateral and ventral stripes (Figure 7.3A). The nrp-1 morpholino injected embryos, by comparison, had small morphological abnormalities in addition to the non-specific edema, including a slight shortening of the body axis and a thinner trunk. In addition, they displayed a number of pigment patterning abnormalities (Figure 7.3B). In the most extreme case, the xanthophores were not evenly distributed through the flank of the embryo but were instead found in isolated patches. There also appeared to be a defect in melanophore patterning as they were often not in the melanophore stripes, but found in ectopic locations throughout the trunk (arrows, Figure 7.3B). In addition, there was a clear defect in the lateral stripe as some melanophores seemed unable to polarise along the antero-posterior axis. Instead, they remained elongated in the dorso-ventral plane or had a stellate, rather than elongated, morphology. To test the specificity of these defects we injected batches of embryos with four different nrp-1 morpholino doses, and with the control morpholino. We assigned three classes of

Figure 7.2. Injection of the nrp1 morpholino resulted in inter-segmental vessel defects

(A-C) Lateral views of 48-52 hpf embryos injected with FITC-dextran highlight the embryonic vasculature. Embryos injected with the control morpholino reveal the large dorsal aorta and a number of small inter-segmental vessels (arrows, A). Injection of small amounts of nrp1 morpholino resulted in a reduction of inter-segmental vessel number (arrows, B). This defect was exacerbated when larger amounts of nrp1 morpholino were injected, and resulted in a complete loss of inter-segmental vessels; however the dorsal aorta remained unaffected (C).

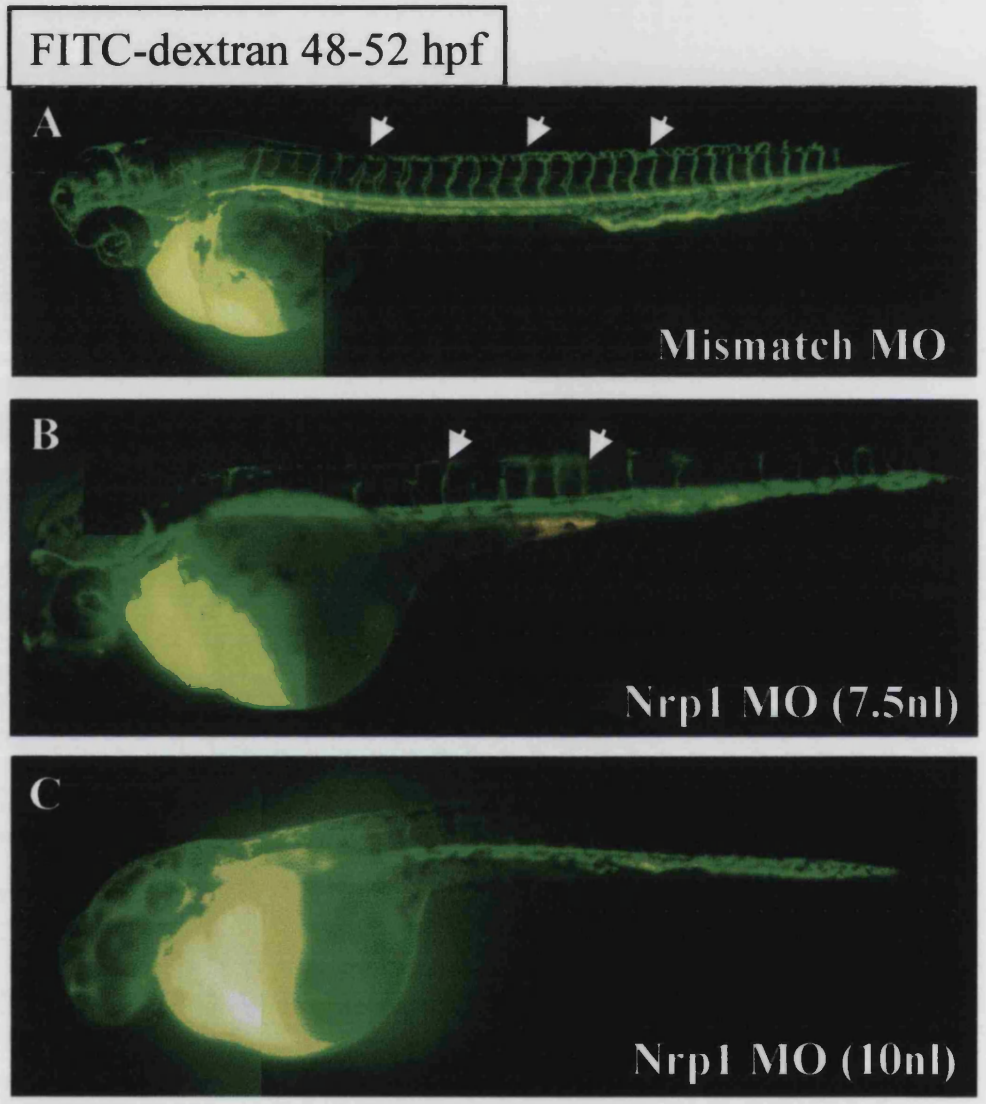
FITC-dextran 48-52 hpf
A
Mismatch MO
B
Nrp1 MO (7.5nl)
C
Nrp1 MO (10nl)

Figure 7.3. Injection of nrp1 morpholino resulted in pigmentation defects at 3 dpf
(A, B) Lateral views of control and nrp1 morpholino injected embryos. Embryos injected with the control morpholino had a normal morphology and pigmentation (A). Most melanophores were found in stripes and the xanthophores were evenly spread throughout the flank of the embryo. By comparison, nrp1 morpholino injected embryos had ectopic melanophores (arrows, B) and xanthophores that were not evenly distributed, resulting in a 'patchy' appearance. (C) Dose response curve revealed that the severity of pigment defects was directly proportional to the dose of injected nrp1 morpholino. For this purpose the pigment phenotypes were grouped into three distinct classes of varying severity. We found that the mild phenotypes decreased and the strong ones increased at progressively higher nrp-1 morpholino doses.

Pigment phenotype 3 dpf

C. Severity of pigment phenotype at different morpholino concentrations

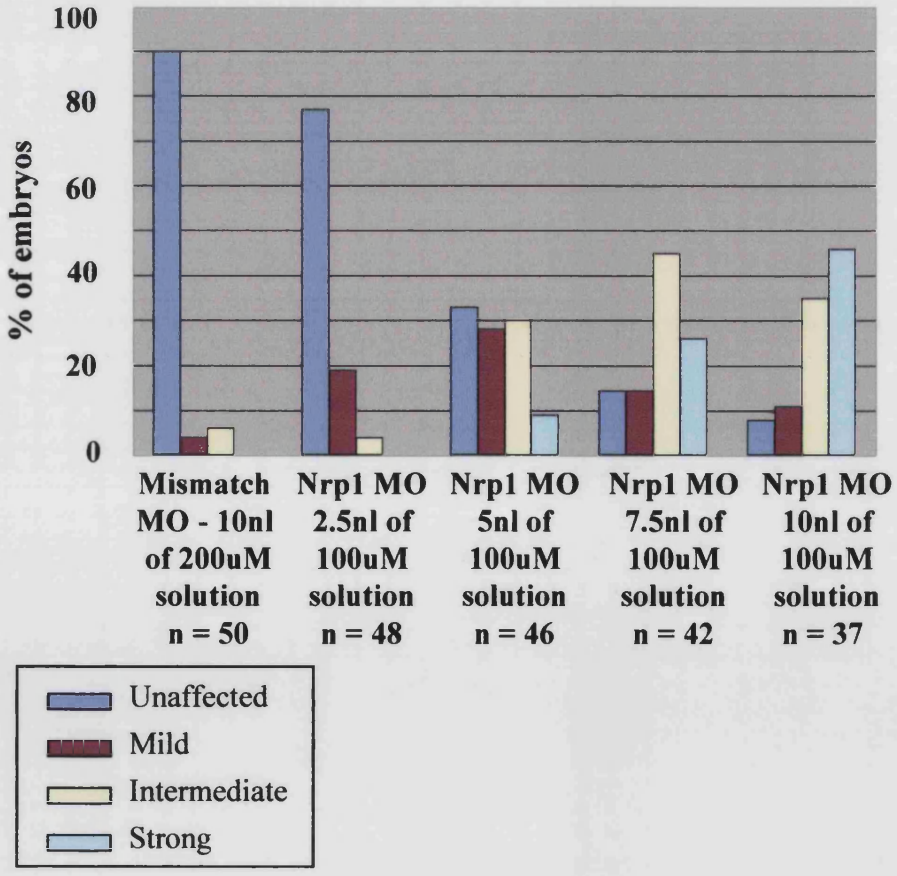

morphant phenotypes, ranging from mild to severe, and counted the number of injected embryos that belonged to each class. The mildest phenotype consisted of an overall normal patterning of xanthophores and melanophores. Some small disturbances were however seen in the lateral stripe where melanophores were not correctly oriented or evenly spread along the horizontal myoseptum. The morphants with intermediate phenotypes had a few ectopic melanophores, whereas the severely affected embryos had many ectopic melanophores and patchy xanthophores. Our counts revealed that most of the embryos injected with the mismatch morpholino were unaffected, but a small percentage (10.5%) had mild and intermediate phenotypes (Figure 7.3C). This could simply reflect normal variation found in a wild-type embryo population. At the lowest concentration of the neuropilin-1 morpholino the number of unaffected embryos decreased and the number of embryos displaying mild and interemediate phentopyes increased proportionally (77.1% and 22.9% respectively) (Figure 7.3C). As the morpholino concentration was increased we observed an increase in the number of severely affected embryos and a concomitant decrease in the less severe phenotypes (Figure 7.3C). At the highest concentration employed, there was a large number of severely affected embryos and only a small percentage of unaffected ones (45.9% and 8.10% respectively) (Figure 7.3C). These observations confirm the specificity of the pigment phenotype to the neuropilin-1 morpholino. At the highest morpholino concentration used we also begun to get a small number of non-specific deformities such as kinking of the tail and severe shortening of the body axis. We thus decided to use this concentration in all our future experiments as at this dose we get strong phenotypes while the deformities are kept to a minimum.

We looked at nrp-1 injected embryos at 5 dpf. However, by this stage the pigment phenotype seems to have recovered (data not shown). The xanthophores are now evenly distributed through the flank and the ectopic melanophores have disappeared. The lateral stripe defects also appeared to have been rectified. However, the embryos look like they are about to die shortly, possibly from the vascular defects caused by the morpholino.

Previous reports suggest that semaphorins have a role in the patterning of the dorsal root ganglia. Neuropilin-1 knock-out mice showed defects in the trajectories of peripheral nervous system efferent fibres (Kitsukawa et al., 1997) and we thus thought it was possible that our nrp-1 morphants might have a DRG phenotype. We used the anti-Hu antibody which detects the pan-neuronal marker Hu, and looked at dorsal root

ganglia in neuropilin-1 and control morpholino injected 3 dpf embryos. At this stage the dorsal root ganglia of a zebrafish embryo are found in stereotypic positions all along the trunk, at the frequency of one DRG per somite. Control injected embryos did indeed display this characteristic pattern (arrows, Figure 7.4A). In contrast, neuropilin-1 injected morphants had several ectopic DRGs (arrows, Figure 7.4B). To confirm that the dorsal root ganglia in neuropilin-1 morphants were supernumerary we counted the number of DRGs in the first 14 somites of 3 dpf neuropilin-1 and control morpholino injected embryos. Our counts revealed that there were indeed more ganglia in the neuropilin-1 morphants when compared to the controls (17 ± 0.6 and 13 ± 0.3 respectively) and this difference was found to be statistically significant using a t-test ($P<0.05$).

Members of the semaphorin family have also been implicated in the patterning of the sympathetic nervous system (Kawasaki et al., 2002), and we thus expected nrp-1 morpholino injected embryos to have some ectopic sympathetic neurons. We used Hu-staining to look at batches of 5 dpf nrp-1 morpholino and control morpholino injected embryos. At this stage the sympathetic ganglia form a chain in the vicinity of the dorsal aorta. The mismatch morpholino injected embryos had a number of cells in the right locations, and extending as far as somite 14 (arrows, Figure 7.4C). The nrp-1 morpholino injected embryos also had a chain of cells in the appropriate location (arrows, Figure 7.4D). There were no significant differences in the number of sympathetic neurons found in mismatch morpholino injected and nrp-1 morpholino injected embryos (8 ± 0.5 and 9 ± 1.0 respectively).

To investigate the basis of the small morphological abnormalities we consistently observed in nrp-1 morpholino injected embryos, we looked at myotome morphology. Previous studies have shown that nrp-1 morphants have a lack of intersegmental vessels, and it was likely that the lack of adequate blood supply may cause some muscle defects. We observed 3 dpf nrp-1 and mismatch morpholino injected embryos by live microscopy. The myotomes of mismatch morpholino injected embryos displayed the characteristic chevron-like shape and regular, strong boundaries. Nrp-1 morpholino injected embryos had relatively normal myotomes. The muscle striations were present and appeared normally organised, suggesting that muscle fibres differentiated normally. The muscle blocks were however slightly U-shaped and the boundaries somewhat weak in places but these defects were vestigial (data not shown). The most striking defect involved myotome size – the nrp-1 morphant somites appeared

Figure 7.4. Nrp1 morpholino injection resulted in DRG defects but did not affect the sympathetic neurons

(A, B) Immunofluorescent detection of the anti-Hu antigen reveals dorsal root ganglia at 3 dpf. Lateral views of control morpholino injected embryos revealed that they have normally patterned DRGs (arrows, A). Nrp1 morpholino injected embryos however had several ectopic DRG neurons (arrows, B). (C, D) Immunofluorescent detection of the anti-Hu antigen reveals sympathetic neurons at 5 dpf. We detected no difference in the number or patterning of sympathetic neurons in control morpholino injected (arrows, C) and nrp1 morpholino injected embryos (arrows, D).

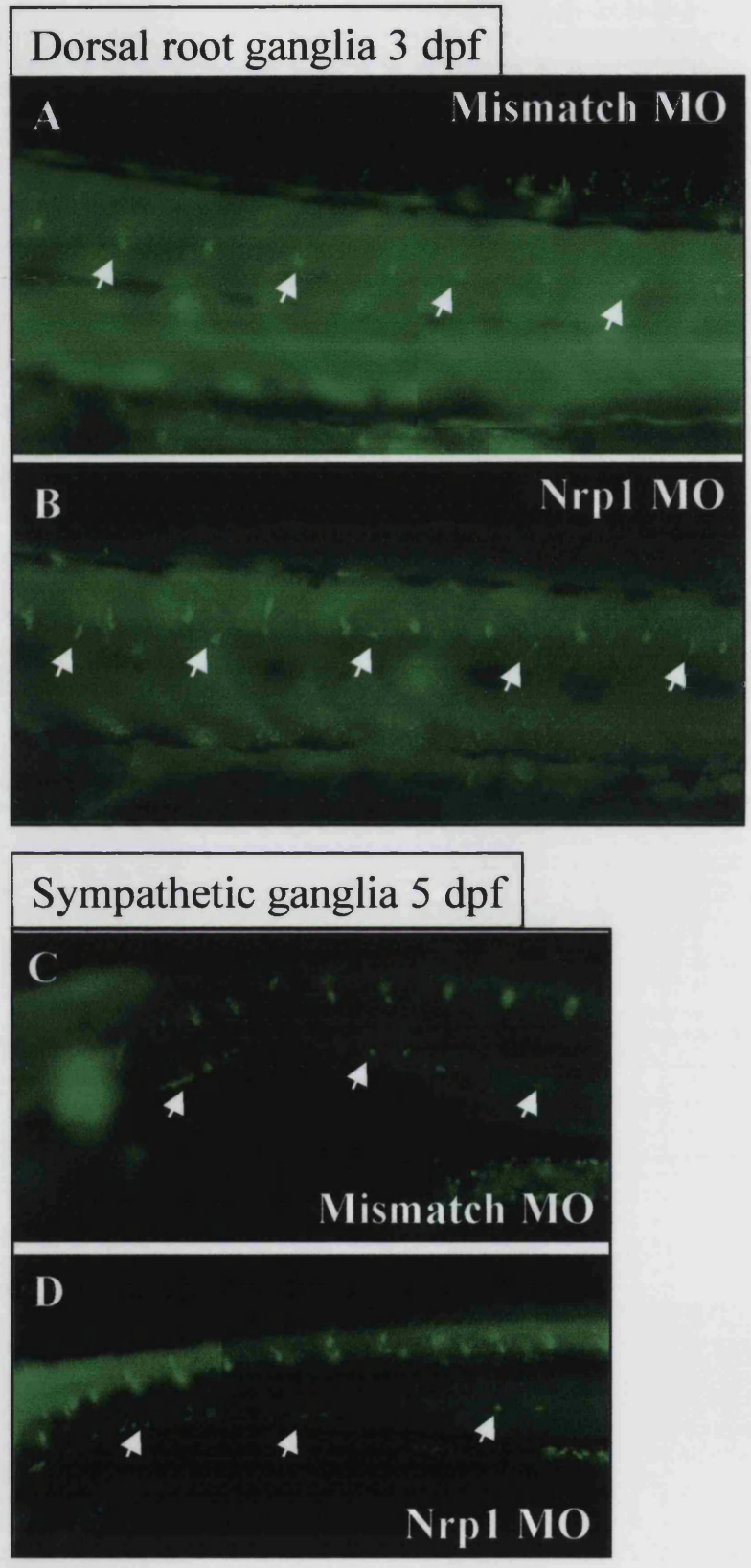
Dorsal root ganglia 3 dpf
A
Mismatch MO
B
Nrp1 MO
Sympathetic ganglia 5 dpf
C
Mismatch MO
D
Nrp1 MO

shorter in the dorso-ventral plane. To confirm this we sectioned some embryos and looked at them in transverse section. This confirmed our initial observations and revealed that the nrp-1 morphant somites are indeed shorter, thus accounting for the thinner body in these embryos (data not shown).

In summary, we found that neuropilin-1 morphants had several neural crest patterning defects. They displayed supernumerary dorsal root ganglia, ectopic melanophores, and a xanthophore patterning defect where the xanthophores do not populate the whole flank of the embryo and are instead found in discrete patches. However, these patterning defects might be a secondary consequence of defective somite morphology.

Neural crest migration defects in neuropilin-1 morphants

To see whether injection of the nrp-1 morpholino had any effect on neural crest migration we used *in situ* hybridisation with the neural crest marker *Sox10.* This marker is expressed in premigratory neural crest, and is maintained in most neural crest cells during the early stages of their migration. After 24 hpf its expression becomes progressively downregulated and restricted to select subpopulations of neural crest cells, however at earlier stages it is thought to label most neural crest cells and is therefore a good marker.

Our prediction was that nrp-1 might have a regulatory role during the early stages of neural crest migration. To see whether knock-down of nrp-1 resulted in neural crest migration defects we injected wild-type embryos with neuropilin-1 and mismatch morpholinos and fixed them at 18, 21 and 24 hpf. At 18 hpf, mismatch morpholino injected embryos had approximately 5-6 distinct streams of neural crest cells migrating on the medial pathway (arrows, Figure 7.5A). A large number of labelled cells were seen in the premigratory position, on top of the neural tube. Nrp-1 morpholino injected embryos displayed a range of phenotypes. The morphants had a number of labelled migrating cells and in the more severely affected embryos these were found all over the medial face of the somite instead of being organised into distinct streams (Figure 7.5B). Even when we were able to discern streams of migrating cells, they were not as tightly organised as in the controls. Instead, cells migrated away from the main stream and lent a disorganised aspect to migration. In addition, there appeared to be more cells migrating in the nrp-1 morpholino injected embryos. To confirm this, we counted the number of migrating cells in nrp-1 and mismatch morpholino injected embryos. Our

Figure 7.5. *Sox10* labelling revealed that neural crest migration is defective in nrp1 morpholino injected embryos

(A, B) *In situ* hybridisation with the neural crest marker *Sox10* revealed several labelled cells at 18 hpf. Mismatch morpholino injected embryos had several labelled cells at the top of the neural tube, and migrating in organised streams on the medial pathway (arrows, A). Nrp1 morpholino injected embryos also had labelled cells on top of the neural tube and on the medial pathway (B). However the migrating cells were disorganised. (C, D) Lateral views of embryos labelled with the neural crest marker Sox10 revealed numerous labelled cells at 21 hpf. Embryos injected with the mismatch morpholino had labelled cells on top of the neural tube and migrating in distinct streams on the medial pathway (arrows, C). By comparison, the migrating cells in nrp1 morphants migrated in a disorganised fashion (D).

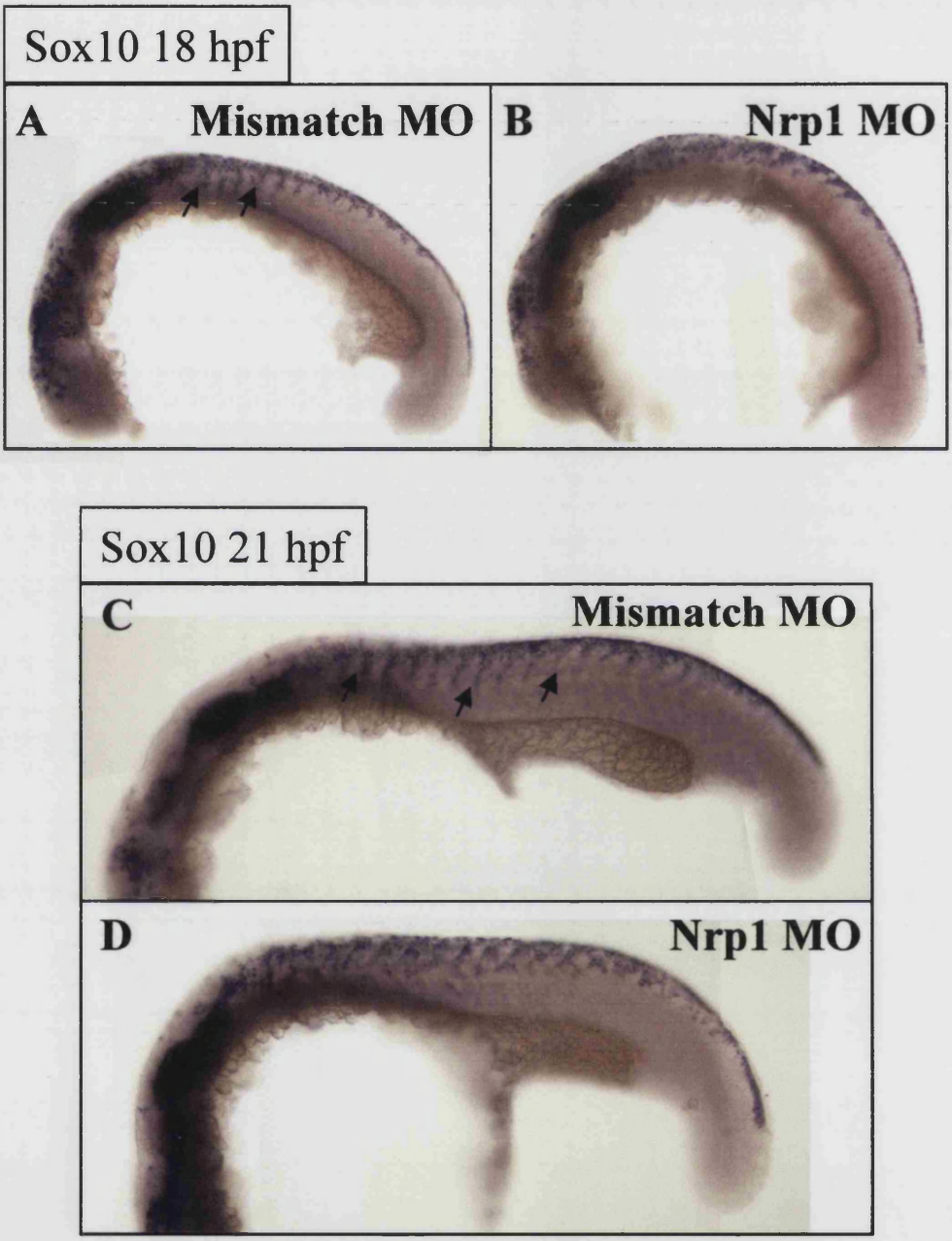
Sox10 18 hpf
A
Mismatch MO
B
Nrp1 MO
Sox10 21 hpf
C
Mismatch MO
D
Nrp1 MO

counts and statistical analyses using a t-test, showed that there was indeed a significantly higher number of neural crest cells ($P<0.05$) undergoing migration on the medial pathway in nrp-1 morpholino morphants compared to mismatch morpholino injected embryos (42 ± 2.2 n=9, and 30 ± 2.8 n=10 respectively) (Figure 7.6A).

By 21 hpf these defects were less pronounced. By now there were approximately 10 streams of migrating cells in each mismatch morpholino injected embryo (arrows, Figure 7.5C). These were well organised and the cells within each stream were tightly associated with one another. In contrast, the streams of migrating neural crest cells in the nrp-1 morpholino injected embryos were disorganised (Figure 7.5D). Counts of migrating cells at 21 hpf revealed that the defect in cell number was less striking at this stage, but there were still a significant difference ($P<0.05$) in the number of migrating neural crest cells in neuropilin-1 and control morpholino injected embryos (81 ± 2.2 n=10 and 70 ± 2.8 n=10 respectively) (Figure 7.6B).

By 24 hpf these defects were almost undetectable. The neural crest cells were now migrating in organised streams of cells throughout the trunk of both mismatch and nrp-1 morpholino injected embryos (Figure 7.7A, B). Although some disorganisation was still apparent in the more severely affected nrp-1 morphants, this was at a much lower level than observed at earlier stages. Similarly, there did not seem to be an excess of migratory cells in nrp-1 morphants at this stage, however it was not possible to confirm this by cell counts due to the high number of cells undergoing migration at this stage.

Thus the neural crest migration defects, which are at first very pronounced, decrease over time, which is what we would expect for a molecule whose role we predicted to be in the regulation of the early stages of neural crest migration.

To see whether the knock-down of neuropilin-1 also has effects on lateral pathway neural crest migration we used *in situ* analysis with the marker *gch* on neuropilin-1 and control morpholino injected embryos. *gch* is a gene involved in the synthesis of pteridine pigments and at early developmental stages (upto 30 hpf) it is expressed in both xanthoblasts and melanoblasts. As these are thought to be the only two types of derivatives that migrate on the lateral pathway in zebrafish we expected to be able to successfully analyse lateral pathway migration with the use of this marker. The onset of neural crest migration on the lateral pathway occurs shortly before 24 hpf thus we decided to analyse neuropilin-1 and control morpholino injected embryos at 24 hpf. Our observations revealed that at this stage mismatch morpholino injected embryos

Figure 7.6. Counts of *Sox10* labelled cells revealed a significantly higher number of cells migrating on the medial pathway of nrp1 morphants

(A, B) Mean number ± SEM of cells migrating on the medial pathway of control morpholino and nrp1 morpholino injected embryos. Statistical analysis using a t-test showed that there was a significant difference in the number of migrating cells on the medial pathway of control and nrp1 morpholino injected embryos at 18 hpf (A). At 21 hpf this difference was smaller however it was still statistically significant (B).

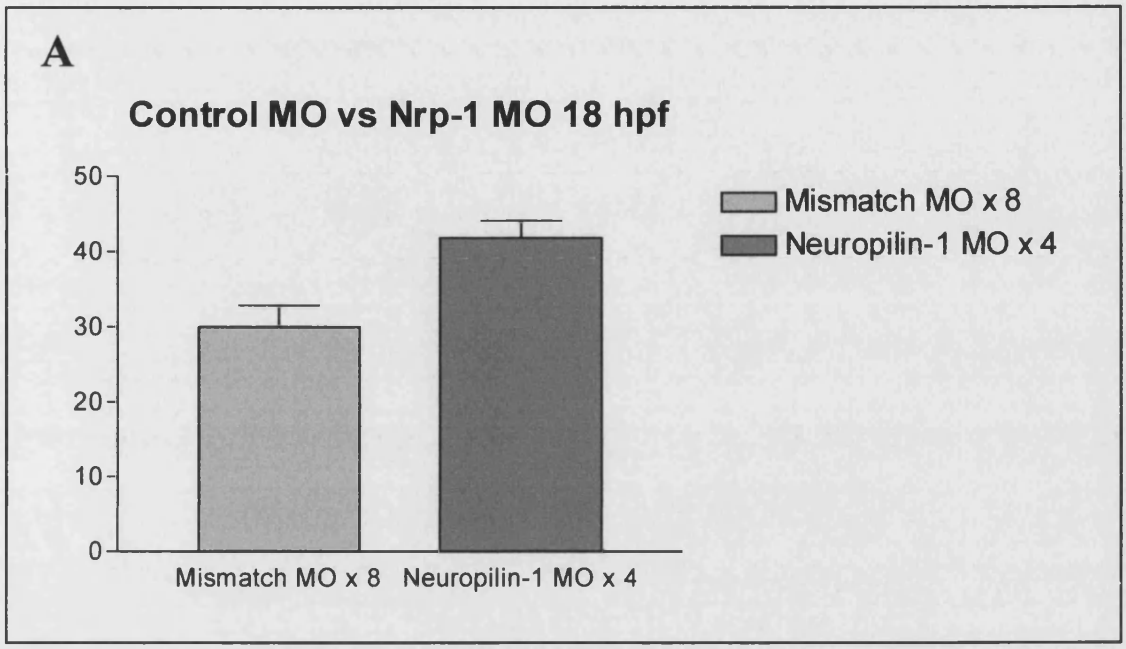
A
Control MO vs Nrp-1 MO 18 hpf
50
40
30
20
10
0
Mismatch MO x 8
Neuropilin-1 MO x 4
Mismatch MO x 8
Neuropilin-1 MO x 4

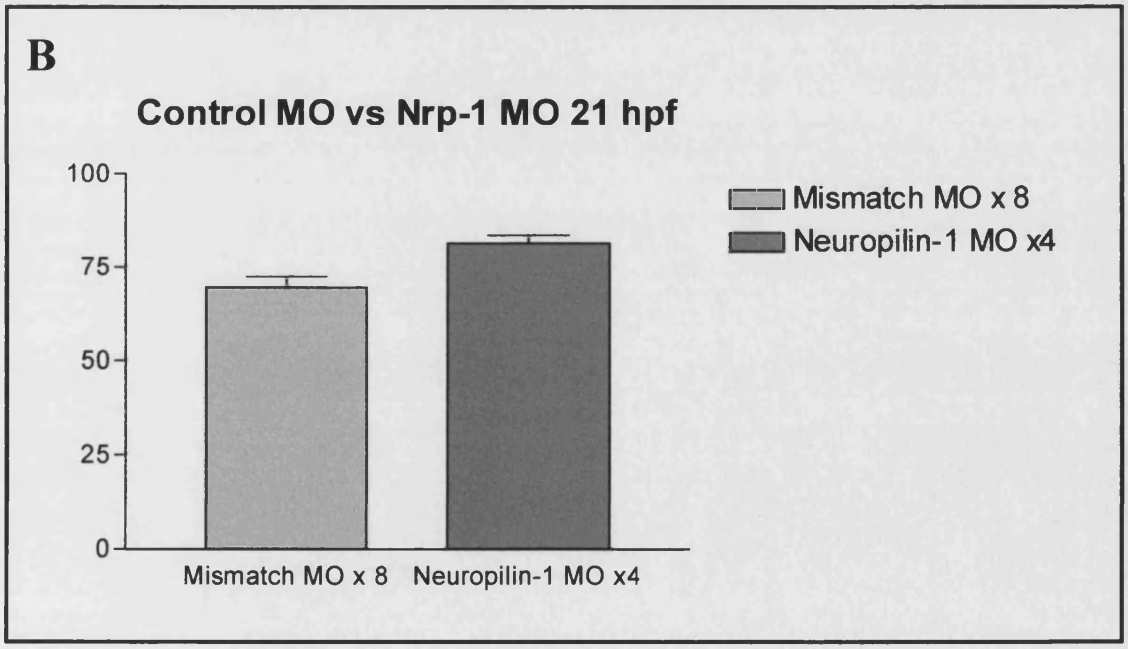
B
Control MO vs Nrp-1 MO 21 hpf
100
75
50
25
0
Mismatch MO x 8
Neuropilin-1 MO x4
Mismatch MO x 8
Neuropilin-1 MO x4

Figure 7.7. *In situ* marker analysis at 24 hpf revealed distinct neural crest phenotypes on the medial and lateral pathways

(A, B) *In situ* hybridisation with the neural crest marker *Sox10* revealed labelled cells migrating on the medial pathway at 24 hpf. Lateral views of control morpholino (A) and nrp1 morpholino injected embryos (B) revealed that they are at this stage indistinguishable. Medially migrating cells are organised into tight streams in both control embryos and nrp1 morphants. (C, D) *In situ* hybridisation with the xanthoblast marker *gch* revealed labelled cells migrating on the lateral pathway at 24 hpf. Lateral views of control morpholino (C) and nrp1 morpholino injected embryos (D) revealed that the number of labelled cells is severely reduced in the morphants.

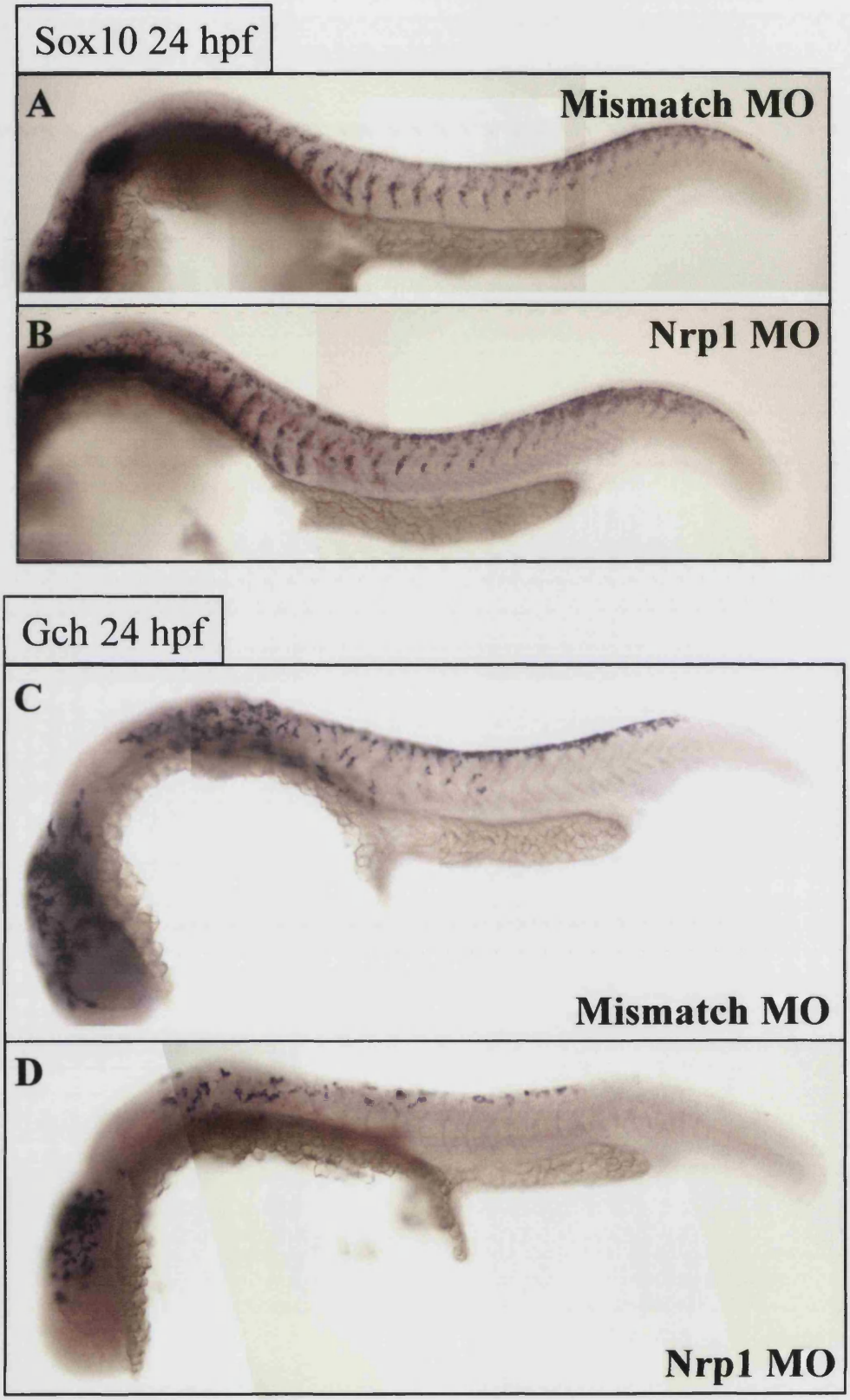
Sox10 24 hpf
A
Mismatch MO
B
Nrp1 MO
Gch 24 hpf
C
Mismatch MO
D
Nrp1 MO

had numerous labelled cells in the head and in the anterior trunk lateral pathway (Figure 7.7C). By comparison, neuropilin-1 morphants had a striking reduction of migrating *gch*-positive cells in both head and trunk regions (Figure 7.7D). Furthermore, there was a drastic reduction in the number of *gch*-labelled premigratory crest cells. Although the cells were present in the right locations, their numbers were decreased in neuropilin-1 morphants.

We have observed distinct effects on medially and laterally migrating neural crest cells. There was an excess of cells migrating on the medial pathway of nrp-1 morpholino injected embryos at 18 and 21 hpf, and a reduction of lateral pathway migrating cells at 24 hpf.

Discussion

The expression of neuropilin-1 *is suggestive of a role in neural crest migration*

We have analysed the expression of *neuropilin-1* at early developmental stages. Our studies revealed that *nrp-1* is expressed in neural crest cells from 14 hpf onwards. Over a period of 4 hours, *nrp-1* expression in the neural crest intensifies, presumably due to the increase in neural crest cell numbers. From 16 hpf onwards expression also becomes evident in the floor plate. This may reflect the role of *nrp-1* in the guidance of subsets of axons found in the floor plate. We never saw any *nrp-1* expression in migrating neural crest cells. We would therefore like to propose that *nrp-1* is downregulated in neural crest cells shortly before they initiate their migration and that this downregulation plays an important part in enabling individual cells to start migrating. Timelapse studies showed that the initiation of medial pathway neural crest migration occurs around 15 hpf and is fully underway by 19 hpf (Jesuthasan, 1996; Raible et al., 1992). We observed a decrease in *nrp-1* expressing premigratory neural crest at 21 hpf, a number of hours after the initiation of neural crest migration, which is consistent with the idea that neural crest cells downregulate *nrp-1* expression before they begin to migrate. As more neural crest cells migrate away from the neural tube, there is a concomitant decrease in the number of neuropilin-1 expressing premigratory neural crest cells. By 24 hpf we saw a complete downregulation of *nrp-1* in the neural crest. If our model is correct, this suggests that by 24 hpf most of the neural crest cells are in a state where they are capable of migrating.

The role of neuropilin-1 in neural crest patterning

We have used a morpholino specific to neuropilin-1 to analyse the role of this protein in neural crest migration and patterning. Our analyses of late embryonic stages revealed a number of neural crest defects, including supernumerary DRGs, ectopic melanophores and a defect in xanthophore patterning. Instead of being evenly distributed over the flank of the embryo, the xanthophores are found in isolated patches. This patterning defect may therefore reflect a possible reduction in xanthophore number. The nrp-1 morphants are however distinct from zebrafish mutants that have a xanthophore reduction such as *salz* and *pfeffer.* These mutants have a defect in a gene required for xanthophore migration (Parichy et al., 2000) and thus they have an almost complete absence of lateral xanthophores. In the nrp-1 morphants we see many lateral xanthophores, thus the xanthophores are clearly able to migrate and differentiate normally. However, they do not populate the whole flank of the embryo suggesting either an insufficient number of cells or defective patterning cues.

Despite previous reports of a neuropilin-1 role in the patterning of the sympathetic nervous system (Kawasaki et al., 2002), our neuropilin-1 morphants had no sympathetic neuron phenotype. However, the earliest stage at which one can see sympathetic ganglia with Hu-staining is 5 dpf and by this stage earlier patterning defects may have recovered.

The dose response study suggests that the pigment defects occur as a result of neuropilin-1 knock-down. However, these defects might be a secondary consequence of the effect of neuropilin-1 on the vascular system. Morphological studies have shown that the morphant myotomes are smaller than their control counterparts, and somewhat disorganised. This might be an effect of intersegmental vessel absence as, without the adequate blood supply, the muscle blocks might atrophy. The pigment and DRG patterning defects that we observed could be a direct consequence of the slight somite disorganisation. We however think this is unlikely. The myotomes of the neuropilin-1 morphant are slightly disorganised and smaller in size than control somites but they still retain a chevron-like shape, have organised muscle striations and weak, but present, boundaries. The mild somite disorganisation seen in several other mutants, including the posterior trunk in *choker,* is not usually associated with a pigment patterning defect, except for the absence of the lateral stripe which is thought to occur as a consequence of the missing horizontal myoseptum. We thus think there is a strong possibility that the

late crest patterning defects in neuropilin-1 morphants occur as a direct result of neuropilin-1 knock-down.

Neuropilin-1 has an early role in neural crest migration

Our analysis of the effects of neuropilin-1 knock-down at earlier developmental stages showed that neural crest migration is defective in neuropilin-1 morphants. We observed severe disorganisation of migrating cells and an increased number of neural crest cells migrating on the medial pathway of neuropilin-1 morphants. We propose that the role of nrp-1 is to control the timing of neural crest migration. In the absence of neuropilin-1, all neural crest cells may be able to start migrating as soon as the pathway opens. Thus, there is an excess of neural crest cells embarking on medial pathway migration simultaneously and this might explain why the migration is disorganised. If there are an increased number of cells migrating at the same time, they might be unable to follow a delineated path and will instead 'spill over' and migrate over the full medial face of the somite.

We also observed an excess of migrating neural crest cells and the concomitant disorganisation at 21 hpf, however at this stage both defects seemed less pronounced. These defects were even less evident at 24 hpf when we saw very little disorganisation and few supernumerary migrating neural crest cells. We believe this to be due to the fact that a large number of neural crest cells emigrated at early stages and there are fewer cells left to migrate at later stages. Thus, the excess of migratory cells and the disorganisation decreases over time. The analysis of the lateral pathway concurs with this idea. The number of cells migrating on this pathway is much lower in neuropilin-1 morphants than in controls suggesting that, due to the excess of medial pathway migration at earlier stages, fewer cells are left to migrate on the lateral pathway. This theory could explain the patterning defects we observe at later developmental stages. An excess of neural crest cells migrates on the medial pathway, and hence, there is an increased number of neural crest precursors that end up differentiating into medial pathway fates, such as neurons and melanophores. Therefore, we see both ectopic melanophores and DRGs. The only neural crest derivatives to migrate exclusively on the lateral pathway are xanthophores. As the number of cells migrating on the lateral pathway is much lower than in controls so is the number of cells that ultimately differentiate into xanthophores, thus accounting for the xanthophore phenotype.

Our analyses of *gch* expression also revealed a reduction of *gch*-labelled cells in the head of *nrp-1* morphants. We found this somewhat surprising as our *nrp-1* expression analyses revealed that *nrp-1* is not expressed in the head and we thus didn't expect it to have a role in cranial neural crest guidance. However, it is possible that the cells we saw in the head were actually trunk neural crest migrating anteriorly to populate head regions.

Interestingly, the pigment patterning defects appear to recover by 5 dpf. This might reflect the ability of zebrafish neural crest cells to regulate their own numbers and recover patterning defects that occur as a consequence of a cell number imbalance. Thus, the xanthophores may proliferate over time to make up for the defect in number. Conversely, the supernumerary melanophores may undergo apoptosis. Studies of the zebrafish mutant *fms* suggest that if a threshold melanophores number is not reached in the stripes, they apoptose due to the lack of community effects (Parichy et al., 2000). Thus, it is conceivable that the isolated ectopic melanophores in the neuropilin-1 morphants undergo apoptosis as a result of the lack of community effects that act as survival factors.

Neuropilin-1 appears to have an important role during the early stages of neural crest migration. It probably isn't involved in neural crest pathfinding as its expression is only maintained in cells that haven't begun to migrate yet. The downregulation of neuropilin-1 might be what enables or permits cells to initiate migration. Previous studies have often dealt with environmental signals that enable neural crest cells to start migrating, such as the change in ECM components and somite architecture, and established the importance of these factors in allowing the initiation of neural crest migration. Our study complements these by characterising an intrinsic change within individual crest cells that has to take place before they can begin to migrate. Thus, our *in situ* analysis has shown that, despite favourable environmental conditions, numerous *nrp-1* expressing neural crest cells stay associated with the neural tube for many hours after the pathway has opened. Future studies may be able to elucidate the mechanism by which *neuropilin-1* expression is regulated in individual cells over time.

Despite the interesting expression of the neuropilin-1 ligand, Sema Z1a during later stages of neural crest migration, the neuropilin-1 expression data gave no evidence for a later role for neuropilin-1 than the one we already described. However, other members of the neuropilin family such as neuropilin-2, the chick homologue of which

has been found to be expressed in crest, might be expressed in migrating zebrafish neural crest cells and have a role in regulating their pathfinding.

Chapter 8

Final Discussion

The processes underlying neural crest development are extremely complex and have fascinated scientist for decades. The study of neural crest migration and patterning has been particularly intriguing – how does a population of cells, which originates in one region of the embryo, migrate towards multiple destinations and generate numerous derivatives in order to establish a complex yet very stereotyped pattern? Much work on this has been done using chick and mouse models and today we have a relatively good understanding of the cellular and molecular basis of neural crest migration in chick. It is now known that somitic muscle has a vital role in guiding neural crest cells as they migrate. Furthermore, a number of muscle-associated molecules that have a role in neural crest pathfinding have been identified and characterised in both chick and mouse. However, the process of neural crest migration is still relatively unexplored in fish and we thus hoped that our studies might contribute to a better understanding of it.

The mutant *choker* is the only known zebrafish mutant that has spatially correlated muscle and pigment patterning defects, and as such, it is unique. By studying this mutant, we hoped to further investigate the relationship between muscle and neural crest development. In addition, we conducted a parallel study in which we characterised a neural crest associated receptor, neuropilin-1, whose interaction with its muscle-associated ligand is thought to be important in the regulation of neural crest migration.

We showed that, in addition to the already described melanophore collar, the *choker* mutant has a number of other neural crest defects. Of these, the only consistent and fully penetrant defect was the loss of xanthophores from the mutant collar. Thus, the region of aberrant muscle development was found to be associated with two separate neural crest patterning defects – an accumulation of melanophores and a loss of xanthophores. We have shown these to be independent of each other, which suggests that they both occur as a consequence of some other primary defect. Since the defect in both the melanophore and slow muscle patterning is one of migration, it is conceivable that the primary defect lies in a molecule that is directly responsible for both the muscle

and neural crest phenotypes. Thus, a recent study identified cadherins as key molecules in the control of slow muscle migration in the zebrafish myotome (Cortes et al., 2003). As cadherins also have an important role in neural crest migration (reviewed in Pla et al., 2001), it is conceivable that a mutation in a cadherin or some other molecule involved in the regulation of migration could cause both the muscle and melanophore migration defects. However, as the muscle defect is quite complex and does not involve solely aberrant slow muscle migration but also a decrease in fast muscle fibres, pectoral fin muscle precursors and muscle pioneers, the real situation is likely to be a lot more complex and not purely dependent upon the loss of function of a molecule involved in migration. A more likely scenario is that the aberrant muscle development is itself responsible for the neural crest defects. Thus, the defective muscle patterning might results in an aberrant distribution of key neural crest guidance molecules over the somite and consequently, neural crest patterning defects.

Our transplant experiments failed to conclusively establish whether the neural crest defects occur as a result of aberrant muscle patterning. However our preliminary transplant data, taken together with the striking spatial correlation between the muscle and neural crest defects and the known role for muscle in the patterning and migration of neural crest derivatives, suggest that the neural crest defects do indeed occur as a secondary consequence of the aberrant muscle development. Consequently, we believe that the melanophore and xanthophore defects are caused by an aberrant distribution of key guidance molecules over the defectively patterned somite. Recent experiments carried out by G Hollway lend proof to this idea, as the transplantation of wild-type somites into a *choker* mutant was found to result in the local rescue of the ectopic melanophore collar.

Using timelapse microscopy we found that the cellular basis of the melanophore defects was aberrant migration. Our studies showed that in wild types the lateral migratory pathway shuts down around 36-39 hpf. In contrast, the mutant melanophores continued to migrate into the *choker* anterior trunk lateral pathway even after it had shut down. We thus believe that the muscle-associated molecules that are defective in *choker* mutants have a role in lateral pathway shutdown. Their expression is likely to be upregulated on the lateral face of the somite at the time of lateral pathway shutdown. By preventing further neural crest emigration onto this pathway they also have an important role in maintaining the integrity of the dorsal and ventral melanophore stripes. Other

molecules expressed in this region may act as survival factors and have a role in the maintenance of xanthophores in the interstripe regions. In their absence, xanthophores are unable to remain in their position and our preliminary data suggests that they undergo apoptosis. As the onset of the xanthophore defect occurs earlier then the melanophore phenotype, the molecules involved in xanthophore maintenance may be distinct from the molecules involved in the shutdown of the lateral pathway.

Previous studies have largely focused on identifying the factors that regulate the initiation of neural crest migration and have established the importance of muscle in the prevention of precocious neural crest migration and in the delay of lateral pathway neural crest migration (Jesuthasan, 1996; Raible et al., 1992). Our study complements these by characterising the process of cessation of lateral pathway migration and revealing the pivotal role of muscle in the regulation of this process. Previous studies have identified numerous factors that play a role in establishing the correct pattern of neural crest derivatives, either as guidance molecules or as stop signals. By comparison, our study has identified the importance of factors that maintain an established pattern. In the absence of these factors, cells migrate to the right locations but are subsequently lost through apoptosis or migration into ectopic locations. A model summarising our findings is shown in Figure 8.1.

By analysing the expression of a number of molecules that are thought to have a role in neural crest guidance we had hoped to identify a molecule or molecules that have an aberrant expression pattern at 36 hpf and that might therefore be responsible for the *choker* defect. However, only one molecule we analysed was expressed at the right time to have a role in lateral pathway shutdown and its expression was normal in *choker* mutants. The guidance of neural crest cells is a very complex process and there are a whole plethora of muscle-associated molecules that have a role in this. Thus it is likely that the *choker* defect lies in a molecule not characterised by us, or as yet unidentified in zebrafish.

Alternatively, the causative agent of the *choker* melanophore phenotype might not be molecular but physical in nature. Thus, the anteriormost somites of *choker* mutants are smaller than their wild-type counterparts due to lack of dorsalmost extension. Even if a putative lateral pathway inhibitor were correctly patterned, smaller amounts of it will be expressed due to the small somite size. This amount may not reach the sufficient threshold to inhibit melanophore migration into the lateral pathway. Furthermore, the stripe melanophores may find the smaller somite easier to bridge.

Figure 8.1 The model summarises our results and proposes that muscle associated cues have a role in maintaining melanophores and xanthophores in their environment.

(A, B) A schematic is shown, depicting transverse views of *choker* mutants and wild-type siblings. During post-migratory stages in wild-type embryos, muscle associated cues prevent melanophores from migrating into the lateral pathway (blue, A). As a result of this, melanophores are maintained in their stripes. In addition, muscle associated cues also have a role in maintaining xanthophores in the lateral pathway environment (blue, A). In the absence of inhibitory cues, melanophores will freely invade the lateral pathway thus giving rise to the ectopic melanophore collar (B). Concomitantly, due to lack of maintenance cues, xanthophores will be progressively lost from the lateral pathway (B).

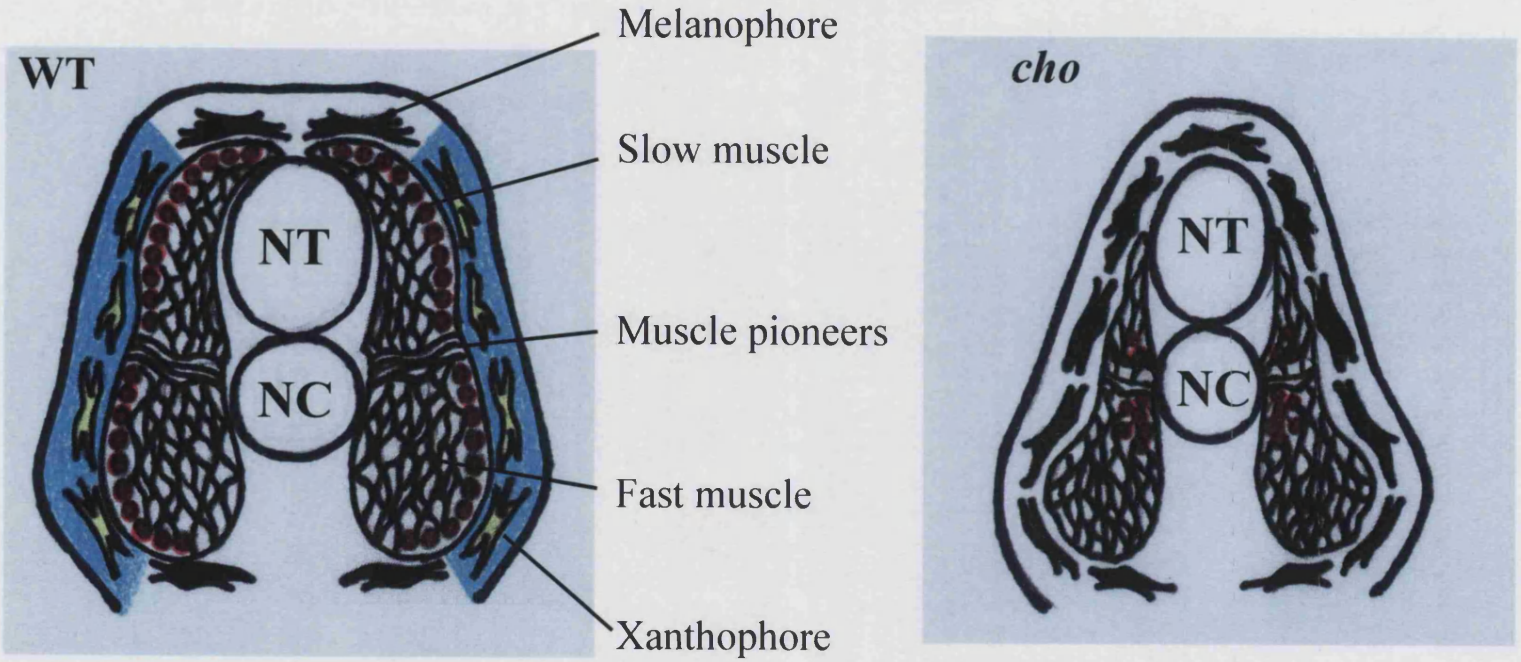
WT
NT
NC
Melanophore
Slow muscle
Muscle pioneers
Fast muscle
Xanthophore
cho
NT
NC

Similarly, the smaller somite might not provide sufficient survival cues to maintain xanthophores in the anterior trunk interstripe region. Alternatively, due to the smaller somite size, a lower number of xanthophores will settle over the anteriormost trunk somites and this number may not be high enough to reach a community effect that normally promotes survival of these cells. If this were the case, we would expect to see xanthophores initially populating the anterior trunk lateral pathway and then being lost over a number of hours. This is indeed what we saw. Whether the causative agent of the neural crest defects is molecular or physical in nature can be further investigated once the *choker* gene is cloned.

On account of the widespread muscle defects we believe *choker* to be a gene involved in muscle patterning. *choker* was initially grouped as a *you*-type mutant on account of its U-shaped somites and morphologically normal notochord. Many of the *you*-type mutants have to date been cloned and identified as members of the hedgehog signalling pathway [Karlstrom, 1999 #235; Roy, 2001 #61; Schauerte, 1998 #110]. However, the detailed muscle characterisation carried out by G Hollway and P Currie suggests that *choker* is not a true *you*-type mutant as it has defects not seen in other *you*-types, such as defective fast muscle and pectoral fin muscle development. Furthermore, *choker* does not have some of the defects usually associated with sonic hedgehog mutants, such as a blood phenotype or grossly defective DRGs (personal observation). We therefore believe that, unlike the other *you*-types, the defect in *choker* does not lie in sonic hedgehog signalling.

Instead, we would like to propose that *choker* is a gene involved in the patterning of the anteriormost 5-6 somites. Evidence suggests that the patterning of the anteriormost somites in zebrafish is distinct from that of more posterior ones. This is based on the observation that the anteriormost 5-6 somites have different properties than their more posterior counterparts. Thus, the first 5-6 somites all bud of from the segmental plate at the same time, whereas the more posterior somites form at regular half-hourly intervals. Secondly, several zebrafish mutants including *after eight* (*aei*) and *deadly seven* (*des*) have normal development of anteriormost somites but defective segmentation in the posterior trunk (van Eeden et al., 1996). In addition, the molecular properties of the anteriormost somites might be distinct from their posterior counterparts as the lateral stripe does not form in the anterior 5 somites. Taken together, these data suggest that the patterning and development of the foremost somites in a zebrafish trunk

is separable from those of the posterior trunk and may involve different molecular players. As *choker* mutants display extensive defects in the development of the foremost 5 somites only, we believe that *choker* is a gene specifically involved in the patterning of anteriormost somites.

Studies of the role of Notch signalling in zebrafish have proposed a theory to account for the defective development of posterior somites in zebrafish mutants such as *des* and *aei.* It has been proposed that Notch signalling is involved in the synchronisation of oscillations in the PSM. In the absence of Notch signalling, the PSM oscillations get started off synchronously by the oscillator but subsequently gradually drift out of synchrony due to the lack of Notch signalling-dependent cell-cell communication. This results in the normal development of anteriormost somites only (Jiang et al., 2000). However, it is unlikely that *choker* is a gene involved in the Notch signalling pathway as the mutants do not display any of the defects typically associated with Notch pathway mutants, such as irregularly spaced boundaries or defective segmentation. Ongoing attempts to clone the *choker* gene may shed some light on these issues (G Hollway, P Currie).

We have further investigated the relationship between muscle and neural crest development, by characterising the transmembrane receptor neuropilin-1. This molecule is expressed on the surface of neural crest cells and we have shown that it is a key regulator of initiation of neural crest migration. We believe that its repulsive interaction with the muscle associated ligand, SemaZ1a prevents neural crest cells from migrating on the medial pathway until a time when *neuropilin-1* is switched off in neural crest cells. In its absence a greater number of neural crest cells starts to migrate as soon as the medial pathway opens, resulting in a greater number of cells emigrating on the medial pathway during the early stages of neural crest migration. These early defects result in late defects in xanthophore, melanophore and dorsal root ganglia patterning. The pigment defects however recover by 5 dpf showing once again the amazing ability of neural crest cells to regulate their own numbers and correct patterning defects.

Our characterisation of *neuropilin-1* complements previous studies that characterised the environmental changes that enable neural crest cells to start migrating, by characterising a molecule whose downregulation is required within neural crest cells themselves to enable initiation of migration. Numerous molecules that have a role in neural crest migration have been identified and characterised so far (reviewed in

Halloran and Berndt, 2003). A role for semaphorins in neural crest migration has been implied in several loss-of-function studies in mouse and chick (Brown et al., 2001; Kawasaki et al., 2002). Our study has added to this by characterising the role of the semaphorin receptor, neuropilin-1, in zebrafish neural crest migration and patterning.

Altogether, our analysis have enhanced our understanding of neural crest migration in zebrafish by describing one cellular and one molecular event by which neural crest migration is regulated.

Appendix

Appendix 1.A. Results for neural crest transplants when embryos were immobilised in orientation 1.

Transplant	Phenotype	Head	Anterior trunk (som 1-7)	Posterior trunk (som 7-14)	Tail
1	WT	Hindbrain N	N	N; Mus	N Mus
	WT	Hindbrain N	N	N; Mus	**FM**; N; Mus; Nc
	WT	Hindbrain N	N	**LS X/Mb; DS crest** Mus	Mus; Axn
	WT	**Crest** Hindbrain N	**LS glia x 2;** N; Mus	**DS X/Mb** N; S	Axn; N; S
	WT	Hindbrain N	N	N	**MP crest; Xb/Mb;** Mus; N; Nc; S
	WT				**MP crest x 4 DS crest x 9** Mus; S
	WT	Hindbrain N	N; Mus	Axn	
	WT	**Crest**	En; Mus; N; S	Axn; N; S	Axn
	WT	Hindbrain N	Axn, N	Axn	
	WT	Hindbrain N	Mus, N	Mus; N	**FM; X/Mb** En; Mus; N; S
	WT	**Crest around ear** Hindbrain N	N	**MP crest** Mus; N; S	
	WT		N x 2		Mus; S
	WT (no label)				
	WT (no label)				

Appendix 1.B. Results for neural crest transplants when embryos were immobilised in orientation 2.

2	WT		Axn; Mus; N	**DS crest x 2** Axn; Mus; N	Axn
	WT		En; Mus; S	**VS crest**	**LS crest x 2**

				Mus; S	P Axn; Mus; Nrm
	WT				DS and MP crest Mus; N; S
	WT				**FM** **MP crest x 2** Mus; Nrm
3	WT	Hindbrain N	Axn; Mus; N; S	Axn; Mus; N	**FM** **MP crest** Axn; N
	WT	Hindbrain N	N	Mus; N	**MP crest** **LS crest** P Axn; N
	WT	Hindbrain N	MP crest **Mus; N**	**LS crest** Mus; N; S	FM; DS and MP crest x 2 **Mus; N; S**
4	WT	Hindbrain N	N	S	Mus; S
	WT		**DS crest** N	VS, DS and LS crest Mus; N	FM; DS and VS crest Mus; N; S
	WT			Mus; S	FM; VS and MP crest Mus; S
	WT	**M**	**5 Xs** (som 1-2) Mus; N; S	**FM;** **LP crest** Mus; N; S	**FM;** **MP crest** Mus; N; P Pr; PG; S
	WT			Mus; S	**FM; X;** **MP crest** Mus; N; S
5	*cho*		**VS crest** **DS M x 5** **(som 6-7)** P Axn; S	Mus; N; S	
	cho (no label)				
	cho			Mus; S	**LP crest** Mus; S
	cho		Mus; N; S	Mus; N; S	**FM;** LP crest; a few X
	cho				**DS crest** Mus
	cho				**LP crest** En; Mus; N;

					S
	cho		S	S	S
	cho			Mus; S	**FM; DS and LP crest** Mus; S
	cho		Bl	Mus; S	**FM** En; Mus; S
	cho				**FM; MP M x 2, DS M** Bl

Appendix 1.C. Results of neural crest transplants when embryos were immobilised in orientation 3.

6 *a	*cho*		**5 X (som 6-8)**	**4 X; X/Mb (som 11-13)** S	**3 Xs** Mus; N
	cho (no label)				
	cho	**X around ear; 3 X/Mb**	N	S	
*b	*cho*	**2 X around ear; a few X/Mb**	N; S	**M** N; S	N
	cho (no label)				
	cho			S	S
	cho	**4 X/Mb in head** S			
*c	*cho*	**3 X (anterior to som 1); 4 X/Mb**	**X (som 1); X/Mb (som 4-6);** M and X (som 7) S	**4 DS X** (som 9-11) S	N; S
7 *d	*cho*		**3 VS Xs (som 1-2); X (som 5); 2 VS X/Mb (som 6-8);** 3 X (som 7-8) N	**Numerous X** N; S	**X; crest** Mus; N; S
	cho				**A few X/Mb** Mus; N; S

8	*cho*			Mus	Mus; N; S
	cho		N; S	Mus; N	Mus; N
	cho			S	**FM** Mus; S
	cho			S	**FM;** **DS X/Mb** Mus; N; S
	cho			S	**FM** Mus; S
	cho	Hindbrain N	N; S	N; S	
	cho	Hindbrain N	N		
	cho	**3 X/Mb** N			
	cho			Mus; S	Mus; N; S
	cho			N; S	N; S
	cho		S	S	N; S
	cho		Axn; N; S	Mus; N; S	N; S
9	WT				**FM** Mus; N; S
	WT		**MP crest** P Axn	P Axn	
	WT		N; S	Mus; N; S	**FM** Mus; N; S
	WT		**4 X** N; S	**FM** Mus; N	**FM; 4X** Mus; N; S
	WT		**4 X** N; S	**2 X;** **MP crest** N; S	N; S
	WT			S	**FM** Mus; N; S
	WT		N	**FM** Mus; N	Mus
	WT			S	Mus; S
	WT		**A few X** N; S	**Numerous X** N; S	**6 X; FM** Mus; N; S
	WT		**LP crest** N	N	N
	WT			S	**FM** Mus; N; S
	WT		S	**2 X**	**2X** Mus; S
	WT			S	S
	WT		N	N	Mus; N
	WT		N; S	**9 X** N; S	**FM** Mus; N; S
	WT		N	S	P Axn; S
	WT				S

	WT			S	S
10	*cho*	Hindbrain N; S	P	P	P
	Deformed	**3X/Mb** Hindbrain N; S	**X/Mb** N; S	S	S
	WT	S	P; S	**2 X** P; S	P; S
	cho	Hindbrain N	N	N; S	Axn
	cho		P Axn; S	S	**FM; 2 X** S
	WT			**2 X; 2 X/Mb** Mus; S	**FM** Mus; N; S
	cho		N	N	Mus; N
	cho	**A few X/Mb** Hindbrain N	N; S		N
11	*cho*			Mus; N	Mus; N; S
	cho		N	Mus; N	
	cho (no label)				
	cho		N		
	cho	**Numerous M/Mb**	S	N; S	S
	Cho/nac				S
	nac	**2 M; 5 X/Mb** Hinbrain N			
	Nac (no label)				
	Nac			**2 X/Mb** S	**X; 3 M** N; S

Appendix 2. Results of neural crest transplants at day 3

Transplant	Phenotype	Head	Anterior Trunk	Posterior Trunk	Tail
a	*cho*		**5 X (som 6-8)**	**2 X (som11) 3 X (som 11-12) 5 X (som 18)**	
b	*cho*	**A few X**			
c	*cho*		**2 X (som 1) 2 DS X (som 5-6)**		
d	*cho*		**2 X (som 1) Some X**	**Numerous X**	

			(posterior to som 5)		

Appendix 3. Results of muscle transplants at day 2

Embryo	Head	Anterior trunk	Posterior trunk	Tail
cho		S	Mus; S	mus; N
cho		N	Mus; N	Mus; N
cho		N	Mus; N	
cho		N	Mus; N	Mus; N
cho		N; S	Mus; N; S	Mus; N; S; Xs
cho			Mus; S	Mus; N; S
cho		N	Mus; N	Mus; N
cho			Mus; S	Mus; N; S; FM
cho	M	N; Xs	Mus; N	Mus;
cho		S	Mus; N; S; Xs	Mus; N; S; FM

Key:

Axn = Axon
Blood = Bl
Crest = unidentified crest
En = Endothelium
FM = Fin Mesenchyme
M = Melanophore
Mb = Melanoblast
Mus = Muscle
Nc = Notochord
N = Neuron
Nrm = Neuromast
P Axn – Posterior Lateral Line axon
P Pr = Posterior Lateral Line primordium
P G = Posterior Lateral Line glia
S = Skin
X = Xanthophore
Xb = Xanthoblast

LS = Lateral Stripe
DS = Dorsal Stripe
VS = Ventral Stripe
MP = Medial Pathway
LP = Lateral pathway

References

Amaya, E., Musci, T. J. and Kirschner, M. W. (1991). Expression of a Dominant Negative Mutant of the Fgf Receptor Disrupts Mesoderm Formation in Xenopus Embryos. *Cell* **66**, 257-270.

An, M., Luo, R. and Henion, P. D. (2002). Differentiation and maturation of zebrafish dorsal root and sympathetic ganglion neurons. *J Comp Neurol* **446**, 267-75.

Andermann, P., Ungos, J. and Raible, D. W. (2002). Neurogenin1 defines zebrafish cranial sensory ganglia precursors. *Developmental Biology* **251**, 45-58.

Aoyama, H. and Asamoto, K. (1988). Determination of Somite Cells - Independence of Cell- Differentiation and Morphogenesis. *Development* **104**, 15-28.

Araki, M., Takano, T., Uemonsa, T., Nakane, Y., Tsudzuki, M. and Kaneko, T. (2002). Epithelia-mesenchyme interaction plays an essential role in trans differentiation of retinal pigment epithelium of silver mutant quail: Localization of FGF and related molecules and aberrant migration pattern of neural crest cells during eye rudiment formation. *Developmental Biology* **244**, 358-371.

Arnott, H. J., Best, A.C., Nicol, J.A. (1970). Occurrence of melanosomes and of crystal sacs within the same cell in the tapetum lucidum of the stingaree. *Journal of Cell Biology* **46**, 426-7.

Aulehla, A. and Johnson, R. L. (1999). Dynamic expression of lunatic fringe suggests a link between notch signaling and an autonomous cellular oscillator driving somite segmentation. *Developmental Biology* **207**, 49-61.

Ayer-Le Lievre, C. S. and Le Douarin, N. M. (1982). The early development of cranial sensory ganglia and the potentialities of their component cells studied in quail-chick chimeras. *Dev Biol* **94**, 291-310.

Bagnara, J. T., Matsumoto, J., Ferris, W., Frost, S. K., Turner, W. A., Jr., Tchen, T. T. and Taylor, J. D. (1979). Common origin of pigment cells. *Science* **203**, 410-5.

Barrantes, I. D., Elia, A. J., Wunsch, K., De Angelis, M. H., Mak, T. W., Rossant, J., Conlon, R. A., Gossler, A. and de la Pompa, J. L. (1999). Interaction between Notch signalling and Lunatic fringe during somite boundary formation in the mouse. *Current Biology* **9**, 470-480.

Behar, O., Golden, J. A., Mashimo, H., Schoen, F. J. and Fishman, M. C. (1996). Semaphorin III Is needed for normal patterning and growth of nerves, bones and heart. *Nature* **383**, 525-528.

Blagden, C. S., Currie, P. D., Ingham, P. W. and Hughes, S. M. (1997). Notochord induction of zebrafish slow muscle mediated by Sonic hedgehog. *Genes Dev* **11**, 2163-75.

Bronner-Fraser, M. (2000). Rostrocaudal differences within the somites confer segmental pattern to trunk neural crest migration. *Curr Top Dev Biol* **47**, 279-96.

Brown, C. B., Feiner, L., Lu, M. M., Li, J., Ma, X., Webber, A. L., Jia, L., Raper, J. A. and Epstein, J. A. (2001). PlexinA2 and semaphorin signaling during cardiac neural crest development. *Development* **128**, 3071-80.

Burgess, R., Rawls, A., Brown, D., Bradley, A. and Olson, E. N. (1996). Requirement of the paraxis gene for somite formation and musculoskeletal patterning. *Nature* **384**, 570-573.

Cano, A., Perez-Moreno, M. A., Rodrigo, I., Locascio, A., Blanco, M. J., del Barrio, M. G., Portillo, F. and Nieto, M. A. (2000). The transcription factor Snail controls epithelial-mesenchymal transitions by repressing E-cadherin expression. *Nature Cell Biology* **2**, 76-83.

Challa, A. K., Beattie, C. E. and Seeger, M. A. (2001). Identification and characterization of roundabout orthologs in zebrafish. *Mechanisms of Development* **101**, 249-253.

Chan, J., Mably, J. D., Serluca, F. C., Chen, J. N., Goldstein, N. B., Thomas, M. C., Cleary, J. A., Brennan, C., Fishman, M. C. and Roberts, T. M. (2001). Morphogenesis of prechordal plate and notochord requires intact Eph/ephrin B signaling. *Dev Biol* **234**, 470-82.

Chang, C. B. and Hemmati-Brivanlou, A. (1998). Neural crest induction by Xwnt7B in Xenopus. *Developmental Biology* **194**, 129-134.

Christian, J. L. and Moon, R. T. (1993). Interactions between Xwnt-8 and Spemann Organizer Signaling Pathways Generate Dorsoventral Pattern in the Embryonic Mesoderm of Xenopus. *Genes & Development* **7**, 13-28.

Cooke, J. (1998). A gene that resuscitates a theory - somitogenesis and a molecular oscillator. *Trends in Genetics* **14**, 85-88.

Cortes, F., Daggett, D., Bryson-Richardson, R. J., Neyt, C., Maule, J., Gautier, P., Hollway, G. E., Keenan, D. and Currie, P. D. (2003). Cadherin-mediated differential

cell adhesion controls slow muscle cell migration in the developing zebrafish myotome. *Developmental Cell* **5**, 865-876.

Currie, P. D. and Ingham, P. W. (1996). Induction of a specific muscle cell type by a hedgehog-like protein in zebrafish. *Nature* **382**, 452-5.

Delmas, V., Pla, P., Feracci, H., Thiery, J. P., Kemler, R. and Larue, L. (1999). Expression of the cytoplasmic domain of E-cadherin induces precocious mammary epithelial alveolar formation and affects cell polarity and cell-matrix integrity. *Developmental Biology* **216**, 491-506.

Devoto, S. H., Melancon, E., Eisen, J. S. and Westerfield, M. (1996). Identification of separate slow and fast muscle precursor cells in vivo, prior to somite formation. *Development* **122**, 3371-80.

Dickinson, M. E., Selleck, M. A., McMahon, A. P. and Bronner-Fraser, M. (1995). Dorsalization of the neural tube by the non-neural ectoderm. *Development* **121**, 2099-106.

Dorsky, R. I., Moon, R. T. and Raible, D. W. (1998). Control of neural crest cell fate by the Wnt signalling pathway. *Nature* **396**, 370-3.

Du, S. J., Devoto, S. H., Westerfield, M. and Moon, R. T. (1997). Positive and negative regulation of muscle cell identity by members of the hedgehog and TGF-beta gene families. *J Cell Biol* **139**, 145-56.

Duband, J. L., Monier, F., Delannet, M. and Newgreen, D. (1995). Epithelium-mesenchyme transition during neural crest development. *Acta Anatomica* **154**, 63-78.

Dupin, E., Glavieux, C., Vaigot, P. and Le Douarin, N. M. (2000). Endothelin 3 induces the reversion of melanocytes to glia through a neural crest-derived glial-melanocytic progenitor. *Proc Natl Acad Sci U S A* **97**, 7882-7.

Dupin, E., Real, C., Glavieux-Pardanaud, C., Vaigot, P. and Le Douarin, N. M. (2003). Reversal of developmental restrictions in neural crest lineages: Transition from Schwann cells to glial-melanocytic precursors in vitro. *Proceedings of the National Academy of Sciences of the United States of America* **100**, 5229-5233.

Durbin, L., Brennan, C., Shiomi, K., Cooke, J., Barrios, A., Shanmugalingam, S., Guthrie, B., Lindberg, R. and Holder, N. (1998). Eph signaling is required for segmentation and differentiation of the somites. *Genes Dev* **12**, 3096-109.

Durbin, L., Sordino, P., Barrios, A., Gering, M., Thisse, C., Thisse, B., Brennan, C., Green, A., Wilson, S. and Holder, N. (2000). Anteroposterior patterning is

required within segments for somite boundary formation in developing zebrafish. *Development* **127**, 1703-1713.

Dutton, K. A., Pauliny, A., Lopes, S. S., Elworthy, S., Carney, T. J., Rauch, J., Geisler, R., Haffter, P. and Kelsh, R. N. (2001). Zebrafish colourless encodes sox10 and specifies non-ectomesenchymal neural crest fates. *Development* **128**, 4113-25.

Eickholt, B. J., Mackenzie, S. L., Graham, A., Walsh, F. S. and Doherty, P. (1999). Evidence for collapsin-1 functioning in the control of neural crest migration in both trunk and hindbrain regions. *Development* **126**, 2181-2189.

Ekker, M., Wegner, J., Akimenko, M. A. and Westerfield, M. (1992). Coordinate embryonic expression of three zebrafish engrailed genes. *Development* **116**, 1001-10.

Englund, C., Steneberg, P., Falileeva, L., Xylourgidis, N. and Samakovlis, C. (2002). Attractive and repulsive functions of Slit are mediated by different receptors in the Drosophila trachea. *Development* **129**, 4941-4951.

Erickson, C. A. and Goins, T. L. (1995). Avian neural crest cells can migrate in the dorsolateral path only if they are specified as melanocytes. *Development* **121**, 915-24.

Erickson, C. A. and Perris, R. (1993). The Role of Cell-Cell and Cell-Matrix Interactions in the Morphogenesis of the Neural Crest. *Developmental Biology* **159**, 60-74.

Evrard, Y. A., Lun, Y., Aulehla, A., Gan, L. and Johnson, R. L. (1998). lunatic fringe is an essential mediator of somite segmentation and patterning. *Nature* **394**, 377-381.

Faraco, C. D., Vaz, S. A., Pastor, M. V. and Erickson, C. A. (2001). Hyperpigmentation in the Silkie fowl correlates with abnormal migration of fate-restricted melanoblasts and loss of environmental barrier molecules. *Dev Dyn* **220**, 212-25.

Forsberg, H., Crozet, F. and Brown, N. A. (1998). Waves of mouse Lunatic fringe expression, in four-hour cycles at two-hour intervals, precede somite boundary formation. *Current Biology* **8**, 1027-1030.

Frost, S. K., Robinson, S. J., Carson, M. K., Thorsteinsdottir, S. and Giesler, J. (1987). Effects of Exogenous Guanosine on Chromatophore Differentiation in the Axolotl. *Pigment Cell Research* **1**, 37-43.

Gilmour, D. T., Maischein, H. M. and Nusslein-Volhard, C. (2002). Migration and function of a glial subtype in the vertebrate peripheral nervous system. *Neuron* **34**, 577-588.

Goodrich, H. B., Nichols, R. (1931). The development and the regeneration of the color pattern in *Brachydanio rerio*. *Journal of Morphology and Physiology* **52**, 513-23.

Griffin, K. J. P., Amacher, S. L., Kimmel, C. B. and Kimelman, D. (1998). Molecular identification of spadetail: regulation of zebrafish trunk and tail mesoderm formation by T-box genes. *Development* **125**, 3379-3388.

Halloran, M. C. and Berndt, J. D. (2003). Current progress in neural crest cell motility and migration and future prospects for the zebrafish model system. *Developmental Dynamics* **228**, 497-513.

Halpern, M. E., Ho, R. K., Walker, C. and Kimmel, C. B. (1993). Induction of Muscle Pioneers and Floor Plate Is Distinguished by the Zebrafish No Tail Mutation. *Cell* **75**, 99-111.

Heisenberg, C. P., Tada, M., Rauch, G. J., Saude, L., Concha, M. L., Geisler, R., Stemple, D. L., Smith, J. C. and Wilson, S. W. (2000). Silberblick/Wnt11 mediates convergent extension movements during zebrafish gastrulation. *Nature* **405**, 76-81.

Holder, N. and Klein, R. (1999). Eph receptors and ephrins: effectors of morphogenesis. *Development* **126**, 2033-2044.

Holley, S. A., Geisler, R. and Nusslein-Volhard, C. (2000). Control of her1 expression during zebrafish somitogenesis by a Delta-dependent oscillator and an independent wave-front activity. *Genes & Development* **14**, 1678-1690.

Holley, S. A., Julich, D., Rauch, G. J., Geisler, R. and Nusslein-Volhard, C. (2002). her1 and the notch pathway function within the oscillator mechanism that regulates zebrafish somitogenesis. *Development* **129**, 1175-1183.

Jen, W. C., Gawantka, V., Pollet, N., Niehrs, C. and Kintner, C. (1999). Periodic repression of Notch pathway genes governs the segmentation of Xenopus embryos. *Genes & Development* **13**, 1486-1499.

Jesuthasan, S. (1996). Contact inhibition/collapse and pathfinding of neural crest cells in the zebrafish trunk. *Development* **122**, 381-9.

Jiang, Y. J., Aerne, B. L., Smithers, L., Haddon, C., Ish-Horowicz, D. and Lewis, J. (2000). Notch signalling and the synchronization of the somite segmentation clock. *Nature* **408**, 475-479.

Johnston, S. H., Rauskolb, C., Wilson, R., Prabhakaran, B., Irvine, K. D. and Vogt, T. F. (1997). A family of mammalian Fringe genes implicated in boundary determination and the Notch pathway. *Development* **124**, 2245-2254.

Karlstrom, R. O., Talbot, W. S. and Schier, A. F. (1999). Comparative synteny cloning of zebrafish you-too: mutations in the Hedgehog target gli2 affect ventral forebrain patterning. *Genes & Development* **13**, 388-393.

Kawasaki, T., Bekku, Y., Suto, F., Kitsukawa, T., Taniguchi, M., Nagatsu, I., Nagatsu, T., Itoh, K., Yagi, T. and Fujisawa, H. (2002). Requirement of neuropilin 1-mediated Sema3A signals in patterning of the sympathetic nervous system. *Development* **129**, 671-80.

Kelsh, R. N., and Raible, D.W. (2002). Specification of zebrafish neural crest. *Results and Problems in Cell Differentiation* **40**, 216-236.

Kelsh, R. N., Brand, M., Jiang, Y. J., Heisenberg, C. P., Lin, S., Haffter, P., Odenthal, J., Mullins, M. C., van Eeden, F. J., Furutani-Seiki, M. et al. (1996). Zebrafish pigmentation mutations and the processes of neural crest development. *Development* **123**, 369-89.

Kelsh, R. N., Dutton, K., Medlin, J. and Eisen, J. S. (2000a). Expression of zebrafish fkd6 in neural crest-derived glia. *Mech Dev* **93**, 161-4.

Kelsh, R. N. and Eisen, J. S. (2000). The zebrafish colourless gene regulates development of non-ectomesenchymal neural crest derivatives. *Development* **127**, 515-25.

Kelsh, R. N., Schmid, B. and Eisen, J. S. (2000b). Genetic analysis of melanophore development in zebrafish embryos. *Dev Biol* **225**, 277-93.

Kidd, T., Bland, K. S. and Goodman, C. S. (1999). Slit is the midline repellent for the robe receptor in Drosophila. *Cell* **96**, 785-794.

Kidd, T., Russell, C., Goodman, C. S. and Tear, G. (1998). Dosage-sensitive and complementary functions of roundabout and commissureless control axon crossing of the CNS midline. *Neuron* **20**, 25-33.

Kil, S. H., Krull, C. E., Cann, G., Clegg, D. and Bronner-Fraser, M. (1998). The alpha 4 subunit of integrin is important for neural crest cell migration. *Developmental Biology* **202**, 29-42.

Kimelman, D. and Griffin, K. J. P. (2000). Vertebrate mesendoderm induction and patterning. *Current Opinion in Genetics & Development* **10**, 350-356.

Kimmel, C. B., Ballard, W. W., Kimmel, S. R., Ullmann, B. and Schilling, T. F. (1995). Stages of embryonic development of the zebrafish. *Dev Dyn* **203**, 253-310.

Kimmel, C. B., Warga, R. M. and Schilling, T. F. (1990). Origin and organization of the zebrafish fate map. *Development* **108**, 581-94.

Kitsukawa, T., Shimizu, M., Sanbo, M., Hirata, T., Taniguchi, M., Bekku, Y., Yagi, T. and Fujisawa, H. (1997). Neuropilin-semaphorin III/D-mediated chemorepulsive signals play a crucial role in peripheral nerve projection in mice. *Neuron* **19**, 995-1005.

Kolodkin, A. L., Levengood, D. V., Rowe, E. G., Tai, Y. T., Giger, R. J. and Ginty, D. D. (1997). Neuropilin is a Semaphorin III receptor. *Cell* **90**, 753-762.

Kozlowski, D. J., Murakami, T., Ho, R. K. and Weinberg, E. S. (1997). Regional cell movement and tissue patterning in the zebrafish embryo revealed by fate mapping with caged fluorescein. *Biochem Cell Biol* **75**, 551-62.

Kramer, S. G., Kidd, T., Simpson, J. H. and Goodman, C. S. (2001). Switching repulsion to attraction: Changing responses to slit during transition in mesoderm migration. *Science* **292**, 737-740.

Krull, C. E. (2001). Segmental organization of neural crest migration. *Mech Dev* **105**, 37-45.

Krull, C. E., Collazo, A., Fraser, S. E. and Bronnerfraser, M. (1995). Segmental Migration of Trunk Neural Crest - Time-Lapse Analysis Reveals a Role for Pna-Binding Molecules. *Development* **121**, 3733-3743.

Krull, C. E., Lansford, R., Gale, N. W., Collazo, A., Marcelle, C., Yancopoulos, G. D., Fraser, S. E. and Bronner-Fraser, M. (1997). Interactions of Eph-related receptors and ligands confer rostrocaudal pattern to trunk neural crest migration. *Curr Biol* **7**, 571-80.

LaBonne, C. and Bronner-Fraser, M. (1998). Neural crest induction in Xenopus: evidence for a two-signal model. *Development* **125**, 2403-2414.

Le Douarin, N. M. and Dupin, E. (2003). Multipotentiality of the neural crest. *Current Opinion in Genetics & Development* **13**, 529-536.

Le Douarin, N. M. and Kalcheim, C. (1999). The Neural Crest: Cambridge University Press.

Lee, J. S., Ray, R. and Chien, C. B. (2001). Cloning and expression of three zebrafish roundabout homologs suggest roles in axon guidance and cell migration. *Developmental Dynamics* **221**, 216-230.

Lee, P., Goishi, K., Davidson, A. J., Mannix, R., Zon, L. and Klagsbrun, M. (2002). Neuropilin-1 is required for vascular development and is a mediator of VEGF-dependent angiogenesis in zebrafish. *Proc Natl Acad Sci U S A* **99**, 10470-5.

Lewis, K. E., Currie, P. D., Roy, S., Schauerte, H., Haffter, P. and Ingham, P. W. (1999). Control of muscle cell-type specification in the zebrafish embryo by Hedgehog signalling. *Dev Biol* **216**, 469-80.

Liem, K. F., Tremml, G., Roelink, H. and Jessell, T. M. (1995). Dorsal Differentiation of Neural Plate Cells Induced by Bmp- Mediated Signals from Epidermal Ectoderm. *Cell* **82**, 969-979.

Lister, J. A., Robertson, C. P., Lepage, T., Johnson, S. L. and Raible, D. W. (1999). nacre encodes a zebrafish microphthalmia-related protein that regulates neural-crest-derived pigment cell fate. *Development* **126**, 3757-67.

Lofberg, J., Nynas-McCoy, A., Olsson, C., Jonsson, L. and Perris, R. (1985). Stimulation of initial neural crest cell migration in the axolotl embryo by tissue grafts and extracellular matrix transplanted on microcarriers. *Dev Biol* **107**, 442-59.

Luo, Y. L., Raible, D. and Raper, J. A. (1993). Collapsin - a Protein in Brain That Induces the Collapse and Paralysis of Neuronal Growth Cones. *Cell* **75**, 217-227.

Mancilla, A. and Mayor, R. (1996). Neural crest formation in Xenopus laevis: mechanisms of Xslug induction. *Dev Biol* **177**, 580-9.

Marchant, L., Linker, C., Ruiz, P., Guerrero, N. and Mayor, R. (1998). The inductive properties of mesoderm suggest that the neural crest cells are specified by a BMP gradient. *Dev Biol* **198**, 319-29.

Marusich, M. F., Furneaux, H. M., Henion, P. D. and Weston, J. A. (1994). Hu neuronal proteins are expressed in proliferating neurogenic cells. *J Neurobiol* **25**, 143-55.

McGrew, M. J., Dale, J. K., Fraboulet, S. and Pourquie, O. (1998). The lunatic Fringe gene is a target of the molecular clock linked to somite segmentation in avian embryos. *Current Biology* **8**, 979-982.

McLennan, R. and Krull, C. E. (2002). Ephrin-As cooperate with EphA4 to promote trunk neural crest migration. *Gene Expression* **10**, 295-305.

Milos, N. and Dingle, A. D. (1978a). Dynamics of pigment pattern formation in the zebrafish *Brachydanio rerio*. *J Exp Zool* **205**, 217-224.

Milos, N. and Dingle, A. D. (1978b). Dynamics of pigment pattern formation in the zebrafish, *Brachydanio rerio*. *J Exp Zool* **205**, 205-216.

Mochii, M., Ono, T., Matsubara, Y. and Eguchi, G. (1998). Spontaneous transdifferentiation of quail pigmented epithelial cell is accompanied by a mutation in the Mitf gene. *Developmental Biology* **196**, 145-159.

Morin-Kensicki, E. M. and Eisen, J. S. (1997). Sclerotome development and peripheral nervous system segmentation in embryonic zebrafish. *Development* **124**, 159-67.

Moury, J. D. and Jacobson, A. G. (1989). Neural fold formation at newly created boundaries between neural plate and epidermis in the axolotl. *Dev Biol* **133**, 44-57.

Moury, J. D. and Jacobson, A. G. (1990). The origins of neural crest cells in the axolotl. *Dev Biol* **141**, 243-53.

Nguyen, M. T. T. and Arnheiter, H. (2000). Signaling and transcriptional regulation in early mammalian eye development: a link between FGF and MITF. *Development* **127**, 3581-3591.

Nguyen, V. H., Schmid, B., Trout, J., Connors, S. A., Ekker, M. and Mullins, M. C. (1998). Ventral and lateral regions of the zebrafish gastrula, including the neural crest progenitors, are established by a bmp2b/swirl pathway of genes. *Developmental Biology* **199**, 93-110.

Nguyen, V. H., Trout, J., Connors, S. A., Andermann, P., Weinberg, E. and Mullins, M. C. (2000). Dorsal and intermediate neuronal cell types of the spinal cord are established by a BMP signaling pathway. *Development* **127**, 1209-1220.

Nieto, M. A., Sargent, M. G., Wilkinson, D. G. and Cooke, J. (1994). Control of Cell Behavior During Vertebrate Development by Slug, a Zinc-Finger Gene. *Science* **264**, 835-839.

Nishimura, E. K., Yoshida, H., Kunisada, T. and Nishikawa, S. I. (1999). Regulation of E- and P-cadherin expression correlated with melanocyte migration and diversification. *Dev Biol* **215**, 155-66.

Oakley, R. A., Lasky, C. J., Erickson, C. A. and Tosney, K. W. (1994). Glycoconjugates mark a transient barrier to neural crest migration in the chicken embryo. *Development* **120**, 103-14.

Odenthal, J., Rossnagel, K., Haffter, P., Kelsh, R. N., Vogelsang, E., Brand, M., van Eeden, F. J., Furutani-Seiki, M., Granato, M., Hammerschmidt, M. et al. (1996). Mutations affecting xanthophore pigmentation in the zebrafish, Danio rerio. *Development* **123**, 391-8.

Palmeirim, I., Henrique, D., IshHorowicz, D. and Pourquie, O. (1997). Avian hairy gene expression identifies a molecular clock linked to vertebrate segmentation and somitogenesis. *Cell* **91**, 639-648.

Parichy, D. M., Ransom, D. G., Paw, B., Zon, L. I. and Johnson, S. L. (2000). An orthologue of the kit-related gene fms is required for development of neural crest-derived xanthophores and a subpopulation of adult melanocytes in the zebrafish, Danio rerio. *Development* **127**, 3031-44.

Pelletier, I., Bally-Cuif, L. and Ziegler, I. (2001). Cloning and developmental expression of zebrafish GTP cyclohydrolase I. *Mech Dev* **109**, 99-103.

Perris, R. and Perissinotto, D. (2000). Role of the extracellular matrix during neural crest cell migration. *Mech Dev* **95**, 3-21.

Pettway, Z., Domowicz, M., Schwartz, N. B. and BronnerFraser, M. (1996). Age-dependent inhibition of neural crest migration by the notochord correlates with alterations in the S103L chondroitin sulfate proteoglycan. *Experimental Cell Research* **225**, 195-206.

Pla, P., Moore, R., Morali, O. G., Grille, S., Martinozzi, S., Delmas, V. and Larue, L. (2001). Cadherins in neural crest cell development and transformation. *J Cell Physiol* **189**, 121-32.

Raible, D. W. and Eisen, J. S. (1994). Restriction of neural crest cell fate in the trunk of the embryonic zebrafish. *Development* **120**, 495-503.

Raible, D. W., Wood, A., Hodsdon, W., Henion, P. D., Weston, J. A. and Eisen, J. S. (1992). Segregation and early dispersal of neural crest cells in the embryonic zebrafish. *Dev Dyn* **195**, 29-42.

Reedy, M. V., Faraco, C. D. and Erickson, C. A. (1998). The delayed entry of thoracic neural crest cells into the dorsolateral path is a consequence of the late emigration of melanogenic neural crest cells from the neural tube. *Dev Biol* **200**, 234-46.

Rickmann, M., Fawcett, J. W. and Keynes, R. J. (1985). The migration of neural crest cells and the growth of motor axons through the rostral half of the chick somite. *J Embryol Exp Morphol* **90**, 437-55.

Roos, M., Schachner, M. and Bernhardt, R. R. (1999). Zebrafish semaphorin Z1b inhibits growing motor axons in vivo. *Mech Dev* **87**, 103-17.

Roy, S., Wolff, C. and Ingham, P. W. (2001). The u-boot mutation identifies a Hedgehog-regulated myogenic switch for fiber-type diversification in the zebrafish embryo. *Genes Dev* **15**, 1563-76.

Saga, Y., Hata, N. and Koseki, H. (1997). Mesp2: A novel mouse gene expressed in the presegmented mesoderm and essential tor segmentation initiation. *Developmental Biology* **186**, B105-B105.

Saga, Y., Yagi, T., Ikawa, Y., Sakakura, T. and Aizawa, S. (1992). Mice Develop Normally without Tenascin. *Genes & Development* **6**, 1821-1831.

SaintJeannet, J. P., He, X., Varmus, H. E. and Dawid, I. B. (1997). Regulation of dorsal fate in the neuraxis by Wnt-1 and Wnt-3a. *Proceedings of the National Academy of Sciences of the United States of America* **94**, 13713-13718.

Santiago, A. and Erickson, C. A. (2002). Ephrin-B ligands play a dual role in the control of neural crest cell migration. *Development* **129**, 3621-32.

Sawada, A., Fritz, A., Jiang, Y. J., Yamamoto, A., Yamasu, K., Kuroiwa, A., Saga, Y. and Takeda, H. (2000). Zebrafish Mesp family genes, mesp-a and mesp-b are segmentally expressed in the presomitic mesoderm, and Mesp-b confers the anterior identity to the developing somites. *Development* **127**, 1691-1702.

Schauerte, H. E., van Eeden, F. J. M., Fricke, C., Odenthal, J., Strahle, U. and Haffter, P. (1998). Sonic hedgehog is not required for the induction of medial floor plate cells in the zebrafish. *Development* **125**, 2983-2993.

Schilling, T. F. and Kimmel, C. B. (1994). Segment and cell type lineage restrictions during pharyngeal arch development in the zebrafish embryo. *Development* **120**, 483-94.

Sela-Donenfeld, D. and Kalcheim, C. (1999). Regulation of the onset of neural crest migration by coordinated activity of BMP4 and Noggin in the dorsal neural tube. *Development* **126**, 4749-62.

Sela-Donenfeld, D. and Kalcheim, C. (2000). Inhibition of noggin expression in the dorsal neural tube by somitogenesis: a mechanism for coordinating the timing of neural crest emigration. *Development* **127**, 4845-54.

Selleck, M. A. J. and Bronnerfraser, M. (1995). Origins of the Avian Neural Crest - the Role of Neural Plate- Epidermal Interactions. *Development* **121**, 525-538.

Shah, N. M., Groves, A. K. and Anderson, D. J. (1996). Alternative neural crest cell fates are instructively promoted by TGFbeta superfamily members. *Cell* **85**, 331-43.

Sherman, L., Stocker, K. M., Morrison, R. and Ciment, G. (1993). Basic Fibroblast Growth-Factor (Bfgf) Acts Intracellularly to Cause the Transdifferentiation of Avian Neural Crest-Derived Schwann-Cell Precursors into Melanocytes. *Development* **118**, 1313-1326.

Shoji, W., Isogai, S., Sato-Maeda, M., Obinata, M. and Kuwada, J. Y. (2003). Semaphorin3a1 regulates angioblast migration and vascular development in zebrafish embryos. *Development* **130**, 3227-3236.

Shoji, W., Yee, C. S. and Kuwada, J. Y. (1998). Zebrafish Semaphorin Z1a collapses specific growth cones and alters their pathway in vivo. *Development* **125**, 1275-1283.

Sosic, D., BrandSaberi, B., Schmidt, C., Christ, B. and Olson, E. N. (1997). Regulation of paraxis expression and somite formation by ectoderm- and neural tube-derived signals. *Developmental Biology* **185**, 229-243.

Stemple, D. L. and Anderson, D. J. (1992). Isolation of a Stem-Cell for Neurons and Glia from the Mammalian Neural Crest. *Cell* **71**, 973-985.

Strachan, L. R. and Condic, M. L. (2003). Neural crest motility and integrin regulation are distinct in cranial and trunk populations. *Developmental Biology* **259**, 288-302.

Taniguchi, M., Yuasa, S., Fujisawa, H., Naruse, I., Saga, S., Mishina, M. and Yagi, T. (1997). Disruption of Semaphorin III/D gene causes severe abnormality in peripheral nerve projection. *Neuron* **19**, 519-530.

Testaz, S. and Duband, J. L. (2001). Central role of the alpha4beta1 integrin in the coordination of avian truncal neural crest cell adhesion, migration, and survival. *Dev Dyn* **222**, 127-40.

Thibaudeau, G. and Holder, S. (1998). Cellular plasticity among axolotl neural crest-derived pigment cell lineages. *Pigment Cell Research* **11**, 38-44.

Tucker, R. P. (2001). Abnormal neural crest cell migration after the in vivo knockdown of tenascin-C expression with morpholino antisense oligonucleotides. *Dev Dyn* **222**, 115-9.

van Eeden, F. J., Granato, M., Schach, U., Brand, M., Furutani-Seiki, M., Haffter, P., Hammerschmidt, M., Heisenberg, C. P., Jiang, Y. J., Kane, D. A. et al. (1996). Mutations affecting somite formation and patterning in the zebrafish, Danio rerio. *Development* **123**, 153-64.

Wang, H. U. and Anderson, D. J. (1997). Eph family transmembrane ligands can mediate repulsive guidance of trunk neural crest migration and motor axon outgrowth. *Neuron* **18**, 383-396.

Wang, K. H., Brose, K., Arnott, D., Kidd, T., Goodman, C. S., Henzel, W. and Tessier-Lavigne, M. (1999). Biochemical purification of a mammalian slit protein as a positive regulator of sensory axon elongation and branching. *Cell* **96**, 771-784.

Weinberg, E. S., Allende, M. L., Kelly, C. S., Abdelhamid, A., Murakami, T., Andermann, P., Doerre, O. G., Grunwald, D. J. and Riggleman, B. (1996). Developmental regulation of zebrafish MyoD in wild-type, no tail and spadetail embryos. *Development* **122**, 271-280.

Woo, K. and Fraser, S. E. (1995). Order and coherence in the fate map of the zebrafish nervous system. *Development* **121**, 2595-609.

Yamamoto, A., Amacher, S. L., Kim, S. H., Bouwmeester, T., Agius, E., Geissert, D., Kimmel, C. B. and De Robertis, E. M. (1998). Paraxial protocadherin is a downsteam target of spadetail involed in morphogenesis of the mesodermal mantle. *Developmental Biology* **198**, 387.

Yee, C. S., Chandrasekhar, A., Halloran, M. C., Shoji, W., Warren, J. T. and Kuwada, J. Y. (1999). Molecular cloning, expression, and activity of zebrafish semaphorin Z1a. *Brain Research Bulletin* **48**, 581-593.

Yuan, W. L., Zhou, L. J., Chen, T. H., Wu, J. Y., Rao, Y. and Ornitz, D. M. (1999). The mouse SLIT family: Secreted ligands for ROBO expressed in patterns that suggest a role in morphogenesis and axon guidance. *Developmental Biology* **212**, 290-306.

Zhang, N. A. and Gridley, T. (1998). Defects in somite formation in lunatic fringe deficient mice. *Nature* **394**, 374-377.

Zhao, S. L., Rizzolo, L. J. and Barnstable, C. J. (1997). Differentiation and transdifferentiation of the retinal pigment epithelium. In *International Review of Cytology - a Survey of Cell Biology, Vol 171*, vol. 171, pp. 225-266.